RECEPTOR-BASED MODELING OF GROUNDWATER CONTAMINATION

by

Roseanna Marie Neupauer

Submitted in Partial Fulfillment
of the Requirements for the Degree of
Doctor of Philosophy in Earth and Environmental Science
with Dissertation in Hydrology

New Mexico Institute of Mining and Technology
Socorro, New Mexico
December, 2000

ABSTRACT

Receptor-based modeling can be used to determine the prior position of contamination observed at a receptor, such as a pumping well or a monitoring well. The results of a receptor-based model are backward location and travel time probability distributions for the observed contamination. For a contaminant parcel that was observed at a receptor, backward location probability is the probability distribution describing the position of the parcel at some time prior to detection, and backward travel time probability is the probability distribution describing the travel time of the parcel from an upgradient position to the detection location. The receptor-based (backward) model can be used to improve characterization of known sources of groundwater contamination, to identify previously unknown contamination sources, and to delineate capture zones.

Backward probabilities are related to adjoint states of resident concentration; therefore, the governing equations of backward probability are adjoints of the forward governing equation. We formally show the relationship between adjoint states and backward probabilities. Using the advection-dispersion equation as the model of forward contaminant transport, we derive the backward governing equation for many conceptual models including one- and multi-

dimensional domains, homogeneous and heterogeneous aquifers, uniform and non-uniform flow, steady and transient flow, and conservative and reactive solutes. Each governing equation contains the adjoint of the advection-dispersion operator and a load term that defines the particular adjoint state. The load term depends on both the type of probability and the type of receptor. We show that forward location and travel time probabilities are also related to the same adjoint states.

The backward governing equations are similar to the forward model; therefore, any forward contaminant transport code can also be used to solve the backward model. The load terms contain generalized functions that cannot be implemented explicitly in numerical codes, so approximations must be used. We show the appropriate load term approximations that can be used with general cell-centered finite difference models and finite element models with linear triangular or prism elements.

In practical situations, contamination is sampled at multiple locations and times, and the concentrations of the samples are known. This additional data provides more information that can be used to characterize the prior position of contamination. This additional information should reduce the variances for the location and travel time probability distributions and improve the characterization of the contamination source. We present approaches for incorporating multiple detections of contamination and concentration measure-

ments into the backward probability model. The variances of the probability distributions are reduced using multiple detections. If the source mass is well-constrained, the variances are also reduced using concentration measurements.

As a test case for applying the backward probability model, we use data from a trichloroethylene (TCE) plume at the Massachusetts Military Reservation (MMR) on Cape Cod to obtain information about the prior positions of the observed TCE. The backward model was based on a forward flow and transport model that had been used to simulation remediation conditions. We adapted the model to pre-remediation conditions and used it to obtain backward probability distributions for detected contamination. The results indicate a low probability that the contamination originated from the major suspected source. This could indicate that other sources of contamination were more likely, or that the model was not optimized for pre-remediation conditions.

ACKNOWLEDGMENT

I was very fortunate to have the opportunity to work with two prominent researchers in hydrology, John Wilson and Allan Gutjahr. I thank my research advisor, John Wilson, for his guidance and support throughout my time at New Mexico Tech. He has been a wonderful source of knowledge regarding this research and other academic and professional topics. I appreciate his willingness to share many hours with me discussing my research progress, problems, and issues. It was through these discussions that I developed a much deeper understanding of the subject area than I ever could have achieved on my own. I have always been impressed by John's enthusiasm and dedication to his work and the work of his students and in the interest he takes in helping students learn. It was a pleasure to work with him, and I hope that I can follow his example.

Allan Gutjahr was an immense help in integrating probability theory with contaminant transport. Very few people have such a vast knowledge of both math and hydrology, and I thank him for cheerfully sharing this with me. Although Allan was involved in the development of most of the theory in this dissertation, he unfortunately did not see these final results. I know that this dissertation would have been improved with Allan's insight. Obviously, he was still needed since several issues in Chapter 9 of this dissertation have not yet been resolved.

I thank my other committee members, Dongxiao (Don) Zhang, Rick Aster, Brian McPherson, and Vince Tidwell, for their guidance, and for their reviews of this dissertation. Don was an excellent source of information for theoretical aspects regarding randomness in contaminant transport. Rick and Brian made sure that I put my theoretical model into a physical context by testing my model with a real-world application. Vince joined my committee only a few months before I defended and provided a fresh view of the material.

Several others have provided me with knowledge and information that I needed to complete this research and I thank them for their help. William D. Stone provided much needed input on operator theory and generalized functions that was very important for developing the backward model equations. Chunmiao Zheng of the University of Alabama gave me his flow and transport model of the CS-10 TCE plume at MMR, and also provided information about MT3DMS. Data for the CS-10 TCE plume at MMR was supplied by Sarah Stuart of Jacobs Engineering Group Inc. at Otis Air National Guard Base. Spence Smith of the Massachusetts Military Reservation provided information on the TCE contamination and remediation.

Two friends and former co-workers at INEL, James McCarthy and Annette Schafer, also deserve some recognition. In different ways, they were each influential in my becoming a groundwater hydrologist and in my decision to study with John Wilson.

Finally, I thank my parents, George and Mary Neupauer, and my sister, Maria Neupauer, for their constant love, support, and encouragement. Although they probably do not understand my research, they still appreciate

my dedication to it.

This research was supported by the Geophysical Research Center at New Mexico Tech, by the Hantush Fellowship from New Mexico Tech, and by the Environmental Protection Agency's STAR Fellowship program under Fellowship No. U-915324-01-0. This work has not been subjected to the EPA's peer and administrative review and therefore may not necessarily reflect the views of the Agency and no official endorsement should be inferred.

This dissertation was typeset with LaTeX[1] by the author.

[1] LaTeX document preparation system was developed by Leslie Lamport as a special version of Donald Knuth's TeX program for computer typesetting. TeX is a trademark of the American Mathematical Society. The LaTeX macro package for the New Mexico Institute of Mining and Technology dissertation format was adapted by the author from Gerald Arnold's modification of the LaTeX macro package for The University of Texas at Austin by Khe-Sing The.

TABLE OF CONTENTS

LIST OF TABLES

LIST OF FIGURES

This dissertation is accepted on behalf of the faculty of the Institute by the following committee:

John L. Wilson, Advisor

Roseanna Marie Neupauer Date

CHAPTER 1

INTRODUCTION

Environmental contaminant transport problems can be broadly divided into two categories—source-based problems and receptor-based problems. In this context, a source is defined as any contributor of contamination, such as an accidental spill or release of chemicals into an aquifer. A receptor is defined as an entity that is exposed to a contamination, such as a drinking water supply well. The distinction between source-based and receptor-based problems is based on the type of information that is known and the type of information that is desired. In a source-based problem, we are interested in the effects of one or a few contaminant sources on many potential receptors. In these types of problems, information about the source is known and information about the receptor is desired. An example of a source-based problem would be if we want to determine the concentration of a chemical in an aquifer downgradient of a spill. The source is known, and we want to determine its impact on the many possible receptors downgradient of the source. In a receptor-based problem, we are interested in the effects of many possible sources on one or a few receptors. In these problems, information is known about the receptor, and information about the source is desired. An example of a receptor-based problem would be if we detect contamination in the aquifer and want to identify the source of

contamination. In this case, the receptor is known but the source is not.

Environmental transport problems are solved using transport models. Transport models can also be classified as source-based and receptor-based. Both types of models can be used to model the same physical, chemical, and biological processes; however, the flow of information is in opposite directions. With a source-based model, the flow of information is away from the source and toward the many possible receptors; and with a receptor-based model, the flow of information is away from the receptor and back toward the many possible sources.

Environmental transport problems can be modeled with either source-based or receptor-based models. In practice, source-based modeling is much more frequently used than receptor-based modeling, regardless of whether the problem is source-based or receptor-based. However, receptor-based models are useful because they provide different information, enabling the modeler to examine preconceived ideas of system behavior from a new perspective. In addition, for certain types of problems, receptor-based models are more computationally efficient than source-based models.

This dissertation describes receptor-based modeling of groundwater contamination. If contamination is detected in an aquifer but the source of contamination is unknown, we can use receptor-based modeling to obtain information about the prior position of the detected contamination or about the travel time of the contamination from an upgradient location (possibly the source) to the detection location. The results of receptor-based modeling are location and travel time probability distributions. Location probability de-

scribes the probability distribution for the position of the detected contamination at some time in the past. It is related to the contaminant plume (resident concentration) in a source-based model. Travel time probability describes the probability distribution for the amount of time prior to detection that the contamination was at an upgradient location. It is related to the mass flux (flux concentration) of contamination in a source-based model. These probabilities can be used to improve characterization of known sources of groundwater contamination, to identify previously unknown contamination sources, to delineate capture zones, and to characterize source release times.

1.1 Background

Transport of a solute in groundwater is usually described by the advection-dispersion equation (ADE)

$$\frac{\partial C}{\partial t} = \frac{\partial}{\partial x_i}\left(D_{ij}\frac{\partial C}{\partial x_j}\right) - \frac{\partial}{\partial x_i}\left(v_i C\right) + \frac{q_I}{\theta}C_I - \frac{q_O}{\theta}C \ , \tag{1.1}$$

where $C(\mathbf{x}, t)$ is resident concentration, t is time, x_i are the spatial directions $(i = 1, 2, 3)$, $\mathbf{x} = (x_1, x_2, x_3)$, D_{ij} is the i, j^{th} entry of the dispersion tensor, v_i is the groundwater velocity in the direction of x_i, q_I is the source flow rate per unit volume, C_I is the source strength, θ is porosity, and q_O is the sink flow rate per unit volume. If the source location and release history of the contamination are specified, the solution of this equation (with its initial and boundary conditions) describes the distribution of contamination at some later time. This is a source-based model because information about the source is known or assumed to be known. Because contamination is modeled as it moves

forward in time, this model can also be called a forward model. We will use the terms "source-based model" and "forward model" interchangeably.

Concentration can be expressed in two different forms—resident concentration and flux concentration [*Kreft and Zuber*, 1978; *Parker and van Genuchten*, 1984]. Resident concentration is a measure of the mass of solute per unit volume of water, or a volume-averaged concentration. Flux concentration is a measure of the solute mass flux per unit water flux, or a flux-averaged concentration. In one dimension, the relationship between the two concentrations is [*Parker and van Genuchten*, 1984]

$$C^f = C - \frac{D}{v}\frac{\partial C}{\partial x} \tag{1.2}$$

where C^f is flux concentration. With spatially-uniform v and D, the forward ADE can be solved for either resident or flux concentration.

Location and travel time probabilities are often used in forward modeling to describe solute transport in groundwater [e.g., *Dagan*, 1982, 1987; *Jury*, 1982; *Jury and Roth*, 1990; *Chin and Chittaluru*, 1994]. Forward location probability describes the position of a solute parcel at a fixed time after its release from the source [*Dagan*, 1982, 1987, 1989; *Jury and Roth*, 1990; *Chin and Chittaluru*, 1994] and is related to resident concentration [*Dagan*, 1987; *Jury and Roth*, 1990]. The normalized concentration distribution at some time t after release from an instantaneous point source is equivalent to the location probability density function at time t, given by

$$f_{\mathbf{x}}(\mathbf{x};t) = \frac{C(\mathbf{x},t)}{\int_\Omega C(\mathbf{x},0^+)\, d\Omega}, \tag{1.3}$$

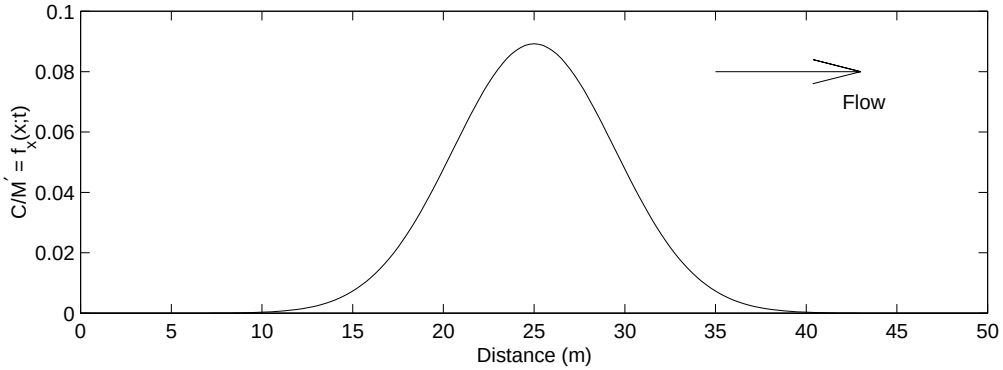

Figure 1.1: One-dimensional normalized resident concentration and location probability distributions at $t = 20$ days after release from a pulse source at $x = 5$ m. ($v = 1$ m/d, $D = 0.5$ m^2/d)

where $f_{\mathbf{x}}(\mathbf{x};t)$ is location probability at time t, $\mathbf{x}$ is the position vector, $C(\mathbf{x},t)$ is the resident concentration distribution from an instantaneous point source, Ω is the spatial domain, and $\int_\Omega C(\mathbf{x},0^+)\ d\Omega = M'$, where M' is a measure of the total mass that entered the system.

For example, Figure 1.1 shows a one-dimensional normalized resident concentration distribution at time $t = 20$ days after a pulse of contaminant is released at location $x = 5$ m. The highest concentration occurs at $x = 25$ m and the concentration is low for $x < 15$ m and $x > 35$ m. Thus, 20 days after a release from a source at $x = 5$ m, more solute parcels are found near $x = 25$ m than near the tails. This curve is also the location probability distribution, $f_x(x;t)$, for a solute parcel that was released at the source 20 days ago. Based on Figure 1.1, the most likely particle location at $t = 20$ days is $x = 25$ m.

Forward travel time probability describes the time required for a solute parcel to travel from its source to a location of interest [*Jury*, 1982; *Jury et al.*, 1986; *Dagan*, 1989; *Dagan and Nguyen*, 1989], and is related to flux

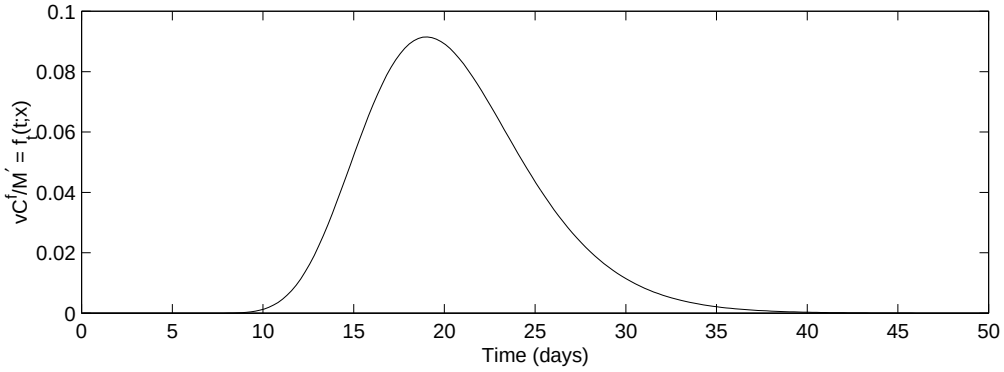

Figure 1.2: One-dimensional normalized flux concentration and travel time probability distributions at $x = 25$ m for a pulse source at $x = 5$ m. ($v = 1$ m/d, $D = 0.5$ m^2/d)

concentration [*Shapiro and Cvetkovic*, 1988; *Rubin and Dagan*, 1992]. For an instantaneous point source of contamination, the normalized flux concentration at a downgradient location, $\mathbf{x}$, is equivalent to the travel time probability density function for that location, given by

$$f_t(t;\mathbf{x}) = \frac{|v|C^f(\mathbf{x},t)}{M'} \tag{1.4}$$

for a one-dimensional domain, where $f_t(t;\mathbf{x})$ is travel time probability from the source to $\mathbf{x}$, v is the groundwater velocity, $C^f(\mathbf{x},t)$ is flux concentration, and M' is a measure of the total amount of mass that entered at the source. Figure 1.2 shows the normalized flux concentration at $x = 25$ m for an instantaneous pulse injection of contaminant from a source at $x = 5$ m. The peak concentration occurs at $t \approx 19$ days, and the concentration is very low for $t < 10$ days and for $t > 35$ days. For a single solute parcel, the travel time from the source location to location $x = 25$ m is more likely to be near $t = 19$ days and less likely

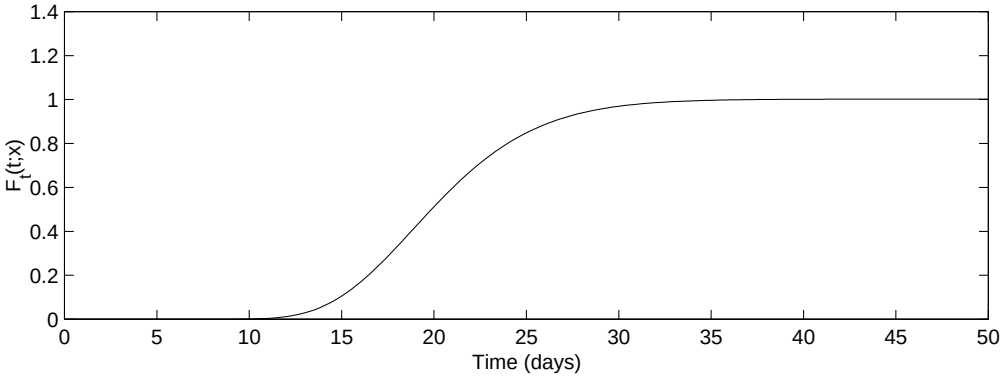

Figure 1.3: Cumulative distribution function for travel time probability at $x = 25$ m for a source at $x = 5$ m. ($v = 1$ m/d, $D = 0.5$ m^2/d)

to be near the tails. This curve is also a travel time probability distribution; thus, the most likely travel time from the source to $x = 25$ m is approximately $t = 19$ days.

The cumulative distribution of travel time probability can be expressed as

$$F_t(t; \mathbf{x}) = \int_0^t f_t(t'; \mathbf{x})\, dt'. \tag{1.5}$$

The cumulative distribution function describes the probability that a contaminant parcel traveled from its source location to a location of interest in time t or less. Figure 1.3 shows the cumulative distribution function for travel time probability at $x = 25$ m for a source at $x = 5$ m. Based on this distribution, a solute parcel released at the source at $x = 5$ m would reach the location $x = 25$ m in 35 days or less.

Since forward location and travel time probabilities are linear functions of resident and flux concentrations, respectively, these probabilities are

also governed by the forward ADE

$$\frac{\partial f}{\partial t} = \frac{\partial}{\partial x_i}\left(D_{ij}\frac{\partial f}{\partial x_j}\right) - \frac{\partial}{\partial x_i}\left(v_i f\right) - \frac{q_O}{\theta} f \ , \tag{1.6}$$

where f represents either location or travel time probability, and the source term from (1.1) was eliminated. Flux concentration is only governed by the forward ADE if v and D are spatially-uniform. Therefore, since travel time probability is related to flux concentration, (1.6) is valid for travel time probability only if v and D are spatially-uniform.

In the source-based (forward) model, we are interested in the future location of a solute parcel, so the flow of information is away from the source, i.e. in the direction of the groundwater velocity. In the receptor-based model, we are interested in the past location of a solute parcel, so the flow of information is away from the detection and back toward the (possibly unknown) source, i.e. in the opposite direction as the groundwater velocity. Because probability in the receptor-based model moves upgradient and backward in time, the receptor-based model can also be called a backward model. We will use the terms "receptor-based model" and "backward model" interchangeably.

Given a forward model, the equivalent backward probability model can be obtained heuristically by reversing the sign on the advection term to account for the reversed flow of information, and by modifying the source term, boundary conditions, and initial condition to include information about the detected solute parcel. The resulting backward location and travel time probabilities can provide information about the prior location of contamination, before it was detected in the aquifer. *Wilson and Liu* [1994], who first derived expres-

sions for backward location and travel time probabilities, used this approach. Although they heuristically obtained accurate expressions for these probabilities, no formal justification was given for the governing equation or boundary conditions. Furthermore, the heuristic approach is difficult to implement and verify for multi-dimensional problems and complex domain geometries.

In this research, we use the adjoint method as a formal approach for obtaining backward probabilities for all model domains. The adjoint method has been used in a variety of applications in groundwater modeling including sensitivity analysis [*Sykes et al.*, 1985; *Wilson and Metcalfe*, 1986], parameter estimation [*Neuman*, 1980; *Sun and Yeh*, 1985; *Townley and Wilson*, 1985; *Lu et al.*, 1988; *Sun and Yeh*, 1990; *Yeh and Sun*, 1990], optimal design [*Ahlfeld et al.*, 1988], and others (see *Sun* [1994]). Central to each of these methods is a linear functional known as a performance measure or an objective function. The performance measure is problem-specific and depends on the goal of the study. With the adjoint method, the forward governing equation (forward operator), with concentration as the dependent variable, is replaced by the adjoint equation (adjoint operator), with the adjoint state as the dependent variable. In the receptor-based model, location and travel time probability are functions of adjoint states, and the particular adjoint state depends on the definition of the performance measure. The adjoint equation models the same physical processes as the forward equation; however, the flow of information is reversed (i.e. the adjoint state is propagated backward in time).

1.2 Purpose and Scope

The main goal of this research is to develop a mathematical modeling technique that can efficiently address receptor-based problems in complex, three-dimensional, heterogeneous aquifers. We use the adjoint approach to obtain the governing equations of the backward model, and we extend the work of *Wilson and Liu* [1994, 1997] to account for multiple detections of contamination and to use the sampled concentration of the detected contamination. With this additional information, the uncertainty of the results is decreased, and the variances of the resulting location and travel time probabilities are reduced.

The method will be most useful if it can be easily applied in practice. A second goal of this research is to develop the mathematical modeling technique so that it can be solved using conventional transport codes. In this way, practitioners who are familiar with forward transport modeling software can readily perform receptor-based modeling.

The specific tasks of this research are:

- Verify that backward probabilities are related to adjoint states of resident concentration.
- Demonstrate the adjoint theory approach for obtaining the governing equations of the receptor-based model.
- Demonstrate the numerical implementation of the receptor-based model.
- Generalize the receptor-based model for multiple detections of contamination.

- Generalize the receptor-based model to use measured concentrations of the detected contamination.
- Illustrate the receptor-based modeling technique through an application at a contaminated site.

The scope of this research covers transport of contaminants in water-saturated porous media. The contaminant can be in the aqueous or sorbed phases. We do not address transport of non-aqueous phase liquids (NAPL); however, the method can be used for dissolved NAPL constituents. The aquifer may be one-dimensional or multi-dimensional; and it may be homogeneous or heterogeneous. We assume that all aquifer parameters and transport parameters are known.

1.3 Literature Review

Receptor-based models produce backward location and travel time probabilities that can be used to characterize sources of groundwater contamination. The probabilities depend on the location and time of detection of contamination in the aquifer. If contamination is detected at multiple locations, the probability distribution must be modified to account for all detections.

Travel time and location probabilities have been used extensively in forward transport modeling. In this section, we provide an overview of the use of probabilities in forward modeling. We also discuss some results of the two-particle forward transport problem. The two-particle problem, which models the relative displacement of two contaminant particles that originate from

the same source, is the forward equivalent of the multiple detection problem. Finally, we review the literature on receptor-based models and source identification.

1.3.1 Forward Location and Travel Time Probabilities

Due to the inherent uncertainty in transport parameters, it is impossible to accurately quantify contaminant transport in groundwater. The travel time approach provides a means of describing solute transport in terms of an arrival time or travel time probability.

Dagan [1982, 1984, 1987] used a Lagrangian approach to develop the location probability for the future position of a solute mass, and showed that the probability is related to resident concentration. The approach was based on stochastic theory of continuous movements, and was applied to heterogeneous porous media. *Shapiro and Cvetkovic* [1989], *Dagan* [1989] and *Dagan and Nguyen* [1989] used a Lagrangian approach to develop the travel time probability for a solute mass, and showed its relationship to the flux of solute across a control plane. *Cvetkovic and Shapiro* [1990] extended the approach to reactive solutes.

Jury [1982], *Jury et al.* [1986], and *Jury and Roth* [1990] use a transfer function approach to describe solute transport through an unsaturated soil unit. The transfer function approach obtains a relationship between the solute input at the soil surface and the solute flux at a particular depth, without modeling the details of transport within the soil unit. The transformation from the solute input to the solute outflow is described by an input response function

(transfer function) that represents the response of the system to a unit pulse input of solute at the soil surface. The transfer function is equivalent to a travel time probability of a single contaminant particle through the soil unit. This approach has been applied successfully in laboratory experiments [e.g., *Dyson and White*, 1989; *Zhang*, 1995] and field tests [e.g., *White et al.*, 1986; *Butters and Jury*, 1989].

Forward probabilities have been used in other fields, such as turbulent diffusion and fish migration. *Batchelor* [1949] theoretically showed the relationship between the location probability of a particle in a turbulent flow and the moments of probability distribution for the velocity of the particle. Using velocity covariances, he showed that the diffusion coefficient increases over time and approaches a constant value for large times. *Monin and Yaglom* [1971] and *Csanady* [1973] related the concentration of a constituent in the atmosphere to a location probability.

Zabel [1994] and *Zabel and Anderson* [1997] studied travel times of migrating juvenile salmon. They developed travel time probability distributions for migrating salmon populations, based on advection due to the river velocity, diffusion due to the random behavior of individual salmon, mortality due to long travel times, and migrational delay due to the effects of dams on the river.

1.3.2 Two-Particle Problem for the Forward Model

The basic premise of the two-particle problem for contaminant transport in groundwater is that contaminant parcels follow random paths through

the aquifer, and the random paths of two parcels originating at the same source are correlated. The contaminant plume is one realization of the many possible transport pathways; therefore, the centroid of the contaminant plume need not travel at a velocity equal to the mean groundwater velocity in the aquifer. The random spread of the plume, which is quantified by the random dispersion coefficient, is controlled by the correlation between transport paths of pairs of contaminant parcels. Much of the two-particle transport theory estimates the expected value of the dispersion coefficient, based on velocity variations and covariances.

Kitanidis [1988] and *Dagan* [1990] found that the expected value of the dispersion coefficient depends on the second spatial moment of the initial plume at the contamination source, the displacement covariance for a single parcel, and the centroid displacement covariance, which is a measure of the separation between the plume centroid from one realization and the ensemble average of the plume centroid location over all possible realizations. Several researchers [e.g. *Dagan*, 1990, 1991; *Salandin et al.*, 1991; *Rajaram and Gelhar*, 1993a, 1993b; *Zhang et al.*, 1996] studied two-particle transport in idealized flow fields and found that the one-particle dispersion coefficient generally overestimates the effective dispersion coefficient, except at large times. *Rajaram and Gelhar* [1993b] verified these results with experimental data from the Borden tracer test.

Few two-particle transport studies develop probability distributions for the future position of the contaminant parcels. *Rajaram and Gelhar* [1993b] developed an expression for the probability density function for the separation distance of particle pairs, where the spread of the distribution is related to the

velocity covariance of the particle pairs.

The two-particle transport problem in groundwater hydrology is related to the two-particle problem in turbulent diffusion. The two-particle problem has received much attention in turbulent diffusion theory because concentration fluctuations, which are affected by the separation distance of particle pairs, are important for determining reaction rates in chemical reactors, predicting air pollution, analysis of turbulent combustion, and other applications [*Durbin*, 1980]. In both turbulent diffusion and groundwater transport, the position of a moving particle is affected by a heterogeneous velocity field. The velocity variations are caused by multiple scales of turbulent eddies in turbulent flow, and by multiple scales of aquifer heterogeneity in groundwater flow.

Csanady [1973] showed that the joint displacement probability of two particles released from the same source is related to the mean product of the concentrations. *Durbin* [1980] showed that the displacement probability of two particles can be related to the random velocities of the particle pairs. These studies used a Lagrangian framework for the analyses, equivalent to the framework commonly used in the two-particle transport problem in groundwater hydrology. More recent studies of two-particle displacements in turbulent diffusion have dealt with two-particle statistics of random velocity fluctuations using Lagrangian statistical descriptions [e.g., *Borgas and Sawford*, 1994; *Pedrizzetti and Novikov*, 1994; *Pope*, 1994].

In the two-particle forward transport problem described above, the position of the two particles are assumed to be correlated. The random particle positions are caused by random velocity fluctuations in the aquifer. The relative

positions of the two particles can be quantified by the velocity covariances between the two particles.

1.3.3 Receptor-based Modeling

Receptor-based modeling has been used in groundwater hydrology to determine pumping well capture zones and to identify prior locations of contamination by using travel time and location probabilities. It has been applied to contaminant transport problems through two different approaches– random walk simulations and continuum approaches to solving the advection-dispersion equation.

Uffink [1989] used backward-in-time random walk simulations to determine capture zones around pumping wells. Capture zones are generally obtained for advective flow only, by considering travel time along streamlines. Uffink used Kolmogorov's backward equation to incorporate dispersion into the capture zone calculations and obtain a location probability density function for the initial location of possible contamination. By integrating this location probability density function over time, he obtained a type of cumulative distribution function that represents the capture zone for the well. *Chin and Chittaluru* [1994] also used a backward random walk model to identify pumping well capture zones. They obtained a backward location probability distribution using the backward random walk method, and then related this to a backward travel time distribution using an approximation to Bayes' theorem. *Bagtzoglou et al.* [1992] also used backward location probabilities to identify sources of contamination. They obtained probability maps using a random walk method,

by reversing the flow field and leaving the dispersion process unchanged.

Wilson and Liu [1994], *Liu* [1995], and *Liu and Wilson* [1995] used receptor-based modeling to identify the prior location of groundwater contamination observed in a pumping well. They used a heuristic method to obtain a backward probabilistic continuum model from the forward advection-dispersion equation, and solved it for travel time and location probabilities. The results of hypothetical test cases of a receptor-based model were verified using results from source-based modeling. They also showed that receptor-based modeling significantly reduced the computational burden. *Wilson and Liu* [1997] further tested the receptor-based model using results of a field tracer test at the Borden Site at the Canadian Forces Base, Borden, Ontario, Canada. Eight tracers were injected into fifteen injection wells upgradient of an extraction well, and tracer concentrations were measured at the extraction well. The receptor-based model was used to determine the travel time probabilities from the injection wells to the extraction well for each tracer. The model results compared well with the tracer test data, especially for tracers that were injected near the extraction well. With one simulation of the receptor-based model, breakthrough curves for all 15 injection wells were reliably predicted [*Wilson and Liu* 1997].

Liu [1995] and *Wilson and Liu* [1994] heuristically developed the backward governing equation for reactive transport processes of first-order decay, and linear equilibrium and non-equilibrium sorption. In addition, *Liu* [1995] heuristically developed a backward model for spatially-varying velocity caused by natural recharge.

Receptor-based modeling has also been applied in other fields includ-

ing atmospheric transport and oceanic transport. In atmospheric transport, receptor-based models are used to determine the principal contributors of airborne contaminants to ambient air samples by using measured concentrations at the receptors [*Daisey et al.*, 1985]. For example, *Voldner et al.* [1981] used a receptor model to estimate the flux of sulfur across the U.S.-Canadian boundary, and to determine deposition patterns of sulfur species in eastern Canada. *Small and Sampson* [1989] predicted the long-range transport and deposition of sulfur species in eastern North America by using the Atmospheric Contributions to Interregional Deposition (ACID) receptor model [*Sampson and Small*, 1984]. *Kenski et al.* [1995] used a receptor model to validate emissions inventories of volatile organic compounds in five U.S. cities. These atmospheric models share the receptor focus of this dissertation but use substantially different methods.

Holzer and Hall [2000] used adjoint theory to develop transit-time probability density functions for fluid transport in the atmosphere and in the ocean. They determine both forward and backward transit time probabilities.

1.3.4 Source History

A related problem that has received much attention in the recent literature addresses source characterization using inverse theory to reproduce the source history. Several researchers have evaluated methods for recovering the release history and plume evolution history from the present-day spatial distribution of a contaminant plume. In general, this problem is ill-posed, and sensitive to measurement errors. Although recovering the release history is not

a direct application of the method presented in this dissertation, it addresses a related source characterization problem. Source characterization is a receptor-based problem because information about the receptors is available (present-day spatial distribution of the plume) and information about the source (source history) is desired. The problem has been solved using source-based modeling with inverse theory. The inverse methods used include Tikhonov regularization [*Skaggs and Kabala* 1994, 1998; *Liu and Ball*, 1999; *Neupauer et al.*, 2000], the method of quasi-reversibility [*Skaggs and Kabala* 1995]; minimum relative entropy inversion [*Woodbury and Ulrych*, 1996, 1998; *Woodbury et al.*, 1998; *Neupauer et al.*, 2000]; and a geostatistical approach [*Snodgrass and Kitanidis*, 1997].

1.4 Organization of this Dissertation

Each chapter of the body of this dissertation is written as a paper for publication. Additional supporting material is included in the Appendix to this dissertation.

The formal adjoint approach for deriving the backward model is presented in Chapters 2 through 6. In Chapters 2 and 3, we present the adjoint approach for a one-dimensional domain, illustrating the approach using a semi-infinite domain with a pumping well at one boundary (Chapter 2) and using an infinite domain with a monitoring well receptor (Chapter 3). Chapter 2 has been published as *Neupauer and Wilson* [1999]. Chapter 4 presents an extension of the adjoint approach to address multi-dimensional problems. Chapters 2–4 deal only with conservative tracers in steady, uniform flow fields. Extensions

to non-uniform or transient flow fields and reactive solutes are presented in Chapters 5 and 6.

Chapter 7 and Appendix A address the numerical implementation of the backward model using conventional transport codes. In Chapter 7, we present the general approach for block-centered finite difference models and finite element models with two-dimensional linear triangular elements and three-dimensional linear triangular prism elements. We also present specific results for applications using MODFLOW [*McDonald and Harbaugh*, 1988] and MT3D [*Zheng*, 1990]. MODFLOW is used to produce a flow field that is used by MT3D. With the backward model, the flow field must be reversed. A Fortran code to reverse the flow field is presented in Appendix A.

In Chapters 2–7, we consider only one detection of contamination. It is realistic to expect multiple detections of contamination, in space or in time, and to have concentration measurements for the detected contamination. This additional information will result in a variance reduction of the probability distributions. In Chapter 8, the backward model is extended to account for multiple detections, and in Chapter 9, we extend the backward model to include concentration measurements.

The single-detection backward model for a pumping well detection was verified by *Wilson and Liu* [1997] at the Borden Site. In Chapter 10, we present another application of the backward model. Finally, Chapter 11 contains conclusions of this research and recommendations for future work.

References

Ahlfeld, D.P., J.M. Mulvey, and G.F. Pinder, Contaminated groundwater remediation design using simulation, optimization, and sensitivity theory, 1, Model development, *Water Resour. Res.*, 24(3), 431–441, 1988.

Bagtzoglou, A.C., D.E. Dougherty, and A.F.B. Thompson, Application of particle methods to reliable identification of groundwater pollution sources, *Water Resources Management*, 6, 15–23, 1992.

Batchelor, G.K., Diffusion in a field of homogeneous turbulence, I, Eulerian analysis, *Austral. J. Sci. Res.*, 2, 437–450, 1949.

Borgas, M.S. and B.L. Sawford, A family of stochastic models for two-particle dispersion in isotropic homogeneous stationary turbulence, *J. Fluid Mech.*, 279, 69–99, 1994.

Butters, G.L. and W.A. Jury, Field scale transport of bromide in an unsaturated soil, 2, Dispersion modeling, *Water Resour. Res.*, 25(7), 1583–1589, 1989.

Chin, D.A. and P.V.K. Chittaluru, Risk management in wellhead protection, *J. Water Resour. Plan. Manage.*, 120(3), 294–315. 1994.

Csanady, G.T., *Turbulent Diffusion in the Environment*, D. Reidel Publishing Company, Boston, Mass., 1973.

Cvetkovic, V. and A.M. Shapiro, Mass arrival of sorptive solute in heterogenous porous media, *Water Resour. Res.*, 26(9), 2057–2067, 1990.

Dagan, G., Stochastic modeling of groundwater flow by unconditional and conditional probabilities, 2, The solute transport, *Water Resour. Res.*,

18(4), 835–848, 1982.

Dagan, G., Solute transport in heterogeneous formations, *J. Fluid Mech.*, 145, 151-177, 1984.

Dagan, G., Theory of solute transport by groundwater, *Ann. Rev. Fluid Mech.*, 19, 183–215, 1987.

Dagan, G., *Flow and Transport in Porous Formations*, Springer-Verlag, New York, 1989.

Dagan, G., Transport in heterogeneous porous formations: spatial moments, ergodicity, and effective dispersion, *Water Resour. Res.*, 26(6), 1281–1290, 1990.

Dagan, G., Dispersion of a passive solute in non-ergodic transport by steady velocity fields in heterogeneous formation, *J. Fluid Mech.*, 233, 197–210, 1991.

Dagan, G., and V. Nguyen, A comparison of travel time and concentration approaches to modeling transport by groundwater, *J. Contam. Hydrol.*, 4, 79–91, 1989.

Daisey, J.M., P.J. Lioy, and T.J. Kneip, *Receptor Models For Airborne Organic Species*, U.S. Environmental Protection Agency, Atmospheric Sciences Research Laboratory, Research Triangle Park, NC, 1985.

Durbin, P.A., A stochastic model of two-particle dispersion and concentration fluctuations in homogeneous turbulence, *J. Fluid Mech.* 100(2), 279–302, 1980.

Dyson, J.S. and R.E. White, A simple predictive approach to solute transport

in layered soils, *J. Soil Sci.*, 40, 525–542, 1989.

Holzer, M., and T.M. Hall, Transit-time and tracer-age distributions in geophysical flows, *J. Atmos. Sci.*, in press, 2000.

Jury, W.A., Simulation of solute transport using a transfer function model, *Water Resour. Res.*, 18(2), 363–368, 1982.

Jury, W.A., G. Sposito, and R.E. White, A transfer function model of solute transport through soil, 1, Fundamental concepts, *Water Resour. Res.*, 22(2), 243–247, 1986.

Jury, W.A. and K. Roth, *Transfer Functions and Solute Movement through Soil: Theory and Applications*, Birkhauser, Boston, 1990.

Kenski, D.M., R.A. Wadden, P.A. Scheff, and W.A. Lonneman, Receptor modeling approach to VOC emission inventory validation, *J. Envir. Engng.*, 121(7), 483–491, 1995.

Kitanidis, P.K., Prediction by the method of moments of transport in a heterogeneous formation, *J. Hydrol.*, 102, 453–473, 1988.

Kreft, A. and A. Zuber, On the physical meaning of the dispersion equation and its solutions for different initial and boundary conditions, *Chem. Eng. Sci.*, 33, 1471–1480, 1978.

Liu, C. and W.P. Ball, Application of inverse methods to contaminant source identification from aquitard diffusion profiles at Dover AFB, Delaware, *Water Resour. Res.*, 35(7), 1975–1985, 1999.

Liu, J., *Travel time and location probabilities for groundwater contaminant sources*, Master's thesis, New Mexico Institute of Mining and Tech-

nology, Socorro, 1995.

Liu, J. and J.L. Wilson, Modeling travel time and source location probabilities in two-dimensional heterogeneous aquifer. *Proceedings 5th Annual WERC Technology Development Conference*, New Mexico State University, Las Cruces, New Mexico, 59–67, 1995.

Lu, A.H., F. Schmittroth, and W.W.-G. Yeh, Sequential estimation of aquifer parameters, *Water Resour. Res.*, 24(5), 670–682, 1988.

McDonald, M.G. and A.W. Harbaugh, *A Modular Three-Dimensional Finite-Difference Groundwater Flow Model*, U.S. Geological Survey Techniques of Water-Resources Investigations, Book 6, Chapter A1, 1988.

Monin, A.S. and A.M. Yaglom, *Statistical Fluid Mechanics*, vol. 1, MIT Press, Cambridge, Mass., 1971.

Neuman, S.P., A statistical approach to the inverse problem of aquifer hydrology, 3, Improved solution method and added perspective, *Water Resour. Res.*, 16(2), 331–346, 1980.

Neupauer, R.M. and J.L. Wilson, Adjoint method for obtaining backward-in-time location and travel time probabilities of a conservative groundwater contaminant, *Water Resour. Res.*, 35(11), 3389–3398, 1999.

Neupauer, R.M., B. Borchers, and J.L. Wilson, Comparison of inverse methods for reconstructing the release history of a groundwater contamination source, *Water Resour. Res.*, 36(9), 2469–2475, 2000.

Parker, J.C. and M. Th. van Genuchten, Flux-averaged and volume-averaged concentrations in continuum approaches to solute transport, *Water*

Resour. Res., 20(7), 866–872, 1984.

Pedrizzetti, G. and E.A. Novikov, On Markov modelling of turbulence, *J. Fluid Mech.*, 280, 69–93, 1994.

Pope, S.B., Lagrangian PDF methods for turbulent flows, *Ann. Rev. Fluid Mech.*, 26, 23–63, 1994.

Rajaram, H. and L.W. Gelhar, Plume scale-dependent dispersion in heterogeneous aquifers, 1, Lagrangian analysis in a stratified aquifer, *Water Resour. Res.*, 29(9), 3249–3260, 1993a.

Rajaram, H. and L.W. Gelhar, Plume scale-dependent dispersion in heterogeneous aquifers, 2, Eulerian analysis and three-dimensional aquifers, *Water Resour. Res.*, 29(9), 3261–3276, 1993b.

Rubin, Y. and G. Dagan, Conditional estimation of solute travel time in heterogeneous formations: impact of transmissivity measurements, *Water Resour. Res.*, 28(4), 1033–1040, 1992.

Salandin, P., A. Rinaldo, and G. Dagan, A note on transport in stratified formations by flow tilted with respect to bedding, *Water Resour. Res.*, 27(11), 3009–3017, 1991.

Sampson, P.J. and M.J. Small, Atmospheric trajectory models for diagnosing the sources of acid precipitation, in *Acid Precipitation, Vol. 9: Modeling of Total Acid Precipitation Impacts*, J.L. Schnoor, ed., Butterworth Publishers, Boston, 1–23, 1984.

Shapiro, A.M. and V.D. Cvetkovic, Stochastic analysis of solute arrival time in heterogeneous porous media, *Water Resour. Res.*, 24(10), 1711–1718,

1988.

Skaggs, T.H. and Z.J. Kabala, Recovering the release history of a groundwater contaminant, *Water Resour. Res.*, 30(1), 71–79, 1994.

Skaggs, T.H. and Z.J. Kabala, Recovering the history of a groundwater contaminant plume: Method of quasi-reversibility, *Water Resour. Res.*, 31(11), 2669–2673, 1995.

Skaggs, T.H. and Z.J. Kabala, Limitations in recovering the history of a groundwater contaminant plume, *J. Contam. Hydrol.*, 33, 347–359, 1998.

Small, M.J. and P.J. Sampson, Stochastic simulation of meteorological variability for long-range atmospheric transport, 1, Dynamic Lagrangian models, *Atmos. Environ.*, 23(12), 2813–2824, 1989.

Snodgrass, M.R. and P.K. Kitanidis, A geostatistical approach to contaminant source identification, *Water Resour. Res.*, 33(4), 537–546, 1997.

Sun, N.-Z., *Inverse Problems in Groundwater Modeling*, Kluwer Academic Publishers, Boston, 1994.

Sun, N.-Z. and W.W.-G. Yeh, Identification of parameter structure in groundwater inverse problems, *Water Resour. Res.*, 21(6), 869–883, 1985.

Sun, N.-Z. and W.W.-G. Yeh, Coupled inverse problems in groundwater modeling, 1, Sensitivity analysis and parameter identification, *Water Resour. Res.*, 26(10), 2507–2525, 1990.

Sykes, J.F., J.L. Wilson, and R.W. Andrews, Sensitivity analysis for steady state groundwater flow using adjoint operators, *Water Resour. Res.*, 21(3), 359–371, 1985.

Townley, L.R. and J.L. Wilson, Computationally efficient algorithms for parameter estimation and uncertainty propagation in numerical models of groundwater flow, *Water Resour. Res.*, 21(12), 1851–1860, 1985.

Uffink, G.J.M., Application of Kolmogorov's backward equation in random walk simulations of groundwater contaminant transport, in *Contaminant Transport in Groundwater*, H.E. Kobus and W. Kinzelbach, editors, pp. 283–289, A.A. Balkema, Brookfield, Vt., 1989.

Voldner, E.C., M.P. Olson, K. Oikawa, and M. Loiselle, Comparison between measured and computed concentrations of sulphur compounds in Eastern North America, *J. Geophys. Res.*, 86(C6), 5339–5346, 1981.

White, R.E., J.S. Dyson, R.A. Haigh, W.A. Jury, and G. Sposito, A transfer function model of solute transport through soil, 2, Illustrative applications, *Water Resour. Res.*, 22(2), 248–254, 1986.

Wilson, J.L. and J. Liu, Backward tracking to find the source of pollution, in *Waste-management: From Risk to Remediation*, edited by R. Bhada *et al.*, ECM Press, Albuquerque, NM, 181–199, 1994.

Wilson, J.L. and J. Liu, Field Validation of the Backward-in-time Advection Dispersion Theory. *Proceedings of the 1996 HSRC/WERC Joint Conf. on the Environment*, Great Plains-Rocky Mountain Hazardous Substance Center, Manhattan, Kansas, http://www.engg.ksu.edu/HSRC/ 96Proceed/wilson.html, 1997.

Wilson, J.L. and D.E. Metcalfe, Illustration and verification of adjoint sensitivity theory for steady state groundwater flow, *Water Resour. Res.*, 21(11), 1602–1610, 1985.

Woodbury, A.D. and T.J. Ulrych, Minimum relative entropy inversion: Theory and application to recovering the release history of a groundwater contaminant, *Water Resour. Res.*, 32(9), 2671–2681, 1996.

Woodbury, A.D. and T.J. Ulrych, Minimum relative entropy and probabilistic inversion in groundwater hydrology, *Stochastic Hydrol. Hydraul.*, 12, 317–358, 1998.

Woodbury, A.D., E. Sudicky, T.J. Ulrych, and R. Ludwig, Three-dimensional plume source reconstruction using minimum relative entropy inversion, *J. Contam. Hydrol.*, 32, 131–158, 1998.

Yeh, W.W.-G. and N.-Z. Sun, Variational sensitivity analysis, data requirements, and parameter identification in a leaky aquifer system, *Water Resour. Res.*, 26(9), 1927–1938, 1990.

Zabel, R.W., Spatial and temporal models of migrating juvenile salmon with application, Doctoral dissertation, University of Washington, Seattle, Washington, 1994.

Zabel, R.W. and J.J. Anderson, A model of the travel time of migrating juvenile salmon, with an application to Snake River spring chinook salmon, *North Am. J. Fish. Manage.*, 17, 93–100, 1997.

Zhang, R., Prediction of solute transport using a transfer function model and the convection-dispersion equation, *Soil Sci.*, 160(1), 18–27, 1995.

Zhang, Y.-K., D. Zhang, and J. Lin, Nonergodic solute transport in three-dimensional heterogeneous isotropic aquifers, *Water Resour. Res.*, 32(9), 2955-2963, 1996.

Zheng, C., *MT3D: A Modular Three-Dimensional Transport Model for Simulation of Advection, Dispersion and Chemical Reactions of Contaminants in Groundwater Systems*, Report to the U.S. Environmental Protection Agency, Ada, Oklahoma, 170 pp., 1990.

CHAPTER 2

ADJOINT METHOD FOR OBTAINING ONE-DIMENSIONAL BACKWARD PROBABILITY MODELS[1]

Abstract

Backward location and travel time probabilities can be used to determine the prior location of contamination in an aquifer. For a contaminant particle that was detected in an aquifer, the backward location probability is the probability of where the particle was located at some prior time. Backward travel time probability is the probability of when the particle was located at some position upgradient of the detection. These probabilities can be used to improve characterization of known sources of groundwater contamination, to identify previously unknown contamination sources, and to delineate capture zones. For simple model domains, backward probabilities can be obtained heuristically from a forward model of contaminant transport. For multidimensional problems and complex domain geometries, the heuristic approach is difficult to implement and verify. The adjoint method provides a formal approach for obtaining backward probabilities for all model domains and geometries. We formally show that the backward model probabilities are adjoint states of resident concentration. We provide a methodology for obtaining the governing equations and boundary and final conditions for these probabilities. The approach is illustrated using a one-dimensional, semi-infinite domain that

[1]This chapter has appeared in *Water Resources Research*: Neupauer, R.M. and J.L. Wilson, Adjoint method for obtaining backward-in-time location and travel time probabilities of a conservative groundwater contaminant, *Water Resourc. Res.*, 35(11), 3389–3398, 1999.

mimics flow to a production well, and these results are compared to equivalent probabilities derived heuristically.

2.1 Introduction

Transport of a conservative solute in groundwater is usually described by the advection-dispersion equation (ADE). Solutions of the ADE express solute concentration as a function of location and time, for all times after the initial release of the solute. This form of the ADE is a forward-in-time model because we track the solute as it moves forward in time.

Concentration can be expressed in two different forms—resident concentration and flux concentration [*Kreft and Zuber*, 1978; *Parker and van Genuchten*, 1984]. Resident concentration is a measure of the mass of solute per unit volume of water, or a volume-averaged concentration. Flux concentration is a measure of the solute mass flux per unit water flux, or a flux-averaged concentration. The forward-in-time (forward) ADE can be solved for either resident or flux concentration.

The forward ADE can also be used to solve for location probability and travel time probability. If we consider an individual solute parcel that was released from the contaminant source, then the location probability of that parcel is the probability that it is located at a given position in space at some later time [*Dagan*, 1989; *Jury and Roth*, 1990; *Chin and Chittaluru*, 1994]. Location probability is related to resident concentration [*Jury and Roth*, 1990]. Resident concentration measures the mass of solute at a given location in space at a snapshot in time. If the resident concentration measurements are normalized by the total mass of solute in the system, the resulting distribution

is the percentage of the total mass that is at a given location in space. Suppose we are interested in the present location of one parcel of mass that was input at the source. The parcel is more likely to be found at a location that has a high solute concentration (or, equivalently, a high normalized solute concentration) than a location that has a low solute concentration. Thus, at any point in time, the normalized concentration distribution is equivalent to a probability density function for the location of the parcel (i.e. location probability). Note that for a unit source, the resulting resident concentration is equal to the location probability.

If we again consider an individual solute parcel that was released from the contaminant source, then the travel time probability of that parcel is the probability that it will arrive at a fixed location after a given amount of time has elapsed [*Jury*, 1982; *Chin and Chittaluru*, 1994]. Travel time probability is related to flux concentration [*Jury*, 1982]. Flux concentration measures the mass of solute passing through a fixed location in space over a finite time interval. Mass flux can be expressed as the product of flux concentration and groundwater velocity. In a one-dimensional system, the entire mass of a conservative solute must eventually pass through every point downstream of the source. For a given location downstream of the source, if the mass flux is normalized by the total mass released from the source, the resulting distribution shows the percentage of the total mass that passes the given location in any finite time interval. Suppose we are interested in determining when one parcel of mass that was input at the source will reach a given location. This parcel is more likely to reach the given location when the flux concentration (or normalized mass flux) is high rather than when it is low. Therefore, for a solute

parcel traveling from the source to any given location, the normalized mass flux distribution is equivalent to the travel time probability density function. Since these forward-in-time probabilities are equivalent to normalized concentrations, the forward ADE can also be solved for location and travel time probabilities.

In this discussion, the probabilities have been defined from the point of view of the contaminant source, i.e. they are probabilities for a solute parcel that originated at the contaminant source. Suppose we detect contaminant in the groundwater, but its prior location and source is unknown. We can use a backward-in-time version of the ADE to solve for the prior location probability of the detected solute parcel, and also for the travel time probability of the detected solute parcel from some upgradient location to the detection location [*Wilson and Liu*, 1995]. These probabilities can be used to improve characterization of known sources of groundwater contamination, to identify previously unknown contamination sources, and to delineate capture zones. A related problem that has received much attention recently is a deterministic problem in which the release history of a contamination source is reconstructed from the present position of the contamination plume (e.g. *Skaggs and Kabala* [1994]). In the source history reconstruction problem, the source location is assumed to be known; while the problem presented here can be used to obtain information about the locations of unknown sources.

In the forward model, we are interested in where the solute parcel is going, so the flow of information is away from the source, i.e. in the direction of the groundwater velocity. In the backward model, we are interested in where the solute parcel has been, so the flow of information is away from the detection and back toward the (possibly unknown) source, i.e. in the opposite

direction as the groundwater velocity. Given a forward model, the equivalent backward probability model can be obtained heuristically by reversing the sign on the advection term to account for the reversed flow of information, and by modifying the source term, boundary conditions, and initial condition to include information about the detected solute parcel. Although the dispersion coefficient is a function of velocity, no sign reversal is performed on the dispersion term. Dispersion is proportional to the magnitude of velocity; therefore reversing the direction of velocity does not affect the sign on the dispersion coefficient. The resulting backward-in-time location and travel time probabilities can provide information about the prior location of contamination, before it was detected in the aquifer. *Wilson and Liu* [1995], who first derived expressions for backward-in-time location and travel time probabilities, used this approach. Although they heuristically obtained accurate expressions for these probabilities (as demonstrated in our Figure 2.1), no formal justification was given for the governing equation or boundary conditions. Furthermore, the heuristic approach is difficult to implement and verify for multi-dimensional problems and complex domain geometries.

Bagtzoglou et al. [1992] also used backward location probabilities to identify sources of contamination. They obtained probability maps using a random walk method, by reversing the flow field and leaving the dispersion process unchanged. *Uffink* [1989] used a similar random walk approach to delineate capture zones around pumping wells.

We propose the adjoint method as a formal approach for obtaining backward probabilities for all model domains. The adjoint method has been used in a variety of applications in groundwater modeling including sensitivity

analysis [*Sykes et al.*, 1985; *Wilson and Metcalfe*, 1985], parameter estimation [*Neuman*, 1980; *Sun and Yeh*, 1985; *Townley and Wilson*, 1985; *Lu et al.*, 1988; *Sun and Yeh*, 1990; *Yeh and Sun*, 1990], optimal design [*Ahlfeld et al.*, 1988], and others (see *Sun* [1994]). Central to each of these methods is a linear functional known as a performance measure or an objective function. The performance measure is problem-specific and depends on the goal of the study. For example, in their sensitivity analysis, *Sykes et al.* [1985] defined one of their performance measures to be piezometric head at a point in an aquifer, and then used the adjoint method to determine sensitivity of this performance measure to the model boundary conditions. *Sun and Yeh* [1985], in a parameter estimation problem, defined their performance measure to be the sum of the squared differences between measured and modeled piezometric head values. They used the adjoint method to determine the sensitivity of this performance measure to the aquifer transmissivity values, and then used these results to find the optimal values.

With the adjoint method, the forward governing equation (forward operator), with concentration as the dependent variable, is replaced by the adjoint equation (adjoint operator), with the adjoint state as the dependent variable. The adjoint state is a function that describes the marginal change in the performance measure due to a unit injection of mass at any point in the system, as we will illustrate later. A different adjoint state can be defined for each performance measure. The adjoint equation models the same physical processes as the forward equation; however, the flow of information is reversed (i.e. the adjoint state is propagated backward in time). A Green's function is an example of an adjoint state.

In this paper, we show that backward-in-time location and travel time probabilities are adjoint states of forward-in-time resident concentration. We provide a methodology for obtaining the governing equations and boundary and initial conditions for these probabilities and show that they are equivalent to those derived by *Wilson and Liu* [1995]. The illustration is shown for a one-dimensional, semi-infinite domain. Although one-dimensional flow and transport is highly idealized, it is equivalent to the domain used by *Wilson and Liu* [1995], and after the methodology has been developed and verified for a one-dimensional system, we can easily extend it to multiple dimensions. The one-dimensional, semi-infinite domain represents flow and transport to a production well. The production well is the driving force for flow, and acts as a sink of water and solute. The adjoint approach can be applied to other domains, such as an infinite domain with an interior monitoring well or weak production well as a detection mechanism. In these infinite domain scenarios, the driving force for flow would be a prescribed velocity field.

In the next section, we present forward models for resident and flux concentration, and we show the relationship between these models and the corresponding forward probabilities. The backward models for location and travel time probabilities are developed heuristically from the forward probability models, following the work of *Wilson and Liu* [1995] and *Liu* [1995]. In the subsequent section, a general form of the adjoint equation is derived. It is then applied to the semi-infinite domain to derive two different adjoint states, one representing location probability and the other representing travel time probability. We show that these probabilities are equivalent to the backward model probabilities that were developed heuristically by *Wilson and Liu* [1995].

2.2 One-Dimensional Contaminant Transport

In this section, solutions to the advection-dispersion equation are described for resident and flux concentration in a one-dimensional system, for an instantaneous point source of contaminant. Using these equations, expressions are developed for location and travel time probabilities for both forward and backward models.

Wilson and Liu [1995] developed expressions for backward-in-time location and travel time probabilities in a one-dimensional, semi-infinite domain. In that work, the domain extended from $0 \leq x < \infty$, with a pumping well (detection mechanism) at $x = 0$ and an instantaneous point source of contaminant at $x_o > 0$. Thus, the velocity was in the direction of $-x$. The equations presented here are taken from *Wilson and Liu* [1995]; however, in this work, the domain extends from $-\infty < x \leq 0$, and velocity is moving in the $+x$ direction. The pumping well is still located at $x = 0$, and the instantaneous point source of contaminant is at $x_o < 0$.

2.2.1 Forward Model

Contaminant transport in a one-dimensional, semi-infinite domain is described by the following form of the advection-dispersion equation

$$\frac{\partial C^r}{\partial t} = \frac{\partial}{\partial x}\left(D\frac{\partial C^r}{\partial x}\right) - \frac{\partial\left(vC^r\right)}{\partial x} \tag{2.1}$$
$$C^r \to 0 \text{ as } x \to -\infty$$
$$\frac{\partial C^r}{\partial x} = 0 \text{ at } x = 0$$
$$C^r(x,0) = \frac{M}{A\theta}\delta(x - x_o)$$

where C^r is resident concentration, D is the dispersion coefficient, v is groundwater velocity, x is the spatial dimension, t is time, M is total source mass, A is cross-sectional area, θ is porosity, $\delta(x)$ is the Dirac delta function, and x_o is the source location ($x_o < 0$). The boundary at $x = 0$ represents a pumping well. The boundary condition specifies that the concentration inside the well bore is equal to the concentration of the fluid in the porous media immediately adjacent to the well bore. Although this might not be exact, it is mathematically convenient and an accepted boundary condition at a pumping well (e.g. *Chen and Woodside* [1988]).

Wilson and Liu [1995] derived the solution to this problem, for constant v and D:

$$\begin{aligned} C^r(x,t) \;=\; & \frac{1}{\sqrt{4\pi Dt}}\frac{M}{A\theta}\exp\left\{-\frac{(x - x_o - vt)^2}{4Dt}\right\}\left[1 + \exp\left\{\frac{-x_o x}{Dt}\right\}\right] \\ & -\frac{v}{2D}\frac{M}{A\theta}\exp\left\{\frac{-vx_o}{D}\right\}\operatorname{erfc}\left[\frac{-x - x_o + vt}{\sqrt{4Dt}}\right]. \end{aligned} \tag{2.2}$$

By normalizing resident concentration by the total mass in the system,

we obtain the following expression for location probability, $f_x(x;t)$;

$$f_x(x;t) = \frac{C^r(x,t)}{\int_{-\infty}^{0} C^r(x,t)\, dx} \; . \tag{2.3}$$

The integral in the denominator evaluates to $M/A\theta$, which can be obtained by integrating (2.2). Alternatively, we see from (2.1) that there are no internal sources or sinks of contamination, and the contaminant is non-reactive; therefore, mass is conserved. In other words, the total mass in the system at any time is equal to the total mass in the system at the initial time. Since $C^r(x,0) = (M/A\theta)\delta(x - x_o)$ where $-\infty < x_o \leq 0$, the total mass in the system at any time is $\int_{-\infty}^{0} C^r(x,0)dx = M/A\theta$; so location probability in (2.3) is equal to $C^r/(M/A\theta)$, and

$$\begin{aligned} f_x(x;t) \;\; = \;\; & \frac{1}{\sqrt{4\pi Dt}} \exp\left\{-\frac{(x - x_o - vt)^2}{4Dt}\right\}\left[1 + \exp\left\{\frac{-x_o x}{Dt}\right\}\right] \\ & -\frac{v}{2D}\exp\left\{\frac{-vx_o}{D}\right\}\mathrm{erfc}\left[\frac{-x - x_o + vt}{\sqrt{4Dt}}\right] \; . \end{aligned} \tag{2.4}$$

This equation could also be obtained by solving (2.1), replacing C^r with f_x, and using the initial condition $f_x(x;0) = \delta(x - x_o) = C^r(x,0)/(M/A\theta)$.

Figure 2.1a shows plots of resident concentration and location probability as a function of position for three different times, $t = 1$, 20, and 50 (dimensionless units). The source location is at $x_o = -100$. Other parameter values are $v = 1.0$, $D = 5.0$, $M = 1.0$, $A = 1.0$, and $\theta = 0.25$. These parameter values were used for all plots in Figure 2.1. A high value of the dispersion coefficient was used to illustrate the effects of dispersion. The left-hand axis represents resident concentration, and the right-hand axis represent location

probability (resident concentration normalized by $M/A\theta = 4.0$).

Flux concentration is related to resident concentration as follows [*Parker and van Genuchten*, 1984]

$$C^f = C^r - \frac{D}{v}\frac{\partial C^r}{\partial x} \tag{2.5}$$

where C^f is flux concentration. For the semi-infinite domain described above, the gradient of C^r at $x = 0$ is zero; therefore, at the pumping well ($x = 0$), flux concentration is equal to resident concentration [*Wilson and Liu*, 1995]

$$C^f(0,t) = \frac{1}{\sqrt{\pi D t}}\frac{M}{A\theta}\exp\left\{-\frac{(x_o + vt)^2}{4Dt}\right\} - \frac{v}{2D}\frac{M}{A\theta}\exp\left\{\frac{-vx_o}{D}\right\}\operatorname{erfc}\left[\frac{-x_o + vt}{\sqrt{4Dt}}\right] . \tag{2.6}$$

Normalizing flux concentration by the total mass in the system results in the following expression for travel time probability, $f_t(t;x)$, for transport from the source to the well:

$$f_t(t;x) = \frac{vC^f(x,t)}{\int_0^\infty vC^f(x,t)\,dt} . \tag{2.7}$$

Integrating the first term in (2.6) over the time domain yields $(2/v)(M/A\theta)$ (*Abramowitz and Stegun* [1972], eqn. 29.3.84), and integrating the second term in (2.6) yields $-(1/v)(M/A\theta)$ (*Abramowitz and Stegun* [1972], eqn. 7.4.21); thus, the integral in the denominator of (2.7) evaluates to $M/A\theta$. The travel

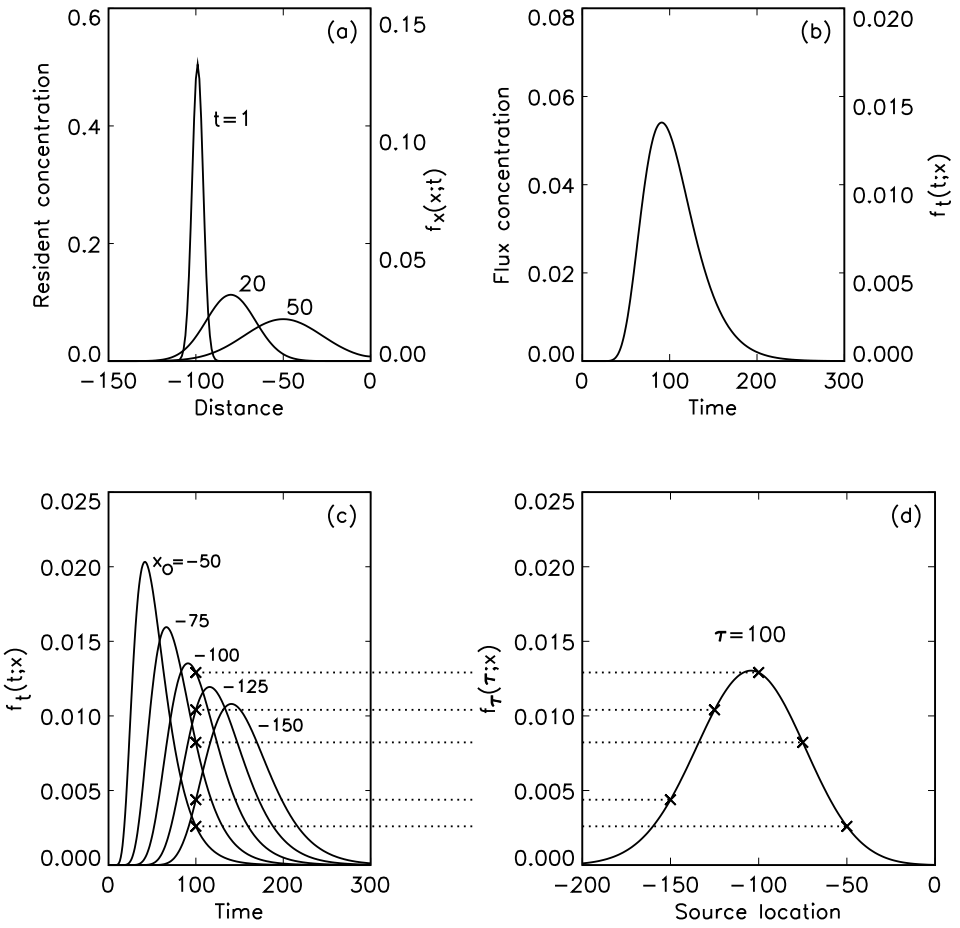

Figure 2.1: Plots of location and travel time probability, similar to plots presented in *Wilson and Liu* [1995]. (a) Plot of resident concentration and forward location probability for a contamination source at $x_o = -100$ for three times. (b) Plot of flux concentration at the pumping well (at $x = 0$) and forward travel time probability to the pumping well for a contamination source at $x_o = -100$. (c) Plot of forward travel time probability to the pumping well for five different contamination source locations. The cross denotes the probability that $t = 100$ for each source location. (d) Plot of backward travel time probability from the pumping well, showing the probability that $\tau = 100$ for all possible source locations. The cross denotes $f_\tau(\tau; x)$ for the source locations in (c).

time probability is equal to $vC^f/(M/A\theta)$, and

$$f_t(t;0) = \frac{v}{\sqrt{\pi D t}} \exp\left\{-\frac{(x_o + vt)^2}{4Dt}\right\} - \frac{v^2}{2D} \exp\left\{\frac{-vx_o}{D}\right\} \operatorname{erfc}\left[\frac{-x_o + vt}{\sqrt{4Dt}}\right] . \quad (2.8)$$

Figure 2.1b shows a plot of flux concentration and travel time probability at the pumping well at $x = 0$, as a function of time, for contamination from a source at location $x_o = -100$. The left-hand axis represents flux concentration, and the right-hand axis represent travel time probability (flux concentration normalized by $M/A\theta = 4.0$).

2.2.2 Backward Model

For constant D and v, *Wilson and Liu* [1995] showed that the backward model for location probability can be obtained by solving the following equation

$$\begin{aligned} \frac{\partial f_x}{\partial \tau} &= D\frac{\partial^2 f_x}{\partial x^2} + v\frac{\partial f_x}{\partial x} \\ f_x &\to 0 \text{ as } x \to -\infty \\ v f_x + D\frac{\partial f_x}{\partial x} &= 0 \text{ at } x = 0 \\ f_x(x;0) &= \delta(x - x_d) \end{aligned} \quad (2.9)$$

where τ is backward time ($\tau = t_d - t$, where t_d is the detection time), and x_d is the detection location, which here is the location of the pumping well at $x_d = 0$. The solution to this equation is the backward-in-time location probability for

a detection at $x_d = 0$, and is given by [*Wilson and Liu*, 1995]

$$f_x(x;\tau) = \frac{1}{\sqrt{\pi D\tau}} \exp\left\{-\frac{(x+v\tau)^2}{4D\tau}\right\} - \frac{v}{2D}\exp\left\{\frac{-vx}{D}\right\} \operatorname{erfc}\left[\frac{-x+v\tau}{\sqrt{4D\tau}}\right] . \quad (2.10)$$

For a contaminant parcel removed at the pumping well ($x_d = 0$), this equation describes the probability density function of the location of the contaminant parcel at time τ before it was observed at the pumping well. *Wilson and Liu* [1995] also showed that the backward model for travel time probability can be obtained by solving

$$\begin{aligned} \frac{\partial f_\tau}{\partial \tau} &= D\frac{\partial^2 f_\tau}{\partial x^2} + v\frac{\partial f_\tau}{\partial x} \\ f_\tau &\to 0 \quad \text{as} \quad x \to -\infty \\ vf_\tau + D\frac{\partial f_\tau}{\partial x} &= v\delta(\tau) \quad \text{at} \quad x = 0 \\ f_\tau(x;0) &= 0 \end{aligned} \quad (2.11)$$

where D and v are constant, and the pumping well is assumed to be at $x_d = 0$. The solution to this equation is the backward-in-time travel time probability from location x to a detection at $x_d = 0$ [*Wilson and Liu*, 1995].

$$f_\tau(\tau;x) = \frac{v}{\sqrt{\pi D\tau}} \exp\left\{-\frac{(x+v\tau)^2}{4D\tau}\right\} - \frac{v^2}{2D}\exp\left\{\frac{-vx}{D}\right\} \operatorname{erfc}\left[\frac{-x+v\tau}{\sqrt{4D\tau}}\right] . \quad (2.12)$$

For a contaminant parcel removed at the pumping well, this equation describes the probability density function of the travel time from some upgradient location x to the pumping well at $x_d = 0$.

Figures 2.1c and d provide an illustration of the relationship between

forward and backward travel-time-probability. Figure 2.1c shows the forward travel time probability from many source locations to the pumping well at $x = 0$. For a travel time of $t = 100$, the travel time probability is denoted with a cross. For a backward time of $\tau = 100$, Figure 2.1d shows the backward travel time probability from the pumping well for all possible source locations. The source locations corresponding to those shown in Figure 2.1c are indicated with a cross. These plots show that the backward probabilities can be obtained from the multiple forward probabilities; however more simulations are needed (one for each possible source location) and less information is obtained (probability is only obtained for a finite number of source locations).

2.3 Derivation of Adjoint Equations

A common application of the adjoint method [*Marchuk et al.*, 1996] in groundwater hydrology is sensitivity analysis (e.g. *Sykes et al.* [1985]; *Wilson and Metcalfe* [1985]; *Sun and Yeh* [1990]), often in the context of an inverse problem. Sensitivity analysis is used to determine the sensitivity of the state of the system (model output) to changes in parameter values (model input). The direct method of performing a sensitivity analysis is to vary the input parameter slightly, rerun the model, and determine the effect on the model output. This method requires one simulation for each parameter. The adjoint method offers a more efficient approach in which the adjoint equation is solved once, and then the result is used to directly compute the sensitivity of the state of the system to all parameters.

Although we are not interested in performing a sensitivity analysis,

we follow the sensitivity analysis approach to obtain the adjoint equation. In this section, the general adjoint equation is derived for the advection-dispersion equation. Then, the derivation is applied to location and travel time probabilities in a semi-infinite domain. By first developing the general adjoint equation, we can adapt the results to address other model domains, such as the infinite domain problem, which could simulate flow and transport through an observation well.

2.3.1 General Adjoint Equation

The adjoint of the advection-dispersion equation (ADE) is developed here following the sensitivity analysis approach of *Sykes et al.* [1985] (see also *Sun and Yeh* [1990]; *Sun* [1994]). In sensitivity analysis, a performance measure is defined that quantifies the state of the system. The goal is to determine the marginal sensitivity of this performance measure to small changes in parameter values. In this section, the adjoint equation is first derived for the advection-dispersion equation using a general performance measure.

The performance measure, P, that quantifies the state of the system can be expressed as

$$P = \iint_{x,t} h(\alpha, C)\, dx\, dt \tag{2.13}$$

where $h(\alpha, C)$ is a functional of the state of the system, α is a vector of system parameters (e.g. $\alpha = [v, D, M, \theta]$), C is concentration, and the integration is over the entire space–time domain. The marginal sensitivity of this performance measure with respect to one parameter, α_k, is obtained by differentiating

(2.13) with respect to α_k:

$$\frac{dP}{d\alpha_k} = \iint_{x,t} \left[\frac{\partial h(\alpha, C)}{\partial \alpha_k} + \frac{\partial h(\alpha, C)}{\partial C} \psi \right] \, dx \, dt \tag{2.14}$$

where $dP/d\alpha_k$ is the marginal sensitivity and ψ is the state sensitivity, $\psi = \partial C/\partial \alpha_k$, where ψ is a measure of the change in system state, C, due to a small change in one of the parameters, α_k, while holding constant x, t, and the other parameters in α. Since the state sensitivity is unknown, adjoint theory can be used to eliminate it from the previous equation. This is done by first differentiating the advection-dispersion equation (including initial and boundary conditions) with respect to the parameter α_k, to obtain a form of the ADE in terms of the state sensitivity, ψ.

One-dimensional contaminant transport can be described by the following general form of the advection-dispersion equation:

$$-\frac{\partial C}{\partial t} + \frac{\partial}{\partial x}\left(D \frac{\partial C}{\partial x} \right) - \frac{\partial (vC)}{\partial x} + Q(x,t) = 0 \tag{2.15}$$

where $Q(x,t)$ describes the contaminant source. The general initial and boundary conditions for this equation are

$$\begin{aligned} a_1 C + b_1 \frac{\partial C}{\partial x} &= g_1(t) \text{ at } x = x_1 \\ a_2 C + b_2 \frac{\partial C}{\partial x} &= g_2(t) \text{ at } x = x_2 \\ C(x,0) &= g_3(x) \end{aligned}$$

where x_1 and x_2 are the boundary locations, $x_2 > x_1$, while a_1, a_2, b_1, and b_2

are known constants, and $g_1(t)$, $g_2(t)$, and $g_3(x)$ are known functions.

Differentiating (2.15) and its boundary and initial conditions with respect to α_k gives

$$-\frac{\partial \psi}{\partial t}+\frac{\partial}{\partial x}\left(D\frac{\partial \psi}{\partial x}\right)+\frac{\partial}{\partial x}\left(\frac{\partial D}{\partial \alpha_k}\frac{\partial C}{\partial x}\right)-\frac{\partial}{\partial x}\left(C\frac{\partial v}{\partial \alpha_k}\right) -\frac{\partial (v\psi)}{\partial x}+\frac{\partial Q(x,t)}{\partial \alpha_k}=0 \qquad (2.16)$$

$$a_1\psi+b_1\frac{\partial \psi}{\partial x}=\frac{\partial g_1(t)}{\partial \alpha_k} \text{ at } x=x_1$$

$$a_2\psi+b_2\frac{\partial \psi}{\partial x}=\frac{\partial g_2(t)}{\partial \alpha_k} \text{ at } x=x_2$$

$$\psi(x,0)=\frac{\partial g_3(x)}{\partial \alpha_k},$$

where we assumed that the coefficients a_1, a_2, b_1, and b_2 are independent of α_k, appropriate for the problems presented in this paper.

The next step is to obtain a similar form of the ADE in terms of the adjoint state, ψ^*, which, at this stage, is just an arbitrary function. First, we define the inner product of two functions, ψ^* and ξ, to be $\iint_{x,t}\psi^*\bar{\xi}\,dx\,dt$, where the overbar denotes complex conjugate. All functions used in this paper are real; therefore $\bar{\xi}=\xi$. Taking the inner product of the adjoint state, ψ^*, and each term on both sides of (2.16) gives

$$\int_0^T\int_{x_1}^{x_2}\Bigg[-\psi^*\frac{\partial \psi}{\partial t}+\psi^*\frac{\partial}{\partial x}\left(D\frac{\partial \psi}{\partial x}\right)-\psi^*\frac{\partial (v\psi)}{\partial x}+\psi^*\frac{\partial Q(x,t)}{\partial \alpha_k} +\psi^*\frac{\partial}{\partial x}\left(\frac{\partial D}{\partial \alpha_k}\frac{\partial C}{\partial x}\right)-\psi^*\frac{\partial}{\partial x}\left(C\frac{\partial v}{\partial \alpha_k}\right)\Bigg]\,dx\,dt=0\,. \qquad (2.17)$$

Integration is carried out over the entire domain: $x_1\le x\le x_2$, and $0\le t\le T$

(we will later show that the final time T is equivalent to the detection time). This equation can be manipulated, term by term, to obtain a similar form of the ADE with ψ^* as the state variable, and with additional divergence terms. Take the first term:

$$\int_0^T \int_{x_1}^{x_2} -\psi^* \frac{\partial \psi}{\partial t} \, dx \, dt = \int_0^T \int_{x_1}^{x_2} \left[-\frac{\partial}{\partial t}(\psi^* \psi) + \psi \frac{\partial \psi^*}{\partial t} \right] \, dx \, dt \, . \tag{2.18}$$

For the second term:

$$\begin{aligned} &\int_0^T \int_{x_1}^{x_2} \psi^* \frac{\partial}{\partial x} \left(D \frac{\partial \psi}{\partial x} \right) \, dx \, dt \\ &\quad = \int_0^T \int_{x_1}^{x_2} \left[\frac{\partial}{\partial x} \left(D \psi^* \frac{\partial \psi}{\partial x} \right) - D \frac{\partial \psi^*}{\partial x} \frac{\partial \psi}{\partial x} \right] \, dx \, dt \\ &\quad = \int_0^T \int_{x_1}^{x_2} \left[\frac{\partial}{\partial x} \left(D \psi^* \frac{\partial \psi}{\partial x} \right) - \frac{\partial}{\partial x} \left(D \psi \frac{\partial \psi^*}{\partial x} \right) + \psi \frac{\partial}{\partial x} \left(D \frac{\partial \psi^*}{\partial x} \right) \right] \, dx \, dt \, . \end{aligned} \tag{2.19}$$

The third term becomes:

$$\int_0^T \int_{x_1}^{x_2} -\psi^* \frac{\partial (v \psi)}{\partial x} \, dx \, dt = \int_0^T \int_{x_1}^{x_2} \left[-\frac{\partial}{\partial x} \left(v \psi^* \psi \right) + \psi v \frac{\partial \psi^*}{\partial x} \right] \, dx \, dt \, . \tag{2.20}$$

No manipulation is done to the remaining terms in (2.17).

Substituting (2.18), (2.19), and (2.20) into (2.17) and rearranging the terms gives

$$\int_0^T \int_{x_1}^{x_2} \Big\{ \psi \left[\frac{\partial \psi^*}{\partial t} + \frac{\partial}{\partial x}\left(D \frac{\partial \psi^*}{\partial x} \right) + v \frac{\partial \psi^*}{\partial x} \right] + \psi^* \frac{\partial Q}{\partial \alpha_k} + \psi^* \frac{\partial}{\partial x}\left(\frac{\partial D}{\partial \alpha_k} \frac{\partial C}{\partial x} \right) - \psi^* \frac{\partial}{\partial x}\left(C \frac{\partial v}{\partial \alpha_k} \right) + \frac{\partial}{\partial x}\left[D\psi^* \frac{\partial \psi}{\partial x} - D\psi \frac{\partial \psi^*}{\partial x} - v\psi^* \psi \right] - \frac{\partial}{\partial t}(\psi^* \psi) \Big\} \, dx \, dt = 0 \, . \quad (2.21)$$

Since the left-hand side of this equation is equal to zero, it can be added to the right-hand side of the marginal sensitivity equation (2.14) yielding

$$\frac{dP}{d\alpha_k} = \int_0^T \int_{x_1}^{x_2} \Big\{ \frac{\partial h(\alpha, C)}{\partial \alpha_k} + \psi \left[\frac{\partial h}{\partial C} + \frac{\partial \psi^*}{\partial t} + \frac{\partial}{\partial x}\left(D \frac{\partial \psi^*}{\partial x} \right) + v \frac{\partial \psi^*}{\partial x} \right] + \psi^* \frac{\partial Q}{\partial \alpha_k} + \psi^* \frac{\partial}{\partial x}\left(\frac{\partial D}{\partial \alpha_k} \frac{\partial C}{\partial x} \right) - \psi^* \frac{\partial}{\partial x}\left(C \frac{\partial v}{\partial \alpha_k} \right) + \frac{\partial}{\partial x}\left[D\psi^* \frac{\partial \psi}{\partial x} - D\psi \frac{\partial \psi^*}{\partial x} - v\psi^* \psi \right] - \frac{\partial}{\partial t}(\psi^* \psi) \Big\} \, dx \, dt \, . \quad (2.22)$$

The last two terms in this equation are divergence terms, which, after integration, are evaluated at the boundary conditions. Thus, these terms can be simplified as follows:

$$\int_0^T \int_{x_1}^{x_2} \frac{\partial}{\partial x}\left[D\psi^* \frac{\partial \psi}{\partial x} - D\psi \frac{\partial \psi^*}{\partial x} - v\psi^* \psi \right] dx \, dt = \int_0^T \left[D\psi^* \frac{\partial \psi}{\partial x} - D\psi \frac{\partial \psi^*}{\partial x} - v\psi^* \psi \right] \Big|_{x_1}^{x_2} dt \quad (2.23)$$

and

$$\int_0^T \int_{x_1}^{x_2} -\frac{\partial}{\partial t}(\psi^* \psi) \, dx \, dt = \int_{x_1}^{x_2} -(\psi^* \psi) \Big|_0^T \, dx \quad (2.24)$$

where the time domain extends from $t = 0$ to $t = T$.

Recall that the intent of this exercise is to eliminate the unknown state sensitivity, ψ, from the (2.14), or, equivalently, from (2.22). Recall also that the adjoint state, ψ^*, is still an arbitrary function. Thus, the adjoint state, ψ^*, can be defined in such a way as to eliminate the state sensitivity, ψ, from (2.22). From these considerations, the governing equation for the adjoint state is

$$\frac{\partial h(\alpha, C)}{\partial C} + \frac{\partial \psi^*}{\partial t} + \frac{\partial}{\partial x}\left(D\frac{\partial \psi^*}{\partial x}\right) + v\frac{\partial \psi^*}{\partial x} = 0 \ , \tag{2.25}$$

and the following statements must be satisfied by the boundary and initial conditions, respectively:

$$\left[D\psi^*\frac{\partial \psi}{\partial x} - D\psi\frac{\partial \psi^*}{\partial x} - v\psi^*\psi\right]\Bigg|_{x_1}^{x_2} = 0 \tag{2.26}$$

$$(\psi^*\psi)\Big|_0^T = 0 \ . \tag{2.27}$$

The boundary and initial conditions of the state sensitivity, ψ, have been defined in the governing equation of the forward model (2.16). By substituting these values for ψ into (2.26) and (2.27), we obtain the boundary and final conditions on ψ^*, in terms of known quantities (e.g. v and D). We have now defined an adjoint equation (2.25) and its boundary (2.26) and final (2.27) conditions, which can be solved to obtain the (no longer arbitrary) functional form of the adjoint state, ψ^*. This function, ψ^*, is an adjoint state of the original

state variable, C.

Through this derivation, we see that there are many different adjoint states of C. For each definition of the performance measure, we have a different functional h, and therefore different forms of the adjoint equation and the adjoint state. Two possible adjoint states are location probability and travel-time probability, which we derive in the next section. Also, in deriving the adjoint equation, we added zero (2.21) to the marginal sensitivity equation (2.14) to obtain an equivalent marginal sensitivity equation (2.22) from which we eliminated the state sensitivity ψ by defining an adjoint equation. We could have added a different form of zero (e.g. by multiplying (2.21) by a constant) to the marginal sensitivity equation. The result would be a different, but equally valid, adjoint equation.

Our intent was to obtain the adjoint of the ADE, which we have done in general form for one dimension. For completeness, we now discuss the relationship between adjoint states and sensitivity analysis. Each adjoint state represents a different measure of the system sensitivity. If we were performing a sensitivity analysis, we would use the appropriate adjoint state in the reduced form of (2.22) to obtain our solution to the marginal sensitivity, $dP/d\alpha_k$. Note that if we were performing a sensitivity analysis with respect to the source strength at one point in space-time, the adjoint state would be equivalent to the marginal sensitivity. In other words, let the contaminant source be an instantaneous point source at $x = x^*$ and $t = t^*$, so $Q(x,t) = Q^*\delta(x - x^*)\delta(t - t^*)$, where Q^* is the source strength. Then, α_k is the source strength, Q^*. Since f, D, and v are independent of Q^*, the terms in (2.22) containing their derivatives with respect to α_k are equal to zero. The terms in (2.22)

that contain ψ are equal to zero by the definition of the adjoint state, ψ^*. Therefore, the only non-zero term in (2.22) is $\psi^* \partial Q/\partial \alpha_k$. Since α_k is defined as Q^*, it can be seen that $\partial Q/\partial \alpha_k$ is equal to $\delta(x - x^*)\delta(t - t^*)$. Thus, we have $\psi^* \partial Q/\partial \alpha_k = \psi^* \delta(x - x^*)\delta(t - t^*)$ and, from (2.22), $dP/d\alpha_k = \psi^*(x^*, t^*)$. Therefore, by choosing α_k to be the magnitude of Q at $x = x^*$ and $t = t^*$, the marginal sensitivity of the performance measure is equal to the adjoint state. In other words, the adjoint state describes the sensitivity of the performance measure to a unit source at any location in the space-time domain.

2.3.2 Complete Adjoint Equations

The general adjoint equations that were derived in the previous section (2.25–2.27) are used to obtain expressions for the adjoint states of resident concentration. The backward-in-time location and travel time probabilities are two possible adjoint states. To use the general equation, we need to define the performance measure, P, in terms of the functional, $h(\alpha, C)$, as shown in (2.13). As we will show, to obtain location probability as the adjoint state, we define the performance measure to be resident concentration at a point in space-time, and for travel time probability, we use flux concentration at a point in space-time.

To complete the adjoint equation, we also need to specify the boundary and initial conditions on the state variable, C. The boundary conditions depend on the system domain (e.g. semi-infinite domain). From the boundary and initial conditions on C, we can obtain their counterparts for the state sensitivity, ψ; through these conditions, we obtain the boundary and final conditions

for the adjoint equation.

The governing equation for contaminant transport in a one-dimensional system in a semi-infinite domain ($-\infty < x \leq 0$) that is bounded at the downgradient boundary by a pumping well is

$$-\frac{\partial C^r}{\partial t} + \frac{\partial}{\partial x}\left(D\frac{\partial C^r}{\partial x}\right) - \frac{\partial (vC^r)}{\partial x} + Q(x,t) = 0 \tag{2.28}$$

where C^r is resident concentration. The appropriate initial and boundary conditions for this equation are

$$\begin{aligned} C^r(x,t) &\rightarrow 0 \quad \text{as} \quad x \rightarrow -\infty \\ \frac{\partial C^r}{\partial x} &= 0 \quad \text{at} \quad x = 0 \\ C^r(x,0) &= 0\,. \end{aligned}$$

Taking the derivative of these equations with respect to an arbitrary parameter, α_k, gives

$$-\frac{\partial \psi}{\partial t} + \frac{\partial}{\partial x}\left(D\frac{\partial \psi}{\partial x}\right) - \frac{\partial (v\psi)}{\partial x} + \frac{\partial}{\partial x}\left(\frac{\partial D}{\partial \alpha_k}\frac{\partial C^r}{\partial x}\right) - \frac{\partial}{\partial x}\left(C^r\frac{\partial v}{\partial \alpha_k}\right) + \frac{\partial Q(x,t)}{\partial \alpha_k} = 0 \tag{2.29}$$

$$\begin{aligned} \psi(x,t) &\rightarrow 0 \text{ as } x \rightarrow -\infty \\ \frac{\partial \psi}{\partial x} &= 0 \text{ at } x = 0 \\ \psi(x,0) &= 0\,. \end{aligned}$$

Using these boundary and initial conditions with (2.26) and (2.27), we can obtain the appropriate boundary and final conditions for the adjoint state. Substituting $\psi(x,t) \rightarrow 0$ as $x \rightarrow -\infty$ and $\partial\psi/\partial x = 0$ at $x = 0$ into (2.26), we are left with

$$-D\psi\frac{\partial\psi^*}{\partial x}\bigg|_{x=0} - v\psi^*\psi|_{x=0} - D\psi^*\frac{\partial\psi}{\partial x}\bigg|_{x\rightarrow-\infty} = 0. \tag{2.30}$$

This equation is satisfied if we set $\psi^*(x,t) \rightarrow 0$ as $x \rightarrow -\infty$ and $D\partial\psi^*/\partial x + v\psi^* = 0$ at $x = 0$. These are the boundary conditions for the adjoint equation. Note that the forward problem had a second-type boundary condition at the well, while the adjoint problem has a third-type boundary condition for the well. For the final condition, we substitute initial condition $\psi(x,0) = 0$ into (2.27), resulting in

$$\psi^*\psi|_T = 0. \tag{2.31}$$

For this equation to be satisfied, the final condition for the adjoint equation must be $\psi^*(x,T) = 0$.

The only remaining undefined item in the adjoint equation is the functional $h(\alpha, C^r)$. Here, we have indicated the dependence of h on resident concentration, C^r (instead of just C), because we wrote the governing ADE (2.28) in terms of resident concentration. The form of $h(\alpha, C^r)$ depends on whether we are looking for location probability or travel time probability.

Location Probability Recall that the normalized distribution of resident concentration, C^r, is equivalent to a probability density function for the location of a solute parcel from a given source. Define the performance measure, P, as the resident concentration at a point, (x', t'), in space-time, which would usually be the location and time of detection. The appropriate functional, h, is

$$h(\alpha, C^r) = C^r(x,t)\delta(x - x')\delta(t - t') \; . \tag{2.32}$$

Substituting (2.32) into (2.13) and integrating over the (x,t) domain gives $P = C^r(x', t')$. For the adjoint equation (2.25), we need $\partial h/\partial C^r$, which is a Fréchet derivative [*Saaty*, 1981] of $h(\alpha, C^r)$ with respect to the function C^r. Taking the Fréchet derivative of both sides of (2.32), we obtain (See Appendix 2.D).

$$\frac{\partial h(\alpha, C^r)}{\partial C^r} = \delta(x - x')\delta(t - t'). \tag{2.33}$$

Note that final time T is an arbitrary upper limit of the time domain in the forward problem. If the performance measure for the forward model is resident concentration at (x', t'), we are only interested in the solution for $t \leq t'$. Thus, the upper limit of the time domain in the forward problem can be arbitrarily set to $T = t'$. For the backward problem (see Section 2.2.2), the backward time τ is given by $\tau = T - t = t' - t$. Using $T = t'$, and v and D constant, the adjoint equation (2.25) and its boundary and final conditions for

location probability in a semi-infinite domain are given by

$$\begin{aligned} -\frac{\partial \psi^*}{\partial t} - D\frac{\partial^2 \psi^*}{\partial x^2} - v\frac{\partial \psi^*}{\partial x} &= \delta(x-x')\delta(t-T)\ , \\ \psi^*(x,t) \to 0 \quad &\text{as} \quad x \to -\infty \\ D\frac{\partial \psi^*}{\partial x} + v\psi^* = 0 \quad &\text{at} \quad x = 0 \\ \psi^*(x,T) &= 0\ . \end{aligned} \tag{2.34}$$

This equation can be solved using Laplace transforms. The solution (derived in Appendix 2.A) is

$$\begin{aligned} \psi^*(x,t) &= \frac{1}{\sqrt{4\pi D(T-t)}} \exp\left\{-\frac{[x-x'+v(T-t)]^2}{4D(T-t)}\right\}\left[1+\exp\left\{\frac{-xx'}{D(T-t)}\right\}\right] \\ &\quad -\frac{v}{2D}\exp\left\{-\frac{vx}{D}\right\}\operatorname{erfc}\left(-\frac{x+x'-v(T-t)}{\sqrt{4D(T-t)}}\right) \end{aligned} \tag{2.35}$$

for $-\infty < x \leq 0$ and $0 < t \leq T$. This equation is equivalent to the backward-in-time location probability proposed by *Wilson and Liu* [1995] for a detection at the pumping well (equation (2.10), where $x' = x_d = 0$ and $\tau = T - t$).

As stated earlier, the adjoint state describes the sensitivity of the performance measure to a unit source at any location in the space–time domain. By this definition, the adjoint state in (2.35) is the sensitivity of the resident concentration at x' to a source at any other location. Not only is resident concentration related to location probability [*Jury and Roth*, 1990], but in this case of a unit source, they are the same. Thus, the adjoint state (2.35) is location probability.

Travel Time Probability Recall that the normalized mass flux, vC^f, is equivalent to the travel time probability for a given source location. Define the performance measure, P, as the mass flux at a point (x', t') in space-time. The appropriate functional, h, is

$$h(\alpha, C^r) = vC^f(x,t)\delta(x-x')\delta(t-t') \; . \tag{2.36}$$

Substituting (2.36) into (2.13) and integrating over the (x,t) domain gives $P = vC^f(x',t')$. For the adjoint equation (2.25), we need $\partial h/\partial C^r$. Flux concentration is defined in terms of resident concentration, as shown in (2.5). Substituting this expression in the functional, h, we obtain

$$h(\alpha, C^r) = \left[vC^r - D\frac{\partial C^r}{\partial x} \right] \delta(x-x')\delta(t-t') \; . \tag{2.37}$$

Using this equation to solve for the Fréchet derivative, $\partial h/\partial C^r$, gives

$$\frac{\partial h(\alpha, C^r)}{\partial C^r} = v\delta(x-x')\delta(t-t') + D\delta'(x-x')\delta(t-t') \; , \tag{2.38}$$

where $\delta'(x)$ is the derivative with respect to x of the Dirac delta function. The second term is derived in Appendix 2.B.

By the argument used in the location probability problem, we can arbitrarily take $T = t'$. Thus, for travel time probability in a semi-infinite domain, with v and D constant, the adjoint equation and its boundary and

final conditions are given by

$$-\frac{\partial \psi^*}{\partial t} - D\frac{\partial^2 \psi^*}{\partial x^2} - v\frac{\partial \psi^*}{\partial x} = v\delta(x-x')\delta(t-T) + D\delta'(x-x')\delta(t-T) \quad (2.39)$$

$$\psi^*(x,t) \to 0 \text{ as } x \to -\infty$$

$$D\frac{\partial \psi^*}{\partial x} + v\psi^* = 0 \text{ at } x = 0$$

$$\psi^*(x,T) \;=\; 0\,.$$

This equation can be solved using Laplace transforms. The solution (derived in Appendix 2.C) is

$$\begin{aligned}
\psi^*(x,t) \;&=\; -\frac{x-x'-v(T-t)}{4\sqrt{\pi D(T-t)^3}}\exp\left\{-\frac{[x-x'+v(T-t)]^2}{4D(T-t)}\right\} \\
&+\; \frac{x+x'+3v(T-t)}{4\sqrt{\pi D(T-t)^3}}\exp\left\{\frac{-xx'}{D(T-t)}\right\}\exp\left\{-\frac{[x-x'+v(T-t)]^2}{4D(T-t)}\right\} \\
&-\; \frac{v^2}{2D}\exp\left\{\frac{-vx}{D}\right\}\operatorname{erfc}\left(\frac{-x-x'+v(T-t)}{\sqrt{4D(T-t)}}\right) \qquad (2.40)
\end{aligned}$$

for $-\infty < x \leq 0$ and $0 < t \leq T$. This equation is equivalent to the backward-in-time travel time probability proposed by *Wilson and Liu* [1995] for a detection at the pumping well (equation (2.12), with $x' = x_d = 0$ and $\tau = T - t$).

The adjoint state in (2.40) is the sensitivity of the mass flux at x', e.g. the detection location, to a unit source at any other location. Not only is mass flux related to travel time probability [*Jury*, 1982], but in this case, they are the same. Thus, the adjoint state (2.40) is travel time probability.

2.4 Conclusions

Backward-in-time location and travel time probabilities can be developed heuristically from the forward-in-time resident and flux concentration distributions, as *Wilson and Liu* [1995] showed for a one-dimensional, semi-infinite domain. Although they arrived at the appropriate governing equation and boundary conditions, their approach was based more on intuition than on proof. To provide a consistent framework for obtaining backward-in-time probabilities for multi-dimensional problems and all spatial domains, we propose the adjoint method.

In this paper, we demonstrated that the adjoint method provides a formal framework for obtaining these backward-in-time probabilities. We derived the one-dimensional adjoint equation for backward-in-time location and travel time probabilities in terms of general boundary conditions. By applying the general form (2.25–2.27) of the equation to the special case of a semi-infinite domain, we derived expressions for location and travel time probabilities; then we verified that these probabilities are equivalent to those obtained by *Wilson and Liu* [1995]. The general form of the adjoint equation can be used to find location and travel time probabilities for other boundary conditions.

Backward-in-time probabilities can be used to obtain information about where contamination was located before it was detected. They have a variety of applications, including capture zone delineation. The backward model is more efficient than the forward model in situations in which the number of known or potential sources is greater than the number of detections. The benefit of the backward model is that, for each detection, we solve the

adjoint equation only once to obtain the backward-in-time location probability for all prior locations at a given time. In other words, for each detection, we obtain information about all possible prior locations after solving the adjoint equation only once. With the forward model, we obtain information about all possible future locations for contamination that was injected at one specified source. Thus, if we have a few detections and many known or possible source locations, the backward model is computationally more efficient than the forward model in that fewer simulations must be run (i.e. one simulation for each detection). However, if we have many detections and only a few possible source locations, the forward model is more computationally efficient than the backward model.

The approach described in this paper is for a simple, idealistic, one-dimensional system. By using the adjoint method, development of the backward probabilities can now formally be extended to a multi-dimensional system.

Acknowledgments

This research was supported in part by the Geophysical Research Center at New Mexico Tech and in part by the Environmental Protection Agency's STAR Fellowship program under Fellowship No. U-915324-01-0. This work has not been subjected to the EPA's peer and administrative review and therefore may not necessarily reflect the views of the Agency and no official endorsement should be inferred. The authors acknowledge William D. Stone for his input on operator theory, and Zbigniew Kabala and an anonymous reviewer for their valuable comments.

References

Abramowitz, M. and I.A. Stegun, *Handbook of Mathematical Functions*, Dover Publications, Inc., New York, 1972.

Ahlfeld, D.P., J.M. Mulvey, and G.F. Pinder, Contaminated groundwater remediation design using simulation, optimization, and sensitivity theory, 1, Model development, *Water Resour. Res.*, 24(3), 431–441, 1988.

Bagtzoglou, A.C., D.E. Dougherty, and A.F.B. Thompson, Application of particle methods to reliable identification of groundwater pollution sources, *Water Resources Management*, 6, 15–23, 1992.

Chen, C.-S. and G.D. Woodside, Analytical solution for aquifer decontamination by pumping, *Water Resour. Res.*, 24(8), 1329–1338, 1988.

Chin, D.A. and P.V.K. Chittaluru, Risk management in wellhead protection, *J. Water Resour. Plan. Manage.*, 120(3), 294–315. 1994.

Dagan, G., *Flow and Transport in Porous Formations*, Springer-Verlag, New York, 1989.

Jury, W.A., Simulation of solute transport using a transfer function model, *Water Resour. Res.*, 18(2), 363–368, 1982.

Jury, W.A. and K. Roth, *Transfer Functions and Solute Movement through Soil: Theory and Applications*, Birkhauser, Boston, 1990.

Kreft, A. and A. Zuber, On the physical meaning of the dispersion equation and its solutions for different initial and boundary conditions, *Chemical Engineering Science*, 33, 1471–1480, 1978.

Liu, J., *Travel time and location probabilities for groundwater contaminant sources*, Master's thesis, New Mexico Institute of Mining and Tech-

nology, Socorro, 1995.

Lu, A.H., F. Schmittroth, and W.W.-G. Yeh, Sequential estimation of aquifer parameters, *Water Resour. Res.*, 24(5), 670–682, 1988.

Marchuk, G.I., V.I. Agoshkov, and V.P. Shutyaev, *Adjoint Equations and Perturbation Algorithms in Nonlinear Problems*, CRC Press, Inc., Boca Raton, FL, 1996.

Neuman, S.P., A statistical approach to the inverse problem of aquifer hydrology, 3, Improved solution method and added perspective, *Water Resour. Res.*, 16(2), 331–346, 1980.

Parker, J.C. and M. Th. van Genuchten, Flux-averaged and volume-averaged concentrations in continuum approaches to solute transport, *Water Resour. Res.*, 20(7), 866–872, 1984.

Saaty, T.L., *Modern Nonlinear Equations*, Dover Publications, Inc., New York, 1981.

Skaggs, T.H. and Z.J. Kabala, Recovering the release history of a groundwater contaminant. *Water Resour. Res.*, 30(1), 71–79, 1994.

Sun, N.-Z., *Inverse Problems in Groundwater Modeling*, Kluwer Academic Publishers, Boston, 1994.

Sun, N.-Z. and W.W.-G. Yeh, Identification of parameter structure in groundwater inverse problems, *Water Resour. Res.*, 21(6), 869–883, 1985.

Sun, N.-Z. and W.W.-G. Yeh, Coupled inverse problems in groundwater modeling, 1, Sensitivity analysis and parameter identification, *Water Resour. Res.*, 26(10), 2507–2525, 1990.

Sykes, J.F., J.L. Wilson, and R.W. Andrews, Sensitivity analysis for steady state groundwater flow using adjoint operators, *Water Resour. Res.*,

21(3), 359–371, 1985.

Townley, L.R. and J.L. Wilson, Computationally efficient algorithms for parameter estimation and uncertainty propagation in numerical models of groundwater flow, *Water Resour. Res.*, 21(12), 1851–1860, 1985.

Uffink, G.J.M., Application of Kolmogorov's backward equation in random walk simulations of groundwater contaminant transport, in *Contaminant Transport in Groundwater*, H.E. Kobus and W. Kinzelbach, editors, pp. 283–289, A.A. Balkema, Brookfield, Vt., 1989.

Wilson, J.L. and J. Liu, Backward tracking to find the source of pollution, in *Waste-management: From Risk to Reduction*, edited by R. Bahda *et al.*, EDM Press, Albuquerque, NM, 181–199, 1995.

Wilson, J.L. and D.E. Metcalfe, Illustration and verification of adjoint sensitivity theory for steady state groundwater flow, *Water Resour. Res.*, 21(11), 1602–1610, 1985.

Yeh, W.W.-G. and N.-Z. Sun, Variational sensitivity analysis, data requirements, and parameter identification in a leaky aquifer system, *Water Resour. Res.*, 26(9), 1927–1938, 1990.

Zwillinger, D., *Handbook of Differential Equations*, 2nd ed., Academic Press, Inc., San Diego, 1989.

2.A Derivation of the Solution to the Adjoint Equation for Location Probability

The adjoint equation for location probability is shown in (2.34). An equivalent equation is given here, with a new time variable, $\tau = T - t$, and a new space variable, $y = -x$.

$$\begin{aligned} \frac{\partial \psi^*}{\partial \tau} - D\frac{\partial^2 \psi^*}{\partial y^2} + v\frac{\partial \psi^*}{\partial y} &= \delta(y - y')\delta(\tau) \ , \\ \psi^*(y,\tau) \to 0 \quad &\text{as} \quad y \to \infty \\ -D\frac{\partial \psi^*}{\partial y} + v\psi^* = 0 \quad &\text{at} \quad y = 0 \\ \psi^*(y,0) &= 0 \end{aligned} \tag{2.41}$$

where $y' = -x'$ and $0 \leq y < \infty$.

Taking the Laplace transform with respect to time ($\tau \to s$) gives

$$\begin{aligned} s\Psi - \psi^*(y,0) - D\frac{d^2\Psi}{dy^2} + v\frac{d\Psi}{dy} &= g(y) \\ \Psi \to 0 \quad &\text{as} \quad y \to \infty \\ v\Psi - D\frac{d\Psi}{dy} = 0 \quad &\text{at} \quad y = 0 \end{aligned} \tag{2.42}$$

where Ψ is the transformed state of ψ^* and $g(y) = \delta(y - y')$. The second term on the left-hand side is equal to zero, according to the initial condition in τ (final condition in t). Taking a second Laplace transform with respect to y ($y \to r$) gives

$$s\hat{\Psi} - Dr^2\hat{\Psi} + Dr\Psi\big|_{y=0} + D\frac{d\Psi}{dy}\bigg|_{y=0} + vr\hat{\Psi} - v\Psi\big|_{y=0} = \hat{g}(r) \tag{2.43}$$

where $\hat{\Psi}$ is the transformed state of Ψ and $\hat{g}(r)$ is the transform of $g(y)$. The fourth and sixth terms on the left-hand side sum to zero according to the boundary condition at $y = 0$. This equation can be rearranged to give

$$\hat{\Psi} = \frac{\hat{g}(r) - Dr\Psi|_{y=0}}{-Dr^2 + vr + s} \,. \tag{2.44}$$

Taking the inverse Laplace transform with respect to r ($r \rightarrow y$) gives

$$\Psi = L^{-1}_{r \rightarrow y} \left[\frac{\hat{g}(r) - Dr\Psi|_{y=0}}{-D(r^2 - vr/D - s/D)} \right] \tag{2.45}$$

where L^{-1} denotes the inverse Laplace transform.

Using partial fractions, the convolution theorem, and applying the boundary condition as $y \rightarrow \infty$, we obtain the following expression for Ψ:

$$\begin{aligned} \Psi \;=\; & \frac{1}{v\xi} \Bigg[\exp\left\{ \frac{vy}{2D}(1+\xi) \right\} \int_y^\infty g(y'') \exp\left\{ -\frac{vy''}{2D}(1+\xi) \right\} dy'' \\ & + \exp\left\{ \frac{vy}{2D}(1-\xi) \right\} \left(\int_0^y g(y'') \exp\left\{ -\frac{vy''}{2D}(1-\xi) \right\} dy'' \right. \\ & \left. - \frac{1-\xi}{1+\xi} \int_0^\infty g(y'') \exp\left\{ -\frac{vy''}{2D}(1+\xi) \right\} dy'' \right) \Bigg] \,, \end{aligned} \tag{2.46}$$

where $\xi = \sqrt{1 + 4sD/v^2}$.

The adjoint state, ψ^*, is found by taking the inverse Laplace transform of the previous equation with respect to s. After some algebraic manipulation and use of the shifting property, we obtain

$$\begin{aligned}\psi^* &= \frac{1}{\sqrt{4\pi D\tau}}\int_0^\infty g(y'')\exp\left\{-\frac{(y-y''-v\tau)^2}{4D\tau}\right\}\,dy'' + \\ &\quad \frac{1}{\sqrt{4\pi D\tau}}\int_0^\infty g(y'')\exp\left\{\frac{-yy''}{D\tau}\right\}\exp\left\{-\frac{(y-y''-v\tau)^2}{4D\tau}\right\}\,dy'' \\ &\quad -\frac{v}{2D}\exp\left\{\frac{vy}{D}\right\}\int_0^\infty g(y'')\mathrm{erfc}\left(\frac{y+y''+v\tau}{\sqrt{4D\tau}}\right)\,dy''\,. \qquad (2.47)\end{aligned}$$

Recall that $g(y'') = \delta(y''-y')$. Substituting this expression into (2.47), evaluating the integrals, and substituting $y = -x$, results in the expression for the adjoint state shown in (2.35).

2.B Verification of the Equality used in the Travel Time Probability Adjoint Equation

In the derivation of the adjoint equations (Section 2.3.2), we made use of the following weak equality.

$$\frac{\partial}{\partial C^r}\left[-D\frac{\partial C^r}{\partial x}\delta(x-x')\delta(t-t')\right] = D\delta'(x-x')\delta(t-t') \; . \tag{2.48}$$

We justify this substitution here.

By taking the Fréchet derivative [*Saaty*, 1981] with respect to C^r of the bracketed term in (2.48), we obtain the following operator, L:

$$L = -D\delta(x-x')\delta(t-t')\frac{\partial}{\partial x} \; . \tag{2.49}$$

Two operators are weakly equal if the results of their operation on a test function are equal, i.e. $L_1 = L_2$ if $\langle L_1, \phi\rangle = \langle L_2, \phi\rangle$, where ϕ is an arbitrary test function, and $\langle \eta, \xi\rangle$ represents the inner product. For the operator shown in (2.49), we have

$$\langle L, \phi\rangle = \iint_{x,t} -D\delta(x-x')\delta(t-t')\frac{\partial \phi}{\partial x}\, dx\, dt \; , \tag{2.50}$$

where integration is over the entire space–time domain. Integrating the right-hand side by parts in x, we see that

$$\langle L, \phi\rangle = \iint_{x,t} D\delta'(x-x')\delta(t-t')\phi\, dx\, dt \; . \tag{2.51}$$

This can be written as

$$\langle L, \phi \rangle \;=\; \langle D\delta'(x - x')\delta(t - t'), \phi \rangle \;\; . \tag{2.52}$$

Therefore, $L = D\delta'(x - x')\delta(t - t')$.

2.C Derivation of the Solution to the Adjoint Equation for Travel Time Probability

The adjoint equation for travel time probability is shown in (2.39). An equivalent equation is given here, with a new time variable, $\tau = T - t$, and a new space variable, $y = -x$.

$$\begin{aligned} \frac{\partial \psi^*}{\partial \tau} - D\frac{\partial^2 \psi^*}{\partial y^2} + v\frac{\partial \psi^*}{\partial y} &= v\delta(y - y')\delta(\tau) - D\delta'(y - y')\delta(\tau)\ , \quad (2.53) \\ \psi^*(y, \tau) \to 0 \quad &\text{as} \quad y \to \infty \\ -D\frac{\partial \psi^*}{\partial y} + v\psi^* = 0 \quad &\text{at} \quad y = 0 \\ \psi^*(y, 0) &= 0 \end{aligned}$$

where $y' = -x'$ and $0 \leq y < \infty$.

Taking the Laplace transform of the previous equation with respect to time ($\tau \to s$) gives

$$\begin{aligned} s\Psi - \psi^*(y, 0) - D\frac{d^2\Psi}{dy^2} + v\frac{d\Psi}{dy} &= g(y) \quad (2.54) \\ \Psi \to 0 \quad &\text{as} \quad y \to \infty \\ v\Psi - D\frac{d\Psi}{dy} = 0 \quad &\text{at} \quad y = 0 \end{aligned}$$

where Ψ is the transformed state of ψ^* and $g(y) = v\delta(y - y') - D\delta'(y - y')$. The second term on the left-hand side is equal to zero, by the initial condition in τ. With the right-hand side written in general terms, (2.54) is equivalent to (2.42). Therefore, the solution to (2.53) in general form is (2.47). Substituting the expression for $g(y)$ into (2.47), evaluating the integrals, and substituting

$y = -x$ gives the expression for the adjoint state shown in (2.40).

2.D Fréchet Derivative

The derivative, $\partial h/\partial C^r$, in (2.14) and (2.25), is a Fréchet (strong) derivative of a functional, h (*Saaty* [1981]; *Zwillinger* [1989]). Consider a function $u(x)$, where x is space, and a functional $w(u) = Wu$, where W is an operator. The Fréchet derivative, $\partial w/\partial u$, is defined as (*Zwillinger* [1989])

$$\lim_{||\epsilon||\to 0} \frac{||W[u+\epsilon] - Wu - \epsilon Lu||}{||\epsilon||} = 0 \,, \tag{2.55}$$

where L the derivative operator, Lu is the Fréchet derivative ($Lu = \partial w/\partial u$), and $||\cdot||$ represents the norm. If, for example, $w(u) = Wu = u^3 + u'' + (u')^2$, then the derivative operator is $L[\ ] = 3u^2[\ ] + [\ ]'' + 2u'[\ ]'$. Contrast this to the derivative of a function; in this example, $\partial w/\partial x = 3u^2u' + u''' + 2u'u''$. In our adjoint problem for location probability, the functional is $h(\alpha, C^r) = C^r(x,t)\delta(x-x')\delta(t-t')$, and its operator is $H[\ ] = [\ ]\delta(x-x')\delta(t-t')$. Rewriting (2.55) to define the derivative of this functional gives

$$\lim_{||\Delta C^r||\to 0} \frac{||H[C^r + \Delta C^r] - HC^r - \Delta C^r LC^r||}{||\Delta C^r||} \quad =$$

$$\lim_{||\Delta C^r||\to 0} \frac{||\Delta C^r \delta(x-x')\delta(t-t') - \Delta C^r LC^r||}{||\Delta C^r||} \quad = \quad 0 \,, \tag{2.56}$$

so that $\partial h/\partial C^r = LC^r = \delta(x-x')\delta(t-t')$. By a similar process, we can show that (2.38) is the Fréchet derivative of (2.37).

CHAPTER 3

ADJOINT METHOD FOR OBTAINING ONE-DIMENSIONAL BACKWARD PROBABILITY MODELS IN AN INFINITE DOMAIN[1]

Abstract

Backward location and travel time probabilities can be used to determine the prior location of contamination in an aquifer. For a contaminant parcel that was detected in an aquifer, the backward location probability is the probability distribution describing the position of the parcel at some time prior to detection. Backward travel time probability is the probability distribution describing the travel time of the parcel from an upgradient position to the detection location. These probabilities can be used to improve characterization of known sources of groundwater contamination, to identify previously unknown contamination sources, and to delineate capture zones. Backward probabilities are functions of adjoint states of concentration; therefore, the governing equation for the backward model is the adjoint of the forward model governing equation, e.g., the advection-dispersion equation. We illustrate the adjoint approach for obtaining backward location and travel time probabilities in a one-dimensional infinite domain, the backward-in-time-and-space version of the classical Gaussian plume. The solution simulates detection of contamination in a monitoring well, and can be used to validate higher dimensional numerical solutions for location and travel time probability.

[1]This chapter has been submitted to *Journal of Contaminant Hydrology*: Neupauer, R.M. and J.L. Wilson, Backward Location and Travel Time Probabilities for Contamination in a One-Dimensional Infinite Aquifer, submitted to *J. Contam. Hydrol.*, September 2000.

3.1 Introduction

If contamination is detected in an aquifer but the source of contamination is unknown, contaminant transport modeling can be used to obtain information about the prior position of the detected contamination. This problem can be addressed with traditional forward modeling (e.g., with the advection-dispersion equation), by modeling the movement of contamination away from its source or a prior location. Since the prior location is unknown, the modeler must select several possible prior locations, run a forward simulation for each one, and compare the results of each simulation to the actual sampled contamination. This approach is inefficient because multiple forward simulations must be run, and information is only obtained for the pre-selected sources.

Backward-in-time modeling is a more efficient approach for obtaining information about the prior position of detected contamination. Backward-in-time modeling produces location and travel time probability distributions. Backward location probability describes the probability distribution for the position of the detected contamination at some time in the past. It is related to resident concentration in forward contaminant transport. Backward travel time probability describes the probability distribution for the amount of time prior to detection that the contamination was at an upgradient location. It is related to flux concentration.

Backward modeling has been used in groundwater hydrology to determine pumping well capture zones and to identify prior locations of contamination. It has been applied to contaminant transport problems through two different approaches—random walk simulations and continuum approaches to

solving the advection-dispersion equation. Uffink (1989) used backward-in-time random walk simulations to determine capture zones around pumping wells. Capture zones are generally obtained for advective flow only, by considering travel time along streamlines. Uffink used Kolmogorov's backward equation to incorporate dispersion into the capture zone calculations and obtained a location probability density function for the initial location of possible contamination. By integrating this location probability density function over time, he obtained a type of cumulative distribution function that represents the capture zone for the well. Chin and Chittaluru (1994) also used a backward random walk model to identify pumping well capture zones. They obtained a backward location probability distribution using the backward random walk method, and then related this to a backward travel time distribution using an approximation to Bayes' theorem. Bagtzoglou et al. (1992) used backward location probabilities to identify sources of contamination. They obtained probability maps using a random walk method, by reversing the flow field and leaving the dispersion process unchanged.

Wilson and Liu (1994), Liu (1995), and Liu and Wilson (1995) used backward-in-time modeling to identify the prior location of groundwater contamination observed in a pumping well. They used a heuristic method to obtain a backward probabilistic continuum model from the forward advection-dispersion equation, and solved it for travel time and location probabilities. Using hypothetical test cases, they verified the results by comparing them to forward modeling results. They also showed that backward modeling required a significantly lower computational burden than forward modeling. Wilson and Liu (1997) further tested the backward model using results of a field tracer test

at the Borden Site at the Canadian Forces Base, Borden, Ontario, Canada. Eight tracers were injected into fifteen injection wells upgradient of an extraction well, and tracer concentrations were measured at the extraction well. The backward model was used to determine the travel time probabilities from the injection wells to the extraction well for each tracer. The model results compared well with the tracer test data, especially for tracers that were injected near the extraction well. With one simulation of the backward model, breakthrough curves for all 15 injection wells were reliably predicted (Wilson and Liu, 1997). Although the heuristic approach for obtaining the backward model produced accurate expressions for backward location and travel time probabilities, no formal justification was given for the governing equation or boundary conditions. Furthermore, the heuristic approach is difficult to implement and verify for multi-dimensional problems and complex domain geometries.

Neupauer and Wilson (1999) showed that, for a one-dimension system with flow to a pumping well, backward location and travel time probabilities are adjoint states of resident concentration. They presented the formal adjoint approach for deriving the governing equations and boundary and initial conditions for the backward model in a one-dimensional domain. The approach was illustrated for one-dimensional flow to a pumping well, modeled as a semi-infinite domain.

In this paper, we obtain backward location and travel time probabilities for contamination detected in a monitoring well. The monitoring well is treated as a passive observer of contamination that does not affect the flow field. This problem can be modeled as an infinite domain, and we consider only one-dimensional flow and transport. This model is the adjoint of the

classical Gaussian plume model. We use the adjoint approach of Neupauer and Wilson (1999) to obtain the governing equations for location and travel time probability. In a one-dimensional, infinite domain, these equations can be solved analytically and we verify the backward model results by comparing them to the equivalent probabilities obtained using a forward model. The one-dimensional solution can be used to validate higher dimensional numerical solutions of the backward model.

3.2 Forward Model

Contaminant transport in a one-dimensional infinite domain is described by the following form of the advection-dispersion equation

$$\begin{aligned} \frac{\partial C^r}{\partial t} &= D\frac{\partial^2 C^r}{\partial x^2} - v\frac{\partial C^r}{\partial x} \\ C^r &\to 0 \text{ as } x \to \pm\infty \\ C^r(x,0) &= \frac{M}{A\theta}\delta(x - x_o) \ , \end{aligned} \tag{3.1}$$

where C^r is resident concentration, D is the dispersion coefficient, v is groundwater velocity, x is the spatial dimension, t is time, M is total source mass, A is cross-sectional area, θ is porosity, $\delta(x)$ is the Dirac delta function, and x_o is the source location. We assume that v and D are constant. The boundary conditions state that the concentration is negligible as $x \to \pm\infty$, and the initial condition indicates an instantaneous point source of contamination. The well-known Gaussian plume solution to this equation is (Carslaw and Jaeger,

1959; Bear, 1972)

$$C^r(x,t) = \frac{1}{\sqrt{4\pi Dt}} \frac{M}{A\theta} \exp\left\{ -\frac{(x - x_o - vt)^2}{4Dt} \right\} . \tag{3.2}$$

Forward location probability, $f_x(x;t)$, is given by

$$f_x(x;t) = \frac{C^r(x,t)}{\int_{-\infty}^{\infty} C^r(x,t)\, dx} . \tag{3.3}$$

The forward location probability describes the probability distribution of the future position of a contaminant parcel. Since the integral of Eq. (3.2) over x evaluates to $M/(A\theta)$, forward location probability for contamination released from an instantaneous point source in an infinite domain is

$$f_x(x;t) = \frac{1}{\sqrt{4\pi Dt}} \exp\left\{ -\frac{(x - x_o - vt)^2}{4Dt} \right\} , \tag{3.4}$$

where $f_x(x;t)$ denotes the location probability at time t.

The resident concentration and forward location probability at times $t = 1$, 20, and 50 are plotted in Fig. 3.1 for $M = 1.0$, $A = 1.0$, $\theta = 0.25$, $v = -1.0$, $D = 5.0$, and $x_o = 100$ (all units are dimensionless). These parameter values are used throughout this paper. The plot shows that the contamination is initially near the source at $x_o = 100$ and it travels downgradient over time. The location probability shows the likely position at $t = 1$, 20, and 50 of one contaminant parcel that was released from the source at $t = 0$. For example, at $t = 20$ after release from the source, the contaminant parcel is most likely to be found near $x = 80$.

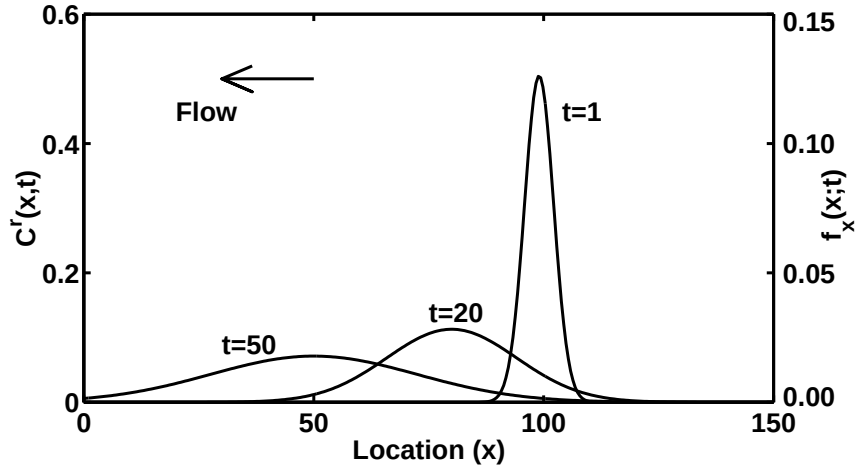

Figure 3.1: Resident concentration and forward location probability for a contamination source at $x_o = 100$.

The relationship between flux and resident concentration in one dimension is (Parker and van Genuchten, 1984)

$$C^f = C^r - \frac{D}{v}\frac{\partial C^r}{\partial x} \tag{3.5}$$

where C^f is flux concentration. Substituting Eq. (3.2) into this expressions gives the following expression for flux concentration:

$$C^f(x,t) = \frac{x - x_o + vt}{4v\sqrt{\pi D t^3}}\frac{M}{A\theta}\exp\left\{-\frac{(x - x_o - vt)^2}{4Dt}\right\} . \tag{3.6}$$

Travel time probability, $f_t(t;x)$, from the source location, x_o, to any other location, x, is given by

$$f_t(t;x) = \frac{vC^f(x,t)}{\int_0^\infty vC^f(x,t)\,dt} . \tag{3.7}$$

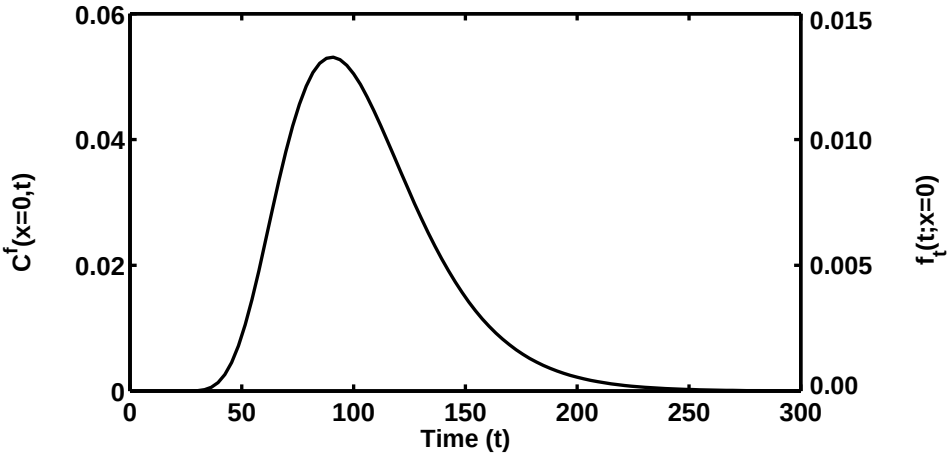

Figure 3.2: Flux concentration and forward travel time probability for a contamination source at $x_o = 100$ and an observation at $x = 0$.

The forward travel time probability describes the probability distribution of the time after release that a contaminant parcel will reach location x. Integrating Eq. (3.6) over the time domain for any downstream location, x, yields $(1/|v|)(M/A\theta)$ (Abramowitz and Stegun, 1972, equations 29.3.82 and 29.3.84); thus the forward travel time probability can be expressed as

$$f_t(t;x) = \frac{|v|(x - x_o + vt)}{4v\sqrt{\pi D t^3}} \exp\left\{-\frac{(x - x_o - vt)^2}{4Dt}\right\} . \tag{3.8}$$

The flux concentration and forward travel time probability at $x = 0$ are plotted in Fig. 3.2 for the parameter values specified above. The plot shows that the peak flux concentration at $x = 0$ occurs at approximately $t \approx 91$ after release. Similarly, the most likely travel time from the source to $x = 0$ is $t \approx 91$.

Suppose we are interested in the travel time probability to $x = 0$

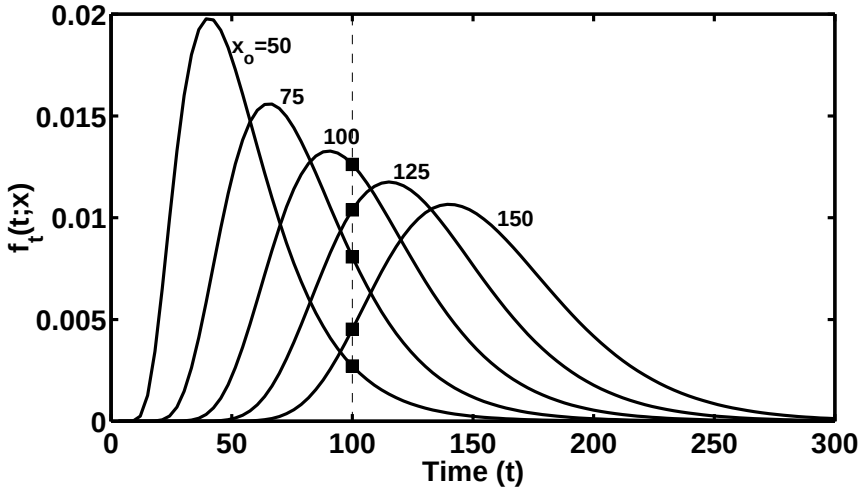

Figure 3.3: Forward travel time probability to $x = 0$ from several source locations. Squares denote the probability that $t = 100$ from each source location to $x = 0$.

for a contaminant parcel released from any source. We could select several possible sources and run a forward probability model for each of them. The travel time probability to $x = 0$ is plotted in Fig. 3.3 for several source locations, using the parameter values specified above. The squares denote the probability that $t = 100$ from each source to $x = 0$. With five simulations of the forward probability model, we determined the probability that $t = 100$ from five sources. Obtaining this information about all possible sources would be inefficient with forward modeling because one simulation would be required for each possible source. However, we could obtain all the desired information with only one simulation of the backward model.

3.3 Backward Model

If contamination is detected in an aquifer, backward location and travel time probabilities can be used to determine the prior position of the contamination. Neupauer and Wilson (1999) showed that, for the conditions they investigated, backward probabilities are adjoint states of resident concentration; therefore, the governing equation for backward probabilities is the adjoint of the advection-dispersion equation, the governing equation for the forward transport model. To obtain the appropriate adjoint equation, Neupauer and Wilson (1999) used the adjoint approach of sensitivity analysis (Sykes et al., 1985; Sun and Yeh, 1990). In sensitivity analysis, a performance measure, P, that quantifies the state of the system is defined as

$$P = \iint_{x,t} h(\alpha, C^r)\, dx\, dt\ , \tag{3.9}$$

where $h(\alpha, C)$ is a performance functional describing the state of the system, α is a vector of system parameters (e.g. $\alpha = [v, D, M, \theta]$), C^r is resident concentration, and integration is performed over the entire space–time domain. The goal of sensitivity analysis is to determine the marginal sensitivity of this performance measure to a small change in the value of one of the parameters, α_k, given by

$$\frac{dP}{d\alpha_k} = \iint_{x,t} \left[\frac{\partial h(\alpha, C^r)}{\partial \alpha_k} + \frac{\partial h(\alpha, C^r)}{\partial C^r} \psi \right] dx\, dt \tag{3.10}$$

where $dP/d\alpha_k$ is the marginal sensitivity and ψ is the state sensitivity, $\psi = \partial C^r / \partial \alpha_k$, where ψ is a measure of the change in system state, C^r, due to a

small change in one of the parameters, α_k, while holding constant x, t, and the other parameters in α. Since the state sensitivity, ψ, is unknown, adjoint theory is used to eliminate it from the previous equation, by defining a new system state called the adjoint state, ψ^*.

In this paper, we present only the results of the adjoint approach. The reader is referred to Neupauer and Wilson (1999) for a complete description of the approach. The governing equation for the backward model is the adjoint of the advection-dispersion equation, Eq. (3.1), given by (Neupauer and Wilson, 1999)

$$\frac{\partial h(\alpha, C^r)}{\partial C^r} + \frac{\partial \psi^*}{\partial t} + D\frac{\partial^2 \psi^*}{\partial x^2} + v\frac{\partial \psi^*}{\partial x} = 0 \ , \tag{3.11}$$

where ψ^* is the adjoint state. If (3.1) is the appropriate governing equation for the forward model, location and travel time probabilities are both adjoint states of resident concentration and can be obtained by solving Eq. (3.11) with the appropriate expression for h, and with the appropriate boundary and final conditions on ψ^*.

The boundary conditions on the adjoint state depend on the aquifer geometry and on the boundary conditions of the forward model. They are selected so that unknown terms vanish from the expression (Neupauer and Wilson, 1999):

$$\left[D\psi^* \frac{\partial \psi}{\partial x} - D\psi \frac{\partial \psi^*}{\partial x} - v\psi^* \psi \right] \Bigg|_{x_1}^{x_2} , \tag{3.12}$$

where $x_1 \to -\infty$ and $x_2 \to \infty$ for the infinite domain problem. For the forward

problem shown in Eq. (3.1), the boundary conditions are $\psi \to 0$ as $x \to \pm\infty$. After substituting these conditions into Eq. (3.12), we have two remaining non-zero terms that must vanish, so we set

$$D\psi^* \frac{\partial \psi}{\partial x}\bigg|_{x\to\infty} = 0 \tag{3.13}$$

$$D\psi^* \frac{\partial \psi}{\partial x}\bigg|_{x\to-\infty} = 0. \tag{3.14}$$

These terms vanish if we set $\psi^*(x,t) \to 0$ as $x \to \pm\infty$; therefore, these are the boundary conditions on ψ^*.

The final condition on ψ^* is defined so that the terms with unknown quantities vanish from the following expression (Neupauer and Wilson, 1999):

$$(\psi^*\psi)\Big|_0^T , \tag{3.15}$$

where T is the detection time. From the forward problem, $\psi(x,0) = 0$, leaving one remaining non-zero term that must vanish, giving $\psi^*\psi = 0$ at $t = T$. This term vanishes if the final condition on ψ^* is $\psi^*(x,T) = 0$.

The remaining unknown term in the adjoint equation is the load term, $\partial h/\partial C^r$, which acts as a source of probability. This is a Fréchet derivative (Saaty, 1981; see also Appendix D of Neupauer and Wilson, 1999) of the performance functional, h, with respect to C^r. The form of h depends on the type of probability. Next we define the appropriate h for location and travel time probabilities.

3.3.1 Location Probability

Since location probability is related to resident concentration, the appropriate performance measure, P, for location probability is the resident concentration at the detection location, x_d, at the time of sampling, T (Neupauer and Wilson, 1999). The appropriate performance functional leading to this P is $h = C^r(x,t)\delta(x - x_d)\delta(t - T)$, and the Fréchet derivative of h with respect to C^r is (Neupauer and Wilson, 1999)

$$\frac{\partial h(\alpha, C^r)}{\partial C^r} = \delta(x - x_d)\delta(\tau) \; , \tag{3.16}$$

where $\tau = T - t$ is backward time, or time prior to detection, and the sampling time is $t = T$ or $\tau = 0$.

For location probability, the complete adjoint equation and its boundary and initial (in τ) conditions are

$$\begin{aligned} \frac{\partial \psi^*}{\partial \tau} - D\frac{\partial^2 \psi^*}{\partial x^2} - v\frac{\partial \psi^*}{\partial x} &= \delta(x - x_d)\delta(\tau) \; , \\ \psi^*(x,\tau) \to 0 \quad &\text{as} \quad x \to \pm\infty \\ \psi^*(x,0) &= 0 \; , \end{aligned} \tag{3.17}$$

This equation can be solved using Fourier and Laplace transforms, and the solution is (Appendix 3.A)

$$\psi^* = f_x(x;\tau) = \frac{1}{\sqrt{4\pi D\tau}} \exp\left\{ -\frac{(x - x_d + v\tau)^2}{4D\tau} \right\} \; , \tag{3.18}$$

which is a Gaussian function that moves backward in time and space, away

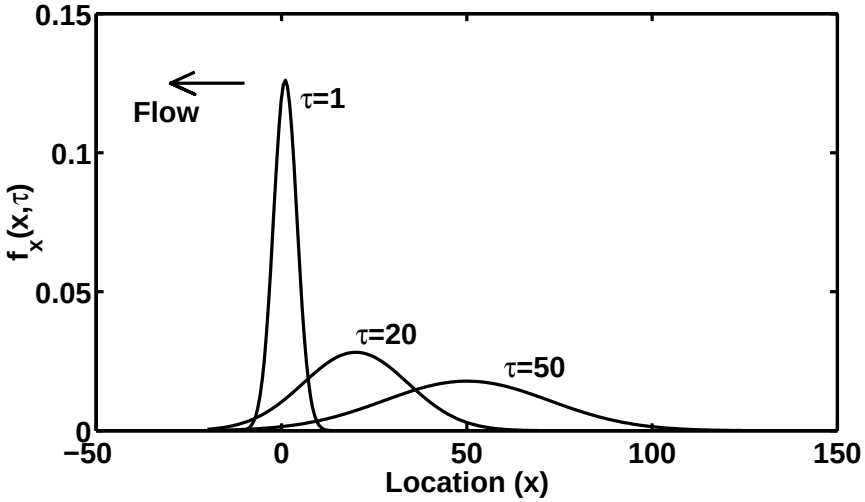

Figure 3.4: Backward location probability for contamination detected at $x_d = 0$ at backward time $\tau = 0$.

from the detection.

Suppose contamination is detected at a monitoring well at $x_d = 0$. The prior location probability of the detected contamination at $\tau = 1$, 20, and 50 is plotted in Fig. 3.4. The mostly likely prior locations of the contamination are $x = 1$ at $\tau = 1$, $x = 20$ at $\tau = 20$, and $x = 50$ at $\tau = 50$.

3.3.2 Travel Time Probability

Since normalized mass flux, vC^f, is related to travel time probability, Neupauer and Wilson (1999) showed that the appropriate performance measure, P, is the normalized mass flux at the detection location at the time of sampling. The performance functional, h, for travel time probability is $h = vC^f\delta(x - x_d)\delta(t - T)$, and the load term on the adjoint equation would be the Fréchet derivative of h with respect to C^r. Because the load represents

a source of probability, it must always be positive; therefore, the complete expression for h is $h = |vC^f|\delta(x - x_d)\delta(t - T)$, where the vertical bars denote absolute value. Neupauer and Wilson (1999) assumed positive velocity; although their form of h was correct for the case they presented, the form using absolute value is more general. Flux concentration is positive if mass flux is in the direction of water flux (i.e., advective flux dominates over dispersive flux), therefore $|vC^f| = |v|C^f$. Using this relationship and Eq. (3.5) in the expression for h, we obtain

$$h(\alpha, C^r) = \left[|v|C^r(x,t) - D\frac{v}{|v|}\frac{\partial C^r}{\partial x}\right]\delta(x - x_d)\delta(t - T)\ , \tag{3.19}$$

where we substituted $v/|v| = |v|/v$. The Fréchet derivative of (3.19) with respect to C^r is (Neupauer and Wilson, 1999)

$$\frac{\partial h(\alpha, C^r)}{\partial C^r} = |v|\delta(x - x_d)\delta(\tau) + D\frac{v}{|v|}\delta'(x - x_d)\delta(\tau)\ , \tag{3.20}$$

where $\delta'(x)$ is the derivative with respect to x of the Dirac delta function, and we have substituted $\tau = T - t$. The complete adjoint equation and its boundary and initial (in τ) conditions for travel time probability are given by

$$\begin{aligned} \frac{\partial \psi^*}{\partial \tau} - D\frac{\partial^2 \psi^*}{\partial x^2} - v\frac{\partial \psi^*}{\partial x} &= |v|\delta(x - x_d)\delta(\tau) + D\frac{v}{|v|}\delta'(x - x_d)\delta(\tau)\ , \\ \psi^*(x,\tau) &\to 0 \quad \text{as} \quad x \to \pm\infty \\ \psi^*(x,0) &= 0\ . \end{aligned} \tag{3.21}$$

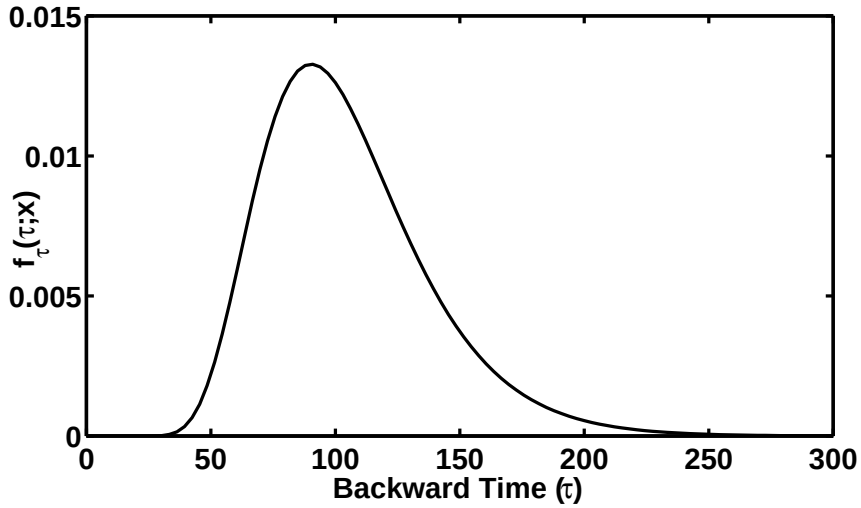

Figure 3.5: Backward travel time probability from $x = 100$ to a monitoring well at $x_d = 0$.

This equation can be solved using Fourier and Laplace transforms, and the solution is (Appendix 3.B)

$$\psi^* = f_\tau(\tau; x) = \frac{-v(x - x_d - v\tau)}{4|v|\sqrt{\pi D\tau^3}} \exp\left\{-\frac{(x - x_d + v\tau)^2}{4D\tau}\right\} . \qquad (3.22)$$

For contamination that is detected at a monitoring well at $x_d = 0$, the travel time probability from $x = 100$ to the monitoring well is plotted in Fig. 3.5. The most likely travel time from $x = 100$ to the well at $x_d = 0$ is $\tau \approx 91$.

Suppose we are interested in the travel time probability to $x_d = 0$ from any source. Fig. 3.3 shows the results of a forward modeling approach to obtain this information. With five forward simulations, we determined the probability that $t = 100$ from five different sources. The results of one backward

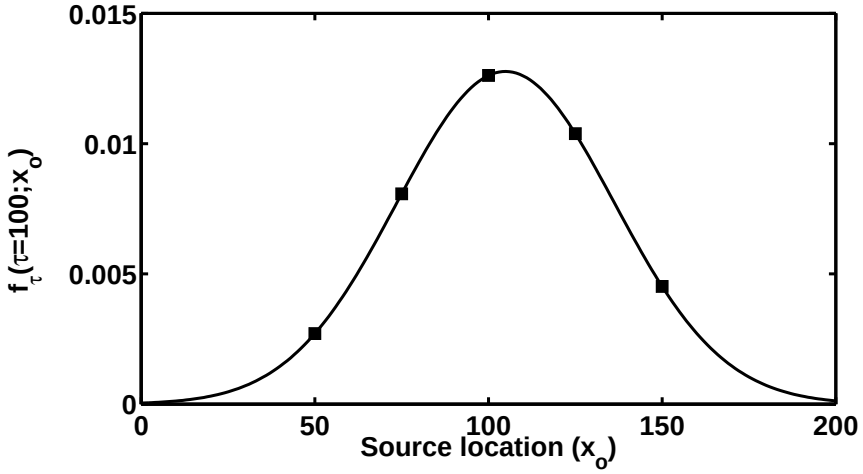

Figure 3.6: Backward travel time probability to $x = 0$ from several source locations. Squares denote the probability that $\tau = 100$ for source locations $x_o = 50, 75, 100, 125$, and 150.

simulation for travel time probability are plotted in Fig. 3.6, which shows the probability that $\tau = 100$ from any source location to $x_d = 0$. The squares denote $f_\tau(\tau; x)$ for the source locations shown in Fig. 3.3. Note that with one simulation of the backward model we obtained more information than with five simulations of a forward model. This plot shows that a contaminant parcel released at $x_o = 105$ is more likely to reach the monitoring well at $\tau = 100$ than parcels released from other upstream or downstream sources.

3.4 Conclusions

Backward-in-time location and travel time probabilities can be developed from the forward-in-time resident and flux concentration distributions, as Wilson and Liu (1995) and Neupauer and Wilson (1999) showed for a one-dimensional, semi-infinite domain using a heuristic approach and adjoint the-

ory, respectively. The semi-infinite domain represents one-dimensional flow to a pumping well, and the backward probabilities are obtained for contamination detected at the pumping well. In this paper, we illustrated the adjoint approach for obtaining backward location and travel time probabilities for contamination detected at a monitoring well, modeled as an internal point in a one-dimensional, infinite domain. This model is the adjoint of the classical Gaussian plume model. We obtained analytical expressions for the backward probabilities, and these can be used to validate higher dimensional numerical solutions of the backward model.

Backward-in-time probabilities can provide information about the position of the contamination before it was detected. They have a variety of applications, including source characterization, source identification, and capture zone delineation. The benefit of the backward model is that, for each detection, we solve the adjoint equation only once to obtain the backward-in-time location probability for all prior locations at a given time. Thus, if we have a few detections and many known or possible source locations, the backward model is computationally more efficient than the forward model in that fewer simulations must be run (i.e., one simulation for each detection). However, if we have many detections and only a few possible source locations, the forward model is more computationally efficient than the backward model because forward modeling results produce information about all possible future locations of contamination.

Acknowledgments

This research was supported in part by the Geophysical Research Center at New Mexico Tech and in part by the Environmental Protection Agency's STAR Fellowship program under Fellowship No. U-915324-01-0. This work has not been subjected to the EPA's peer and administrative review and therefore may not necessarily reflect the views of the Agency and no official endorsement should be inferred.

3.A Solution to the Adjoint Equation for Location Probability

Taking the Fourier transform in space of Eq. (3.17) and its initial condition gives

$$\begin{aligned} \frac{d\Psi}{d\tau} - D(i\lambda)^2\Psi - vi\lambda\Psi &= e^{-i\lambda x_d}\delta(\tau) \\ \Psi(\lambda, 0) &= 0 \end{aligned} \tag{3.23}$$

where Ψ is the transformed state of ψ^*, and λ is the transform variable. Taking the Laplace transform in time of Eq. (3.23), using the initial condition, and rearranging yields

$$\hat{\Psi} = \frac{e^{-i\lambda x_d}}{s + D\lambda^2 - vi\lambda} \, . \tag{3.24}$$

where $\hat{\Psi}$ is the transformed state of Ψ and s is the transform variable. After taking the inverse Laplace transform of this equation, we have

$$\Psi = \exp\left\{-D\tau\lambda^2 + (v\tau - x_d)i\lambda\right\} \, . \tag{3.25}$$

The expression for the adjoint state, ψ^*, can be obtained by taking the inverse Fourier transform of Ψ, given by

$$\psi^* = \frac{1}{2\pi}\int_{-\infty}^{\infty} \exp\left\{-D\tau\left[\lambda^2 - \frac{(x - x_d + v\tau)i\lambda}{D\tau}\right]\right\} d\lambda \, . \tag{3.26}$$

After completing the square in the exponent and evaluating the integral, this reduces to the final expression for backward location probability shown in

Eq. (3.18).

3.B Solution to the Adjoint Equation for Travel Time Probability

Taking the Fourier transform in space of Eq. (3.21) and its initial condition gives

$$\begin{aligned} \frac{d\Psi}{d\tau} - D(i\lambda)^2\Psi - vi\lambda\Psi &= |v|e^{-i\lambda x_d}\delta(\tau) + Di\lambda\frac{v}{|v|}e^{-i\lambda x_d}\delta(\tau) \qquad (3.27) \\ \Psi(\lambda,0) &= 0 \end{aligned}$$

where Ψ is the transformed state of ψ^*, and λ is the transform variable. Taking the Laplace transform in time of Eq. (3.27), using the initial condition, and rearranging gives

$$\hat{\Psi} = \frac{(|v| + Di\lambda v/|v|)e^{-i\lambda x_d}}{s + D\lambda^2 - vi\lambda} \; . \qquad (3.28)$$

where $\hat{\Psi}$ is the transformed state of Ψ and s is the transform variable. After taking the inverse Laplace transform of this equation, we have

$$\Psi = \left(|v| + Di\lambda\frac{v}{|v|}\right)\exp\left\{-D\tau\lambda^2 + (v\tau - x_d)i\lambda\right\} \; . \qquad (3.29)$$

The expression for the adjoint state, ψ^*, can be obtained by taking the inverse Fourier transform of Ψ, defined as

$$\begin{aligned} \psi^* &= \frac{|v|}{2\pi}\int_{-\infty}^{\infty}\exp\left\{-D\tau\lambda^2 + (v\tau + x - x_d)i\lambda\right\}\, d\lambda \qquad (3.30) \\ &\quad + \frac{Div}{2\pi|v|}\int_{-\infty}^{\infty}\lambda\exp\left\{-D\tau\lambda^2 + (v\tau + x - x_d)i\lambda\right\}\, d\lambda \; . \end{aligned}$$

The first integral is equivalent to the product of $|v|$ and Eq. (3.26); therefore

the first integral evaluates to the product of $|v|$ and Eq. (3.18).

The second term, (T2), can be evaluated by first completing the square in the exponent and writing the result as a sum of two integrals:

$$\begin{aligned}(\mathrm{T2}) \;=\; & \frac{Div}{2\pi|v|}\exp\left\{-\frac{(x-x_d+v\tau)^2}{4D\tau}\right\} \\ & \left\{\int_{-\infty}^{\infty}\left(\lambda-\frac{(x-x_d+v\tau)i}{2D\tau}\right)\exp\left[-D\tau\left(\lambda-\frac{(x-x_d+v\tau)i}{2D\tau}\right)^2\right]\,d\lambda\right. \\ & \left.+\frac{(x-x_d+v\tau)i}{2D\tau}\int_{-\infty}^{\infty}\exp\left[-D\tau\left(\lambda-\frac{(x-x_d+v\tau)i}{2D\tau}\right)^2\right]\,d\lambda\right\}.\end{aligned} \tag{3.31}$$

The first integral is the product of an even function and an odd function, which integrates to zero, and the second integral evaluates to

$$(\mathrm{T2}) = \frac{-v(x-x_d+v\tau)}{4|v|\sqrt{\pi D\tau^3}}\exp\left\{-\frac{(x-x_d+v\tau)^2}{4D\tau}\right\}. \tag{3.32}$$

The final expression for backward travel time probability is the sum of Eq. (3.32) and the product of $|v|$ and Eq. (3.18), which is shown in Eq. (3.22).

References

Abramowitz, M. and I.A. Stegun, *Handbook of Mathematical Functions*, Dover Publications, Inc., New York, 1972.

Bagtzoglou, A.C., D.E. Dougherty, and A.F.B. Thompson, Application of particle methods to reliable identification of groundwater pollution sources, *Water Resources Management*, 6, 15–23, 1992.

Bear, J., *Dynamics of Fluids in Porous Media*, American Elsevier Publishing Company, New York, 1972.

Carslaw, H.S. and J.C. Jaeger, *Conduction of Heat in Solids*, 2nd ed., Clarendon Press, Oxford, 1959.

Chin, D.A. and P.V.K. Chittaluru, Risk management in wellhead protection, *J. Water Resour. Plan. Manage.*, 120(3), 294–315. 1994.

Liu, J., *Travel time and location probabilities for groundwater contaminant sources*, Master's thesis, New Mexico Institute of Mining and Technology, Socorro, 1995.

Liu, J. and J.L. Wilson, Modeling travel time and source location probabilities in two-dimensional heterogeneous aquifer. *Proceedings 5th Annual WERC Technology Development Conference*, New Mexico State University, Las Cruces, New Mexico, 59–67, 1995.

Neupauer, R.M. and J.L. Wilson, Adjoint method for obtaining backward-in-time location and travel time probabilities of a conservative groundwater contaminant, *Water Resour. Res.*, 35(11), 3389–3398, 1999.

Parker, J.C. and M. Th. van Genuchten, Flux-averaged and volume-averaged concentrations in continuum approaches to solute transport, *Water Resour. Res.*, 20(7), 866–872, 1984.

Saaty, T.L., 1981. Modern Nonlinear Equations. Dover Publications, Inc., New York.

Sun, N.-Z. and W.W.-G. Yeh, Coupled inverse problems in groundwater modeling, 1, Sensitivity analysis and parameter identification, *Water Resour. Res.*, 26(10), 2507–2525, 1990.

Sykes, J.F., J.L. Wilson, and R.W. Andrews, Sensitivity analysis for steady state groundwater flow using adjoint operators, *Water Resour. Res.*, 21(3), 359–371, 1985.

Uffink, G.J.M., Application of Kolmogorov's backward equation in random walk simulations of groundwater contaminant transport, in *Contaminant Transport in Groundwater*, H.E. Kobus and W. Kinzelbach, editors, pp. 283–289, A.A. Balkema, Brookfield, Vt., 1989.

Wilson, J.L. and J. Liu, Backward tracking to find the source of pollution, in *Waste-management: From Risk to Remediation*, edited by R. Bhada *et al.*, EDM Press, Albuquerque, NM, 181–199, 1994.

Wilson, J.L. and J. Liu, Field Validation of the Backward-in-time Advection Dispersion Theory. *Proceedings of the 1996 HSRC/WERC Joint Conf. on the Environment*, Great Plains-Rocky Mountain Hazardous Substance Center, Manhattan, Kansas, http://www.engg.ksu.edu/HSRC/ 96Proceed/wilson.html, 1997.

CHAPTER 4

ADJOINT METHOD FOR OBTAINING MULTI-DIMENSIONAL BACKWARD PROBABILITY MODELS[1]

Abstract

Backward location and travel time probabilities can be used to determine the former location of contamination in an aquifer. For a contaminant parcel that was detected in an aquifer, the backward location probability describes its position at some time prior to sampling, and the backward travel time probability describes the amount of time required for it to travel to the sampling location from some upgradient position. These probabilities, which can provide information about the source of contamination, are related to adjoint states of resident concentration. The governing equations of the backward probabilities are adjoints of the forward governing equation, e.g., the advection-dispersion equation. We derive these backward governing equations and their boundary and final conditions for both location and travel time probabilities in a multi-dimensional system. Each governing equation contains the adjoint of the advection-dispersion operator and a load term that defines the particular adjoint state (probability). The load term depends on both the type of probability (location or travel time) and the sampling device (pumping well or monitoring well) with which the contamination was detected. The adjoint equation can also be used to efficiently determine forward location and travel time probabilities describing the future location of groundwater contamination,

[1]This chapter has been accepted for publication in *Water Resources Research*: Neupauer, R.M. and J.L. Wilson, Adjoint-derived location and travel time probabilities for a multi-dimensional groundwater system, *Water Resourc. Res.*, in press.

a feature most useful for delineating pumping well captures zones. We illustrate the use of the backward model for obtaining location and travel time probabilities in a hypothetical two-dimensional domain.

4.1 Introduction

When contamination is detected in an aquifer, the source of contamination is often unknown. To address aquifer remediation or to assign responsibility we might want to answer questions such as: "Where is the contamination source?" or "When was the contamination released from the source?" A common modeling approach to answer these questions is to run one forward simulation for each potential source, modeling the movement of the contamination away from the source (forward modeling). If the number of potential sources is large, this approach can result in a significant computational burden since one simulation must be run for each potential source. Furthermore, all potential sources must be identified.

Backward modeling [*Wilson and Liu*, 1994, 1997] is a more efficient approach for answering these questions. With backward modeling we solve for the probability of the former position of the contamination (location probability) or for the probability of the contaminant's travel time from some upgradient location to the sampling location (travel time probability). With one backward simulation we obtain these probabilities for all locations. This reduces the computational burden of forward modeling and is not limited to the pre-identified possible source locations. Not only can backward location and travel time probabilities be used to improve characterization of known sources of groundwater contamination or to identify previously unknown contamina-

tion sources, but a backward model can also be used to efficiently compute forward travel time probabilities that delineate capture zones.

Location and travel time probabilities are often used in forward modeling to describe solute transport in groundwater [e.g., *Dagan*, 1982, 1987; *Jury*, 1982; *Jury and Roth*, 1990; *Chin and Chittaluru*, 1994]. Forward location probability describes the position of a solute parcel at a fixed time after its release from the source [*Dagan*, 1982, 1987, 1989; *Jury and Roth*, 1990; *Chin and Chittaluru*, 1994] and is related to resident concentration [*Dagan*, 1987; *Jury and Roth*, 1990]. The normalized concentration distribution at some time t after release from an instantaneous point source is equivalent to the location probability density function at time t, given by

$$f_{\mathbf{x}}(\mathbf{x};t) = \frac{C(\mathbf{x},t)}{\int_{\Omega} C(\mathbf{x},0^{+})\, d\Omega}, \tag{4.1}$$

where $f_{\mathbf{x}}(\mathbf{x};t)$ is location probability at time t, $\mathbf{x}$ is the position vector, $C(\mathbf{x},t)$ is the resident concentration distribution from an instantaneous point source, Ω is the spatial domain, and $\int_{\Omega} C(\mathbf{x},0^{+})\, d\Omega = M'$, where M' is a measure of the total mass that entered the system.

Forward travel time probability describes the time required for a solute parcel to travel from its source to a location of interest [*Jury*, 1982; *Jury et al.*, 1986; *Dagan*, 1989; *Dagan and Nguyen*, 1989], and is related to flux concentration [*Shapiro and Cvetkovic*, 1988; *Rubin and Dagan*, 1992]. For an instantaneous point source of contamination, the normalized flux concentration at a downgradient location, $\mathbf{x}$, is equivalent to the travel time probability

density function for that location, given by

$$f_t(t;\mathbf{x}) = \frac{v(\mathbf{x})A(\mathbf{x})C^f(\mathbf{x},t)}{M'} \,, \tag{4.2}$$

where $f_t(t;\mathbf{x})$ is travel time probability from the source to $\mathbf{x}$, v is the magnitude of the groundwater velocity, $C^f(\mathbf{x},t)$ is flux concentration, A is the flow area across which flux concentration is defined, and M' is the same measure of total mass described above.

For a conservative solute in a one-dimensional domain, all mass that was released at the source must eventually pass all downgradient points provided there are no intermediate sinks; for this case $\int_t f_t(t;x)\ dt = 1$ for all x downgradient of the source. Most work dealing with travel time probability in multiple dimensions addresses travel time to a control plane extending across the entire domain, where all pathlines intersect the control plane [e.g., *Shapiro and Cvetkovic*, 1988 *Dagan*, 1989; *Dagan and Nguyen*, 1989; *Naff*, 1992; *Rubin and Dagan*, 1992]. In these studies $\int_t f_t(t;\mathbf{x})\ dt = 1$ on the control plane, since all mass must eventually cross the control plane in these models.

Since location probability is related to resident concentration and travel time probability is related to flux concentration, the relationship between the two probabilities can be easily obtained from the relationship between the two concentrations (e.g., in one dimension, $C^f = C - (D/v)\,\partial C/\partial s$ where D is the dispersion coefficient and s is the flow direction [*Parker and van Genuchten*, 1984]). Also, if concentration is modeled with the advection-dispersion equation (ADE), probability can also be modeled with the ADE.

In forward modeling we model the movement of solute (or probabil-

ity) downgradient away from the contamination source and obtain information about the future position of the contamination. With backward modeling we treat the sampling location as a source of probability (there is a probability of one that the contamination was at the sampling location at the time of sampling) and allow the probability to advect upgradient in backward time and to spread out by dispersion, resulting in a plume of backward probability that gives us information about the former position of contamination. For a solute parcel that was detected in the groundwater, backward location probability describes its position at some time prior to sampling, and travel time probability describes the amount of time required for the solute parcel to travel to the sampling location from some upgradient position, such as a known or suspected contamination source. Since this source has a limited size there is a finite probability that a solute parcel detected at the sampling location did not originate from this source, but from some place else. Therefore, with backward travel time probability in multi-dimensional domains, $\int_\tau f_\tau(\tau;\mathbf{x})\ d\tau < 1$ for any $\mathbf{x}$, where τ denotes backward time or time prior to sampling. This is unlike previous work [e.g., *Shapiro and Cvetkovic*, 1988 *Dagan*, 1989; *Dagan and Nguyen*, 1989; *Naff*, 1992; *Rubin and Dagan*, 1992] that considered travel time probability to a control plane that intersected all pathlines; however, if the control plane did not extend across the entire transverse extent of the domain, there would be a finite probability of missing the control plane and we would have $\int_t f_t(t;\mathbf{x})\ dt < 1$ along the control plane.

The uncertainty in the former position of the particle is characterized by the spread of the probability plume and depends on dispersion. Dispersion accounts for the unmodeled spatial variability in groundwater velocity and

for the spatial heterogeneity that causes different portions of the contaminant plume to sample different local velocities. It can be quantified by a dispersion coefficient that reflects both the length scale and variance of the velocity field. At early times, when the travel distance of a contaminant particle is small relative to the length scale of the velocity field, the particle continually samples new scales of heterogeneity as it travels through the aquifer. Thus, the degree of dispersion depends on the particle's travel distance or travel time, and the dispersion coefficient is scale-dependent. Over a sufficiently long period of time, all portions of the plume will sample all scales of velocity variations, and the dispersion coefficient approaches an asymptotic value [*Dagan*, 1990]. This occurs when the travel distance of the particles exceeds the length scale of the velocity variations. In this paper, we use the asymptotic (non-scale-dependent) approximation to the dispersion coefficient, although the model can be modified for scale-dependent dispersion, if desired. Thus, the calculations here assume that the degree of variability in the velocity field is known, and that the length scale of variability is less than the length scale of the problem.

The governing equation of the backward model is similar to the forward model for contaminant transport with some modifications to account for the upgradient movement of probability. By reversing the flow field in a random walk method, *Bagtzoglou et al.* [1992] obtained backward location probabilities for identifying sources of contamination. *Uffink* [1989] and *Chin and Chittaluru* [1994] used a similar random walk approach to delineate capture zones around pumping wells. *Wilson and Liu* [1994, 1997] used a heuristic method to obtain a backward probabilistic continuum model from the forward advection-dispersion equation. The approach was validated using data from a

field-scale tracer experiment at the Borden site [*Wilson and Liu*, 1997]. As we show later, they obtained the correct form of the backward equation; however, their tracer test results and their backward model described forward probabilities which they misinterpreted as backward probabilities. Also, no formal justification was given for their model.

Neupauer and Wilson [1999] showed that backward location and travel time probabilities are related to adjoint states of resident concentration; therefore, the adjoint of a forward model is the appropriate model for backward probabilities. In groundwater hydrology, adjoint theory has been used in sensitivity analysis [*Sykes et al.*, 1985; *Wilson and Metcalfe*, 1985], parameter estimation [*Neuman*, 1980; *Sun and Yeh*, 1985, 1990; *Townley and Wilson*, 1985; *Lu et al.*, 1988; *Yeh and Sun*, 1990], optimal design [*Ahlfeld et al.*, 1988], and others applications (see *Sun* [1994]). In mathematics, adjoint theory can be employed in solving differential equations [e.g., *Zauderer*, 1989; *Zwillinger*, 1989]. The adjoint method provides a rigorous mathematical approach for obtaining the backward model, and it can be easily applied to complex problems. *Neupauer and Wilson* [1999] demonstrated the adjoint approach for obtaining the backward model of a one-dimensional system.

In this paper we extend the results of *Neupauer and Wilson* [1999] to multiple dimensions. We derive the adjoint of the multi-dimensional advection-dispersion equation, and use it to obtain the governing equation and initial and boundary conditions for backward location and travel time probabilities. There are many different adjoint states of concentration, and we show the relationship between backward probabilities and two particular adjoint states. We also explain the relationship between forward location and travel time probabilities

and these same two adjoint states. Each adjoint state is defined by a different load term on the governing equation, and we show that the appropriate load term depends on the type of probability (location or travel time) and the sampling device (monitoring well or pumping well), and we provide several examples of these. We limit our discussion to conservative solutes in a steady flow field. If other processes are considered, adjoint theory can easily be applied to obtain the backward (adjoint) model from the appropriate forward model.

4.2 Adjoint of the Multi-Dimensional Advection Dispersion Equation

The advection-dispersion equation (ADE) is a forward model of contaminant transport in groundwater. Its multi-dimensional form for a conservative chemical is

$$\frac{\partial C}{\partial t} = \frac{\partial}{\partial x_i}\left(D_{ij}\frac{\partial C}{\partial x_j}\right) - \frac{\partial}{\partial x_i}\left(v_i C\right) - \frac{q_O}{\theta}C + \frac{q_I}{\theta}C_I \ , \tag{4.3}$$

$$C(\mathbf{x},0) = C_o(\mathbf{x})$$

$$C(\mathbf{x},t) = g_1(t) \text{ on } \Gamma_1$$

$$D_{ij}\frac{\partial C}{\partial x_j}\mathrm{n}_i = g_2(t) \text{ on } \Gamma_2$$

$$\left(v_i C - D_{ij}\frac{\partial C}{\partial x_j}\right)\mathrm{n}_i = g_3(t) \text{ on } \Gamma_3$$

where $C(\mathbf{x},t)$ is resident concentration, t is time, x_i are the spatial directions $(i = 1,2,3)$, $\mathbf{x} = (x_1, x_2, x_3)$, θ is porosity, D_{ij} is the i,j^{th} entry of the dispersion tensor, v_i is the groundwater velocity in the direction of x_i, q_O is the outflow rate per unit volume, q_I is the inflow rate per unit volume, C_I is the source

strength, C_o is the initial concentration, g_1, g_2, and g_3 are known functions, Γ_1, Γ_2, and Γ_3 are the domain boundaries, and n_i is the outward unit normal vector in the x_i direction. Based on this equation, the advection-dispersion operator is

$$L[\,] = -\frac{\partial[\,]}{\partial t} + \frac{\partial}{\partial x_i}\left(D_{ij}\frac{\partial[\,]}{\partial x_j}\right) - \frac{\partial}{\partial x_i}\left(v_i[\,]\right) - \frac{q_O}{\theta}[\,]\,, \tag{4.4}$$

and (4.3) can be written as $L[C] = -q_I C_I/\theta$, where the right-hand side is called the load term.

The governing equation for the backward probability model is the adjoint of (4.3). We follow the sensitivity analysis approach of *Sykes et al.* [1985] for deriving the adjoint equation. In sensitivity analysis, a performance measure, P, that quantifies some state of the system is defined as

$$P = \iint_{\Omega,t} h(\alpha, C)\; d\Omega\; dt\,, \tag{4.5}$$

where $h(\alpha, C)$ is a functional of the state of the system, α is a parameter (such as v, D, q_I, or others), C is resident concentration, Ω is the spatial domain, and integration is over the entire space–time domain. The appropriate performance functionals, h, are defined later. The marginal sensitivity of this performance measure with respect to the parameter α is obtained by differentiating (4.5) with respect to α:

$$\frac{dP}{d\alpha} = \iint_{\Omega,t}\left[\frac{\partial h(\alpha, C)}{\partial \alpha} + \frac{\partial h(\alpha, C)}{\partial C}\psi\right]\; d\Omega\; dt \tag{4.6}$$

where $dP/d\alpha$ is the marginal sensitivity, ψ is the state sensitivity, $\psi = \partial C/\partial\alpha$, and $\partial h/\partial C$ is a Frèchet derivative (*Saaty* [1981], *Zwillinger*, [1989]) of the functional h with respect to the function C (See Appendix D of *Neupauer and Wilson* [1999] for a derivation of this Frèchet derivative). The state sensitivity in (4.6) is unknown; therefore the marginal sensitivity cannot be obtained directly from that equation. Instead, adjoint theory can be used to eliminate the unknown ψ, and the marginal sensitivity can be obtained in terms of the adjoint state. With judicious choices of h and α, the marginal sensitivity is equivalent to the adjoint state, and is related to location or travel time probability, as we discuss later.

To eliminate ψ from (4.6), we first obtain a governing equation for ψ by differentiating the terms in (4.3) with respect to the parameter α, yielding

$$-\frac{\partial\psi}{\partial t}+\frac{\partial}{\partial x_i}\left(D_{ij}\frac{\partial\psi}{\partial x_j}\right)-\frac{\partial}{\partial x_i}\left(v_i\psi\right)-\frac{q_O}{\theta}\psi=L_\alpha \tag{4.7}$$

$$\psi(\mathbf{x},0)=\frac{\partial C_o}{\partial\alpha}$$

$$\psi(\mathbf{x},t)=0 \text{ on } \Gamma_1$$

$$\left(D_{ij}\frac{\partial\psi}{\partial x_j}+\frac{\partial D_{ij}}{\partial\alpha}\frac{\partial C}{\partial x_j}\right)\mathrm{n}_i=0 \text{ on } \Gamma_2$$

$$\left(v_i\psi+\frac{\partial v_i}{\partial\alpha}C-D_{ij}\frac{\partial\psi}{\partial x_j}-\frac{\partial D_{ij}}{\partial\alpha}\frac{\partial C}{\partial x_j}\right)\mathrm{n}_i=0 \text{ on } \Gamma_3$$

where L_α contains the remaining terms, all independent of ψ, given by

$$L_\alpha=-\frac{\partial}{\partial x_i}\left(\frac{\partial D_{ij}}{\partial\alpha}\frac{\partial C}{\partial x_j}\right)+\frac{\partial}{\partial x_i}\left(\frac{\partial v_i}{\partial\alpha}C\right)-\frac{\partial}{\partial\alpha}\left(\frac{q_I}{\theta}C_I\right)+C\frac{\partial}{\partial\alpha}\left(\frac{q_O}{\theta}\right)\ . \tag{4.8}$$

The governing equation for the backward probability model is the adjoint of

(4.7). In (4.7), g_1, g_2, and g_3 are assumed to be independent of α, although this assumption is not necessary for the adjoint method. In the backward probability model presented here, the parameter α is related to the contamination source; therefore the derivatives of D_{ij}, v_i, q_I, q_O, θ, and C_I with respect to α all vanish, and $L_\alpha = 0$.

Next we take the inner product of each remaining term in (4.7) with respect to an arbitrary function, ψ^*. We see later that this function is the adjoint state. The inner product in the space of continuous, square-integrable, real functions is defined as $<f, g> = \int\int_{\Omega,t} f\, g\, d\Omega\, dt$. This inner product yields

$$\int\int_{\Omega,t} \left\{ -\psi^* \frac{\partial \psi}{\partial t} + \psi^* \frac{\partial}{\partial x_i}\left(D_{ij} \frac{\partial \psi}{\partial x_j} \right) - \psi^* \frac{\partial}{\partial x_i}\left(v_i \psi \right) - \psi^* \frac{q_O}{\theta} \psi \right\} d\Omega\, dt = 0 \; . \quad (4.9)$$

Since the left-hand side of this equation evaluates to zero, we can add it to the right-hand side of (4.6) without changing the equality. Performing this addition, after using the product rule once on each of the first derivative terms and twice on the second derivative term and rearranging terms, we obtain

$$\begin{aligned} \frac{dP}{d\alpha} \;=\; & \int\int_{\Omega,t} \left\{ \frac{\partial h(\alpha, C)}{\partial \alpha} + \psi \left[\frac{\partial h}{\partial C} + \frac{\partial \psi^*}{\partial t} + \frac{\partial}{\partial x_i}\left(D_{ij} \frac{\partial \psi^*}{\partial x_j} \right) + v_i \frac{\partial \psi^*}{\partial x_i} - \frac{q_O}{\theta} \psi^* \right] \right. \\ & \left. - \frac{\partial}{\partial t}\left(\psi \psi^* \right) + \frac{\partial}{\partial x_i}\left[\psi^* D_{ij} \frac{\partial \psi}{\partial x_j} - \psi D_{ij} \frac{\partial \psi^*}{\partial x_j} - v_i \psi \psi^* \right] \right\} d\Omega\, dt \; , \quad (4.10) \end{aligned}$$

where we used the fact that the dispersion tensor is symmetric.

The goal of this exercise was to eliminate the unknown ψ from the marginal sensitivity equation (4.10) by appropriately defining a new function,

ψ^*. The second term in the integral can be eliminated if we define

$$L^*[\psi^*] = \frac{\partial \psi^*}{\partial t} + \frac{\partial}{\partial x_i}\left(D_{ij}\frac{\partial \psi^*}{\partial x_j}\right) + v_i\frac{\partial \psi^*}{\partial x_i} - \frac{q_O}{\theta}\psi^* = -\frac{\partial h}{\partial C}\ . \tag{4.11}$$

This equation is the adjoint equation; $L^*[\ ]$ is the adjoint operator of (4.4), and ψ^* is an adjoint state.

The remaining terms in (4.10) that contain ψ are the spatial and temporal divergence terms. We define the boundary and final conditions on the adjoint state ψ^* such that these terms containing unknown values of ψ vanish. Integrating the temporal divergence term over the time domain and applying Gauss' divergence theorem ($\int_\Omega \nabla \cdot F\ d\Omega = \int_\Gamma F \cdot \mathbf{n}\ d\Gamma$, where $\mathbf{n}$ is the outward normal direction on the boundary Γ) to the spatial divergence terms results in

$$\begin{aligned}\frac{dP}{d\alpha} = &\iint_{\Omega,t} \frac{\partial h(\alpha, C)}{\partial \alpha}\ d\Omega\ dt - \int_\Omega \left(\psi\psi^*\right)\Big|_{t=0}^{t=t_f}\ d\Omega \\ &+ \iint_{\Gamma,t}\left[\psi^* D_{ij}\frac{\partial \psi}{\partial x_j} - \psi D_{ij}\frac{\partial \psi^*}{\partial x_j} - v_i\psi\psi^*\right]\mathrm{n}_i\ d\Gamma\ dt\ ,\end{aligned} \tag{4.12}$$

where t_f is the final time of the time domain and is equal to the time of sampling. Substituting the initial and boundary conditions on ψ from (4.7), which are known values, we obtain

$$\frac{dP}{d\alpha} = \iint_{\Omega,t} \frac{\partial h(\alpha, C)}{\partial \alpha}\, d\Omega\, dt - \int_{\Omega} \left[(\psi\psi^*)\Big|_{t=t_f} - \left(\psi^* \frac{\partial C_o}{\partial \alpha} \right)\Big|_{t=0} \right] d\Omega \qquad (4.13)$$
$$+ \iint_{\Gamma_1,t} \left[\psi^* D_{ij} \frac{\partial \psi}{\partial x_j} \right] \mathrm{n}_i\, d\Gamma_1\, dt - \iint_{\Gamma_2,t} \left[\psi D_{ij} \frac{\partial \psi^*}{\partial x_j} + v_i \psi\psi^* \right] \mathrm{n}_i\, d\Gamma_2\, dt$$
$$- \iint_{\Gamma_3,t} \left[\psi D_{ij} \frac{\partial \psi^*}{\partial x_j} \right] \mathrm{n}_i\, d\Gamma_3\, dt\,.$$

Several integrals still contain unknowns (e.g., $\psi(\mathbf{x}, t_f)$, $\psi^*(\mathbf{x}, t_f)$, and $\psi^*(\mathbf{x}, t)$ on Γ_1). Since the boundary conditions (on Γ_1, Γ_2, and Γ_3) and final condition (at $t = t_f$) for the adjoint state, ψ^*, are still arbitrary, we can assign to them values that cause the remaining integrals to vanish. For the boundary integrals to vanish, we must have $\psi^*(\mathbf{x}, t) = 0$ on Γ_1, $[D_{ij}\partial\psi^*/\partial x_j + v_i\psi^*]\mathrm{n}_i = 0$ on Γ_2, and $[D_{ij}\partial\psi^*/\partial x_j]\mathrm{n}_i = 0$ on Γ_3. For the final condition, the integral over Ω must vanish, so the final condition on ψ^* must be $\psi^*(\mathbf{x}, t_f) = 0$.

We define a new time variable, backward time, $\tau = t_f - t$. The initial condition on ψ^* in backward time (at $\tau = 0$, or, equivalently, at $t = t_f$) is $\psi^*(\mathbf{x}, \tau) = 0$ at $\tau = 0$. The complete adjoint equation in terms of backward time, τ, with initial and boundary conditions as defined above, corresponding to those shown in (4.7), is

$$L^*[\psi^*] = -\frac{\partial \psi^*}{\partial \tau} + \frac{\partial}{\partial x_i}\left(D_{ij}\frac{\partial \psi^*}{\partial x_j}\right) + \frac{\partial}{\partial x_i}\left(v_i \psi^*\right) - \frac{q_I}{\theta}\psi^* = -\frac{\partial h}{\partial C} \qquad (4.14)$$

$$\psi^*(\mathbf{x}, 0) = 0$$

$$\psi^*(\mathbf{x}, \tau) = 0 \text{ on } \Gamma_1$$

$$\left[D_{ij}\frac{\partial \psi^*}{\partial x_j} + v_i \psi^*\right] \mathrm{n}_i = 0 \text{ on } \Gamma_2$$

$$\left[D_{ij}\frac{\partial \psi^*}{\partial x_j}\right] \mathrm{n}_i = 0 \text{ on } \Gamma_3 \ ,$$

where we have assumed steady flow, so $\nabla \cdot v = q_I/\theta - q_O/\theta$, thereby replacing the advection and sink terms in (4.11) with the advection and source terms in (4.14). With backward time τ in (4.14), the sign on the time derivative is reversed (compare with (4.11)).

Note that the adjoint of the first-type boundary condition is also first-type (boundary condition on Γ_1); the adjoint of the second-type boundary condition is third-type (boundary condition on Γ_2), and the adjoint of the third-type boundary condition is second-type (boundary condition on Γ_3). We have now defined the adjoint equation and the initial and boundary conditions of the adjoint state. The load term, $\partial h/\partial C$, is still arbitrary and we develop it in the next section.

4.3 Adjoint States and Probabilities

The adjoint equation was developed using the sensitivity analysis approach, based on a marginal sensitivity of a performance measure, P, to a system parameter, α. The equation defines a family of adjoint states, and the

particular adjoint state depends on the choice of the performance functional h in the load term. In this paper, we are interested in the adjoint states related to location probability and travel time probability. We use marginal sensitivity to define the appropriate performance functionals for these adjoint states.

Using the complete adjoint equation (4.14) in (4.13), the marginal sensitivity reduces to

$$\frac{dP}{d\alpha} = \int\int_{\Omega,t} \frac{\partial h(\alpha, C)}{\partial \alpha}\, d\Omega\, dt + \int_{\Omega} \psi^*(x, t=0) \frac{\partial C_o}{\partial \alpha} d\Omega\ , \tag{4.15}$$

showing the relationship between marginal sensitivity and the adjoint state. If we consider the sensitivity of P to an instantaneous point source anywhere in the aquifer, the marginal sensitivity is equivalent to the adjoint state. For an instantaneous point source of contamination, we can define $C_o(\mathbf{x}, t=0) = M'\delta(\mathbf{x}-\mathbf{x}_o)$, where M' is the source strength and $\mathbf{x}_o$ is the source location. Using $\alpha = M'$ and assuming h is independent of M', (4.15) becomes $dP/d\alpha = \psi^*(\mathbf{x}_o, t=0)$. For appropriate choices of P (or equivalently, h), this marginal sensitivity (adjoint state) is related to backward location or travel time probability. For these same choices of P, the marginal sensitivity is also related to the forward location and travel time probabilities shown in (4.1) and (4.2), respectively. In this section, we show the relationship between adjoint states and probabilities, and we present the appropriate performance functionals for each case.

4.3.1 Load Term for Location Probability

From (4.1), we see that location probability is related to resident concentration. Rearranging (4.1), we obtain $C(\mathbf{x}, t = t_f) = M' f_{\mathbf{x}}(\mathbf{x}; t = t_f, \mathbf{x}_o)$, where $f_{\mathbf{x}}(\mathbf{x}; t = t_f, \mathbf{x}_o)$ is the forward location probability describing the probability that a particle that was released from $\mathbf{x}_o$ will be at position $\mathbf{x}$ (random variable) at time $t = t_f$ ($\tau = 0$). It is useful to define forward location probability at a specific location, $\mathbf{x} = \mathbf{x}_w$, such as for a detection at a monitoring or pumping well. Taking the derivative of C at $\mathbf{x} = \mathbf{x}_w$ with respect to M', we obtain

$$\frac{dC(\mathbf{x}_w, t = t_f)}{dM'} = f_{\mathbf{x}}(\mathbf{x}_w; t = t_f, \mathbf{x}_o) = \psi^*_{\mathbf{x}}(\mathbf{x}_w, \tau = t_f - t = 0) \ , \qquad (4.16)$$

where $\psi^*_{\mathbf{x}}$ is the adjoint state for location probability. This equation shows that forward location probability is equivalent to the marginal sensitivity of resident concentration at the detection location to the source mass. If $P = C(\mathbf{x}_w, t = t_f)$ and $\alpha = M'$, the adjoint state, $\psi^*_{\mathbf{x}}$, represents forward location probability.

For a contaminant parcel that is detected at a well at location $\mathbf{x}_w$ at $\tau = 0$, let $f_{\mathbf{x}}(\mathbf{x}; \tau, \mathbf{x}_w)$ be its backward location probability, defined as the probability that the parcel was at some other location $\mathbf{x}$ (random variable) at some other time τ (deterministic parameter) in the past. Forward location probabilities and backward location probabilities represent the same processes from different points of view. The forward location probability at $\mathbf{x}_w$ due to a source at $\mathbf{x}_o$ represents the probability that contamination from $\mathbf{x}_o$ will be at $\mathbf{x}_w$ in the future; while the backward location probability at $\mathbf{x}_o$ due to a detection at $\mathbf{x}_w$ represents the probability that contamination at $\mathbf{x}_w$ was at $\mathbf{x}_o$

sometime in the past. In both cases, the solute must travel between the same two points and is affected by the same transport processes. Therefore, if there is a high probability that contamination from $\mathbf{x}_o$ will reach $\mathbf{x}_w$ (high forward location probability), then there is also a high probability that contamination detected at $\mathbf{x}_w$ was at $\mathbf{x}_o$ (high backward location probability). The backward location probability for any $(\mathbf{x}_o, \mathbf{x}_w)$ pair is proportional to the forward location probability for the same $(\mathbf{x}_o, \mathbf{x}_w)$ pair.

For a conservative solute in an infinite flow field with no internal sources or sinks of water, a contaminant parcel that is at $\mathbf{x}_o$ at $t = 0$ must also be in the system at $t = t_f$. Therefore, the integral of the forward location probability over all space at $t = t_f$ evaluates to one. Likewise, a contaminant parcel that was detected at $\mathbf{x}_w$ at $t = t_f$ ($\tau = 0$) must have been in the system at $t = 0$ ($\tau = t_f$). Therefore, the integral of the backward location probability over all space at $\tau = t_f$ evaluates to one.

Since forward location probability is proportional to backward location probability and since both probabilities integrate to the same value (one) over the spatial domain, forward location probability for a given $(\mathbf{x}_o, \mathbf{x}_w)$ pair must be equivalent to backward location probability for the same $(\mathbf{x}_o, \mathbf{x}_w)$ pair. It follows from (4.16) that backward location probability is equivalent to the adjoint state ($f_{\mathbf{x}}(\mathbf{x}; \tau, \mathbf{x}_w) = \psi^*_{\mathbf{x}}$) if $P = C(\mathbf{x}_w, t = t_f)$ and $\alpha = M'$. The performance functional, h, must be defined so that its integral over all space and time (4.5) evaluates to this average resident concentration. If we assume that a well can be approximated as a point in the x_1, x_2-plane, with some finite length

in the x_3-direction, then the appropriate performance functional is given by

$$h = C(\mathbf{x},t)\delta(x_1 - x_{1_w})\delta(x_2 - x_{2_w})\frac{B_{x_3}(x_{3_{wb}}, x_{3_{wt}})}{x_{3_{wt}} - x_{3_{wb}}}\delta(\tau)\ , \tag{4.17}$$

where x_{1_w} and x_{2_w} are the coordinates of the center of the well, $x_{3_{wb}}$ and $x_{3_{wt}}$ are the bottom and top elevations, respectively, of the well screen, $\delta(\cdot)$ is the Dirac delta function, and $B_{x_i}(a,b)$ is a boxcar function defined as

$$B_{x_i}(a,b) = \begin{cases} 1 & a < x_i < b \\ 0 & \text{otherwise}\ . \end{cases} \tag{4.18}$$

Integrating (4.17) over the space-time domain, as in (4.5), results in the average resident concentration in the well. The boxcar and Dirac delta functions in space in (4.17) force the integral to be evaluated only over the well volume; the normalizing factor $(x_{3_{wt}} - x_{3_{wb}})$ averages the concentration over the sampled volume; and the Dirac delta function in time causes the integral to be evaluated only at $\tau = 0$. With this h, the resulting load term on the adjoint equation (4.14) is

$$L^*[\psi^*_{\mathbf{x}}(\mathbf{x};\tau)] = -\frac{\partial h}{\partial C} = -\delta(x_1 - x_{1_w})\delta(x_2 - x_{2_w})\frac{B_{x_3}(x_{3_{wb}}, x_{3_{wt}})}{x_{3_{wt}} - x_{3_{wb}}}\delta(\tau)\ , \tag{4.19}$$

where the adjoint state, $\psi^*_{\mathbf{x}}$, is equivalent to location probability, $\psi^*_{\mathbf{x}}(\mathbf{x},\tau) = f_{\mathbf{x}}(\mathbf{x};\tau)$.

The load terms for location probability for one-, two-, and three-dimensional domains are shown in Table 4.1a. In one dimension and in two-dimensional (x_1, x_2) space, the load term is a product of Dirac delta functions;

Table 4.1: Typical load terms for the backward model. (a) Location probability and travel time probability with sampling at a pumping well. (b) Travel time probability with sampling at a monitoring well.

(a) Dimensions	Load Term, $\partial h/\partial C$	Eq. No.
3-D	$\delta(x_1-x_{1_w})\delta(x_2-x_{2_w})B_{x_3}(x_{3_{wb}},x_{3_{wt}})\delta(\tau)/(x_{3_{wt}}-x_{3_{wb}})$	(4.19)
2-D (x_1,x_2)	$\delta(x_1-x_{1_w})\delta(x_2-x_{2_w})\delta(\tau)$	
2-D (x_1,x_3)	$\delta(x_1-x_{1_w})B_{x_3}(x_{3_{wb}},x_{3_{wt}})\delta(\tau)/(x_{3_{wt}}-x_{3_{wb}})$	
1-D (x_1)	$\delta(x_1-x_{1_w})\delta(\tau)$	

(b) Dimensions	Load Term, $\partial h/\partial C$	Eq. No.
3-D	$\big[\delta(x_1-x_{1_w})\delta(x_2-x_{2_w})$ $+a_L(v_1/v)\delta'_{x_1}(x_1-x_{1_w})\delta(x_2-x_{2_w})$ $+a_L(v_2/v)\delta(x_1-x_{1_w})\delta'_{x_2}(x_2-x_{2_w})\big]$ $B_{x_3}(x_{3_{wb}},x_{3_{wt}})\delta(\tau)/(x_{3_{wt}}-x_{3_{wb}})$	(4.26)
2-D (x_1,x_2)	$\big[\delta(x_1-x_{1_w})\delta(x_2-x_{2_w})$ $+\ a_L(v_1/v)\delta'_{x_1}(x_1-x_{1_w})\delta(x_2-x_{2_w})$ $+a_L(v_2/v)\delta(x_1-x_{1_w})\delta'_{x_2}(x_2-x_{2_w})\big]\ \delta(\tau)$	
2-D (x_1,x_3)	$\Big[\delta(x_1-x_{1_w})+a_L(v_1/v)\delta'_{x_1}(x_1-x_{1_w})\Big]$ $B_{x_3}(x_{3_{wb}},x_{3_{wt}})\delta(\tau)/(x_{3_{wt}}-x_{3_{wb}})$	
1-D (x_1)	$\Big[\delta(x_1-x_{1_w})+a_L(v_1/v)\delta'_{x_1}(x_1-x_{1_w})\Big]\ \delta(\tau)$	

in these cases, the location probability is a Green's function. If the well has a finite size in the x_1, x_2 plane, the performance functional must be modified to account for the well geometry, as shown in Appendix 4.A.

4.3.2 Load Term for Travel Time Probability

From (4.2), we see that travel time probability is related to flux concentration. Rearranging (4.2), we obtain

$$C^f(\mathbf{x}_w, t) = \frac{M'}{v(\mathbf{x}_w)A(\mathbf{x}_w)} f_t(t; \mathbf{x}_w, \mathbf{x}_o) \ , \tag{4.20}$$

where $f_t(t; \mathbf{x}_w, \mathbf{x}_o)$ is the forward travel time probability describing the probability that a particle that was released from $\mathbf{x}_o$ will be at $\mathbf{x}_w$ at time t (random variable). Taking the derivative of C^f with respect to M' and using $t = t_f$ ($\tau = 0$), we obtain

$$\frac{dC^f(\mathbf{x}_w, t_f)}{dM'} = \frac{f_t(t_f; \mathbf{x}_w, \mathbf{x}_o)}{v(\mathbf{x}_w)A(\mathbf{x}_w)} = \psi^*_\tau(\mathbf{x}_o, \tau = 0) \ , \tag{4.21}$$

where ψ^*_τ is the adjoint state for travel time probability. This equation shows that forward travel time probability is related to the marginal sensitivity of flux concentration at the detection location to the source mass. In other words, if $P = C^f(\mathbf{x}_w, t_f)$ and $\alpha = M'$, the adjoint state, ψ^*_τ, is related to forward travel time probability through

$$f_t(\tau = t_f - t; \mathbf{x}_w, \mathbf{x}) = \frac{v(\mathbf{x}_w)A(\mathbf{x}_w)C^f(\mathbf{x}_w, t_f)}{M'} = v(\mathbf{x}_w)A(\mathbf{x}_w)\psi^*_\tau(\mathbf{x}, \tau = 0) \ . \tag{4.22}$$

where $\mathbf{x}$ is any source location. Forward travel time probability is related to the flux of the adjoint state at the detection, $\mathbf{x}_w$. For a monitoring well detection, $v(\mathbf{x}_w)$ is the magnitude of the groundwater velocity and A is the flow area. For a pumping well detection $v(\mathbf{x}_w)A(\mathbf{x}_w) = Q/\theta$ where Q is the pumping rate.

With one simulation of the backward model, we obtain the forward travel time probability from all possible source locations to one well. If we were interested in the forward travel time probability from many possible sources to one downstream location, such as for delineating pumping well capture zones, the backward (adjoint) model would more efficient than the forward model. If we are interested in the forward travel time probability from one source location to many possible downstream locations, the backward (adjoint) model is less efficient.

For forward travel time probability, we were interested in the arrival of the particle at detection location $\mathbf{x}_w$, and the probability was related to the flux of the adjoint state at that location. For backward travel time probability, we are interested in the arrival (in backward time) of the particle at some upgradient location $\mathbf{x}$; therefore, the probability is related to mass flux of the adjoint state at $\mathbf{x}$, given by

$$f_\tau(\tau; \mathbf{x}, \mathbf{x}_w) = v(\mathbf{x}) A(\mathbf{x}) \psi^*_\tau(\mathbf{x}, \tau) \ , \tag{4.23}$$

where $f_\tau(\tau; \mathbf{x}, \mathbf{x}_w)$ is backward travel time probability, defined as the probability that a parcel detected at $\mathbf{x}_w$ was located at $\mathbf{x}$ (deterministic parameter) at backward time τ (random variable).

To obtain the adjoint state, ψ^*_τ, the performance functional, h, is defined such that $P = C^f(\mathbf{x}_w, \tau = 0)$. Assuming that the well can be approximated as a point in x_1, x_2-space, with a finite length in the x_3-direction, the

appropriate performance functional, h, is defined as

$$h = C^f \delta(x_1 - x_{1_w})\delta(x_2 - x_{2_w}) \frac{B_{x_3}(x_{3_{wb}}, x_{3_{wt}})}{x_{3_{wt}} - x_{3_{wb}}} \delta(\tau) \; . \tag{4.24}$$

Integrating (4.24) over the space-time domain as in (4.5) results in the average flux concentration in the well at the time of sampling.

The load term for the adjoint equation is $-\partial h/\partial C$, where C is resident concentration; therefore the performance functional, h, must be written in terms of resident concentration, C, rather than flux concentration, C^f. In multi-dimensional systems, flux and resident concentrations are related according to [*Sposito and Barry*, 1987]

$$C^f = C - \frac{1}{v}\left[\left(D_{ij}\frac{\partial C}{\partial x_j}\right)\frac{v_i}{v}\right] \; , \tag{4.25}$$

where v is the magnitude of the velocity vector. Substituting (4.25) into (4.24) and taking the Fréchet derivative with respect to C, we obtain the load term

$$\begin{aligned} L^*[\psi^*_\tau] = -\frac{\partial h}{\partial C} \quad = \quad & -[\delta(x_1 - x_{1_w})\delta(x_2 - x_{2_w}) + \\ & a_L \frac{v_1}{v}\delta'_{x_1}(x_1 - x_{1_w})\delta(x_2 - x_{2_w}) \\ & + a_L \frac{v_2}{v}\delta(x_1 - x_{1_w})\delta'_{x_2}(x_2 - x_{2_w})\Big] \frac{B_{x_3}(x_{3_{wb}}, x_{3_{wt}})}{x_{3_{wt}} - x_{3_{wb}}}\delta(\tau) \; , \end{aligned} \tag{4.26}$$

where $\delta'_{x_i}(x_i - x_{i_w})$ is the derivative of the Dirac delta function with respect to x_i, we assumed flow is essentially horizontal in the vicinity of the well, and the

dispersion coefficient is given by [*Bear*, 1972]

$$D_{ij} = a_T v \delta_{ij} + (a_L - a_T)\frac{v_i v_j}{v} \tag{4.27}$$

where a_L and a_T are the longitudinal and transverse dispersivities, and δ_{ij} is the Kronecker delta function. The terms in (4.26) that contain $\delta'_{x_i}(x_i - x_{i_w})$ are based on derivations in *Neupauer and Wilson* [1999].

At a pumping well, we often assume $\partial C/\partial r = 0$, where r is radial direction measured from the well center. With this assumption and (4.25), flux concentration at the well becomes $C^f = C$, and the performance functional for a travel time probability with a pumping well detection is equivalent to (4.17). For one– and two–dimensional domains, the appropriate load terms for travel time probability are shown in Table 4.1b for a monitoring well detection and Table 4.1a for a pumping well detection. For one-dimensional and two-dimensional horizontal domains, the adjoint state for travel time probability with a pumping well detection is a Green's function.

We used one adjoint state, ψ^*_τ, to obtain both the forward and backward travel time probabilities; therefore these probability distributions have similar shapes but may have different magnitudes. The integral of forward probability f_t over all t shows the probability that the solute parcel released from the source will ever reach the well; while the integral of backward probability f_τ over all τ shows the probability that the detected solute parcel was ever at the source. The difference between these two can be best explained with a strong pumping well in a two-dimensional flow field. An example is radial flow. A particle released from any source will eventually reach the pumping

well; therefore, $\int_t f_t(t;\mathbf{x}_w,\mathbf{x}_o)dt = 1$ for all $\mathbf{x}_o$. However, a particle detected at the pumping well could not have been at every possible source location in the past; therefore, $\int_\tau f_\tau(\tau;\mathbf{x}_o,\mathbf{x}_w)d\tau < 1$ for all $\mathbf{x}_o$. We illustrate this with an example in the next section. In the one-dimensional system studied by *Neupauer and Wilson* [1999], the forward and backward travel time probabilities were equivalent, and therefore they did not discuss the relationship between the two.

So far, we have only dealt with probability density functions; however we can also obtain the cumulative distribution function (cdf). The physical meaning of the location probability cdf is unclear; however, the travel time cdf is important for capture zone delineation. For a contaminant parcel that was detected at a well at $\tau = 0$, the travel time cdf, $F_\tau(\tau)$, defines the probability that the parcel will travel from location $\mathbf{x}$ to the well in time τ or less. The backward travel time cdf can be obtained from the travel time probability density function as

$$F_\tau(\tau) = \int_0^\tau f_\tau(\tau';\mathbf{x})\, d\tau' \,. \tag{4.28}$$

The forward travel time cdf, $F_t(t)$, can be obtained through a similar integration. We can also solve for the travel time cdf directly by performing this integration on the load term for ψ_τ^* to obtain a new adjoint state, Ψ_τ^*, that is related to the travel time cdf. For example, for a pumping well detection, the load term for Ψ_τ^* is obtained by integrating the load term in (4.17) to obtain

$$L^*[\Psi_\tau^*(\tau;\mathbf{x})] = -\delta(x_1 - x_{1_w})\delta(x_2 - x_{2_w})\frac{B_{x_3}(x_{3_{wb}}, x_{3_{wt}})}{x_{3_{wt}} - x_{3_{wb}}} \,, \tag{4.29}$$

and $F_t(t;\mathbf{x}_w) = v(\mathbf{x}_w)A(\mathbf{x}_w)\Psi^*_\tau(\mathbf{x},\tau)$ for the forward travel time cdf, and $F_\tau(\tau;\mathbf{x}_o,\mathbf{x}_w) = v(\mathbf{x}_o)A(\mathbf{x}_o)\Psi^*_\tau(\mathbf{x},\tau)$ for the backward travel time cdf. The forward travel time cdf for a pumping well detection defines a capture zone. *Uffink* [1989], *Chin and Chittaluru* [1994], and *Wilson and Liu* [1997] all delineated pumping well captures zones using backward models, essentially using forward travel time probabilities.

4.3.3 Relationship Between Backward Location and Travel Time Probabilities

Chin and Chittaluru [1994] and *Wilson and Liu* [1994] suggested that location and travel time probabilities are related by Bayes' theorem. For one spatial dimension, $x_1 = x$, Bayes' theorem states that

$$f_x(x|\tau)f_\tau(\tau) = f_\tau(\tau|x)f_x(x) = f(x,\tau)\ , \tag{4.30}$$

where $f_\tau(\tau) = \int_x f(x,\tau)\ dx$ and $f_x(x) = \int_\tau f(x,\tau)\ d\tau$. So, from (4.30)

$$f_\tau(\tau|x) = \frac{f_\tau(\tau)}{f_x(x)} f_x(x|\tau)\ . \tag{4.31}$$

This relationship shows that if location and travel time probabilities were related by Bayes' theorem, they would be conditional probabilities. They are not. Furthermore, location and travel time probabilities are functionally related by Bayes' theorem only if their relationship can be expressed in the form of (4.31).

Using operator theory, we find that backward location and travel time

probabilities are related by (see Appendix 4.B)

$$f_\tau(\tau; x, x_w) = v(x) f_x(x; \tau, x_w) + a_L v(x) \frac{v_1(x_w)}{v(x_w)} \frac{\partial f_x}{\partial x} \ , \tag{4.32}$$

for a monitoring well detection. This relationship cannot be written in the form of (4.31). Therefore, these probabilities cannot be related by Bayes' theorem.

Similarly, for a pumping well detection, backward location and travel time probabilities are related by (see Appendix 4.B)

$$f_\tau(\tau; x, x_w) = v(x) f_x(x; \tau, x_w) \ . \tag{4.33}$$

This expression is coincidentally in the form of (4.31). However, if these probabilities were related by Bayes' theorem, comparison of (4.33) and (4.31) would imply that $f_\tau(\tau) = 1$ and $f_x(x) = 1/v(x)$, which is not necessarily true. Thus, location and travel time probabilities are not conditional and cannot be related by Bayes' theorem.

4.4 Example

Consider the two-dimensional, rectangular, 600 m $\times$ 350 m confined aquifer shown in Figure 4.1. Flow is assumed to be steady, and the flow boundary conditions are specified head on the east and west boundaries and no flow on the north and south boundaries, with flow from east to west. A pumping well is located at $(x_{1_w}, x_{2_w}) = (200 \text{ m}, 175 \text{ m})$ and pumps at a rate of $Q = 1 \times 10^{-4}$ m^3/s. The aquifer thickness is 1 m and the transmissivity is $T = 5 \times 10^{-5}$ m^2/s. The head distribution and velocity field are shown in

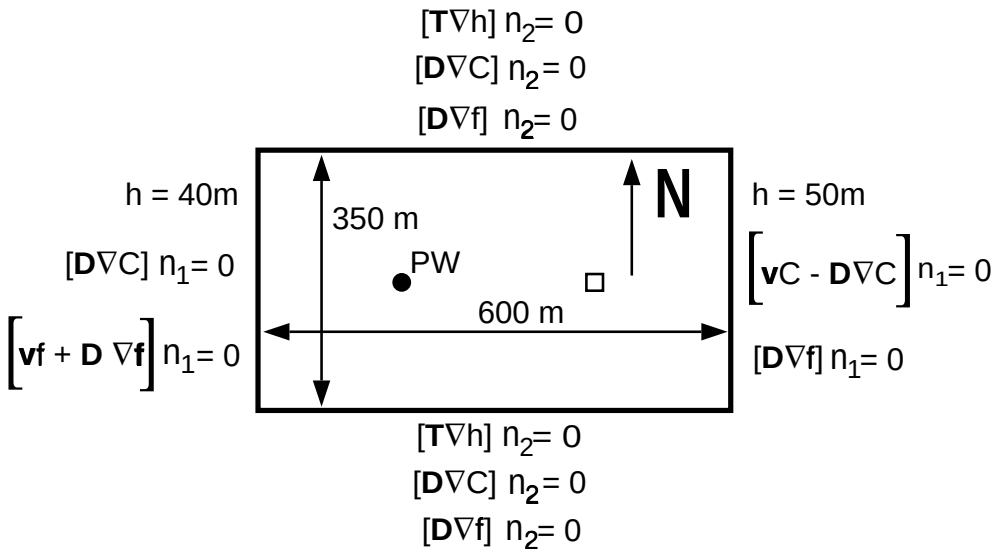

Figure 4.1: Aquifer geometry and boundary conditions. The filled circle denotes the pumping well location; open square denotes the source location.

Figure 4.2.

The boundary conditions for the forward transport model are zero flux at the east boundary and zero gradient at all other boundaries (see Figure 4.1). If 300 g of a conservative chemical enters the aquifer instantaneously at $(x_{1_o}, x_{2_o}) = (400 \text{ m}, 175 \text{ m})$ at $t = 0$, the contaminant plume after 800 days is shown in Figure 4.3. We used longitudinal and transverse dispersivities of $\alpha_L = 10$ m and $\alpha_T = 2$ m, and an aquifer porosity of $\theta = 0.3$. The plume centroid travels almost 200 m in 800 days, and the plume is captured by the well.

Suppose contamination is detected at the pumping well at time $t_f =$ 800 days. We can solve (4.14) for the backward location and travel time probabilities for the detected contamination. The flow field from the forward model

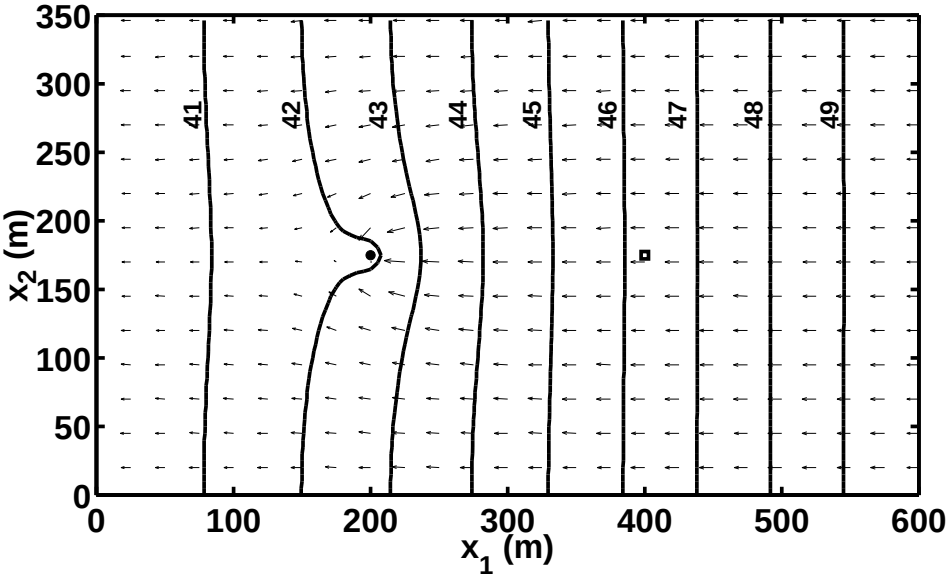

Figure 4.2: Hydraulic head distribution (units are m) and velocity vectors. The filled circle denotes the pumping well location; open square denotes the source location.

must be reversed, and the boundary conditions for the forward model must be modified for the backward simulations. The third-type boundary in the forward model (east boundary) becomes a second-type boundary in the backward model, and the second-type boundaries in the forward model (north, west, and south boundaries) becomes third-type boundaries. However, since the northern and southern boundaries are no-flow boundaries (i.e., $v_2 = 0$ at these boundaries), the third-type boundary reduces to a second-type boundary.

The appropriate governing equation for the backward model for both location and travel time probabilities is (4.14). For a detection at the pumping well, the load term, taken from Table 4.1, is $\partial h/\partial C = \delta(x_1 - x_{1_w})\delta(x_2 - x_{2_w})\delta(\tau)$. For location probability, $f_{\mathbf{x}} = \psi^*_{\mathbf{x}}$; for backward travel time probability, $f_\tau(\tau; \mathbf{x}, \mathbf{x}_w) = v(\mathbf{x})A\psi^*_\tau$; and for forward travel time probability, $f_t(t; \mathbf{x}_w, \mathbf{x})$

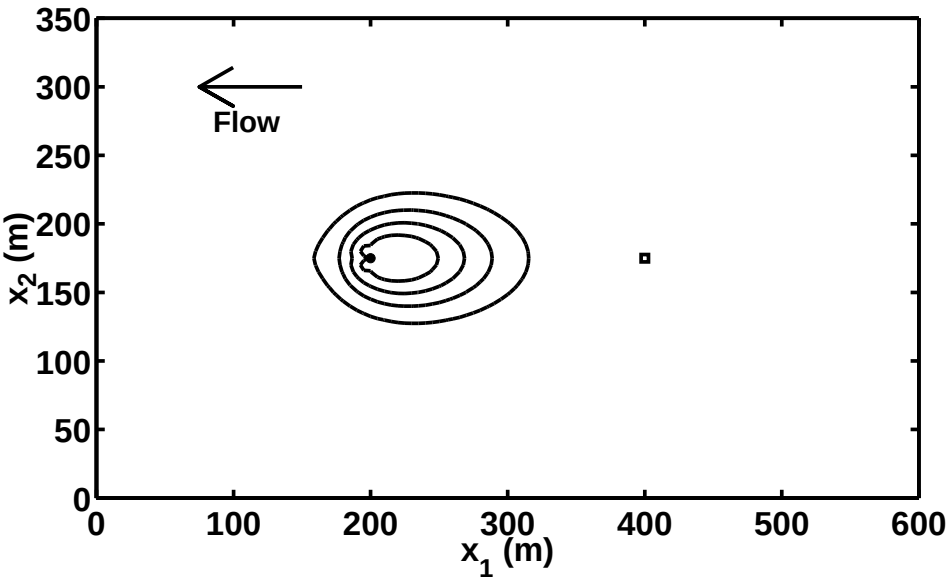

Figure 4.3: Resident concentration at $t = 800$ days (contour interval 0.01 g/m^3). The filled circle denotes the pumping well location; open square denotes the source location.

$= (Q/\theta)\psi^*_\tau$. Figure 4.4 shows the resulting backward location probability at $\tau = 800$ days prior to detection at the pumping well. The plot shows that the detected particle was most likely near $(x_1, x_2) = (440\text{ m}, 175\text{ m})$ at $\tau = 800$ days prior to detection. Of course, the actual source was 40 m farther west, at a location with a slightly lower probability.

Figure 4.5 shows the forward and backward travel time probabilities to the pumping well from $(x_{1_o}, x_{2_o}) = (400\text{ m}, 175\text{ m})$. The forward travel time probability curve represents the time at which a particle that was released from (x_{1_o}, x_{2_o}) will arrive at the pumping well. The most likely arrival time is $t \approx 600$ days. The area under the travel time probability distribution shows the probability that the particle will ever reach the well. The area under the f_t curve in Figure 4.5 is 0.90, indicating that there is a probability of 0.10 that the

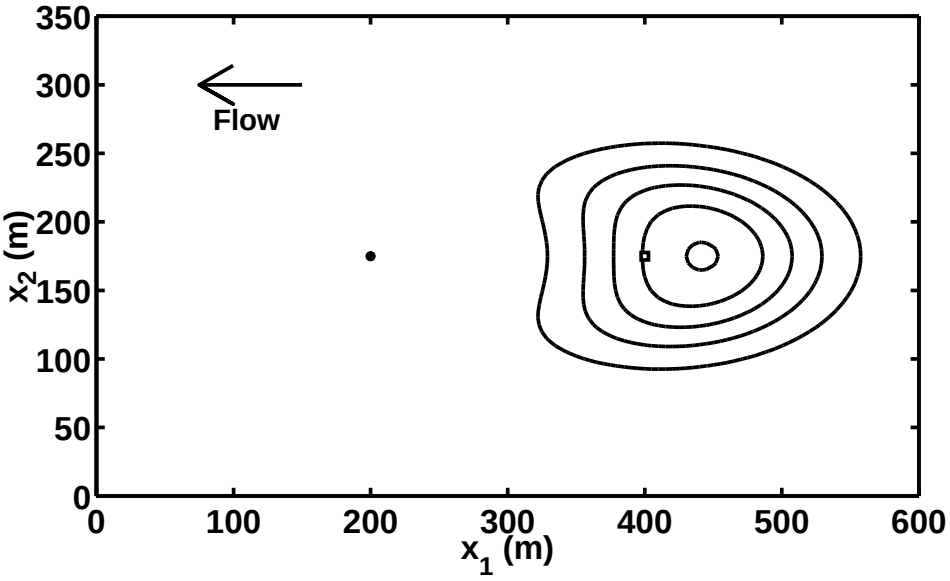

Figure 4.4: Backward location probability at $\tau = 800$ days prior to detection at the pumping well (filled circle) (contour interval is 1×10^{-5} m^{-2}).

particle will bypass the pumping well and not be captured. The backward travel time probability curve represents the time in the past at which a particle that was detected at the pumping well would have been at $(x_1, x_2) = (400 \text{ m}, 175 \text{ m})$. The most likely travel time is $\tau \approx 600$ days. The area under the f_τ curve in Figure 4.5 is 0.04, indicating a 4% probability that the detected particle was ever at $(x_1, x_2) = (400 \text{ m}, 175 \text{ m})$.

The appropriate governing equation for the travel time cumulative distribution function is (4.14), with the load term $\partial h/\partial C = \delta(x_1 - x_{1_w})\delta(x_2 - x_{2_w})$. Figure 4.6 presents the resulting forward travel time cdf at $\tau = 800$ days prior to detection at the pumping well, showing the probability that the travel time from any location to the pumping well is 800 days or less. This is the 800-day capture zone. For example, at $(x_1, x_2) = (400 \text{ m}, 175 \text{ m})$, $F_t(t =$

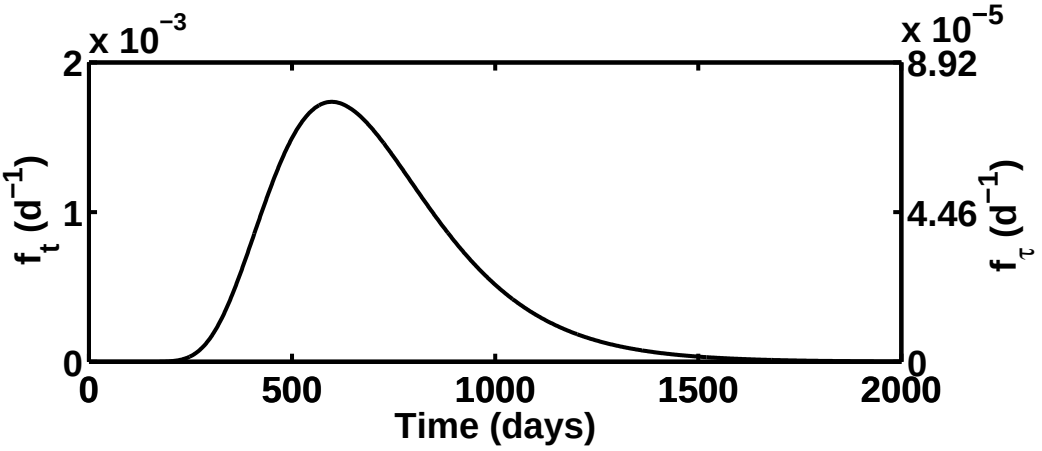

Figure 4.5: Forward (f_t) and backward (f_τ) travel time probabilities from the source area to the pumping well.

800 days) ≈ 0.60, indicating a 60% probability that particle released at this location will reach the pumping well in 800 days or less. With one simulation of the backward model, we obtain the entire time-dependent capture zone.

4.5 Comparison of Heuristic and Adjoint Approaches

Wilson and Liu [1997] used a heuristic method to develop the backward probability model. Their two-dimensional domain was rectangular, similar to the domain shown in Figure 4.1, also with an internal pumping well. However, they treated the well circumference as a boundary, with the well itself outside of the problem domain. They chose the operator

$$L[\,] = -\frac{\partial[\,]}{\partial\tau} + \frac{\partial}{\partial x_i}\left(D_{ij}\frac{\partial[\,]}{\partial x_j}\right) + v_i\frac{\partial[\,]}{\partial x_i}\,. \tag{4.34}$$

This is slightly different than the adjoint operator we obtained in (4.14) because

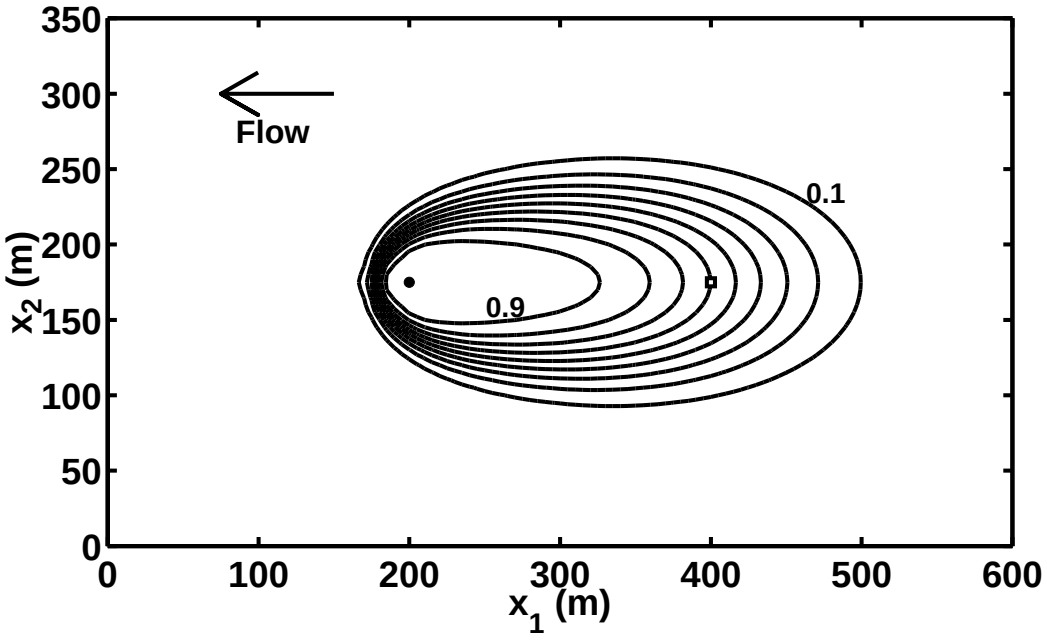

Figure 4.6: Forward travel time cumulative distribution function for a detection at the pumping well. Contour interval is 0.1.

velocity is outside of the derivative ($q_I = 0$, for this problem, so the source term vanishes). However, using $\nabla \cdot v = q_I/\theta - q_O/\theta$, the divergence $\nabla \cdot v$ is non-zero only at the pumping well. Since the well is outside of their problem domain, the operator in (4.34) is correct.

Wilson and Liu [1997] used the flow boundary conditions shown in Figure 4.1. For their forward transport model, they used the boundaries shown in Figure 4.1 on the north, west, and east sides; and $C = 0$ at the eastern boundary. For the backward transport model, they assigned the boundary conditions as first-type on the eastern boundary, and second-type on the other three sides. The first-type boundary condition on the eastern boundary is verified in (4.14) (boundary condition on Γ_1). From (4.14), we see that the boundary condition on the western boundary should have been a third-type boundary. This boundary is downgradient of the pumping well, which is the source of probability. Since probability is transported upgradient in the backward model, no probability reached this boundary (i.e., $f_\tau(\tau; \mathbf{x}) = 0$ on this boundary), and the second-type boundary condition used by *Wilson and Liu* [1997] is effectively equivalent to the third-type boundary condition in (4.14). Their boundary conditions on the north and south boundaries are consistent with Figure 4.1. By using the adjoint method, we have verified that *Wilson and Liu* [1997] heuristically obtained the correct backward governing equation and the appropriate boundary conditions for the edges of their rectangular domain.

Wilson and Liu [1997] treated the pumping well as a boundary, and obtained the correct boundary condition, which we verify here. If the well is

modeled as a point in the x_1, x_2-plane, the boundary condition at the well is

$$\lim_{r_w \to 0} \frac{\partial C}{\partial r} = 0 \ \text{ at } \mathbf{x} = \mathbf{x}_w \ , \tag{4.35}$$

where r_w is the well radius and $\mathbf{x}_w$ is the well location. The appropriate boundary condition at $\mathbf{x} = \mathbf{x}_w$ for the adjoint equation is obtained from (4.35) and (4.12):

$$\lim_{r_w \to 0} \left[D_r \frac{\partial \psi^*}{\partial r} + v_r \psi^* \right] = 0 \ \text{ at } \mathbf{x} = \mathbf{x}_w \ , \tag{4.36}$$

where D_r is the dispersion coefficient in the radial direction, v_r is the radial velocity near the well, and ψ^* is the adjoint state. Recall, from Table 4.1, that the load terms in the adjoint equations for an internal pumping well are non-zero only at $\mathbf{x} = \mathbf{x}_w$. Since $\mathbf{x} = \mathbf{x}_w$ is no longer in the domain when the well is treated as a boundary, we incorporate the load term into the boundary condition at $\mathbf{x} = \mathbf{x}_w$. The load terms vanish for $\tau \neq 0$, so we only modify the boundary condition at $\tau = 0$. For location probability, the load term is an instantaneous source acting at $\mathbf{x} = \mathbf{x}_w$; therefore, the boundary condition at $\mathbf{x} = \mathbf{x}_w$ must be an instantaneous source. The governing equation is $L^*[\psi^*(\mathbf{x}; \tau)] = 0$, and the equivalent boundary condition is

$$\lim_{r_w \to 0} \left[D_r \frac{\partial \psi^*(\mathbf{x}, \tau)}{\partial r} + v_r \psi^*(\mathbf{x}, \tau) \right] = \ -\delta(\tau) \text{ at } \mathbf{x} = \mathbf{x}_w \ . \tag{4.37}$$

For $\tau \neq 0$, the boundary condition is homogeneous, which is consistent with the boundary condition shown in (4.36). For $\tau = 0$, this boundary

condition gives an instantaneous pulse injection at the well, equivalent to the load term shown in Table 4.1. For location probability, $f_{\mathbf{x}} = \psi^*$; for forward travel time probability $f_t = (Q/\theta)\psi^*$; and for backward travel time probability, $f_\tau = v(\mathbf{x})A\psi^*$. *Wilson and Liu* [1997] treated their pumping well as an internal boundary and assumed the boundary condition in (4.37), using it to calculate forward location and travel time probabilities. For this case, forward and backward location probabilities are coincidentally equivalent, and therefore, they correctly calculated backward location probability; however they misidentified their forward travel time probability as backward travel time probability.

4.6 Practical Considerations

The backward probability model is the adjoint of a forward contaminant transport model; therefore all of the assumptions that are made in the forward model (e.g., non-scale-dependent dispersion) are implicitly made in the backward model. Since the backward model is the adjoint of the forward model, the governing equation has the same form as the advection-dispersion equation. Several commercial codes are written to numerically solve the multidimensional ADE. These codes can also be used to solve the backward model, after carefully addressing such issues as reversing the flow field, using the appropriate boundary conditions, and using the correct load term. To run a transport model, we need a flow field from a flow model. In the backward model, the flow field is reversed, so we must reverse the sign on the flow components from the forward flow model.

The boundary conditions for the backward model are obtained using

the adjoint method. First-type boundary conditions in the forward model remain first-type boundary conditions in the backward model; the second-type and third-type boundary conditions are switched from forward to backward models. Since most codes are capable of handling all three boundary types, the boundary conditions for the backward model can be easily implemented in conventional transport codes.

The load term on the adjoint operator can be treated as a source term in conventional transport codes. Several load terms shown in Table 4.1 act instantaneously at a point in space (for location probability, or travel time probability with a pumping well detection). In some cases, the load acts over a line of finite length in the vertical direction. The point sources can be handled in finite difference and finite element codes by injecting mass at a node. Some features in the load terms in Table 4.1, such as the derivative of the Dirac delta function, cannot be implemented exactly, and must be numerically approximated.

4.7 Conclusions

If contamination is sampled in an aquifer but the contamination source is unknown, backward location and travel time probabilities can be used to obtain information about the prior position of contamination. Backward location probability describes the position of the contamination at some time prior to sampling, and backward travel time probability describes the amount of time required for the contamination to travel to the sampling location from some upgradient position, such as a known or suspected contamination source.

We proposed the adjoint method as a tool for obtaining the governing equations for these probabilities. In previous work [*Neupauer and Wilson*, 1999], the governing equations were developed for a one-dimensional system. In this paper, we extended the approach to multi-dimensional advection-dispersion problems.

The governing equation and initial and boundary conditions for the backward model come directly from the forward model, using the adjoint method. The only additional term in the backward model is the load term, describing the particular adjoint state. The load term depends on the type of probability and the sampling device. For location probability, the load term is the Fréchet derivative of the average resident concentration in the sampled region. For travel time probability, the load term in the Fréchet derivative of the flux concentration at the sample location. For a pumping well detection, flux concentration and resident concentration are equivalent; therefore, in this case, the load term for travel time probability reduces to the load term for location probability. With these load terms, the adjoint equation can be solved to obtain the appropriate adjoint state. We showed that if the adjoint state represents the marginal sensitivity of resident concentration at the detection to the source strength, then the adjoint state is equivalent to forward and backward location probabilities. Forward and backward travel time probabilities are related to the flux of the adjoint state if the adjoint state represents the marginal sensitivity of flux concentration at the detection to the source strength.

We have limited our derivations to conservative solutes; however, the adjoint method is sufficiently robust that the approach can be extended to reactive transport, flow transients, and other conditions. Adjoint theory applies to all differential operators, so any transport process that can be modeled with a

differential operator in a forward model can also be modeled with the backward (adjoint) equation. As we have shown here, adjoint theory can easily be applied to linear differential operators. Adjoint theory can also be applied to non-linear problems [*Marchuk et al.*, 1996], although it is more difficult.

Acknowledgments

This research was supported in part by the New Mexico Tech Geophysical Research Center and in part by the Environmental Protection Agency's STAR Fellowship program under Fellowship No. U-915324-01-0. This work has not been subjected to the EPA's peer and administrative review and therefore may not necessarily reflect the views of the Agency and no official endorsement should be inferred. The authors acknowledge William D. Stone for his input on operator theory, and Bert Kerr and two anonymous reviewers for their valuable comments.

References

Ahlfeld, D.P., J.M. Mulvey, and G.F. Pinder, contaminated groundwater remediation design using simulation, optimization, and sensitivity theory, 1, Model development, *Water Resour. Res.*, 24(3), 431–441, 1988.

Bagtzoglou, A.C., D.E. Dougherty, and A.F.B. Thompson, Application of particle methods to reliable identification of groundwater pollution sources, *Water Resources Management*, 6, 15–23, 1992.

Bear, J., *Dynamics of Fluids in Porous Media*, American Elsevier Publishing Company, New York, 1972.

Chin, D.A. and P.V.K. Chittaluru, Risk management in wellhead protection, *J. Water Resour. Plan. Manage.*, 120(3), 294–315. 1994.

Dagan, G., Stochastic modeling of groundwater flow by unconditional and conditional probabilities, 2, The solute transport, *Water Resour. Res.*, 18(4), 835–848, 1982.

Dagan, G., Theory of solute transport by groundwater, *Ann. Rev. Fluid Mech.*, 19, 183–215, 1987.

Dagan, G., *Flow and Transport in Porous Formations*, Springer-Verlag, New York, 1989.

Dagan, G., Transport in heterogeneous porous formations: spatial moments, ergodicity, and effective dispersion, *Water Resour. Res.*, 26(6), 1281–1290, 1990.

Dagan, G., and V. Nguyen, A comparison of travel time and concentration approaches to modeling transport by groundwater, *Journal of Con-*

taminant Hydrology, 4, 79–91, 1989.

Jury, W.A., Simulation of solute transport using a transfer function model, *Water Resour. Res.*, 18(2), 363–368, 1982.

Jury, W.A., G. Sposito, and R.E. White, A transfer function model of solute transport through soil, 1, Fundamental concepts, *Water Resour. Res.*, 22(2), 243–247, 1986.

Jury, W.A. and K. Roth, *Transfer Functions and Solute Movement through Soil: Theory and Applications*, Birkhauser, Boston, 1990.

Lu, A.H., F. Schmittroth, and W.W.-G. Yeh, Sequential estimation of aquifer parameters, *Water Resour. Res.*, 24(5), 670–682, 1988.

Marchuk, G.I., V.I. Agoshkov, and V.P. Shutyaev, *Adjoint Equations and Perturbation Algorithms in Nonlinear Problems*, CRC Press, Inc., Boca Raton, FL, 1996.

Naff, R.L., Arrival times and temporal moments of breakthrough curves for an imperfectly stratified aquifer, *Water Resour. Res.*, 28(1), 53–68, 1992.

Neuman, S.P., A statistical approach to the inverse problem of aquifer hydrology, 3, Improved solution method and added perspective, *Water Resour. Res.*, 16(2), 331–346, 1980.

Neupauer, R.M. and J.L. Wilson, Adjoint method for obtaining backward-in-time location and travel time probabilities of a conservative groundwater contaminant, *Water Resour. Res.*, 35(11), 3389–3398, 1999.

Parker, J.C. and M. Th. van Genuchten, Flux-averaged and volume-averaged

concentrations in continuum approaches to solute transport, *Water Resour. Res.*, 20(7), 866–872, 1984.

Rubin, Y. and G. Dagan, Conditional estimation of solute travel time in heterogeneous formations: impact of transmissivity measurements, *Water Resour. Res.*, 28(4), 1033–1040, 1992.

Saaty, T.L., *Modern Nonlinear Equations*, Dover Publications, Inc., New York, 1981.

Shapiro, A.M. and V.D. Cvetkovic, Stochastic analysis of solute arrival time in heterogeneous porous media, *Water Resour. Res.*, 24(10), 1711–1718, 1988.

Sposito, G. and D.A. Barry, On the Dagan model of solute transport in groundwater: Foundational aspects, *Water Resour. Res.*, 23(10), 1867–1875, 1987.

Sun, N.-Z., *Inverse Problems in Groundwater Modeling*, Kluwer Academic Publishers, Boston, 1994.

Sun, N.-Z. and W.W.-G. Yeh, Identification of parameter structure in groundwater inverse problems, *Water Resour. Res.*, 21(6), 869–883, 1985.

Sun, N.-Z. and W.W.-G. Yeh, Coupled inverse problems in groundwater modeling, 1, Sensitivity analysis and parameter identification, *Water Resour. Res.*, 26(10), 2507–2525, 1990.

Sykes, J.F., J.L. Wilson, and R.W. Andrews, Sensitivity analysis for steady state groundwater flow using adjoint operators, *Water Resour. Res.*, 21(3), 359–371, 1985.

Townley, L.R. and J.L. Wilson, Computationally efficient algorithms for parameter estimation and uncertainty propagation in numerical models of groundwater flow, *Water Resour. Res.*, 21(12), 1851–1860, 1985.

Uffink, G.J.M., Application of Kolmogorov's backward equation in random walk simulations of groundwater contaminant transport, in *Contaminant Transport in Groundwater*, H.E. Kobus and W. Kinzelbach, editors, pp. 283–289, A.A. Balkema, Brookfield, Vt., 1989.

Wilson, J.L. and J. Liu, Backward tracking to find the source of pollution, in *Waste-management: From Risk to Remediation*, edited by R. Bhada *et al.*, ECM Press, Albuquerque, NM, 181–199, 1994.

Wilson, J.L. and J. Liu, Field Validation of the Backward-in-time Advection Dispersion Theory. *Proceedings of the 1996 HSRC/WERC Joint Conf. on the Environment*, Great Plains-Rocky Mountain Hazardous Substance Center, Manhattan, Kansas, http://www.engg.ksu.edu/HSRC/ 96Proceed/wilson.html, 1997.

Wilson, J.L. and D.E. Metcalfe, Illustration and verification of adjoint sensitivity theory for steady state groundwater flow, *Water Resour. Res.*, 21(11), 1602–1610, 1985.

Yeh, W.W.-G. and N.-Z. Sun, Variational sensitivity analysis, data requirements, and parameter identification in a leaky aquifer system, *Water Resour. Res.*, 26(9), 1927–1938, 1990.

Zauderer, E., *Partial Differential Equations of Applied Mathematics*, 2nd ed., John Wiley and Sons, New York, 1989.

Zwillinger, D., *Handbook of Differential Equations*, 2nd ed., Academic Press, Inc., San Diego, 1989.

4.A Load Term Extensions

The load term for location probability was defined assuming that the well is approximated as a point in the x_1, x_2-plane. If the well has a finite radius and screen length, the performance functional is given by

$$h(\mathbf{x}, \tau) = C(\mathbf{x}, \tau) \, \frac{R_{x_1,x_2}(x_{1_w}, x_{2_w}, 0, r_w)}{\pi r_w^2} \, \frac{B_{x_3}(x_{3_{wb}}, x_{3_{wt}})}{x_{3_{wt}} - x_{3_{wb}}} \, \delta(\tau) \, , \tag{4.38}$$

where r_w is the well radius and $R_{x_1,x_2}(x_{1_w}, x_{2_w}, r_i, r_o)$ is a radial boxcar function in the x_1, x_2 plane, whose value is one within the sampled region ($r_i < r < r_o$) and zero outside of it (see Figure 4.7), defined by

$$R_{x_1,x_2}(x_{1_w}, x_{2_w}, r_i, r_o) = \begin{cases} 1 & r_i^2 \leq (x_1 - x_{1_w})^2 + (x_2 - x_{2_w})^2 \leq r_o^2 \\ 0 & \text{otherwise} \, . \end{cases} \tag{4.39}$$

The performance functional in (4.38) assumes that the sampled volume is the entire wellbore ($r_i = 0$ and $r_o = r_w$). If a monitoring well is purged prior to sampling, the sampled region can be approximated instead by an annulus centered at the well center with $r_i > 0$ and $r_o > r_w$, assuming that the aquifer is locally homogeneous in the vicinity of the well and that local flow is essentially horizontal. For an annulus centered at (x_{1_w}, x_{2_w}) with an inner radius of r_i and an outer radius of r_o, the inner and outer radii of the sampled region are related to the number of purged well volumes, N: $r_i = r_w\sqrt{N}$ and $r_o = r_w\sqrt{N+1}$. Modifying the performance functional in (4.38) to account for this new sampled volume, we obtain the appropriate adjoint equation for

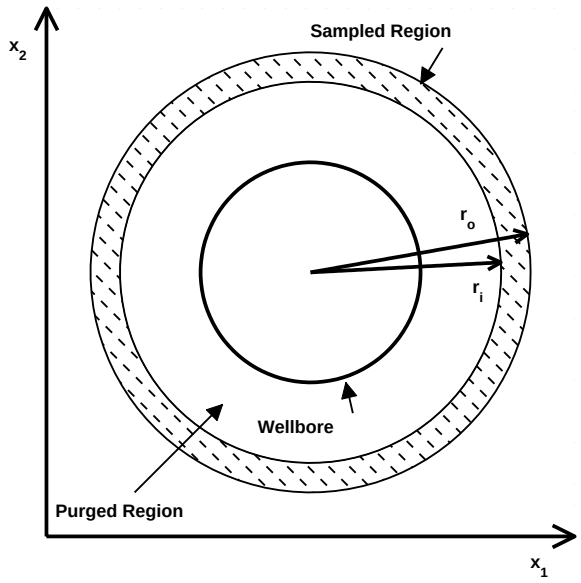

Figure 4.7: Plan view of sampled region in a monitoring well.

location probability at a monitoring well that is purged prior to sampling:

$$L^*[f_{\mathbf{X}}(\mathbf{x};\tau)] = -\frac{\partial h}{\partial C} = -\frac{R_{x_1,x_2}(x_{1_w}, x_{2_w}, r_i, r_o)}{\pi[r_o^2 - r_i^2]} \frac{B_{x_3}(x_{3_{wb}}, x_{3_{wt}})}{x_{3_{wt}} - x_{3_{wb}}} \delta(\tau) \ . \quad (4.40)$$

In the limit as $r_w \to 0$, and with $r_i = 0$, (4.40) approaches (4.19). Equation (4.19) is sufficient if one is interested only in probabilities some distance from the well. In practice this is also a requirement of the model in (4.14) since, like (4.3), it assumes an asymptotic value of the dispersion coefficient. Equation (4.40) is more appropriate for scale-dependent dispersion models, when looking for probabilities near the well.

4.B Relationship Between One-Dimensional Location and Travel Time Probabilities

In this appendix, we show the functional relationship between backward location and travel time probabilities. We look at probabilities in a one-dimensional system ($x = x_1$) with sampling at a monitoring well. From Table 4.1, location probability is described by

$$L^*[f_x(x;\tau)] = -\delta(x - x_w)\delta(\tau) \ , \tag{4.41}$$

and for travel time probability with sampling at a monitoring well, the adjoint equation is

$$L^*[\psi^*_\tau(\tau, x)] = -\delta(x - x_w)\delta(\tau) - a_L \frac{v_1(x_w)}{v(x_w)} \frac{\partial}{\partial x} \left[\delta(x - x_w)\delta(\tau)\right] \ , \tag{4.42}$$

where v denotes the magnitude of v_1. Since τ is independent of x, we moved $\delta(\tau)$ inside the derivative. Substituting (4.41) into (4.42), and realizing that L^* is a linear operator, we obtain

$$L^*[\psi^*_\tau(\tau, x)] = L^* \left[f_x(x;\tau, x_w) + a_L \frac{v_1(x_w)}{v(x_w)} \frac{\partial f_x}{\partial x} \right] \ . \tag{4.43}$$

This equation implies that $\psi^*_\tau(\tau, x) - f_x(x;\tau) - a_L[v_1(x_w)/v(x_w)]$ $(\partial f_x/\partial x)$ is in the null space of L^*, denoted by $NS(L^*)$. The null space is defined as the set of all functions, ϕ, such that $L^*[\phi] = 0$, $(NS(L^*) = \{\phi : L^*[\phi] = 0\})$. Since L^* always has homogeneous boundary and initial conditions (see (4.14)) and no internal sources, the only function in the null space of L^*

is the zero function, i.e. $NS(L^*) = \{0\}$. Therefore, the relationship between location and travel time probability is given by (4.32) for a monitoring well detection. Through a similar approach, the relationship between location and travel time probabilities for sampling at a pumping well is (4.33).

CHAPTER 5

BACKWARD PROBABILITY MODEL FOR NON-UNIFORM AND TRANSIENT FLOW

Abstract

Backward location and travel time probabilities can be used to determine the former location of contamination in an aquifer. For a contaminant parcel that was detected in an aquifer, the backward location probability describes its position at some time prior to sampling and the backward travel time probability describes the amount of time required for it to travel to the sampling location from some upgradient position. These probabilities can provide information about the source of contamination. Backward probabilities are related to adjoint states of resident concentration. The governing equation for these adjoint states is the adjoint of the forward governing equation, e.g., the advection-dispersion equation. The backward probability model has been developed for steady, uniform flow [*Neupauer and Wilson*, 1999, 2000a]. Using adjoint theory to obtain the appropriate governing equation, we extend the backward probability model to account for non-uniform and transient flow.

5.1 Introduction

When contamination is detected in an aquifer, the source of contamination is often unknown. To remediate the aquifer or to assign responsibility we might need to identify the contamination source or estimate the release time of contamination from a known source. A common modeling approach to addressing these issues is to run one forward simulation for each potential source,

modeling the movement of the contamination away from the source (forward modeling). If the number of potential sources is large, this approach can result in a significant computational burden since one simulation must be run for each potential source. Furthermore, all potential sources must be pre-identified.

Backward modeling [*Wilson and Liu*, 1994, 1997] is a more efficient approach to addressing these issues. With backward modeling we obtain the probability distributions for the former position of the contamination (location probability) or for the contaminant's travel time from some upgradient location to the sampling location (travel time probability). With one backward simulation we obtain these probabilities for all locations. This reduces the computational burden of forward modeling, and the results are not limited to the pre-identified possible source locations. Not only can the backward model be used to improve characterization of known sources of groundwater contamination or to identify previously unknown contamination sources, but it can also be used to delineate capture zones.

Location and travel time probabilities are often used in forward modeling to describe solute transport in groundwater [e.g., *Dagan*, 1982, 1987; *Jury*, 1982; *Jury and Roth*, 1990; *Chin and Chittaluru*, 1994]. Forward location probability describes the position of a solute parcel at a fixed time after its release from the source [*Dagan*, 1982, 1987, 1989; *Jury and Roth*, 1990; *Chin and Chittaluru*, 1994] and is related to resident concentration [*Dagan*, 1987; *Jury and Roth*, 1990]. The normalized concentration distribution at some time t after release from an instantaneous point source is equivalent to the location

probability density function at time t, given by

$$f_{\mathbf{x}}(\mathbf{x};t) = \frac{C(\mathbf{x},t)}{\int_{\Omega} C(\mathbf{x},0^{+})\, d\Omega}, \tag{5.1}$$

where $f_{\mathbf{x}}(\mathbf{x};t)$ is location probability at time t, $\mathbf{x}$ is the position vector, $C(\mathbf{x},t)$ is the resident concentration distribution from an instantaneous point source, Ω is the spatial domain, and $\int_{\Omega} C(\mathbf{x},0^{+})\, d\Omega = M_o/\theta$, where M_o is the source mass and θ is porosity.

Forward travel time probability describes the time required for a solute parcel to travel from its source to a location of interest [*Jury*, 1982; *Jury et al.*, 1986; *Dagan*, 1989; *Dagan and Nguyen*, 1989], and is related to flux concentration [*Shapiro and Cvetkovic*, 1988; *Rubin and Dagan*, 1992]. For an instantaneous point source of contamination, the normalized flux concentration at a downgradient location, $\mathbf{x}$, is equivalent to the travel time probability density function for that location, given by

$$f_t(t;\mathbf{x}) = \frac{|\mathbf{v}| A\theta C^f(\mathbf{x},t)}{M_o}\ , \tag{5.2}$$

where $f_t(t;\mathbf{x})$ is travel time probability from the source to $\mathbf{x}$, $\mathbf{v}$ is the groundwater velocity (vector quantity), $C^f(\mathbf{x},t)$ is flux concentration, M_o is the total amount of mass that entered at the source, vertical bars denote magnitude, and A is a flow area. We consider travel time probability across a plane perpendicular to flow, and A is the cross-sectional area of this plane. Since location probability is related to resident concentration and travel time probability is related to flux concentration, the relationship between the two probabilities

can be easily obtained from the relationship between the two concentrations. For example, the relationship between flux and resident concentration in one dimension is [*Parker and van Genuchten*, 1984]

$$C^f = C - \frac{D}{v}\frac{\partial C}{\partial x} \ , \tag{5.3}$$

where D is the dispersion coefficient and v is the groundwater velocity in the x direction. Substituting (5.1) and (5.2) into this expression results in the relationship between forward location and travel time probabilities

$$f_t = |v| f_x - \frac{D|v|}{v}\frac{\partial f_x}{\partial x} \ , \tag{5.4}$$

where we assume constant porosity and $A = 1$.

In forward modeling we model the movement of solute (or probability) downgradient away from the contamination source and obtain information about the future position of the contamination. With backward modeling we treat the sampling location as a source of probability (there is a probability of one that the contamination was at the sampling location at the time of sampling) and allow the probability to advect upgradient in backward time and to spread out by dispersion, resulting in a plume of backward probability that gives us information about the former position of contamination. For a solute parcel that was detected in the groundwater, backward location probability describes its position at some time prior to sampling, and travel time probability describes the amount of time required for the solute parcel to travel to the sampling location from some upgradient position, such as a known or suspected

contamination source.

The mathematical model governing backward probabilities is similar to the model for forward probabilities with some modifications to account for the upgradient movement of probability. By reversing the flow field in a random walk method, *Bagtzoglou et al.* [1992] obtained backward location probabilities for identifying sources of contamination. *Uffink* [1989] and *Chin and Chittaluru* [1994] used a similar random walk approach to delineate capture zones around pumping wells. *Wilson and Liu* [1994, 1997] used a heuristic method to obtain a backward probabilistic continuum model from the forward advection-dispersion equation, and *Liu* [1995] heuristically developed the backward model for non-uniform flow caused by areal recharge. The approach was validated using data from a field-scale tracer experiment at the Borden site [*Wilson and Liu*, 1997]; however, no formal justification was given for the model. *Neupauer and Wilson* [1999, 2000a,b] showed that backward location and travel time probabilities are related to adjoint states of resident concentration. They illustrated the formal adjoint approach for obtaining the governing equations of the backward model for a conservative chemical in one dimension [*Neupauer and Wilson*, 1999, 2000b] and in multiple dimensions [*Neupauer and Wilson*, 2000a].

In this paper, we extend the adjoint approach of *Neupauer and Wilson* [1999] to develop the backward probability model for non-uniform and transient flow. We address non-uniform velocity caused by spatially-varying porosity and by areal recharge. We also consider a transient flow field. We illustrate the approach for a one-dimensional domain, although it can be extended to multiple dimensions following the approach of *Neupauer and Wilson* [2000a].

5.2 Backward Probability Model

Transport of a conservative chemical in a one-dimensional flow field can be modeled using the advection-dispersion equation (ADE), given by

$$\frac{\partial}{\partial t}(\theta C) = \frac{\partial}{\partial x}\left(\theta D \frac{\partial C}{\partial x}\right) - \frac{\partial}{\partial x}(\theta v C) + q_I C_I - q_O C \ , \tag{5.5}$$

$$C(x,0) = C_i(x)$$

$$\frac{\partial C}{\partial x} = g_1(t) \text{ at } x = x_1$$

$$C(x,t) = g_2(t) \text{ at } x = x_2$$

where C is resident concentration, t is time, x is the spatial direction, $D = a_L|v|$ is the dispersion coefficient, a_L is the longitudinal dispersivity, v is the groundwater velocity, θ is porosity, q_I is the source inflow rate per unit volume, C_I is the source strength, q_O is the sink outflow rate per unit volume, C_i is the initial concentration, x_1 and x_2 are the boundaries, and g_1 and g_2 are known functions. The boundary conditions were chosen for illustration; other boundary conditions can also be used. From (5.1), resident concentration is proportional to forward location probability; therefore (5.5) is also the governing equation for forward location probability.

Backward location and travel time probabilities are related to adjoint states of resident concentration; therefore, the governing equation for the backward model is the adjoint of the forward ADE, (5.5), written in terms of the variation of C, rather than in terms of C itself. This approach is used to obtain the adjoint equation in sensitivity analysis [e.g., *Sykes et al.*, 1985; *Wilson and Metcalfe*, 1985] and parameter estimation [e.g., *Sun*, 1994; *Sun and Yeh*, 1990].

Sensitivity analysis measures the sensitivity of a performance measure, P, to a marginal change in a system parameter, α (e.g., $\alpha = v$ or $\alpha = D$). The performance measure quantifies the state of the system, and can be expressed as

$$P = \iint_{x,t} h(\alpha, C)\, dx\, dt\ , \tag{5.6}$$

where $h(\alpha, C)$ is a functional of the state of the system, C is concentration, and integration is over the entire space–time domain. The marginal sensitivity of this performance measure with respect to the parameter α is obtained by differentiating (5.6) with respect to α:

$$\frac{dP}{d\alpha} = \iint_{x,t} \left[\frac{\partial h(\alpha, C)}{\partial \alpha} + \frac{\partial h(\alpha, C)}{\partial C} \psi \right]\, dx\, dt\ , \tag{5.7}$$

where $dP/d\alpha$ is the marginal sensitivity and $\psi = \partial C/\partial \alpha$ is the variation of C, or the state sensitivity.

Backward location probability is equivalent to the marginal sensitivity of the resident concentration at the detection location and time (performance measure, P) to a unit source of mass anywhere in the system (system parameter, α). Let the initial concentration be $C_i(x) = C^* \delta(x - x_o)$, where C^* is the source strength and x_o is the source location. The performance measure for location probability is $P = C(x_w, T)$, where x_w is the well location, T is the detection time, and the system parameter of interest is $\alpha = C^*$. Similarly, the performance measure for backward travel time probability is $P = C^f(x_w, T)$, and travel time probability is equivalent to the magnitude of the flux of $dP/d\alpha$

[*Neupauer and Wilson*, 2000a].

The marginal sensitivity cannot be calculated directly from (5.7) because the state sensitivity is unknown, so we use adjoint theory to eliminate ψ from the equation. The marginal sensitivity becomes (see Appendix 5.A)

$$\frac{dP}{d\alpha} = \iint_{x,t} \frac{\partial h(\alpha, C)}{\partial \alpha}\, dx\, dt + \int_x \left(\theta \psi^* \frac{\partial C_i}{\partial \alpha} \right) \Bigg|_{t=0} dx \;, \tag{5.8}$$

where ψ^*, the adjoint state, is the solution to the following adjoint equation (see Appendix 5.A)

$$\frac{\partial}{\partial \tau}(\theta \psi^*) = \frac{\partial}{\partial x}\left(\theta D \frac{\partial \psi^*}{\partial x} \right) + \frac{\partial}{\partial x}(\theta v \psi^*) - q_I \psi^* + \frac{\partial h(\alpha, C)}{\partial C} \tag{5.9}$$

$$\psi^*(x, 0) = 0$$

$$D\frac{\partial \psi^*}{\partial x} + v\psi^* = 0 \text{ at } x = x_1$$

$$\psi^* = 0 \text{ at } x = x_2 \;,$$

where τ is backward time representing time prior to sampling ($\tau = T - t$, where $t = T$ ($\tau = 0$) is the sampling time). The differences between the forward equation (5.5) and the backward (adjoint) equation (5.9) are the reversal of sign on the velocity term to account for upgradient flow of information, the reversal of sign on the time derivative term to account for flow of information backward in time, and the replacement of sinks in the forward model with sources in the backward model as a consequence of the flow-field reversal. Also, the boundary conditions in the backward model are different than those of the forward model. The first-type boundaries in the forward model remain first-type in the backward model; however, the second-type boundaries in the

forward model become third-type in the backward model, and vice versa. In the adjoint model, all boundary conditions are homogeneous.

Location probability is equivalent to the marginal sensitivity if $\alpha = C^*$, with $C_i = C^*\delta(x - x_o)$, and if h in 5.6 is defined such that $P = C(x_w, T)$. From (5.6), $P = C(x_w, T)$ when the performance functional, h, is defined as

$$h(x, \tau) = C\delta(x - x_w)\delta(\tau) \ , \tag{5.10}$$

where $\delta(x)$ is a Dirac delta function. The load term in the adjoint equation, $\partial h/\partial C$, is the Fréchet derivative [*Saaty*, 1981; see also Appendix D of *Neupauer and Wilson*, 1999] of this performance functional, h, with respect to C. Therefore, for location probability, the load term in (5.9) is $\partial h/\partial C = \delta(x - x_w)\delta(\tau)$. Since h is independent of α ($\alpha = C^*$), the first integral in (5.8) vanishes, and the marginal sensitivity (and backward location probability) reduces to

$$\frac{dP}{d\alpha} = f_x(x = x_o; \tau = T) = \theta(x_o, \tau = T)\psi_x^*(x_o, \tau = T), \tag{5.11}$$

where ψ_x^* is the adjoint state corresponding to location probability.

Travel time probability is equivalent to the magnitude of the flux of marginal sensitivity using $\alpha = C^*$, with $C_i = C^*\delta(x - x_o)$, and $P = C^f(x_w, T)$. Therefore, for travel time probability, the performance functional, h, is defined as

$$h(x, \tau) = C^f\delta(x - x_w)\delta(\tau) \ . \tag{5.12}$$

Substituting (5.3) into this equation and taking the Fréchet derivative with respect to C, we obtain the load term for backward travel time, given by

$$\frac{\partial h}{\partial C} = \delta(x - x_w)\delta(\tau) + \frac{D}{v}\delta'(x - x_w)\delta(\tau) \ , \tag{5.13}$$

where $\delta'(x)$ is the derivative of the Dirac delta function with respect to x. With the appropriate substitutions in (5.8), the marginal sensitivity can be reduced and the travel time probability becomes

$$\begin{aligned} \left(|v(x, \tau = T)| \frac{dP}{d\alpha} \right) \Bigg|_{x_o} &= f_\tau(\tau = T; x = x_o) \\ &= |v(x_o, \tau = T)| \theta(x_o, \tau = T) \psi^*_\tau(x_o, \tau = T), \end{aligned} \tag{5.14}$$

for a one-dimensional domain, where ψ^*_τ is the adjoint state corresponding to backward travel time probability.

5.3 Applications of the General Backward Probability Model

In this section we present several examples of the backward probability model for a conservative tracer. We use the hypothetical one-dimensional aquifer shown in Figure 5.1. The confined aquifer is semi-infinite with a pumping well at $x = 0$, and a source of contamination at $x_o > 0$, where x_o is the source location. Flow is steady from right to left in the figure, with no internal sources or sinks of water or contamination.

The governing equation for the forward model is shown in (5.5), with $q_I = q_O = 0$, $x_1 = 0$, $x_2 \to \infty$, $g_1(t) = g_2(t) = 0$, and $C_i(x) = C^*\delta(x - x_o) = (M_o/\theta)\delta(x - x_o)$, where M_o is the source mass per unit cross-sectional area of

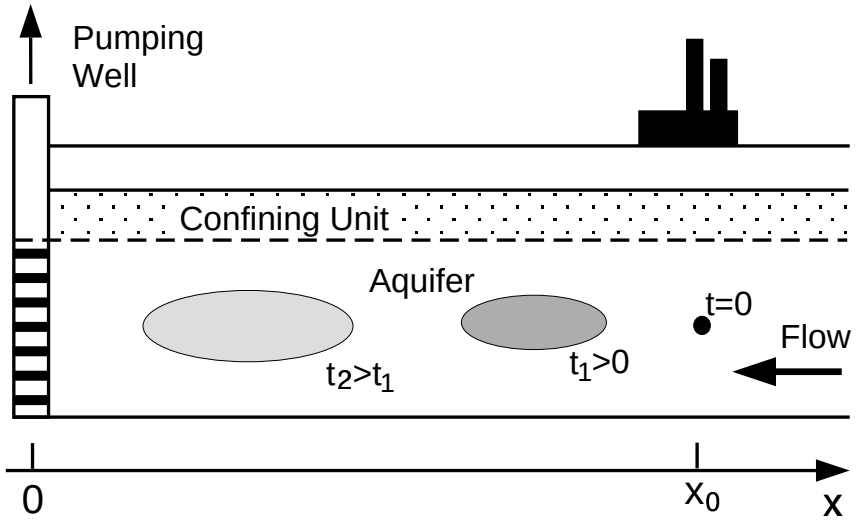

Figure 5.1: Aquifer geometry for example problem.

the aquifer. The solution to (5.5) for constant v, D, and θ is *Wilson and Liu* [1994]

$$C(x,t) = \frac{M_o}{\theta\sqrt{4\pi Dt}} \exp\left\{-\frac{(x-x_o-vt)^2}{4Dt}\right\}\left[1+\exp\left\{\frac{-x_o x}{Dt}\right\}\right] + \frac{M_o v}{2D\theta}\exp\left\{\frac{-vx_o}{D}\right\}\operatorname{erfc}\left[\frac{x+x_o-vt}{\sqrt{4Dt}}\right], \quad (5.15)$$

for $v < 0$ (i.e., flow in the direction of $-x$). This equation is plotted in Figure 5.2 using the transport parameters values shown in Table 5.1. The figure shows the resident concentration for $t = 20$ days and $t = 50$ days after release from the source at $x_o = 100$ m. At $t = 20$ days, the contamination has not yet reached the pumping well, but by $t = 50$ days, some contamination has reached the well.

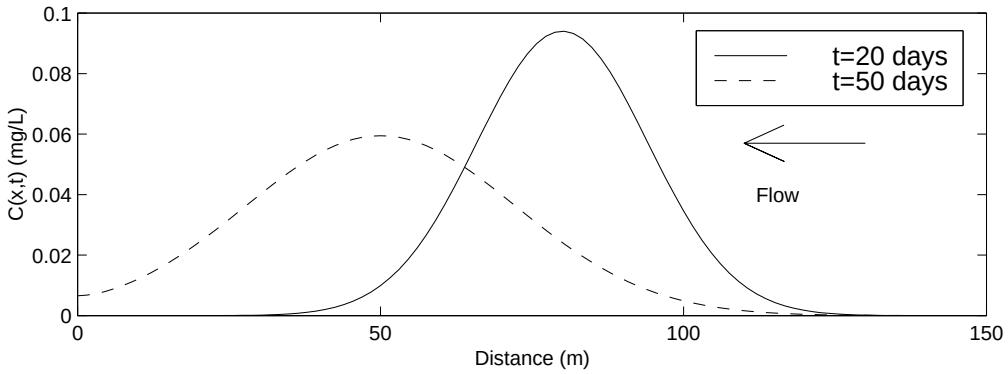

Figure 5.2: Resident concentration of a conservative tracer at $t = 20$ days and $t = 50$ days after release. ($x_o = 100$ m, $v = -1$ m/d, $D = 5$ m^2/d, $M_o = 1$ g/m^2, $\theta = 0.3$).

Table 5.1: Transport parameters for the example problem.

Parameter	Value
Source location, x_o	100 m
Groundwater velocity, v	-1 m/d
Longitudinal dispersivity, a_L	5 m
Dispersion coefficient, D	5 m^2/d
Porosity, θ	0.3
Source mass, M_o	1 g/m^2

5.3.1 Backward Probability Model in a Steady and Uniform Flow Field

Suppose we detect contamination in the pumping well and want to know its location at some time in the past. To determine the likely prior locations, we could use the backward location probability for contamination detected at the pumping well ($x_w = 0$). The governing equation for this case is (5.9) with h defined in (5.10), $q_I = 0$, $x_1 = 0$, and $x_2 \to \infty$, and the backward location probability (5.11) is defined by $f_x = \theta\psi^*$. The solution to this equation is [*Wilson and Liu*, 1994]

$$f_x(x;\tau) = \frac{1}{\sqrt{\pi D\tau}} \exp\left\{-\frac{(x+v\tau)^2}{4D\tau}\right\} + \frac{v}{2D} \exp\left\{\frac{-vx}{D}\right\} \operatorname{erfc}\left[\frac{x-v\tau}{\sqrt{4D\tau}}\right] , \quad (5.16)$$

for $v < 0$. This equation is plotted in Figure 5.3 for $\tau = 20$ days and $\tau = 50$ days prior to detection at the pumping well, showing the probability of the position of the detected contamination at $\tau = 20$ and $\tau = 50$ days prior to detection. The most likely prior position of the contamination is $x \approx 23$ m at $\tau = 20$ days prior to detection, and $x \approx 55$ m at $\tau = 50$ days prior to detection. Note also that $f_x(x = 100 \text{ m}; \tau = 20 \text{ days}) \approx 0$; this is consistent with Figure 5.2, which shows that mass originating at $x_o = 100$ m does not reach the pumping well in 20 days. At $\tau = 50$ days, however, the location probability at $x = 100$ m is non-zero, indicating that the mass that originated at $x = 100$ m has a finite probability of reaching the pumping well in 50 days. This is also consistent with Figure 5.2.

Suppose that we detect contamination in the pumping well and would like to know when it could have been released from a known or suspected

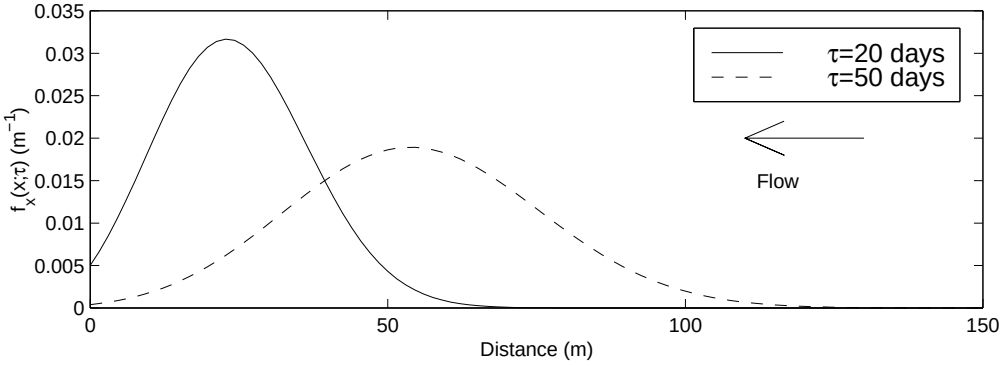

Figure 5.3: Backward location probability for a conservative tracer at $\tau = 20$ days and $\tau = 50$ days prior to detection at the pumping well. ($x_w = 0$, $v = -1$ m/d, $D = 5$ m^2/d).

source at $x = x_o = 100$ m. To determine the likely travel times from the source to the pumping well, we would use the backward travel time probability. The governing equation for backward travel time probability is (5.9) with $h = C^f \delta(x - x_w)\delta(\tau)$, where x_w is the pumping well location (i.e., $x_w = 0$). In this example, the pumping well is at a domain boundary that is modeled with a zero-gradient boundary condition; therefore from (5.3), $C^f = C$ at the well, and the load term in the adjoint equation is $\partial h/\partial C = \delta(x - x_w)\delta(\tau)$, giving $\psi^*_\tau = \psi^*_x$ for this case.

From (5.14) and (5.16), backward travel time probability for this case is

$$f_\tau(\tau; x) = \frac{-v}{\sqrt{\pi D \tau}} \exp\left\{-\frac{(x + v\tau)^2}{4D\tau}\right\} - \frac{v^2}{2D} \exp\left\{\frac{-vx}{D}\right\} \operatorname{erfc}\left[\frac{x - v\tau}{\sqrt{4D\tau}}\right], \quad (5.17)$$

for $v < 0$. This equation is plotted in Figure 5.4, showing the backward travel time probability from the pumping well to the source at $x = x_o = 100$ m. This

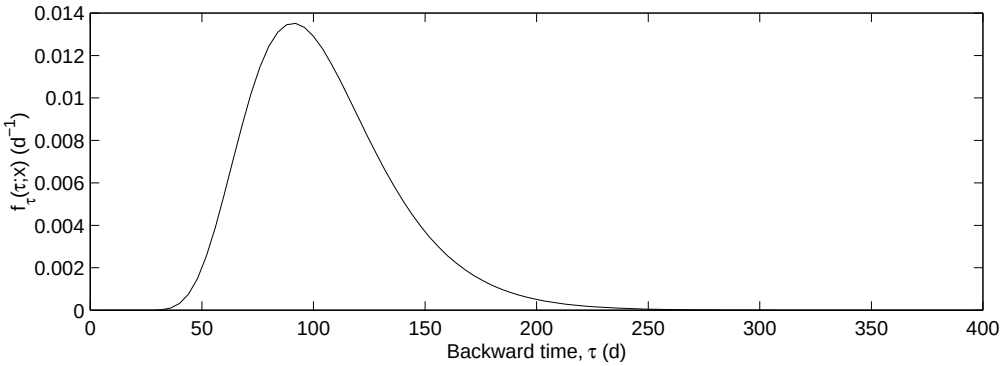

Figure 5.4: Backward travel time probability for a conservative tracer from the pumping well to $x = 100$ m. ($x_w = 0$, $v = -1$ m/d, $D = 5$ m^2/d).

travel time probability distribution shows that the most likely travel time from $x_o = 100$ m to the pumping well is $\tau \approx 92$ days. Note also that $f_\tau > 0$ at $\tau = 50$ days, indicating a non-zero probability that mass from $x_o = 100$ m will reach the pumping well in 50 days. This is consistent with the results shown in Figure 5.2.

5.3.2 Backward Probability Model with Spatially-varying Aquifer Porosity

For a one-dimensional domain with no internal sources or sinks of water, as in Figure 5.1, the specific discharge, q, is uniform because of mass conservation. If aquifer porosity is spatially-varying, groundwater velocity also varies in space, because $v = q/\theta$. The governing equation for forward contaminant transport is (5.5). Because velocity is spatially-varying, this equation does not have a simple analytical solution. We used MODFLOW–96 [*Harbaugh and McDonald*, 1996] and MT3DMS [*Zheng and Wang*, 1999] simulate flow and transport using the parameter values shown in Tables 5.1 and 5.2,

Table 5.2: Flow parameters for numerical simulations.

Parameter	Value
Downstream boundary, x_1	0
Upstream boundary, x_2	201 m
Specified head at x_2	100 m
Spatial discretization	2 m (1 m at x_1)
Aquifer thickness, B	10 m
Aquifer width	1 m
Transmissivity	0.0002 m^2/d
Specific storage, S_s	0.001 m^{-1}
Pumping rate, Q	3 m^3/d

with porosity given by

$$\theta(x) = \theta_o + .0005x \tag{5.18}$$

where $\theta_o = 0.3$ is the porosity at $x = 0$ and x has units of m. With these values, the velocity at the well is $v = Q/(B\theta_o) = -1$ m/d.

The transport model results are plotted in Figure 5.5, showing the resident concentration at $t = 20$ days and $t = 50$ days after release from the source at $x_o = 100$ m. For comparison, the plumes for the constant porosity ($\theta = 0.3$) case are also shown. With spatially-varying porosity, the porosity at the source is $\theta(x_o) = 0.35$; therefore the velocity ($v = q/\theta$) near the source is slower for the spatially-varying porosity case. This is confirmed in Figure 5.5, which illustrates that the constant-porosity plume moves faster than the spatially-varying-porosity plume. Also, because porosity is higher in the aquifer with spatially-varying porosity, the spatially-varying-porosity plume

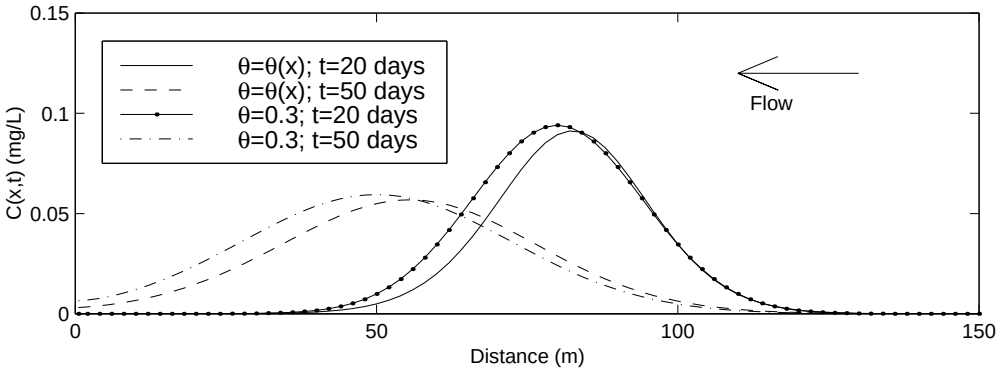

Figure 5.5: Resident concentration of a conservative tracer in an aquifer with spatially-varying porosity. (x_o = 100 m, $v = -1$ m/d, D = 5 m^2/d, M_o = 1 g/m^2).

occupies a smaller portion of the total aquifer volume.

For backward location probability, the appropriate governing equation is (5.9) with h as defined in (5.10). We solved this equation numerically using MODFLOW–96 and MT3DMS, with the parameters in Tables 5.1 and 5.2 and porosity shown in (5.18). (See Chapter 7 for details of the numerical implementation of the backward probability model). The results from MT3DMS produce $\psi_x^*(x,\tau)$, and from (5.11) $f_x(x;\tau) = \theta(x,\tau)\psi_x^*(x,\tau)$. The location probability is plotted in Figure 5.6 for τ = 20 days and τ = 50 days prior to detection at the pumping well. For comparison, the location probability for the constant-porosity case is also shown. Because the velocity is slower for the spatially-varying-porosity case, the upstream movement of its location probability plume is slower and less disperse.

With the zero-gradient boundary condition at the pumping well, $\psi_\tau^* = \psi_x^*$. We obtained ψ_x^* for location probability using MT3DMS. Using (5.14), backward travel time probability from the pumping well to the source at $x =$

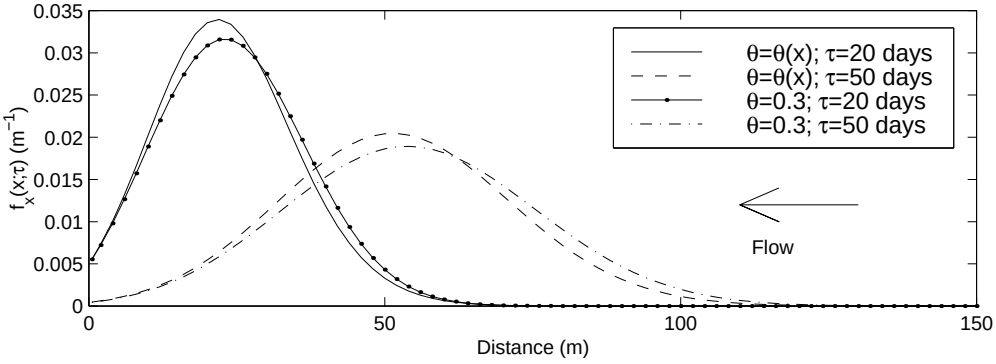

Figure 5.6: Location probability of a conservative tracer in an aquifer with spatially-varying porosity. ($x_w = 0$, $v = -1$m/d at x_w, $a_L = 5$ m).

$x_o = 100$ m is given by $f_\tau(\tau; x = x_o) = |v(x_o)|\theta(x_o, \tau)\psi^*_\tau(x_o, \tau)$. These results are plotted in Figure 5.7. For comparison, the travel time probability is also shown for the constant-porosity case. Because the velocity is slower for the spatially-varying-porosity case, the travel time probability plume also travels slower (and arrives further back in time) for this case, suggesting an earlier release time at the source.

5.3.3 Backward Probability Model with Natural Recharge

Natural recharge is a spatially-distributed source of water, and possibly of contamination. In the absence of any other internal sources or sinks, the forward governing equation (5.5) is modified as

$$\frac{\partial(\theta C)}{\partial t} = \frac{\partial}{\partial x}\left(\theta D \frac{\partial C}{\partial x}\right) - \frac{\partial}{\partial x}(\theta v C) + \frac{N}{B} C_I \ , \tag{5.19}$$

where the sink term, $-q_O C$, is eliminated because we are assuming no internal sinks, N is the natural recharge rate (spatially-uniform), B is the aquifer

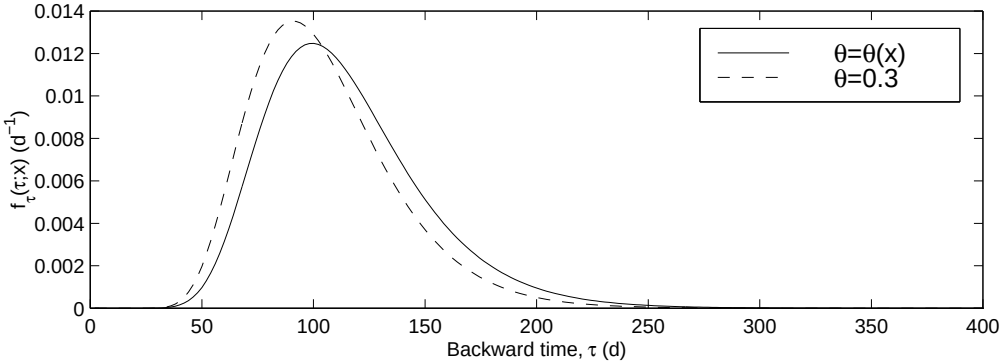

Figure 5.7: Backward travel time probability from the source area to the pumping well for a conservative tracer in an aquifer with spatially-varying porosity. ($x_o = 100$ m, $x_w = 0$, $v = -1$ m/d at x_w, $a_L = 5$ m).

thickness, and the ratio N/B is the source inflow rate, q_I. We assume that the natural recharge is free of contamination (i.e., $C_I = 0$); therefore, the final term in (5.19) vanishes.

Since natural recharge is a spatially-distributed source, the velocity in the aquifer varies in space. For the aquifer shown in Figure 5.1, if the velocity at the pumping well is $v_o = -1$ m/d, the equation describing the aquifer velocity is

$$v(x) = v_o + \frac{Nx}{B\theta}, \tag{5.20}$$

where velocity increases in the flow direction, i.e., to the left. The concentration distribution for the aquifer shown in Figure 5.1 can be found by numerically solving (5.19). Again, we used MODFLOW–96 [*Harbaugh and McDonald*, 1996] and MT3DMS [*Zheng and Wang*, 1999] with the parameters listed in Tables 5.1 and 5.2, and with $N = 0.009$ m/d. We used an unrealistically large N to

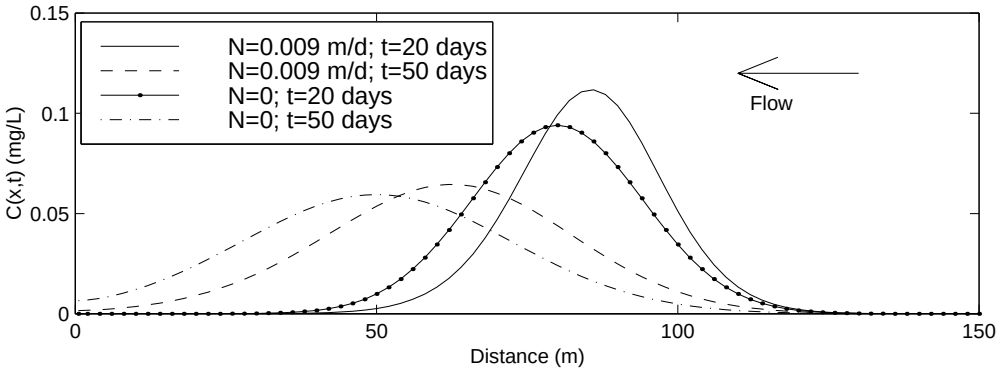

Figure 5.8: Resident concentration of a conservative tracer in a confined aquifer with natural recharge. ($x_o = 100$ m, $v_o = -1$ m/d, $a_L = 5$ m, $M_o = 1\text{g/m}^2$, $\theta = 0.3$).

amplify the effects of natural recharge. The results are plotted in Figure 5.8, showing the resident concentration for $t = 20$ days and $t = 50$ days after release from the source. For comparison, the plumes for the no-recharge case are also shown. The plume with recharge travels more slowly than the plume without recharge because the magnitude of the velocity is lower. The plume with recharge is less disperse because the dispersion coefficient is proportional to velocity.

The governing equation for backward location probability for the aquifer in Figure 5.1 with recharge is (5.9) with $q_I = N/B$, and location probability is given as $f_x = \theta\psi^*$. We solved this equation numerically using MODFLOW-96 and MT3DMS. The results are plotted in Figure 5.9, showing the backward location probability distribution for $\tau = 20$ days and $\tau = 50$ days prior to detection at the pumping well (at $x_w = 0$). For comparison, the location probability for the no-recharge case is also shown. Because of a lower velocity, the location probability with recharge travels more slowly upstream

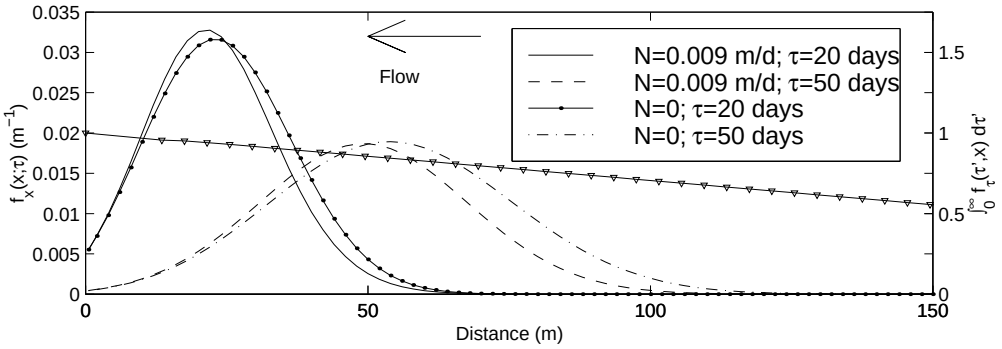

Figure 5.9: Backward location probability for a conservative tracer in a confined aquifer with natural recharge, and the integral over time of backward travel time probability, $f_\tau(\tau, x)$ (solid line with triangles) ($x_w = 0$, $v_o = -1$ m/d, $a_L = 5$ m).

and is less disperse than the location probability for the no-recharge case.

The recharge term in the adjoint equation has the same form as a first-order decay term with an equivalent decay rate of $\lambda = N/(B\theta) = 0.003$ d^{-1} for the parameters used in this example, where the θ is contributed by (5.11). Since probability is "decaying", $\int_x f_x \, dx < 1$, for $\tau > 0$. This indicates a finite probability that the detected contamination entered the system through the natural recharge and therefore was not in the system at the time of interest. In other words, $1 - \int_x f_x(x; \hat{\tau}) \, dx$ is equivalent to the probability that the detected contamination entered the system via natural recharge in the interval $0 < \tau < \hat{\tau}$. With first-order decay, $\int_x f_x(x; \tau) \, dx = e^{-\lambda\tau}$. For $\tau = 20$ days (solid line in Figure 5.9), $\int_x f_x(x; \tau) \, dx = 0.9401$, and $\int_x f_x(x; \tau) \, dx = 0.8622$ for $\tau = 50$ (dashed line in Figure 5.9). These values are essentially equivalent to $e^{-\lambda\tau}$.

With the zero-gradient boundary condition at the pumping well, $\psi^*_\tau = \psi^*_x$. We have already obtained ψ^*_x for location probability using MT3DMS.

From (5.14), the backward travel time probability from the pumping well to the source at $x = x_o = 100$ m is given by $f_\tau(\tau; x = x_o) = |v(x_o)|\theta(x_o, \tau)\psi^*_\tau(x_o, \tau)$. These results are plotted in Figure 5.10, showing the backward travel time probability from the pumping well to the source at $x = x_o = 100$ m. For comparison, the travel time probability is also shown for the no-recharge case. Because the velocity is slower with recharge, the travel time probability plume travels slower (and arrives later) for this case. The travel time probability curve also decays over time because the recharge term in the adjoint equation acts like a first-order decay term. This is demonstrated by comparing the areas under the two curves in Figure 5.10. The integral of backward travel time probability over the time domain (from $\tau = 0$ to $\tau \to \infty$) for a given x represents the probability that the detected particle was ever in the system at x. From Figure 5.10, $\int_0^\infty f_\tau(\tau', x_o)d\tau' \approx 0.71$ at $x_o = 100$ m, indicating a 71% probability that the detected particle was ever at $x_o = 100$ m, and a 29% probability that the particle entered the system between $x_w = 0$ and $x_o = 100$ m, and therefore was never at $x_o = 100$ m. For the conservative solute, $\int_0^\infty f_\tau(\tau', x_o)d\tau' = 1.0$ at $x_o = 100$ m, indicating that, for this one-dimensional domain, a conservative particle must have been at x_o at some time in the past. The values of this integral for other x are shown in Figure 5.9 (right-hand axis).

It is clear from this example that the adjoint equation (5.9) assumes that location and travel time probabilities are related to the recharge rate, N. The recharge term in the adjoint equation (5.9) acts as a first-order decay term, leading to the decay of probability. Suppose you know that the detected contamination did not enter the aquifer through recharge. In this case the

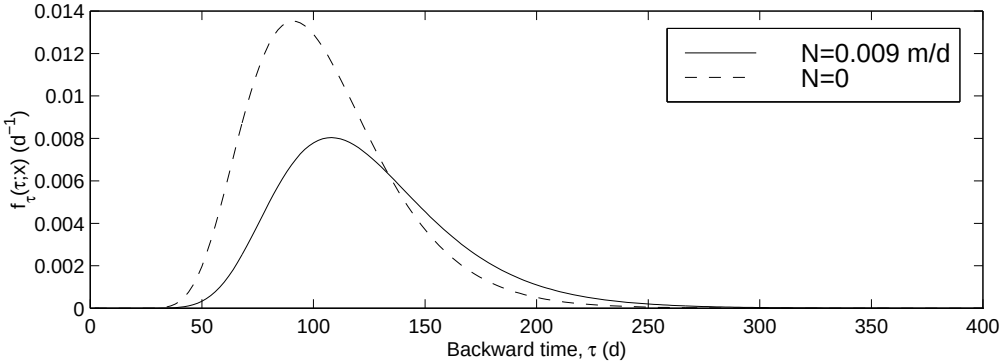

Figure 5.10: Backward travel time probability from the pumping well to the source area for a conservative tracer in an aquifer with natural recharge. ($x_w = 0$, $x_o = 100$ m, $v_o = -1$ m/d, $a_L = 5$ m).

location and travel time probabilities should be independent of the recharge rate and there would be no decay of probability, i.e., $\int_{\mathbf{X}} f_{\mathbf{X}}(\mathbf{x})d\mathbf{x} = 1$ when integrated over the entire spatial domain. For this case, the adjoint equation is still (5.9), but with $q_I = 0$. The backward probabilities would still be influenced by recharge, but only through the flow field.

5.3.4 Backward Probability Model with Transient Flow

If the flow field in an aquifer is transient, the forward contaminant transport model is governed by (5.5), with $v = v(x,t)$. Neglecting water compressibility, the accumulation term of the continuity equation becomes $S_s \partial h/\partial t = \partial\theta/\partial t$, where S_s is specific storage and h is hydraulic head, indicating that porosity is also temporally variable. To emphasize the variability in these parameters, we generalize (5.5) for these temporally-varying parameters as

$$\frac{\partial}{\partial t}\left[\theta(x,t)C\right] = \frac{\partial}{\partial x}\left[\theta(x,t)D(x,t)\frac{\partial C}{\partial x}\right] - \frac{\partial}{\partial x}\left[\theta(x,t)v(x,t)C\right] + q_I C_I - q_O C \ . \tag{5.21}$$

The governing equation for the backward probability model is the adjoint of (5.21). Rewriting the adjoint equation (5.9), emphasizing the temporal and spatial variability in the parameter values, we obtain

$$\frac{\partial}{\partial \tau}\left[\theta(x,T-\tau)\psi^*\right] = \frac{\partial}{\partial x}\left[\theta(x,T-\tau)D(x,T-\tau)\frac{\partial \psi^*}{\partial x}\right] + \frac{\partial}{\partial x}\left[\theta(x,T-\tau)v(x,T-\tau)\psi^*\right] - q_I\psi^* + \frac{\partial h(\alpha,C)}{\partial C} \ , \tag{5.22}$$

where we have substituted $t = T - \tau$. By inspection of this equation, we see that the flow field in the forward model, $v(x,t)$, must be reversed in both space and time to be used in the backward (adjoint) model, and the porosity must also be reversed in time. Since $D = a_L|v|$, reversal in time of D is accomplished by the flow-field reversal. The backward location and travel time probabilities are still defined by (5.11) and (5.14), respectively.

As an example, suppose the aquifer in Figure 5.1 is at steady state with pumping at a rate of $Q = 4$ m^3/d, and at $t = 0$ the pumping rate is decreased to $Q = 3$ m^3/d. After the pumping rate is decreased, head increases and the flow field will be in a transient until it reaches a new steady state. We used MODFLOW-96 [*Harbaugh and McDonald*, 1996] and MT3DMS [*Zheng and Wang*, 1999] to solve this problem. In MT3DMS, porosity is constant

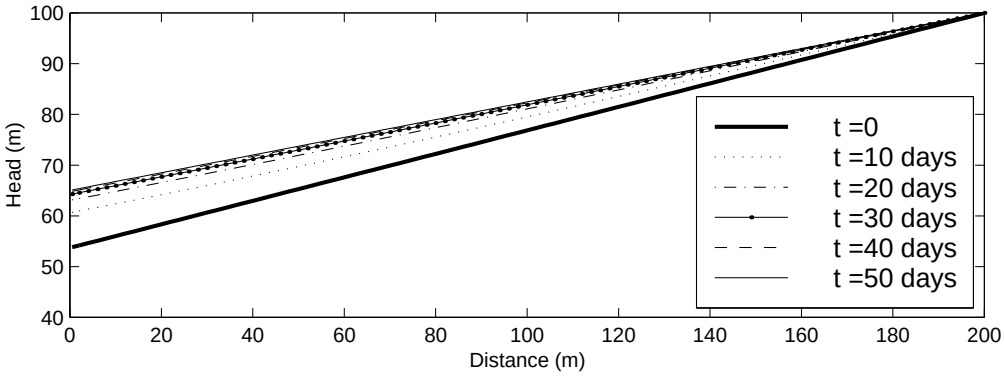

Figure 5.11: Head distribution in transient simulation.

throughout the simulation (i.e., $\partial\theta/\partial t$ is neglected), therefore we only considered temporally-varying v and D (See Appendix 5.B for more details).

The head distribution in the aquifer at five different times is shown in Figure 5.11. The aquifer reaches a new steady state in approximately 50 days. Figure 5.12 shows resident concentration at $t = 20$ days and $t = 50$ days after release from a source at $x_o = 100$ m. For comparison, the plumes from the steady flow simulation ($Q = 3$ m^3/d; $v = -1$ m/d) are also shown. In the transient flow case, the velocity is slightly faster than in the steady flow simulation; therefore, the plume moves slightly faster.

The governing equation for backward location probability for the aquifer in Figure 5.1 with transient flow is (5.22) with h as defined in (5.10). We solved this equation numerically using MODFLOW-96 and MT3DMS, with $\tau = T - t$, and $T = 50$ days. The results are plotted in Figure 5.13, showing the backward location probability distribution for $\tau = 20$ days and $\tau = 50$ days prior to detection at the pumping well (at $x_w = 0$). For comparison, the location probability for the steady flow case is also shown. For early τ (later

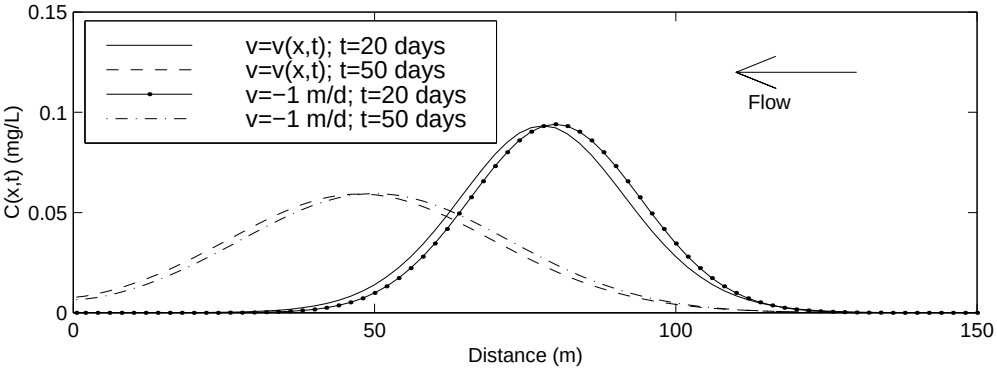

Figure 5.12: Resident concentration of a conservative tracer in an aquifer with transient flow. ($x_o = 100$ m, $a_L = 5$ m, $M_o = 1$ g/m^2, $\theta = 0.3$).

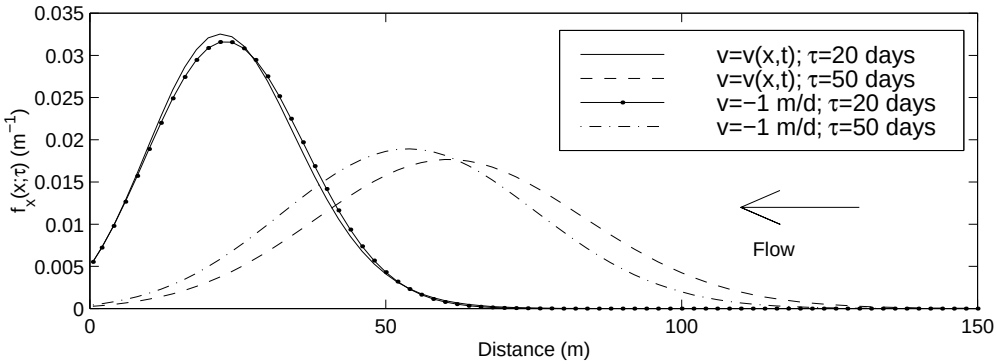

Figure 5.13: Location probability of a conservative tracer in an aquifer with transient flow. ($x_o = 100$ m, $a_L = 5$ m, $M_o = 1$ g/m^2, $\theta = 0.3$).

forward time), the aquifer is essentially at steady state with the lower pumping rate ($Q = 3$ m^3/d; $v = -1$ m/d); therefore, the steady-flow and transient-flow location probability plumes at $\tau = 20$ days are essentially equivalent. At $\tau = 50$ days, the aquifer is at steady state with the higher pumping rate ($Q = 4$ m^3/d); therefore the transient-flow probability plume has traveled farther than the steady-flow plume.

With the zero-gradient boundary condition at the pumping well, $\psi^*_\tau =$

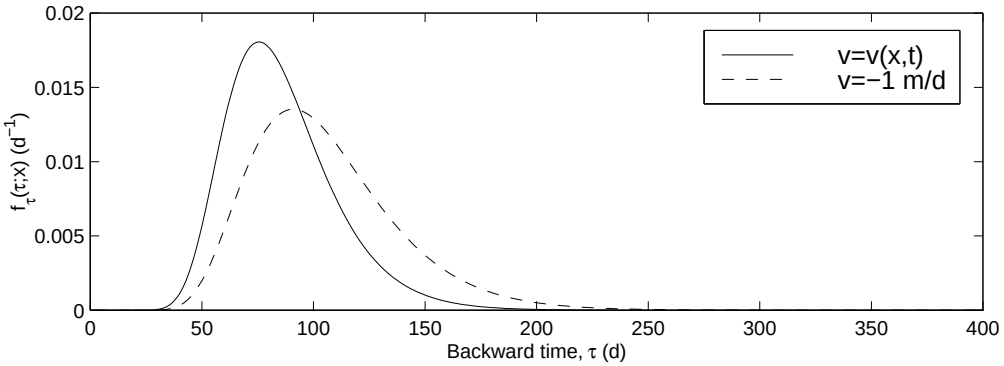

Figure 5.14: Backward travel time probability from the pumping well to the source area for a conservative tracer in an aquifer with transient flow. ($x_w = 0$, $x_o = 100$ m, $a_L = 5$ m).

ψ_x^*. Using (5.14), backward travel time probability from the pumping well to the source at $x = x_o = 100$ m is given by $f_\tau(\tau; x = x_o) = |v(x_o, \tau)|\theta(x_o, \tau)\psi_\tau^*(x_o, \tau)$. These results are plotted in Figure 5.14. For comparison, the travel time probability is also shown for the steady-flow case. Because the velocity is faster in the transient-flow case, the travel time probability plume travels faster (and arrives sooner) for this case.

5.4 Conclusions

Backward location and travel time probabilities were developed heuristically by *Liu* [1995] and *Wilson and Liu* [1994] for several cases including transport of conservative chemicals in uniform and non-uniform flow fields. *Neupauer and Wilson* [1999, 2000a,b] demonstrated that these backward probabilities are related to adjoint states of resident concentration, and they used adjoint theory to obtain the governing equations of the backward probability model for conservative tracers. The advantage of the adjoint approach over the

heuristic approach in obtaining the governing equations is that adjoint theory provides a rigorous mathematical procedure for developing the equations for all aquifer geometries and for all transport processes.

In this paper, we used adjoint theory to obtain backward location and travel time probabilities for the cases of spatially-varying porosity, natural recharge, and transient flow in a one-dimensional domain. Using the approach of *Neupauer and Wilson* [2000a], the results presented here can be applied to multiple dimensions. Spatially-varying porosity produces a non-uniform velocity field that affects both the movement and the spread of the probability plumes. We would observe similar results for a variable aquifer thickness, or for a variable hydraulic conductivity in multiple dimensions. Transient flow produces a spatially- and temporally-varying velocity field and porosity. The forward model flow field must be reversed in both space and time to obtain the appropriate flow field for the backward model.

Areally-distributed natural recharge produces a non-uniform velocity field, with velocity increasing downgradient. In the adjoint (backward) equation, the natural recharge term is equivalent to a first-order decay term; therefore, the backward probabilities decay in time. For location probability at a fixed time, $\hat{\tau}$, this decay quantifies the probability that the detected contaminant parcel entered the aquifer through natural recharge during the time interval $0 < \tau < \hat{\tau}$, and was not in the system at $\hat{\tau}$. For travel time probability at a fixed point, $\hat{x}$, the decay indicates a non-zero probability that the contaminant parcel entered the system downgradient of $\hat{x}$, and therefore it was never at $\hat{x}$. If it is known that the source of contamination has no causal or correlative link to recharge, then the backward probability can be calculated

without decay.

Acknowledgments

This research was supported in part by the Geophysical Research Center at New Mexico Tech and in part by the Environmental Protection Agency's STAR Fellowship program under Fellowship No. U-915324-01-0. This work has not been subjected to the EPA's peer and administrative review and therefore may not necessarily reflect the views of the Agency and no official endorsement should be inferred. The authors acknowledge William D. Stone for his input on operator theory.

References

Bagtzoglou, A.C., D.E. Dougherty, and A.F.B. Thompson, Application of particle methods to reliable identification of groundwater pollution sources, *Water Resources Management*, 6, 15–23, 1992.

Chin, D.A. and P.V.K. Chittaluru, Risk management in wellhead protection, *J. Water Resour. Plan. Manage.*, 120(3), 294–315. 1994.

Dagan, G., Stochastic modeling of groundwater flow by unconditional and conditional probabilities, 2, The solute transport, *Water Resour. Res.*, 18(4), 835–848, 1982.

Dagan, G., Theory of solute transport by groundwater, *Ann. Rev. Fluid Mech.*, 19, 183–215, 1987.

Dagan, G., *Flow and Transport in Porous Formations*, Springer-Verlag, New York, 1989.

Dagan, G., and V. Nguyen, A comparison of travel time and concentration approaches to modeling transport by groundwater, *Journal of Contaminant Hydrology*, 4, 79–91, 1989.

Harbaugh A.W. and M.G. McDonald, *User's Documentation for MODFLOW-96, an update to the U.S. Geological Survey Modular Finite-Difference Ground-Water Flow Model*, U.S. Geological Survey, Open-File Report 96-485, 1996.

Jury, W.A., Simulation of solute transport using a transfer function model, *Water Resour. Res.*, 18(2), 363–368, 1982.

Jury, W.A., G. Sposito, and R.E. White, A transfer function model of solute transport through soil, 1, Fundamental concepts, *Water Resour. Res.*, 22(2), 243–247, 1986.

Jury, W.A. and K. Roth, *Transfer Functions and Solute Movement through Soil: Theory and Applications*, Birkhauser Verlag, Boston, 1990.

Liu, J., *Travel time and location probabilities for groundwater contaminant sources*, Master's thesis, New Mexico Institute of Mining and Technology, Socorro, 1995.

Neupauer, R.M. and J.L. Wilson, Adjoint method for obtaining backward-in-time location and travel time probabilities of a conservative groundwater contaminant, *Water Resour. Res.*, 35(11), 3389–3398, 1999.

Neupauer, R.M. and J.L. Wilson, Adjoint-derived location and travel time probabilities in a multi-dimensional groundwater flow system, *Water Resour. Res.*, in press, 2000a.

Neupauer, R.M. and J.L. Wilson, Backward location and travel time probabilities for contamination in a one-dimensional infinite aquifer, submitted to *J. Contam. Hydrol.*, 2000b.

Parker, J.C. and M. Th. van Genuchten, Flux-averaged and volume-averaged concentrations in continuum approaches to solute transport, *Water Resour. Res.*, 20(7), 866–872, 1984.

Rubin, Y. and G. Dagan, Conditional estimation of solute travel time in heterogeneous formations: impact of transmissivity measurements, *Water Resour. Res.*, 28(4), 1033–1040, 1992.

Shapiro, A.M. and V.D. Cvetkovic, Stochastic analysis of solute arrival time in heterogeneous porous media, *Water Resour. Res.*, 24(10), 1711–1718, 1988.

Sun, N.-Z., *Inverse Problems in Groundwater Modeling*, Kluwer Academic Publishers, Boston, 1994.

Sun, N.-Z. and W.W.-G. Yeh, Coupled inverse problems in groundwater modeling, 1, Sensitivity analysis and parameter identification, *Water Resour. Res.*, 26(10), 2507–2525, 1990.

Sykes, J.F., J.L. Wilson, and R.W. Andrews, Sensitivity analysis for steady state groundwater flow using adjoint operators, *Water Resour. Res.*, 21(3), 359–371, 1985.

Uffink, G.J.M., Application of Kolmogorov's backward equation in random walk simulations of groundwater contaminant transport, in *Contaminant Transport in Groundwater*, H.E. Kobus and W. Kinzelbach, editors, pp. 283–289, A.A. Balkema, Brookfield, Vt., 1989.

Wilson, J.L. and J. Liu, Backward tracking to find the source of pollution, in *Waste-management: From Risk to Remediation*, edited by R. Bhada *et al.*, ECM Press, Albuquerque, NM, 181–199, 1994.

Wilson, J.L. and J. Liu, Field Validation of the Backward-in-time Advection Dispersion Theory. *Proceedings of the 1996 HSRC/WERC Joint Conf. on the Environment*, Great Plains-Rocky Mountain Hazardous Substance Center, Manhattan, Kansas, http://www.engg.ksu.edu/HSRC/ 96Proceed/wilson.html, 1997.

Wilson, J.L. and D.E. Metcalfe, Illustration and verification of adjoint sensitivity theory for steady state groundwater flow, *Water Resour. Res.*, 21(11), 1602–1610, 1985.

Zheng, C. and P.P. Wang, *MT3DMS: Documentation and User's Guide*, Release DoD_3.50.A, U.S. Army Corps of Engineers, Contract Report, SERDP-99, 1999.

5.A Adjoint Derivation

Following the approach of *Sykes et al.* [1985] and *Neupauer and Wilson* [2000a], adjoint theory can be used to eliminate the unknown state sensitivity, ψ from (5.7). We present the derivation here since previous derivations assumed steady flow and constant porosity, θ. We first obtain a governing equation for ψ by differentiating each term of (5.5) with respect to the parameter α, resulting in

$$-\frac{\partial}{\partial t}(\theta\psi)+\frac{\partial}{\partial x}\left(\theta D\frac{\partial\psi}{\partial x}\right)-\frac{\partial}{\partial x}(\theta v\psi)-q_O\psi+L_\alpha=0\ , \tag{5.23}$$

$$\psi(x,0)=\frac{\partial C_i(x)}{\partial\alpha}$$

$$\frac{\partial\psi}{\partial x}=0 \text{ at } x=x_1$$

$$\psi=0 \text{ at } x=x_2$$

where L_α contains the remaining terms, all independent of ψ, and is given by

$$L_\alpha=\frac{\partial}{\partial x}\left[\frac{\partial(\theta D)}{\partial\alpha}\frac{\partial C}{\partial x}\right]-\frac{\partial}{\partial x}\left[\frac{\partial(\theta v)}{\partial\alpha}C\right]+\frac{\partial(q_IC_I)}{\partial\alpha}-C\frac{\partial q_O}{\partial\alpha}-\frac{\partial}{\partial t}\left[C\frac{\partial\theta}{\partial\alpha}\right]. \tag{5.24}$$

In (5.23), we assume that g_1, and g_2 are independent of α, although this assumption is not necessary for the adjoint method. In this paper, $L_\alpha = 0$ because the only parameter α considered is $\alpha = C^*$, the source strength.

Next we take the inner product of the left-hand side of (5.23) with an arbitrary function, ψ^*, called the adjoint state. The inner product of two real functions f and g is defined as $\langle f,g\rangle = \int_0^T\int_{x_1}^{x_2} f\,g\;dx\;dt$, where the time

domain is $0 \leq t \leq T$. The inner product of (5.23) with ψ^* produces

$$\iint_{x,t}\left[-\psi^*\frac{\partial}{\partial t}(\theta\psi)+\psi^*\frac{\partial}{\partial x}\left(\theta D\frac{\partial\psi}{\partial x}\right)-\psi^*\frac{\partial}{\partial x}(\theta v\psi)-\psi^* q_O\psi\right]dxdt=0. \quad (5.25)$$

Using the product rule on each derivative term, the inner product can be rewritten as

$$\begin{aligned}\iint_{x,t}\Bigg[&-\frac{\partial}{\partial t}(\psi^*\theta\psi)+\theta\psi\frac{\partial\psi^*}{\partial t}+\psi\frac{\partial}{\partial x}\left(\theta D\frac{\partial\psi^*}{\partial x}\right)+\frac{\partial}{\partial x}\left(\psi^*\theta D\frac{\partial\psi}{\partial x}\right) \\ &-\frac{\partial}{\partial x}\left(\psi\theta D\frac{\partial\psi^*}{\partial x}\right)-\frac{\partial}{\partial x}(\psi^*\theta v\psi)-\theta v\psi\frac{\partial\psi^*}{\partial x}-\psi^* q_O\psi\Bigg]\,dx\,dt=0\,.\end{aligned} \quad (5.26)$$

Since the left-hand side of this equation evaluates to zero, it can be added to the right-hand side of (5.7) without changing the equality. With this addition and after rearranging the terms, (5.7) becomes

$$\begin{aligned}\frac{dP}{d\alpha}=\iint_{x,t}\Bigg\{&\psi\left[\frac{\partial h(\alpha,C)}{\partial C}+\theta\frac{\partial\psi^*}{\partial t}+\frac{\partial}{\partial x}\left(\theta D\frac{\partial\psi^*}{\partial x}\right)-\theta v\frac{\partial\psi^*}{\partial x}-q_O\psi^*\right] \\ &+\frac{\partial h(\alpha,C)}{\partial\alpha}-\frac{\partial}{\partial t}(\psi^*\theta\psi)+\frac{\partial}{\partial x}\left(\psi^*\theta D\frac{\partial\psi}{\partial x}-\psi\theta D\frac{\partial\psi^*}{\partial x}-\psi^*\theta v\psi\right)\Bigg\}\,dx\,dt\,.\end{aligned} \quad (5.27)$$

To eliminate the unknown values of ψ from the divergence terms, we define boundary and final conditions on the adjoint state, ψ^*, so that the divergence terms containing unknown values of ψ vanish. After integration over the spatial domain, the divergence terms in space become

$$\int_t\left[\psi^*\theta D\frac{\partial\psi}{\partial x}-\psi\theta D\frac{\partial\psi^*}{\partial x}-\psi^*\theta v\psi\right]\Bigg|_{x_1}^{x_2}dt\,. \quad (5.28)$$

After we substitute the boundary conditions on ψ from (5.23), the terms involving unknown values of ψ can be eliminated from (5.28) if we set $D\partial\psi^*/\partial x + v\psi^* = 0$ at $x = x_1$, and $\psi^* = 0$ at $x = x_2$. Similarly, after integration over the time domain, the divergence term in time becomes

$$\int_x \psi^* \theta \psi \Big|_{t=0}^{t=T} dx \; . \tag{5.29}$$

After we substitute the initial condition on ψ from (5.23), we can eliminate the term involving $\psi(x, T)$ by setting $\psi^* = 0$ at $t = T$. These are the final and boundary conditions for the adjoint state, ψ^*. Note that the first-type boundary (at $x = x_2$) in the forward model remains a first-type boundary in the backward model, and the second-type boundary (at $x = x_1$) in the forward model becomes a third-type boundary in the backward model. Similarly, a third-type boundary in the forward model would become a second-type boundary in the backward model. All boundary conditions in the backward model are homogeneous.

The only remaining term containing ψ in (5.27) is the first term in the integral. To eliminate ψ from the expression, we set the quantity inside the square brackets to zero, producing the adjoint equation

$$-\theta \frac{\partial \psi^*}{\partial t} = \frac{\partial}{\partial x}\left(\theta D \frac{\partial \psi^*}{\partial x}\right) - \theta v \frac{\partial \psi^*}{\partial x} - q_O \psi^* + \frac{\partial h(\alpha, C)}{\partial C} \; , \tag{5.30}$$

and the marginal sensitivity in (5.27) is simplified to the expression in (5.8). Using the continuity equation for an incompressible fluid,

$$\frac{\partial \theta}{\partial t} + \frac{\partial}{\partial x}\left(\theta v\right) = q_I - q_O \; , \tag{5.31}$$

the adjoint equation, (5.30), can be rewritten as (5.9).

5.B Backward Probability Simulations using MT3DMS with Transient Flow

In a transient flow field, the hydraulic head distribution is transient. For an incompressible fluid,

$$S_s \frac{\partial h}{\partial t} = \frac{\partial \theta}{\partial t} \; ; \tag{5.32}$$

and the porosity also varies in time and space.

In MT3DMS [*Zheng and Wang*, 1999], porosity remains unchanged throughout the simulation. Transient flow is handled by modifying the time-derivative term as

$$\frac{\partial(\theta C)}{\partial t} = \theta \frac{\partial C}{\partial t} + C \frac{\partial \theta}{\partial t} = \theta \frac{\partial C}{\partial t} + C q_s' \; , \tag{5.33}$$

where θ is porosity, C is resident concentration, t is time, and $q_s' = \partial\theta/\partial t$ is the "flow rate" (per unit volume) of water into or out of storage. The term involving q_s' is modeled as a source/sink term. This accounts for the transient porosity in the accumulation term. The transient porosity in the advection and dispersion terms are accounted for in the flow field, because the specific discharge $q = v\theta$ is obtained directly from the flow model results. Therefore, for a conservative tracer, the correct concentration is obtained. However, the total mass of solute (or probability) in the aquifer is not conserved in MT3DMS. Total mass, M, can be calculated as

$$M = \sum_{k}^{N_B} C_k (\Delta x)_k (\Delta y)_k B_k \theta_k \; , \tag{5.34}$$

where N_B is the number of grid blocks, Δx and Δy is the grid block size in the x- and y-directions, B is the cell thickness, and k is the cell index, $k = 1, 2, \ldots, N_B$. For mass conservation, it is necessary to update θ_k in this calculation; otherwise internal mass (or probability) is not preserved.

The values of q_s' are calculated in the flow simulation (MODFLOW-96) and entered into MT3DMS via the MODFLOW/MT3D link file. To preserve mass and probability, we set $q_s' = 0$ for all forward and backward transient transport simulations.

CHAPTER 6

BACKWARD PROBABILITY MODEL WITH REACTIVE TRANSPORT

Abstract

Backward location and travel time probabilities can be used to determine the former location of contamination in an aquifer. For a contaminant parcel that was detected in an aquifer, the backward location probability describes its position at some time prior to sampling and the backward travel time probability describes the amount of time required for it to travel to the sampling location from some upgradient position. These probabilities, which can provide information about the source of contamination, are related to adjoint states of resident concentration. The governing equation of the backward probability model is the adjoint of the forward governing equation, e.g., the advection-dispersion equation. These equations have been previously developed for a conservative chemical [e.g., *Neupauer and Wilson*, 1999, 2000a,b]. We present the backward model for reactive transport including first-order decay, linear equilibrium sorption, and linear non-equilibrium sorption.

6.1 Introduction

When contamination is detected in an aquifer, the source of contamination is often unknown. To remediate the aquifer or to assign responsibility we might need to identify the contamination source or estimate the release time of contamination from a known source. A common modeling approach to addressing these issues is to run one forward simulation for each potential source,

modeling the movement of the contamination away from the source (forward modeling). If the number of potential sources is large, this approach can result in a significant computational burden since one simulation must be run for each potential source. Furthermore, all potential sources must be identified.

Backward modeling [*Wilson and Liu*, 1994, 1997] is a more efficient approach that can be used to address these issues. With backward modeling we obtain the probability distributions for the former position of the contamination (location probability) or for the contaminant's travel time from some upgradient location to the sampling location (travel time probability). With one backward simulation we obtain these probabilities for all locations. This reduces the computational burden of forward modeling, and the results are not limited to the pre-identified possible source locations. Not only can the backward probability model be used to improve characterization of known sources of groundwater contamination or to identify previously unknown contamination sources, but it can also be used to delineate capture zones.

Location and travel time probabilities are often used in forward modeling to describe solute transport in groundwater [e.g., *Dagan*, 1982, 1987; *Jury*, 1982; *Jury and Roth*, 1990; *Chin and Chittaluru*, 1994]. Forward location probability describes the position of a solute parcel at a fixed time after its release from the source [*Dagan*, 1982, 1987, 1989; *Jury and Roth*, 1990; *Chin and Chittaluru*, 1994] and is related to resident concentration [*Dagan*, 1987; *Jury and Roth*, 1990]. The normalized concentration distribution at some time t after release from an instantaneous point source is equivalent to the location

probability density function at time t, given by

$$f_{\mathbf{x}}(\mathbf{x};t) = \frac{C(\mathbf{x},t)}{\int_{\Omega} C(\mathbf{x},0^{+})\, d\Omega}, \tag{6.1}$$

where $f_{\mathbf{x}}(\mathbf{x};t)$ is location probability at time t, $\mathbf{x}$ is the position vector, $C(\mathbf{x},t)$ is the resident concentration distribution from an instantaneous point source, Ω is the spatial domain, and $\int_{\Omega} C(\mathbf{x},0^{+})\, d\Omega = M_o/\theta$, where M_o is the source mass and θ is porosity.

Forward travel time probability describes the time required for a solute parcel to travel from its source to a location of interest [*Jury*, 1982; *Jury et al.*, 1986; *Dagan*, 1989; *Dagan and Nguyen*, 1989], and is related to flux concentration [*Shapiro and Cvetkovic*, 1988; *Rubin and Dagan*, 1992]. For an instantaneous point source of contamination, the normalized flux concentration at a downgradient location, $\mathbf{x}$, is equivalent to the travel time probability density function for that location, given by

$$f_t(t;\mathbf{x}) = \frac{|\mathbf{v}| A\theta C^f(\mathbf{x},t)}{M_o}\ , \tag{6.2}$$

where $f_t(t;\mathbf{x})$ is travel time probability from the source to $\mathbf{x}$, $\mathbf{v}$ is the groundwater velocity (vector quantity), $C^f(\mathbf{x},t)$ is flux concentration, M_o is the total amount of mass that entered at the source, vertical bars denote magnitude, and A is a flow area. We consider travel time probability across a plane perpendicular to flow, and A is the cross-sectional area of this plane. Since location probability is related to resident concentration and travel time probability is related to flux concentration, the relationship between the two probabilities

can be easily obtained from the relationship between the two concentrations. For example, the relationship between flux and resident concentration in one dimension is [*Parker and van Genuchten*, 1984]

$$C^f = C - \frac{D}{v}\frac{\partial C}{\partial x} \ , \tag{6.3}$$

where D is the dispersion coefficient and v is the groundwater velocity in the x direction. Substituting (6.1) and (6.2) into this expression results in the relationship between forward location and travel time probabilities

$$f_t = |v| f_x - \frac{D|v|}{v}\frac{\partial f_x}{\partial x} \ , \tag{6.4}$$

where $A = 1$ for this one-dimensional domain.

In forward modeling we model the movement of solute (or probability) downgradient away from the contamination source and obtain information about the future position of the contamination. With backward modeling we treat the sampling location as a source of probability (there is a probability of one that the contamination was at the sampling location at the time of sampling) and allow the probability to advect upgradient in backward time and to spread out by dispersion, resulting in a plume of backward probability that gives us information about the former position of contamination. For a solute parcel that was detected in the groundwater, backward location probability describes its position at some time prior to sampling, and travel time probability describes the amount of time required for the solute parcel to travel to the sampling location from some upgradient position, such as a known or suspected

contamination source.

The mathematical model governing backward probabilities is similar to the model for forward probabilities with some modifications to account for the upgradient movement of probability. By reversing the flow field in a random walk method, *Bagtzoglou et al.* [1992] obtained backward location probabilities for identifying sources of contamination. *Uffink* [1989] and *Chin and Chittaluru* [1994] used a similar random walk approach to delineate capture zones around pumping wells. *Wilson and Liu* [1994, 1997] used a heuristic method to obtain a backward probabilistic continuum model from the forward advection-dispersion equation. *Liu* [1995] heuristically developed the backward model for reactive transport, with first-order decay, and linear equilibrium and non-equilibrium sorption. The backward modeling approach was validated using data from a field-scale tracer experiment at the Borden site [*Wilson and Liu*, 1997]; however, no formal justification was given for the model. *Neupauer and Wilson* [1999, 2000a,b] showed that backward-in-time location and travel time probabilities are related to adjoint states of resident concentration. They illustrated the formal adjoint approach for obtaining the governing equations of the backward model for a conservative chemical in one dimension [*Neupauer and Wilson*, 1999, 2000b] and in multiple dimensions [*Neupauer and Wilson*, 2000a].

In this paper, we extend the adjoint approach of *Neupauer and Wilson* [1999] to develop the backward probability model for reactive transport, and compare the results to those obtained heuristically by *Liu* [1995]. We consider the reactive transport processes of first-order decay, and linear equilibrium and non-equilibrium sorption. We illustrate the approach for a one-dimensional

domain, although it can be extended to multiple dimensions following the approach of *Neupauer and Wilson* [2000a].

6.2 Backward Probability Model for a Conservative Tracer

In this section, we present the governing equations for backward location probability for a conservative tracer in a steady, uniform flow field. Backward location and travel time probability are related to adjoint states of the forward concentration; therefore, the governing equation for backward probabilities can be obtained from the adjoint of the forward contaminant transport operator. The relationship between a differential operator, L, and its adjoint, L^*, is [*Zauderer*, 1989]

$$gL[f] - fL^*[g] = \text{divergence terms} , \tag{6.5}$$

where f and g are two arbitrary functions, and the right-hand side contains divergence terms in both space ($\partial\{\ \}/\partial x$, in one spatial dimension) and time ($\partial\{\ \}/\partial t$).

Transport of a conservative chemical in a one-dimensional flow field can be modeled using the advection-dispersion equation (ADE), given by

$$\frac{\partial C}{\partial t} = \frac{\partial}{\partial x}\left(D\frac{\partial C}{\partial x}\right) - \frac{\partial}{\partial x}(vC) + \frac{q_I}{\theta}C_I - \frac{q_O}{\theta}C , \tag{6.6}$$

$$C(x,0) = C_i(x)$$

$$\frac{\partial C}{\partial x} = g_1(t) \text{ at } x = x_1$$

$$C(x,t) = g_2(t) \text{ at } x = x_2$$

where C is resident concentration, t is time, x is the spatial direction, $D = a_L|v|$ is the dispersion coefficient, a_L is the longitudinal dispersivity, v is the groundwater velocity, θ is porosity, q_I is the source inflow rate per unit volume, C_I is the source strength, q_O is the sink outflow rate per unit volume, C_i is the initial concentration, x_1 and x_2 are the boundaries, and g_1 and g_2 are known functions. The boundary conditions were chosen for illustration; other boundary conditions can also be used. The differential operator of (6.6) is the advection-dispersion operator, given by

$$L[\,] = -\frac{\partial[\,]}{\partial t} + \frac{\partial}{\partial x}\left(D\frac{\partial[\,]}{\partial x}\right) - \frac{\partial}{\partial x}\left(v[\,]\right) - \frac{q_O}{\theta}[\,]\,, \tag{6.7}$$

and (6.6) can be expressed as $L[C] = -q_I C_I/\theta$.

Neupauer and Wilson [1999, 2000a,b] used a sensitivity analysis approach to obtain the governing equation for the backward model. Sensitivity analysis measures the sensitivity of a performance measure, P, to a marginal change in a system parameter, α (e.g., $\alpha = v$ or $\alpha = D$). The performance measure quantifies the state of the system, and can be expressed as

$$P = \iint_{x,t} h(\alpha, C)\; dx\; dt\;, \tag{6.8}$$

where $h(\alpha, C)$ is a functional of the state of the system, C is concentration, and integration is over the entire space–time domain. The marginal sensitivity of this performance measure with respect to the parameter α is obtained by

differentiating (6.8) with respect to α:

$$\frac{dP}{d\alpha} = \iint_{x,t} \left[\frac{\partial h(\alpha, C)}{\partial \alpha} + \frac{\partial h(\alpha, C)}{\partial C} \psi \right] \, dx \, dt \, , \tag{6.9}$$

where $dP/d\alpha$ is the marginal sensitivity and $\psi = \partial C / \partial \alpha$ is the variation of C, or the state sensitivity.

Location and travel time probabilities are related to the marginal sensitivity of concentration to a source of solute anywhere in the aquifer [*Neupauer and Wilson*, 2000a]. For location probability, the performance measure, P, is resident concentration at the detection location and time; and for travel time probability, P is flux concentration at the detection location and time. In both cases, the system parameter, α, is the source strength. Let the initial concentration be $C_i(x) = C^* \delta(x - x_o)$, where C^* is the source strength and x_o is the source location. Then, with $\alpha = C^*$ and P as defined above, the marginal sensitivity in (6.9) is related to location or travel time probability.

The marginal sensitivity (and therefore probability) cannot be calculated directly from (6.9) because the state sensitivity is unknown, so we use adjoint theory to eliminate ψ from the equation. The new marginal sensitivity equation in terms of the adjoint state becomes [*Neupauer and Wilson*, 2000a]

$$\frac{dP}{d\alpha} = \iint_{x,t} \frac{\partial h(\alpha, C)}{\partial \alpha} \, dx \, dt + \int_x \left(\psi^* \frac{\partial C_i}{\partial \alpha} \right) \Bigg|_{t=0} dx \, , \tag{6.10}$$

where ψ^*, the adjoint state, is the solution to the adjoint of (6.6)

$$L^*[\psi^*] = -\frac{\partial \psi^*}{\partial \tau} + \frac{\partial}{\partial x}\left(D\frac{\partial \psi^*}{\partial x}\right) + \frac{\partial}{\partial x}(v\psi^*) - \frac{q_I}{\theta}\psi^* = -\frac{\partial h}{\partial C} \qquad (6.11)$$

$$\psi^*(x,0) = 0$$

$$D\frac{\partial \psi^*}{\partial x} + v\psi^* = 0 \text{ at } x = x_1$$

$$\psi^* = 0 \text{ at } x = x_2 \quad ,$$

which is the governing equation for the backward model [*Neupauer and Wilson*, 2000a]. In (6.11), τ is backward time, representing time prior to sampling ($\tau = T - t$, where $\tau = 0$ ($t = T$) is the sampling time), h is a performance functional that depends on the type of probability (location or travel time) and the detection mechanism (e.g., pumping well or monitoring well), and the load term $\partial h/\partial C$ is a Fréchet derivative. The boundary conditions in (6.11) are specific to the boundary conditions in the forward model (6.6). In general, a first-type boundary in the forward model remains a first-type boundary in the backward model, a second-type boundary in the forward model becomes a third-type boundary in the backward model, and vice versa. All boundary and initial conditions in the backward model are homogeneous.

The performance functional, h, in (6.11) depends on the type of probability desired. For location probability, h must be defined such that P in (6.8) is the resident concentration at the detection location x_w at the detection time $\tau = 0$ ($t = T$); therefore, we need $P = C(x_w, t = T) = C(x_w, \tau = 0)$, and the appropriate performance functional is given by $h = C\delta(x - x_w)\delta(\tau)$, where $\delta(\cdot)$ is a Dirac delta function. With this expression for the performance functional,

(6.11) becomes

$$L^*[\psi_x^*] = -\frac{\partial h}{\partial C} = -\delta(x - x_w)\delta(\tau) \ , \tag{6.12}$$

where ψ_x^* is the adjoint state for location probability. By simplifying (6.10), we see that this adjoint state is equivalent to the marginal sensitivity, $dP/d\alpha$. Since h is independent of α ($\alpha = C^*$), the first integral in (6.10) vanishes. Let the initial concentration be $C_i(x) = C^*\delta(x - x_o)$, where C^* is the source strength and x_o is the source location. Then, with $\alpha = C^*$, (6.10) evaluates to $dP/d\alpha = \psi_x^*(x_o, \tau = T)$. Since location probability is equivalent to this marginal sensitivity, we have $f_x(x; \tau = T, x_w) = \psi_x^*(x, \tau = T)$, where $f_x(x; \tau = T, x_w)$ is the probability that a parcel detected at x_w at time $\tau = 0$ was at location x (random variable) at time $\tau = T$ prior to detection [*Neupauer and Wilson*, 2000a].

For travel time probability, h must be defined such that P in (6.8) is the flux concentration at the detection location x_w at the detection time $\tau = 0$ ($t = T$); therefore, we need $P = C^f(x_w, t = T) = C^f(x_w, \tau = 0)$, and the appropriate performance functional is given by $h = C^f\delta(x - x_w)\delta(\tau)$. Substituting (6.3) into this expression and taking the Fréchet derivative with respect to C, (6.11) becomes [*Neupauer and Wilson*, 1999, 2000a]

$$L^*[\psi_\tau^*] = -\frac{\partial h}{\partial C} = -\left[\delta(x - x_w) + \frac{D}{v}\delta'(x - x_w)\right]\delta(\tau) \ , \tag{6.13}$$

where ψ_τ^* is the adjoint state for travel time probability and $\delta'(x)$ is the derivative of the Dirac delta function with respect to x. Travel time probability is

equal to the magnitude of the flux of $dP/d\alpha$ with $\alpha = C^*$ [*Neupauer and Wilson*, 2000a]. From (6.10), this becomes $f_\tau(\tau; x, x_w) = |v(x,\tau)|\psi^*_\tau(x,\tau)$, for a one-dimensional domain, where the vertical bars denote magnitude and $f_\tau(\tau; x, x_w)$ is the probability that a parcel detected at x_w at time $\tau = 0$ traveled from x to the detection location in time τ (random variable). We often assume that $\partial C/\partial x = 0$ at a pumping well. Therefore, for a pumping well detection, (6.3) reduces to $C^f = C$, and (6.13) is replaced by

$$L^*[\psi^*_\tau] = -\frac{\partial h}{\partial C} = -\delta(x - x_w)\delta(\tau) \ , \tag{6.14}$$

indicating that $\psi^*_\tau = \psi^*_x$ for a pumping well detection.

We have now defined the complete governing equations for location and travel time probabilities of a conservative tracer in a one-dimensional, steady flow field. As an example, consider the hypothetical aquifer shown in Figure 6.1. The aquifer is confined and one-dimensional; it is semi-infinite with a pumping well at $x = 0$, and a source of contamination at $x_o > 0$, where x_o is the source location. Flow is from right to left in the figure, with no internal sources or sinks of water or contamination.

The governing equation for the forward model is shown in (6.6), with $q_I = q_O = 0$, $x_1 = 0$, $x_2 \to \infty$, $g_1(t) = g_2(t) = 0$, and $C_i(x) = (M_o/\theta)\delta(x - x_o)$, where M_o is the source mass per unit cross-sectional area of the aquifer. The solution to (6.6) for constant v and D is *Wilson and Liu* [1994]

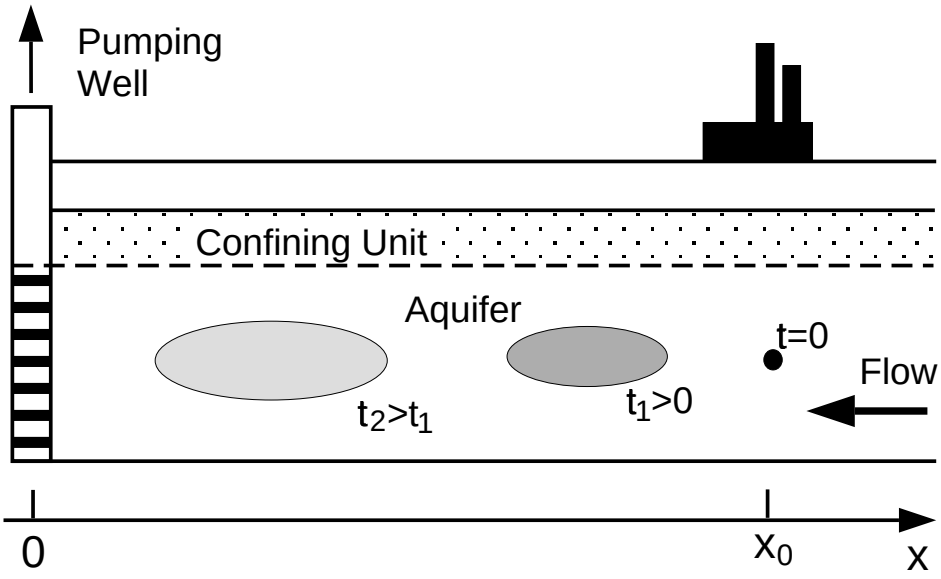

Figure 6.1: Aquifer geometry for example problem.

$$C(x,t) = \frac{M_o}{\theta\sqrt{4\pi Dt}} \exp\left\{-\frac{(x-x_o-vt)^2}{4Dt}\right\}\left[1+\exp\left\{\frac{-x_o x}{Dt}\right\}\right] + \frac{M_o v}{2D\theta}\exp\left\{\frac{-vx_o}{D}\right\}\operatorname{erfc}\left[\frac{x+x_o-vt}{\sqrt{4Dt}}\right], \quad (6.15)$$

for $v < 0$ (i.e., flow in the direction of $-x$). This solution is plotted in Figure 6.2 for $x_o = 100$ m, $a_L = 5$ m, $v = -1$ m/d, $D = 5$ m^2/d, $\theta = 0.3$, and $M_o = 1.0$ g/m^2. These parameter values, also shown in Table 6.1, are used throughout the paper unless otherwise stated. The figure shows the resident concentration for $t = 20$ days and $t = 50$ days after release from the source. At $t = 20$ days, the contamination has not yet reached the pumping well, but by $t = 50$ days, some contamination has reached the well.

Suppose we detect contamination in the pumping well and would like to know its location at some time in the past. To determine the likely prior locations, we could use the backward-in-time location probability for contamination detected at the pumping well ($x_w = 0$). The governing equation for this

Table 6.1: Transport parameters for the example problem.

Parameter	Value
Source location, x_o	100 m
Groundwater velocity, v	-1 m/d
Longitudinal dispersivity, a_L	5 m
Dispersion coefficient, D	5 m^2/d
Porosity, θ	0.3
Source mass, M_o	1 g/m^2

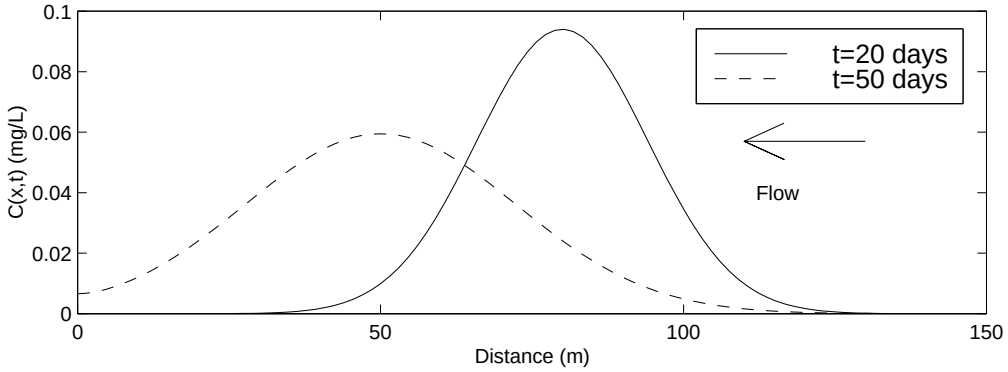

Figure 6.2: Resident concentration of a conservative tracer at $t = 20$ days and $t = 50$ days after release.

case is (6.11) with the load term defined in (6.12), again with $q_I = 0$, $x_1 = 0$, and $x_2 \to \infty$. With $f_x = \psi^*$, the solution to this equation is [*Wilson and Liu*, 1994]

$$f_x(x;\tau) = \frac{1}{\sqrt{\pi D\tau}} \exp\left\{-\frac{(x+v\tau)^2}{4D\tau}\right\} + \frac{v}{2D} \exp\left\{\frac{-vx}{D}\right\} \operatorname{erfc}\left[\frac{x-v\tau}{\sqrt{4D\tau}}\right] , \quad (6.16)$$

for $v < 0$. This solution is plotted in Figure 6.3 for $\tau = 20$ days and $\tau = 50$ days prior to detection at the pumping well. The curves show the probability that the detected contamination was at any upgradient location at $\tau = 20$ and $\tau = 50$ days prior to detection. The most likely prior position of the contamination is $x \approx 23$ m at $\tau = 20$ days prior to detection, and $x \approx 55$ m at $\tau = 50$ days prior to detection. Note also that at $\tau = 20$ days, $f_x \approx 0$ for $x = 100$ m; this is consistent with the results in Figure 6.2, which show that mass originated at $x_o = 100$ m does not reach the pumping well in 20 days. At $\tau = 50$ days, however, the location probability at $x = 100$ m is non-zero, indicating that had mass originated at $x = 100$ m, it would have a finite probability of reaching

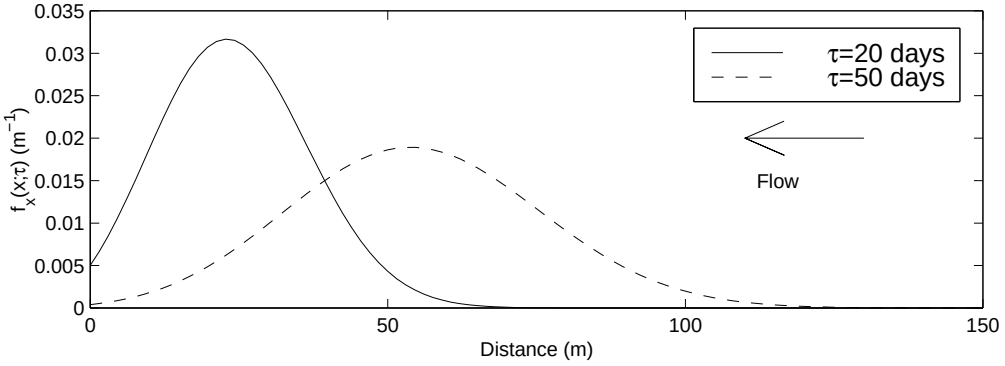

Figure 6.3: Backward location probability for a conservative tracer at $\tau =$ 20 days and $\tau = 50$ days prior to detection at the pumping well.

the pumping well in 50 days. This is also consistent with the forward results in Figure 6.2.

Suppose again that we detect contamination in the pumping well and would like to know when it could have been released from a known or suspected source at $x = x_o = 100$ m. To determine the likely travel times from the source to the pumping well, we could use the backward-in-time travel time probability. The governing equation for this pumping well detection is (6.14). Using $f_\tau = |v|\psi^*_\tau$, the solution to this equation is [*Wilson and Liu*, 1994]

$$f_\tau(\tau; x) = \frac{-v}{\sqrt{\pi D\tau}} \exp\left\{-\frac{(x+v\tau)^2}{4D\tau}\right\} - \frac{v^2}{2D} \exp\left\{\frac{-vx}{D}\right\} \operatorname{erfc}\left[\frac{x-v\tau}{\sqrt{4D\tau}}\right], \quad (6.17)$$

for $v < 0$, where f_τ is travel time probability. This solution is plotted in Figure 6.4 showing the backward travel time probability from the pumping well to the source at $x = x_o = 100$ m. This travel time probability distribution shows that the most likely travel time from $x_o = 100$ m to the pumping well is $\tau \approx 92$ days. Note also that $f_\tau > 0$ at $\tau = 50$ days, indicating a non-zero

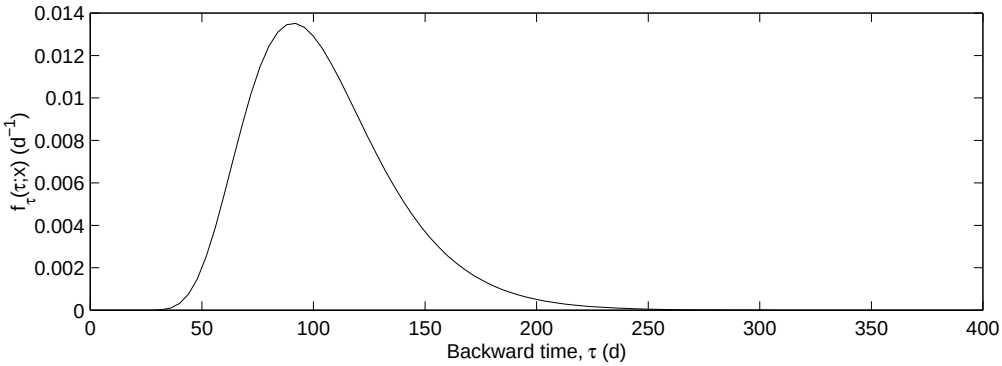

Figure 6.4: Backward travel time probability for a conservative tracer from the pumping well to $x = 100$ m.

probability that mass from $x_o = 100$ m will reach the pumping well in 50 days. This is consistent with the forward results shown in Figure 6.2.

6.3 Extensions of the Backward Probability Model

In this section, we present backward probability models for more complex cases than those described above. We consider the additional transport processes of first-order decay and sorption. In all cases, the forward governing equation (forward operator) must be modified to account for the additional processes. We present the modified form of the forward equation and forward operator, and use adjoint theory to obtain the appropriate adjoint operator, and the new load terms, if necessary. With the extensions presented here, the boundary and initial conditions in the forward model are unchanged; therefore, the boundary and final conditions of the backward model in (6.11) also hold here.

6.3.1 Backward Probability Model with Decay

Radioactive decay and some biodegradation processes can be modeled as first-order decay processes. With first-order decay, the forward equation (6.6) can be modified as

$$\frac{\partial C}{\partial t} = \frac{\partial}{\partial x}\left(D\frac{\partial C}{\partial x}\right) - \frac{\partial}{\partial x}(vC) + \frac{q_I}{\theta}C_I - \frac{q_O}{\theta}C - \lambda C \ , \tag{6.18}$$

where λ is the first-order decay rate. With this form of the ADE, the forward operator has an additional term

$$L_\lambda[\,] = L[\,] - \lambda[\,] \ , \tag{6.19}$$

where $L[\,]$ is the forward operator shown in (6.7) and $L_\lambda[\,]$ is the new forward operator that includes the decay term.

The backward operator is the adjoint of (6.19), given by

$$L^*_\lambda[\,] = L^*[\,] - \lambda[\,] \ , \tag{6.20}$$

where $L^*[\,]$ is the adjoint of $L[\,]$, shown in (6.11), and $L^*_\lambda[\,]$ is the new adjoint operator that includes the decay term. Using (6.5), it can be verified that this operator is the adjoint of (6.19).

For the one-dimensional aquifer in Figure 6.1, the governing equation for backward location probability with decay is

$$L^*_\lambda[\psi^*_x] + \delta(x - x_w)\delta(\tau) = 0 \ , \tag{6.21}$$

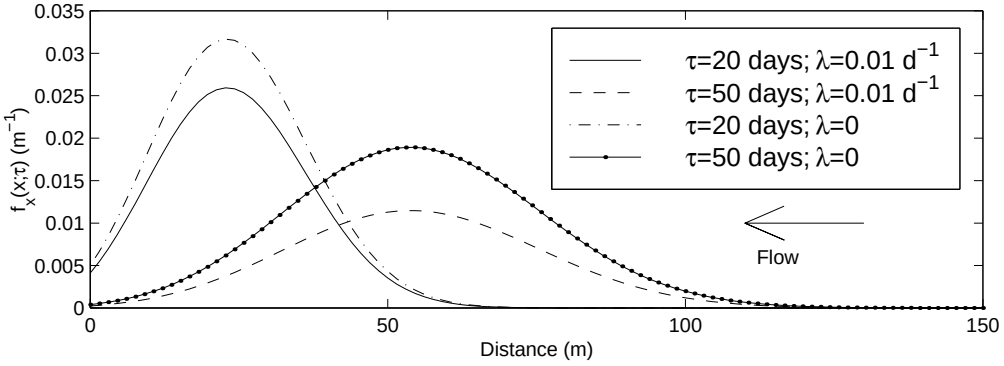

Figure 6.5: Backward location probability for a decaying contaminant, for $\tau = 20$ days and $\tau = 50$ days prior to detection at the pumping well.

with boundary and initial conditions shown in (6.11). The load term comes from (6.12). Using $f_x = \psi_x^*$ and $x_w = 0$, the solution to this equation is

$$\begin{aligned} f_x(x;\tau) &= \frac{1}{\sqrt{\pi D\tau}} \exp\left\{-\frac{(x+v\tau)^2}{4D\tau} - \lambda\tau\right\} \\ &\quad + \frac{v}{2D} \exp\left\{-\frac{vx}{D} - \lambda\tau\right\} \operatorname{erfc}\left[\frac{x - v\tau}{\sqrt{4D\tau}}\right], \end{aligned} \tag{6.22}$$

for $v < 0$. The derivation is given in Appendix 6.A. Results are plotted in Figure 6.5 using $\lambda = 0.01$ d^{-1} (half-life of $t_{1/2} \approx 69$ days), for $\tau = 20$ days and $\tau = 50$ days prior to detection at the pumping well. For comparison, the location probability curves for the conservative tracer are also shown on the plot. For the decaying contaminant, the location probability also decays; therefore, $\int_x f_x \, dx < 1$ for $\tau > 0$. This represents a non-zero probability that the contaminant parcel would have decayed before reaching the pumping well if it had been in the system at backward time τ. As backward time τ increases, the probability that the contaminant parcel would have decayed before reaching the pumping well also increases. In this example, $\int_x f_x dx = 0.82$

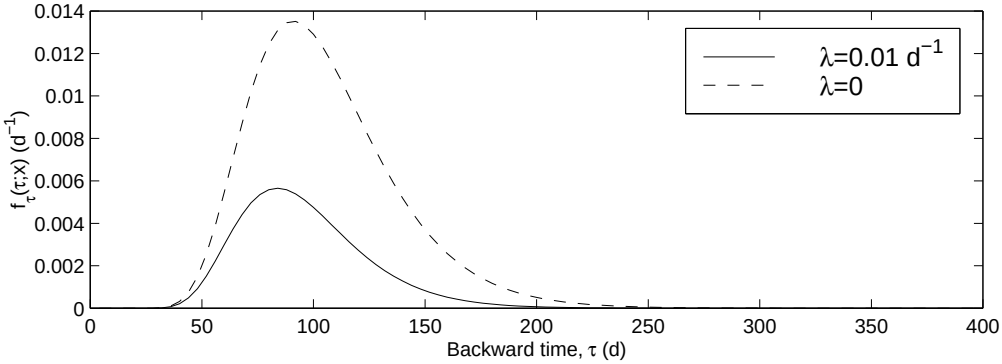

Figure 6.6: Backward travel time probability from the pumping well to $x_o = 100$ m for a decaying contaminant and a conservative tracer.

for $\tau = 20$ days, indicating an 18% probability that a contaminant parcel in the aquifer at $\tau = 20$ days would have decayed before reaching the pumping well. For $\tau = 50$ days, $\int_x f_x dx = 0.61$, indicating a 39% probability that a contaminant parcel in the aquifer at $\tau = 50$ days would have decayed before reaching the pumping well.

For the one-dimensional aquifer in Figure 6.1 with a pumping well detection, $\psi_\tau^* = \psi_x^*$. Using (6.22) and $f_\tau = |v|\psi_\tau^*$, the backward travel time probability is

$$\begin{aligned} f_\tau(\tau; x) &= \frac{-v}{\sqrt{\pi D\tau}} \exp\left\{-\frac{(x+v\tau)^2}{4D\tau} - \lambda\tau\right\} \\ &\quad -\frac{v^2}{2D} \exp\left\{-\frac{vx}{D} - \lambda\tau\right\} \operatorname{erfc}\left[\frac{x - v\tau}{\sqrt{4D\tau}}\right] . \end{aligned} \tag{6.23}$$

for $v < 0$. Figure 6.6 shows the backward travel time probability from the pumping well to a source at $x = x_o = 100$ m using $\lambda = 0.01\text{d}^{-1}$ and $\lambda = 0$. For the decaying contaminant, the travel time probability also decays; therefore,

$\int_\tau f_\tau d\tau < 1$ for $x > x_w$. This accounts for the non-zero probability that the detected contaminant parcel would have decayed before reaching the pumping well if it had ever been at location x. In this example, $\int_\tau f_\tau d\tau = 0.37$ at $x_o = 100$ m for the decaying solute ($\int_\tau f_\tau d\tau = 1.0$ for the conservative solute). Thus, there is a 63% probability that a contaminant parcel at $x_o = 100$ m would have decayed before reaching the pumping well at $x_w = 0$.

An alternative approach is to consider that regardless of whether the chemical is conservative or decaying, a contaminant parcel that arrives at the pumping well has not decayed. We can use a non-decaying location probability to determine the prior location of the detected parcel at time τ, given that the parcel was in the aquifer at time τ. Similarly, the non-decaying travel time probability determines the detected parcel's travel time from an upgradient location, x, to the pumping well, given that the parcel had been present at x at some time in the past. With this interpretation, the appropriate backward model is equivalent to the model for the conservative tracer which is also shown in Figures 6.5 and 6.6.

The expressions obtained in this section for location and travel time probability are equivalent to those developed heuristically by *Liu* [1995] for a one-dimensional domain with constant parameters. Liu chose the non-decaying interpretation for location probability and the decaying interpretation for travel time probability.

6.3.2 Backward Probability Model with Linear Equilibrium Sorption

In this section, we develop the adjoint model for linear reversible equilibrium sorption. With sorption, the contaminant can be in the aqueous phase or the sorbed phase, so the forward contaminant transport problem is a multi-phase problem. In the backward probability model, contamination can be detected in the aqueous phase, the sorbed phase, or both. Prior to detection, the contamination could be in either the aqueous or sorbed phase, or the phase can be unspecified (i.e., either phase). The term "prior" refers to any time before the detection was made, not just to a time immediately before detection. We refer to the phase of the contamination at these prior times as the "prior phase". Using all combinations of detected and prior phases, we have nine possible phases of location probability. We use the notation that $f_{x_{i|j}}(x;\tau,x_w)$ is the probability that a contaminant particle was at location x (random variable) in phase i (random variable) at backward time τ, given that it was detected in phase j (deterministic parameter) at location x_w (deterministic parameter) and time $\tau = 0$. We use the subscripts $_A$, $_S$, and $_T$ to denote aqueous, sorbed, and total (detection in both phases or prior state in either phase) phases, respectively. Table 6.2 summarizes the backward probabilities. Since the particle must be in either the aqueous or sorbed phase at any time, the relationship between the three probabilities is $f_{x_{T|j}} = f_{x_{A|j}} + f_{x_{S|j}}$.

With linear equilibrium sorption, aqueous phase resident concentra-

Table 6.2: Notation for backward probabilities with sorption.

Probability	Prior Phase	Detection Phase
$f_{x_{A\|A}}$	aqueous	aqueous
$f_{x_{A\|S}}$	aqueous	sorbed
$f_{x_{A\|T}}$	aqueous	both
$f_{x_{S\|A}}$	sorbed	aqueous
$f_{x_{S\|S}}$	sorbed	sorbed
$f_{x_{S\|T}}$	sorbed	both
$f_{x_{T\|A}}$	either	aqueous
$f_{x_{T\|S}}$	either	sorbed
$f_{x_{T\|T}}$	either	both
f_{τ_A}	aqueous	aqueous
f_{τ_S}	sorbed	aqueous
f_{τ_T}	total	aqueous

tion, C, and sorbed phase resident concentration, C_S, are related by

$$C_S = \frac{K_d \rho_b}{\theta} C \ , \tag{6.24}$$

where K_d is a partition coefficient (in units of volume of water per mass of solids), ρ_b is the bulk density of the porous medium (in units of mass of solids per total volume), θ is porosity, and C and C_S have units of mass of solute per volume of water. With this equilibrium model, partitioning between the aqueous and the solid phases is instantaneous. Often C_S has units of mass of solute per mass of solids. We found that using the same units for C and C_S simplifies the interpretation of the backward model (see also *Liu* [1995]). The resulting adjoint states have units equivalent to those of location probability.

For an instantaneous point source of contamination in the aquifer

shown in Figure 6.1, the governing equation for forward contaminant transport with linear equilibrium sorption is given by

$$\begin{aligned}
\frac{\partial C}{\partial t} + \frac{\partial C_S}{\partial t} &= D\frac{\partial^2 C}{\partial x^2} - v\frac{\partial C}{\partial x} \\
C_S &= \frac{K_d \rho_b}{\theta} C \\
C(x,0) &= \frac{M_o}{R\theta}\delta(x - x_o) = C_{Ao}\delta(x - x_o) \\
C_S(x,0) &= \frac{(R-1)M_o}{R\theta}\delta(x - x_o) = C_{So}\delta(x - x_o) \\
\frac{\partial C}{\partial x} = 0 \quad &\text{at} \quad x = 0 \\
C(x,t) \to 0 \quad &\text{as} \quad x \to \infty \,,
\end{aligned} \tag{6.25}$$

where $R = 1 + \rho_b K_d/\theta$ is the retardation coefficient, and the initial source mass is partitioned between the aqueous and sorbed phases according to (6.24). The first equation in (6.25) is equivalent to (6.6) with $q_I = q_O = 0$, $x_1 = 0$, $x_2 \to \infty$, $g_1(t) = g_2(t) = 0$, $C_i = (M_o/[\theta R])\delta(x - x_o)$, and with v and D in (6.6) replaced by v/R and D/R, respectively, in (6.25). With these parameter definitions, the solution to the first equation in (6.25) can be obtained by inspection of (6.15); therefore, the solution to this system of equations in (6.25) is

$$\begin{aligned}
C(x,t) &= \frac{M_o}{\theta\sqrt{4\pi DRt}} \exp\left\{-\frac{(R[x - x_o] - vt)^2}{4DRt}\right\}\left[1 + \exp\left\{\frac{-x_o x R}{Dt}\right\}\right] \\
&\quad + \frac{M_o v}{2DR\theta} \exp\left\{\frac{-v x_o}{D}\right\} \operatorname{erfc}\left[\frac{R[x + x_o] - vt}{\sqrt{4DRt}}\right] \,,
\end{aligned} \tag{6.26}$$

$$C_S(x,t) = \frac{M_o(R-1)}{\theta\sqrt{4\pi DRt}}\exp\left\{-\frac{(R[x-x_o]-vt)^2}{4DRt}\right\}\left[1+\exp\left\{\frac{-x_o x R}{Dt}\right\}\right] + \frac{M_o v(R-1)}{2DR\theta}\exp\left\{\frac{-vx_o}{D}\right\}\operatorname{erfc}\left[\frac{R[x+x_o]-vt}{\sqrt{4DRt}}\right], \quad (6.27)$$

for $v < 0$. These concentrations are plotted in Figure 6.7 using the parameters in Table 6.1 and the additional sorption parameters in Table 6.3. The plots show the resident concentration (aqueous, sorbed, and total) for $t = 50$ days after release from the source. Total concentration, C_T, is defined as $C_T = C + C_S$. With $R = 2.5$, 40% of the mass $(1/R)$ is in the aqueous phase and 60% of the mass $([R-1]/R)$ is in the sorbed phase. For comparison, the aqueous concentration for the conservative tracer $(R = 1)$ is also shown on the plot. With linear equilibrium sorption, the solute velocity and dispersion coefficient are v/R and D/R, respectively, where v and D are the velocity and dispersion coefficient of a conservative tracer. With $R = 2.5$, the total concentration at $t = 50$ days for the sorbing solute is equivalent to the concentration of the conservative tracer at $t = 20$ days. This can be seen by comparing C_T in Figure 6.7 with $C(x, t = 20)$ in Figure 6.2.

Forward location probabilities are related to the concentration distributions shown in Figure 6.7. The forward aqueous phase location probability, $f^f_{x_A}(x;t,x_o)$, is the probability that a particle originating at x_o (deterministic parameter) will be at location x (random variable) in the aqueous phase (random variable) at time t. Similarly, forward sorbed phase location probability, $f^f_{x_S}(x;t,x_o)$, is the probability that a particle originating at x_o will be at

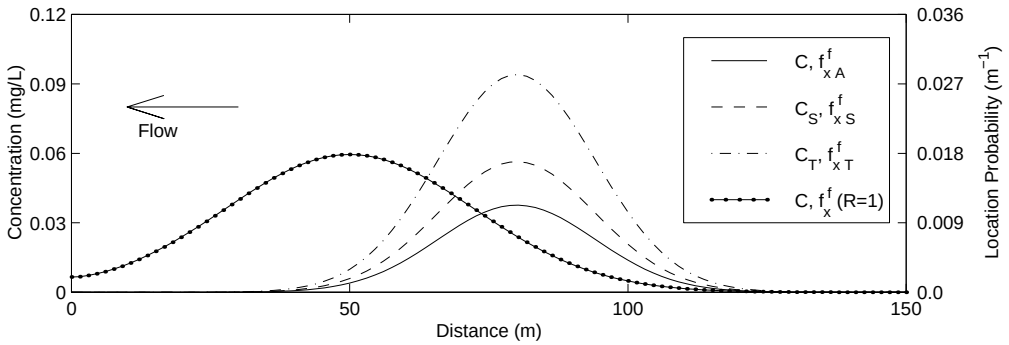

Figure 6.7: Resident concentration and forward location probabilities with linear equilibrium sorption at $t = 50$ days after release from the source at $x_o = 100$ m.

Table 6.3: Sorption parameters for the example problem.

Parameter	Value
Partition coefficient, K_d	0.3 cm^3/g
Bulk density, ρ_b	1.5 g/cm^3
Retardation coefficient, R	2.5
Rate constant, α_s	0.02 d^{-1}

location x in the sorbed phase at time t, and forward total location probability, $f^f_{x_T}(x;t,x_o)$, is the probability that a particle originating at x_o will be at location x in either phase at time t. From (6.1),

$$f^f_{x_A}(x;t,x_o) = \frac{C(x,t)}{M_o/\theta} \tag{6.28}$$

$$f^f_{x_S}(x;t,x_o) = \frac{C_S(x,t)}{M_o/\theta} \tag{6.29}$$

$$f^f_{x_T}(x;t,x_o) = \frac{C_T(x,t)}{M_o/\theta}\,. \tag{6.30}$$

The curves in Figure 6.7 also represent forward location probability, using the scale on the right-hand axis. For the case of linear equilibrium sorption, the forward location probability does not depend on the phase of the contamination at the source. A contaminant particle in the aqueous phase at the source (at x_o) can partition instantaneously into the sorbed phase at x_o; therefore, we need not distinguish between the possible sources phases. As we show later, this is not true for non-equilibrium sorption.

The governing equations for backward probabilities form a system of equations that is the adjoint of (6.25). Using sensitivity analysis, we obtained the adjoint equations and the relationship between the adjoint states and the backward probabilities. The complete adjoint equations are (see Appendix 6.B)

$$
\begin{aligned}
\frac{\partial \psi_A^*}{\partial \tau} &= D\frac{\partial^2 \psi_A^*}{\partial x^2} + v\frac{\partial \psi_A^*}{\partial x} + \frac{K_d \rho_b}{\theta}\psi_S^* + \frac{\partial h}{\partial C} \qquad (6.31)\\
\frac{\partial \psi_A^*}{\partial \tau} &= -\psi_S^* + \frac{\partial h}{\partial C_S}\ ,\\
\psi_A^*(x;0) &= 0\\
D\frac{\partial \psi_A^*}{\partial x} + v\psi_A^* = 0 \quad &\text{at} \quad x = x_w = 0\\
\psi_A^* \to 0 \quad &\text{as} \quad x \to \infty\ ,
\end{aligned}
$$

where τ is backward time, i.e., time prior to detection, and ψ_A^* and ψ_S^* are adjoint states of aqueous and sorbed concentrations, respectively. By comparing (6.25) and (6.31), we see that the forms of the forward and backward equations are different. In the forward equation (6.25), sorption appears in a time derivative in the first equation, and the aqueous phase concentration appears in the second equation as a first-order term. By substituting the second equation into the first for C_S, the system of equations can be reduced to one equation. In contrast, in the backward equation (6.31), sorption appears in a first-order source term in the first equation, and the adjoint state of aqueous concentration appears as a time-derivative in the second equation. However, the system of equations can be reduced to one equation by substituting the second equation into the first for ψ_S^* (as we show in (6.34), for example). The resulting equation, which has the same form as the reduced forward model, contains only one adjoint state, ψ_A^*, and the backward probabilities for all phases are functions of this one adjoint state.

With (6.31), the marginal sensitivity becomes (see Appendix 6.B;

compare to (6.10))

$$\frac{dP}{d\alpha} = \iint_{x,t} \frac{\partial h(\alpha, C)}{\partial \alpha}\, dx\, dt + \int_x \left[\psi_A^* \frac{\partial C_{Ao}}{\partial \alpha} \delta(x - x_o) + \psi_A^* \frac{\partial C_{So}}{\partial \alpha} \delta(x - x_o) \right] dx\,. \tag{6.32}$$

As discussed above, location and travel time probabilities are related to the marginal sensitivity of concentration (performance measure, P) to a source of contamination anywhere in the aquifer. For a non-sorbing solute, the performance measure, P, for location probability is the resident concentration at the detection location; and for travel time probability P is the flux concentration at the detection. For a sorbing solute, the sampled concentration at the detection can be in either the aqueous or sorbed phase, or both; therefore, the performance measure, P, also depends on the phase of the observed contamination. Likewise, the contaminant source (or prior phase) can be in either the aqueous or sorbed phase; therefore, the choice of the parameter α depends on the desired prior (or source) phase.

For backward location probability, the phase of the detected contamination is known, but the prior phase and location are random variables; therefore, we can think of it as the probability that a contaminant particle was at location x (random variable) in phase i (random variable) at time τ (deterministic parameter) in the past, conditioned on the particle having been at the detection location x_w in phase j at time $\tau = 0$. The marginal sensitivities (and adjoint states) obtained from (6.32) are slightly different than this. The adjoint state represents a probability that is conditioned on the prior phase rather than

on the detection phase. We will denote these probabilities as $g_{x_{j|i}}$, representing the probability that a particle detected at x_w in phase j (random variable) was located at x (random variable) in phase i (conditioned on this random variable) at time τ in the past, with $i, j = A$ (aqueous phase) or S (sorbed phase). For example, $g_{x_{A|S}}$ is the adjoint state obtained for an aqueous-phase detection ($h = C\delta(x - x_w)\delta(\tau)$) and a sorbed prior phase. Using Bayes' theorem, we can relate the adjoint states, $g_{x_{j|i}}$, to the desired backward probabilities, $f_{x_{i|j}}$. We explain the procedure here.

Location probability is equivalent to the marginal sensitivity of resident concentration at the detection location; therefore, the appropriate performance functional, h, in (6.31) is:

$$h = \begin{cases} C\delta(x - x_w)\delta(\tau) & \text{for aqueous} - \text{phase detection} \\ C_S\delta(x - x_w)\delta(\tau) & \text{for sorbed} - \text{phase detection} \\ C_T\delta(x - x_w)\delta(\tau) & \text{for a detection in both phases .} \end{cases} \tag{6.33}$$

The appropriate α in (6.32) depends on the former phase of the contamination; therefore, $\alpha = C_{Ao}$ if we are interested in the probability that the detected contamination was in the aqueous phase at its former position, and $\alpha = C_{So}$ for the probability that the detected contamination was in the sorbed phase at its former position. It is not necessary that the "former" location be the source of contamination; it is simply a location of the contamination at some time prior to detection.

For an aqueous phase detection, we use $h = C\delta(x - x_w)\delta(\tau)$ from

(6.33) in the governing adjoint equations (6.31), which reduce to

$$R\frac{\partial \psi_A^*}{\partial \tau} = D\frac{\partial^2 \psi_A^*}{\partial x^2} + v\frac{\partial \psi_A^*}{\partial x} + \delta(x - x_w)\delta(\tau) \ . \tag{6.34}$$

For the aquifer shown in Figure 6.1, the solution to this equation is

$$\begin{aligned} \psi_A^* \ = \ & \frac{1}{\sqrt{\pi DR\tau}} \exp\left\{-\frac{(Rx + v\tau)^2}{4DR\tau}\right\} + \\ & \frac{v}{2DR} \exp\left\{\frac{-vx}{D}\right\} \operatorname{erfc}\left[\frac{Rx - v\tau}{\sqrt{4DR\tau}}\right] \ , \end{aligned} \tag{6.35}$$

for $v < 0$. For an aqueous prior phase, $\alpha = C_{Ao}$ and from (6.32), $dP/d\alpha = \psi_A^*$ for an aqueous detection and aqueous prior phase; therefore, $g_{x_{A|A}} = \psi_A^*$. Similarly, for a sorbed prior phase, $\alpha = C_{So}$ and from (6.32), $dP/d\alpha = \psi_A^* = g_{x_{A|S}}$. These marginal sensitivities represent backward location probabilities conditioned on the prior phase, and they are both equivalent to ψ_A^* from (6.35) regardless of the prior phase of the particle.

For a sorbed phase detection, we substitute $h = C_S\delta(x - x_w)\delta(\tau)$ from (6.33) into (6.31), which reduces to

$$R\frac{\partial \psi_A^*}{\partial \tau} = D\frac{\partial^2 \psi_A^*}{\partial x^2} + v\frac{\partial \psi_A^*}{\partial x} + \frac{K_d\rho_b}{\theta}\delta(x - x_w)\delta(\tau) \ . \tag{6.36}$$

For the aquifer shown in Figure 6.1, the solution to this equation is

$$\begin{aligned} \psi_A^* \ = \ & \frac{R-1}{\sqrt{\pi DR\tau}} \exp\left\{-\frac{(Rx + v\tau)^2}{4DR\tau}\right\} + \\ & \frac{v(R-1)}{2DR} \exp\left\{\frac{-vx}{D}\right\} \operatorname{erfc}\left[\frac{Rx - v\tau}{\sqrt{4DR\tau}}\right] \ , \end{aligned} \tag{6.37}$$

for $v < 0$, where $R - 1 = K_d \rho_b / \theta$.

Using this result in (6.32) with $\alpha = C_{Ao}$ for an aqueous prior phase, we have $dP/d\alpha = g_{x_{S|A}} = \psi_A^*$. Similarly, with $\alpha = C_{So}$ for a sorbed prior phase, we have $dP/d\alpha = g_{x_{S|S}} = \psi_A^*$. Again these marginal sensitivities are both equivalent to ψ_A^* from (6.37), regardless of the prior phase of the particle.

The adjoint states are plotted in Figure 6.8 (lines) for $\tau = 50$ days using the parameter values in Tables 6.1 and 6.3, and the expressions from (6.35) and (6.37). The solid line represents the probability that a particle at location x (random variable) at $\tau = 50$ days prior to detection will be in the aqueous phase at the pumping well at $\tau = 0$. The prior phase of the particle does not affect the distribution. Similarly, the dashed line represents the same probability, but for a sorbed phase detection. The most likely location of the detected particle at $\tau = 50$ days is $x \approx 23$ m, regardless of the detected phase. However, with $R = 2.5$, the detection is more likely to be in the sorbed phase (60% probability; $(R-1)/R = 0.60$) than in the aqueous phase (40% probability; $1/R = 0.40$). The plot also shows the forward location probability (symbols) for several sources. We ran forward simulations for sources at $x_o = 10, 20, \ldots, 140$ m, with a source of probability partitioned between the aqueous and sorbed phases according to (6.25). For each simulation, we determined the aqueous and sorbed phase forward location probabilities at the pumping well ($x_w = 0$) at $t = 50$ days after release from the source. These values are plotted in Figure 6.8, where the circles represent the aqueous phase location probability at $x_w = 0$ due to a source at x, and the squares represent the sorbed phase location probability at $x_w = 0$ due to a source at x. These forward probabilities are equivalent to the adjoint states, indicating that, because the adjoint states

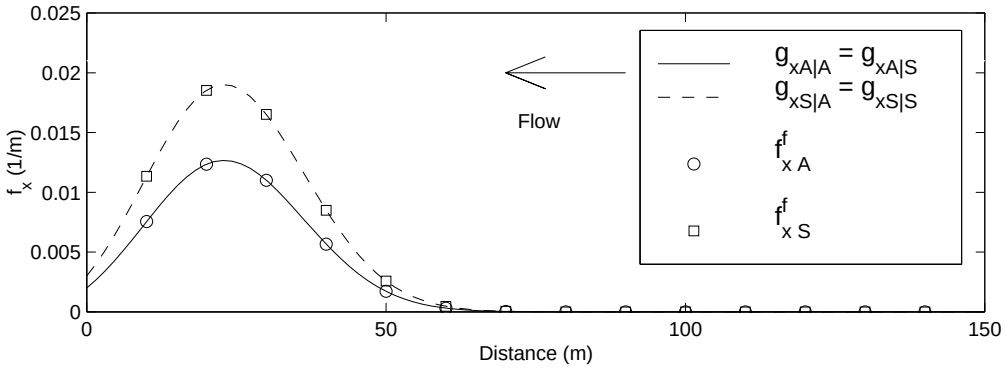

Figure 6.8: Adjoint states (lines) and forward aqueous and sorbed phase location probabilities (symbols) with linear equilibrium sorption at 50 days prior to detection at $x_w = 0$.

represent probabilities conditioned on the prior phase, the adjoint states are related to forward location probabilities.

The probabilities represented by these adjoint states are not the backward location probabilities that we would like to obtain. They are conditioned on the prior phase of the contamination, rather than on the phase at the detection, which is the desired conditioning for backward probabilities. We can obtain the desired backward probabilities from these adjoint states by using Bayes' theorem. Let $\mathrm{P}(x_w, p_w; \tau = 0 | x_o, p_o; \tau = T)$ define the probability of finding a particle at x_w in phase p_w at $\tau = 0$, given that it was located at x_o in phase p_o at backward (earlier) time $\tau = T$. Here, the location and phase are random, but the times are deterministic parameters. With this notation, the adjoint states (marginal sensitivities) can be defined as

$$g_{x_{j|i}} = \mathrm{P}(x_w, p_w = j; \tau = 0 | x_o = x, p_o = i; \tau = T) \,, \tag{6.38}$$

where $i, j = A, S$.

The backward location probabilities can be defined as

$$f_{x_{i|j}} = \mathrm{P}(x_o = x, p_o = i; \tau = T | x_w, p_w = j; \tau = 0) \ , \tag{6.39}$$

where the right-hand side denotes the probability that a particle that was detected at location x_w at backward time (i.e., earlier time) $\tau = 0$ in phase $p_w = j$ would have been located at $x_o = x$ (random variable) at backward time $\tau = T$ in phase $p_o = i$ (random variable), and $i, j = A, S$. These $f_{x_{i|j}}$ are related to $g_{x_{j|i}}$ through Bayes' theorem, yielding (see Appendix 6.C)

$$f_{x_{A|j}} = \frac{g_{x_{j|A}}[R(x_o)]^{-1}}{\int_{x_o} \left[g_{x_{j|A}}[R(x_o)]^{-1} + g_{x_{j|S}}(R(x_o) - 1)[R(x_o)]^{-1} \right] \, dx_o} \tag{6.40}$$

$$f_{x_{S|j}} = \frac{g_{x_{j|S}}(R(x_o) - 1)[R(x_o)]^{-1}}{\int_{x_o} \left[g_{x_{j|A}}[R(x_o)]^{-1} + g_{x_{j|S}}(R(x_o) - 1)[R(x_o)]^{-1} \right] \, dx_o} \ . \tag{6.41}$$

If the retardation coefficient R is spatially uniform, these two equations simplify to $f_{x_{A|j}} = g_{x_{j|A}}$ and $f_{x_{S|j}} = (R - 1) g_{x_{j|S}}$. By definition, the total location probabilities for a detection in phase j are $f_{x_{T|j}} = f_{x_{A|j}} + f_{x_{S|j}}$.

For an aqueous detection, the backward aqueous, sorbed, and total location probabilities are calculated from (6.40) and (6.41) and plotted in Figure 6.9 for $\tau = 50$ days. The most likely prior location at $\tau = 50$ days is $x \approx 23$ m. At $\tau = 50$ days, with $R = 2.5$, $\int_x f_{x_{A|A}} \, dx = 0.4$; $\int_x f_{x_{S|A}} \, dx = 0.6$; and $\int_x f_{x_{T|A}} \, dx = 1.0$. Thus, a particle detected at the pumping well is most likely to have been at location $x \approx 23$ m at time $\tau = 50$ days in the past, and it is more likely to have been in the sorbed phase than in the aqueous

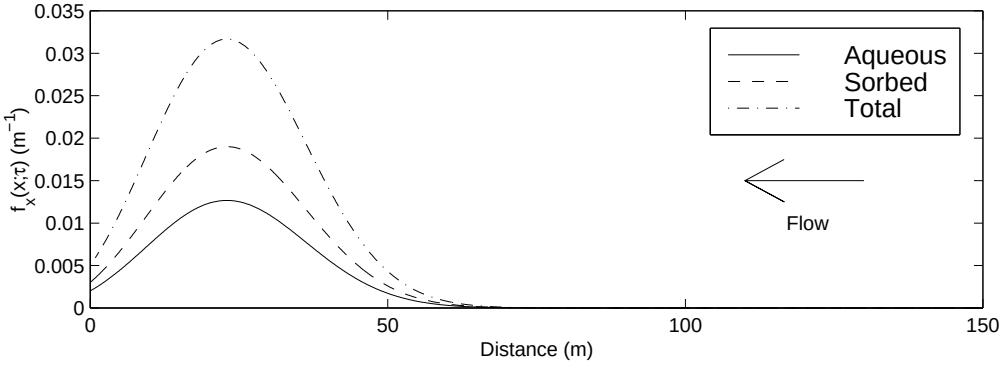

Figure 6.9: Location probability with linear equilibrium sorption at $\tau = 50$ days based on a aqueous phase detection at $x_w = 0$.

phase. Since R is spatially uniform in this case, these backward aqueous and sorbed phase location probabilities are equivalent to the marginal sensitivities shown in Figure 6.8. In this linear equilibrium sorption case, the backward location probabilities for a detection in the sorbed phase or in both phases would produce the same results as those shown in Figure 6.9.

For travel time probability, the performance functional is related to flux concentration at the detection location. By definition, flux concentration only exists in the aqueous phase; therefore, in contrast to the nine different location probabilities, we have only three different travel time probabilities, representing the three possible prior phases—aqueous, sorbed, or either. Aqueous phase travel time probability, f_{τ_A}, is the probability distribution describing the amount of time in the past (random variable) that the detected contamination was at a specified location, x (deterministic parameter), in the aqueous phase (random variable). Sorbed phase travel time probability, f_{τ_S}, is the probability distribution describing the amount of time in the past that the detected contamination was at x in the sorbed phase. Finally, total travel time probability,

f_{τ_T}, is the probability distribution describing the amount of time in the past that the detected contamination was at x in either phase. These probabilities are listed in Table 6.2.

For backward travel time probability, the phase of the detected contamination is known, but the prior phase and travel time are random variables. In other words, the backward travel time probability is conditioned on the phase on the detection. As with location probability, the adjoint states for travel time probability represent a probability that is conditioned on the prior phase. Using similar notation as in (6.38), we denote these probabilities as

$$g_{\tau_{A|i}} = \mathrm{P}(p_w = A, \tau = 0; x_w | p_o = i, \tau = T; x_o) \tag{6.42}$$

where the right-hand side denotes the probability that a particle that originated at x_o at time $\tau = T$ (random variable) in phase $p_o = j$ was detected at location x_w at backward time $\tau = 0$ in the aqueous phase (random variable), with $j = A, S$. Here, the time and phase are random and the locations are deterministic parameters. Since flux concentration cannot be detected in the sorbed phase, $g_{\tau_{S|i}} = 0$.

The performance functional for the governing equation for travel time probability is $h = C^f \delta(x - x_w)\delta(\tau)$. At the pumping well, we assume $\partial C/\partial x = 0$; therefore, from (6.3), $C^f = C$, yielding $h = C\delta(x - x_w)\delta(\tau)$ for a pumping well detection. The adjoint equation is equivalent to (6.34), whose solution is shown in (6.35) for $v < 0$. For an aqueous prior phase, $\alpha = C_{Ao}$ and from (6.32), $dP/d\alpha = \psi_A^*$. Similarly, for a sorbed prior phase, we also have $dP/d\alpha = \psi_A^*$. Travel time probability is equivalent to the magnitude of the flux of marginal

sensitivity, therefore $g_{\tau_{A|A}} = g_{\tau_{A|S}} = |v(x)|\psi_A^*$.

The backward travel time probabilities can be defined as

$$f_{\tau_j} = \mathrm{P}(p_o = j, \tau = T; x_o | p_w = A, \tau = 0; x_w) \ , \tag{6.43}$$

where the right-hand side denotes the probability that a particle that was detected at location x_w at backward time $\tau = 0$ in the aqueous phase would have been at x_o at backward time $\tau = T$ (random variable) in phase $p_o = j$ (random variable) with $j = A, S$. These travel time probabilities are related to $g_{\tau_{A|j}}$ through Bayes' theorem, yielding (see Appendix 6.C)

$$f_{\tau_A} = \frac{g_{\tau_{A|A}}[R(x_o)]^{-1}}{\int_\tau \left[g_{\tau_{A|A}}[R(x_o)]^{-1} + g_{\tau_{A|S}}(R(x_o)-1)[R(x_o)]^{-1}\right] \, d\tau} \tag{6.44}$$

$$f_{\tau_S} = \frac{g_{\tau_{A|S}}(R(x_o)-1)[R(x_o)]^{-1}}{\int_\tau \left[g_{\tau_{A|A}}[R(x_o)]^{-1} + g_{\tau_{A|S}}(R(x_o)-1)[R(x_o)]^{-1}\right] \, d\tau} \ , \tag{6.45}$$

and by definition, $f_{\tau_T} = f_{\tau_A} + f_{\tau_S}$. If the retardation coefficient, R, is spatially-uniform, these equations reduce to $f_{\tau_A} = g_{\tau_{A|A}}$ and $f_{\tau_S} = (R-1)g_{\tau_{A|S}}$.

The backward aqueous, sorbed, and total travel times probabilities are plotted in Figure 6.10, which shows that the most likely backward travel time from the pumping well at $x = 0$ to $x = 100$ m is $\tau \approx 230$ days. For $x = 100$ m and $R = 2.5$, $\int_\tau f_{\tau_A} \, d\tau = 0.4$; $\int_\tau f_{\tau_S} \, d\tau = 0.6$; and $\int_\tau f_{\tau_T} \, d\tau = 1.0$. Thus, a particle detected at the pumping well is most likely to have been at location $x = 100$ m at time $\tau \approx 230$ days in the past, and it was in the aqueous phase 40% of the time and in the sorbed phase 60% of the time at that location. For comparison, the travel time probability for a non-sorbing

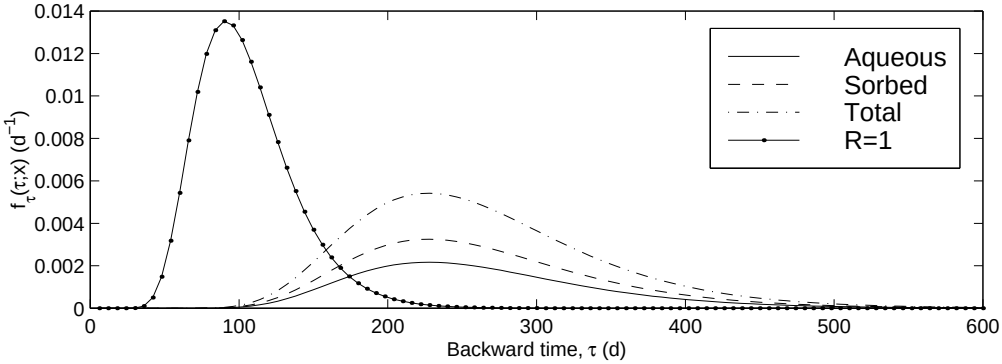

Figure 6.10: Backward travel time probability from the pumping well to $x = 100$ m for the linear equilibrium sorption case.

tracer is also shown in Figure 6.10. Note that the probable travel times from $x = 100$ m to the well are much earlier for the non-sorbing tracer than for the sorbing solute because transport is retarded for the sorbing solute.

In his heuristic development of the backward probability model for linear equilibrium sorption, *Liu* [1995] did not distinguish between the possible phases of the detection. Since the detection phase is irrelevant for the linear equilibrium sorption case, his location probabilities are equivalent to those presented here. The travel time probabilities obtained heuristically by *Liu* [1995] are equivalent to the $g_{\tau_{A|i}}$ calculated here.

6.3.3 Backward Probability Model with Linear Non-Equilibrium Sorption

In this section, we develop the adjoint model for linear reversible non-equilibrium sorption. With linear equilibrium sorption, the transfer between the aqueous and sorbed phases occurs instantaneously, and the sorbed

and aqueous phases are always in equilibrium. With non-equilibrium sorption, transfer between the phases is rate-limited, given by

$$\frac{\partial C_S}{\partial t} = \alpha_s \left(\frac{K_d \rho_b}{\theta} C - C_S \right) , \tag{6.46}$$

where α_s is the first-order rate constant (in units of reciprocal time), and C and C_S have units of mass of solute per unit volume of water. In the limit as $\alpha_s \to \infty$, this equation reduces to (6.24).

For an instantaneous point source of aqueous contamination in the aquifer shown in Figure 6.1, the governing equation for forward contaminant transport with linear non-equilibrium sorption is

$$\begin{aligned}
\frac{\partial C}{\partial t} + \frac{\partial C_S}{\partial t} &= D \frac{\partial^2 C}{\partial x^2} - v \frac{\partial C}{\partial x} \\
\frac{\partial C_S}{\partial t} &= \alpha_s \left(\frac{K_d \rho_b}{\theta} C - C_S \right) \\
C(x,0) &= \frac{M_o}{\theta} \delta(x - x_o) = C_{Ao} \delta(x - x_o) \\
C_S(x,0) &= 0 = C_{So} \delta(x - x_o) \\
\frac{\partial C}{\partial x} = 0 \quad &\text{at} \quad x = 0 \\
C(x,t) \to 0 \quad &\text{as} \quad x \to \infty \, .
\end{aligned} \tag{6.47}$$

We assumed that the initial contamination was entirely in the aqueous phase; therefore, no mass is initially in the sorbed phase. This system of equations can be solved analytically using Laplace transforms in time.

The Laplace transforms in time ($t \rightarrow s$) of C and C_S are [*Liu*, 1995]

$$\hat{C} = \frac{M_o}{\theta D(r_2 - r_1)} \left[\exp\{r_o(x - x_o)\} - \frac{Dr_1 - v}{Dr_2 - v} \exp\{r_1 x - r_2 x_o\} \right] \quad (6.48)$$

$$\hat{C_S} = \frac{\alpha_s K_d \rho_b}{\theta(s + \alpha_s)} \hat{C} \quad (6.49)$$

where $\hat{C}$ and $\hat{C_S}$ are the Laplace transformed functions for C and C_S, respectively, s is the transform variable, and

$$r_o = \begin{cases} r_1 & x_o < x \\ r_2 & x_o > x \end{cases} \quad (6.50)$$

$$r_1 = \frac{v}{2D}(1 + \xi) \qquad r_2 = \frac{v}{2D}(1 - \xi)$$

$$\xi = \sqrt{1 + \frac{4\gamma D}{v^2}} \qquad \gamma = s\left[1 + \frac{\rho_b \alpha_s K_d}{\theta(s + \alpha_s)}\right] .$$

We numerically inverted the Laplace transform using a Stehfest algorithm [*Jury and Roth*, 1990] to obtain the aqueous and sorbed phase concentrations. The results are shown in Figure 6.11 for the parameter values listed in Tables 6.1 and 6.3. The figure shows the resident concentration (aqueous, sorbed, and total) at $t = 50$ days after release from the source. At $t = 50$ days, 45% of the mass is in the aqueous phase and 55% of the mass is in the sorbed phase. For comparison, the aqueous concentration for the conservative tracer is also shown on the plot. With linear non-equilibrium sorption, the aqueous solute moves slightly slower than the conservative tracer because the sorbing solute is somewhat retarded. The sorbed solute wave travels slower than the aqueous solute wave because sorption is rate-limited. If the curves in Figure 6.11 are normalized by M_o/θ,

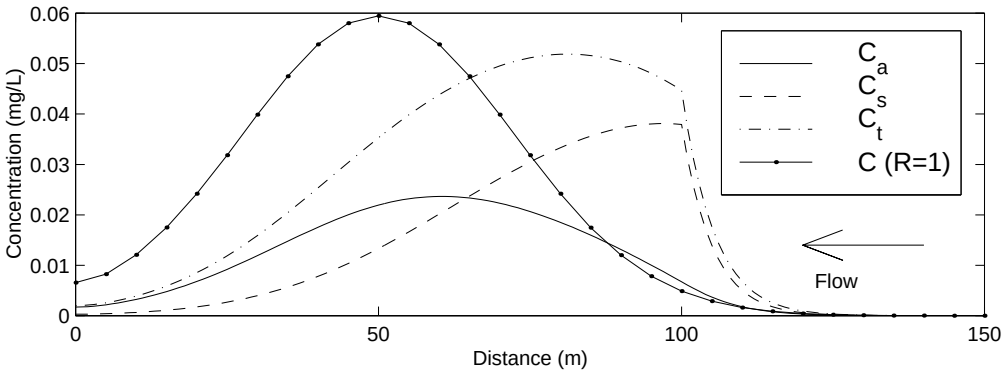

Figure 6.11: Resident concentration with linear non-equilibrium sorption at $t = 50$ days after release at $x_o = 100$ m in the aqueous phase.

they represent forward location probabilities. The normalized aqueous (sorbed) concentration curve describes the probability that a particle originating at x_o in the aqueous phase will be at location x in the aqueous (sorbed) phase at time t. Because sorption is rate-limited, the probability distributions depend on the phase of initial mass of solute. If the initial source mass was in the sorbed phase, the resulting concentration (and location probability) distributions would be shifted toward the source location, with more mass in the sorbed phase because of the rate-limited transfer between the phases.

The governing equations for backward probabilities form a system of equations that is the adjoint of (6.47). Using sensitivity analysis, we obtained the adjoint equations and the relationship between the adjoint states and backward probabilities. The complete system of adjoint equations is (see Appendix 6.D)

$$
\begin{aligned}
\frac{\partial \psi_A^*}{\partial \tau} = D\frac{\partial^2 \psi_A^*}{\partial x^2} \quad &+ \quad v\frac{\partial \psi_A^*}{\partial x} + \frac{\alpha_s K_d \rho_b}{\theta}\psi_S^* + \frac{\partial h}{\partial C} \\
\frac{\partial \psi_A^*}{\partial \tau} + \frac{\partial \psi_S^*}{\partial \tau} \quad &= \quad -\alpha_s \psi_S^* + \frac{\partial h}{\partial C_S} \\
\psi_A^*(x;0) \quad &= \quad \psi_S^*(x;0) = 0 \\
D\frac{\partial \psi_A^*}{\partial x} + v\psi_A^* = 0 \quad &\text{at} \quad x = x_w = 0 \\
\psi_A^* \to 0 \quad &\text{as} \quad x \to \infty \, ,
\end{aligned}
\tag{6.51}
$$

where τ is backward time, and ψ_A^* and ψ_S^* are adjoint states of aqueous and sorbed concentrations, respectively. By comparing (6.47) and (6.51), we see that the forms of the forward and backward equations are different. The forward equation has time derivatives of both C and C_S in the first equation and a first-order term in C in the second equation. The backward equation has a first-order term of ψ_S^* in the first equation and time derivatives of both ψ_A^* and ψ_S^* in the second equation. In contrast to the linear equilibrium sorption case, the forward and backward models with non-equilibrium sorption must both be solved as a system of equations. Therefore, the backward model contains two adjoint states, ψ_A^* and ψ_S^*, and the backward probabilities are related to linear combinations of these adjoint states, as we show below.

The marginal sensitivity equation for linear non-equilibrium sorption becomes (see Appendix 6.D)

$$
\begin{aligned}
\frac{dP}{d\alpha} \quad = \quad & \iint_{x,t} \frac{\partial h(\alpha, C)}{\partial \alpha} \, dx \, dt \; + \\
& \int_x \left[\psi_A^* \frac{\partial C_{Ao}}{\partial \alpha}\delta(x - x_o) + (\psi_A^* + \psi_S^*)\frac{\partial C_{So}}{\partial \alpha}\delta(x - x_o) \right] \, dx \, .
\end{aligned}
\tag{6.52}
$$

The only difference between this equation and the marginal sensitivity equation for linear equilibrium sorption (6.32) is in the coefficient on the $\partial C_{So}/\partial\alpha$ term.

We can now use the adjoint equation (6.51) and the marginal sensitivity equation (6.52) to calculate backward location and travel time probabilities. For location probability, the performance functionals are defined in (6.33). For an aqueous phase detection, the appropriate performance functional is $h = C\delta(x - x_w)\delta(\tau)$, and the adjoint equation (6.51) becomes

$$\begin{aligned} \frac{\partial\psi_A^*}{\partial\tau} &= D\frac{\partial^2\psi_A^*}{\partial x^2} + v\frac{\partial\psi_A^*}{\partial x} + \frac{\alpha_s K_d \rho_b}{\theta}\psi_S^* + \delta(x - x_w)\delta(\tau) \\ \frac{\partial\psi_A^*}{\partial\tau} &+ \frac{\partial\psi_S^*}{\partial\tau} = -\alpha_s\psi_S^* \ . \end{aligned} \tag{6.53}$$

This system of equations can be solved analytically using Laplace transforms. The solution at $x_w = 0$ is (see Appendix 6.E)

$$\begin{aligned} \hat{\psi_A^*} &= \frac{1}{Dr_1}\exp\{r_2 x\} \\ \hat{\psi_S^*} &= \frac{-s}{s + \alpha_s}\hat{\psi_A^*} \ , \end{aligned} \tag{6.54}$$

where $\hat{\psi_A^*}$ and $\hat{\psi_S^*}$ are the Laplace transforms of ψ_A^* and ψ_S^*, respectively, $r_1 = -v/(2D)[1+\xi]$, $r_2 = -v/(2D)[1-\xi]$, and ξ is defined in (6.50). For an aqueous prior phase, $\alpha = C_{Ao}$, and from (6.52), $dP/d\alpha = g_{x_{A|A}} = \psi_A^*$. For a sorbed prior phase, $\alpha = C_{So}$, and $dP/d\alpha = g_{x_{A|S}} = \psi_A^* + \psi_S^*$. The $g_{x_{j|i}}$ are defined in (6.38).

Although it is unlikely that contamination would be detected in the sorbed phase at a pumping well, we consider a sorbed phase detection to il-

lustrate some important concepts about backward probabilities for sorbing solutes. For a sorbed phase detection, the appropriate performance functional is $h = C_S\delta(x - x_w)\delta(\tau)$, and (6.51) becomes

$$\begin{aligned} \frac{\partial\psi_A^*}{\partial\tau} &= D\frac{\partial^2\psi_A^*}{\partial x^2} + v\frac{\partial\psi_A^*}{\partial x} + \frac{\alpha_s K_d\rho_b}{\theta}\psi_S^* \\ \frac{\partial\psi_A^*}{\partial\tau} + \frac{\partial\psi_S^*}{\partial\tau} &= -\alpha_s\psi_S^* + \delta(x - x_w)\delta(\tau)\ . \end{aligned} \tag{6.55}$$

Solving this system of equations analytically at $x_w = 0$ using Laplace transforms, we obtain (see Appendix 6.E)

$$\begin{aligned} \hat{\psi_A^*} &= \frac{\alpha_s K_d\rho_b}{Dr_1\theta(s + \alpha_s)}\exp\{r_2 x\} \\ \hat{\psi_S^*} &= \frac{-s}{s + \alpha_s}\hat{\psi_A^*} + \frac{\delta(x - x_w)}{s + \alpha_s}\ . \end{aligned} \tag{6.56}$$

For an aqueous prior phase, $\alpha = C_{Ao}$, and from (6.52), $dP/d\alpha = g_{x_{S|A}} = \psi_A^*$. For a sorbed prior phase, $\alpha = C_{So}$, and $dP/d\alpha = g_{x_{S|S}} = \psi_A^* + \psi_S^*$.

The probabilities represented by these marginal sensitivities are conditioned on the prior phase of the contamination, rather than on the detection phase, which is the desired conditioning for backward probabilities. The backward location probabilities are related to the $g_{x_{j|i}}$ through Bayes' theorem (see Appendix 6.C and (6.40) and (6.41)). We calculated the adjoint states by numerically inverting the Laplace transforms using a Stehfest algorithm [*Jury and Roth*, 1990] with the parameter values in Tables 6.1 and 6.3. Using the adjoint states and their relationships with $g_{x_{j|i}}$, we calculated the backward location probabilities from (6.40) and (6.41). The backward aqueous, sorbed, and total

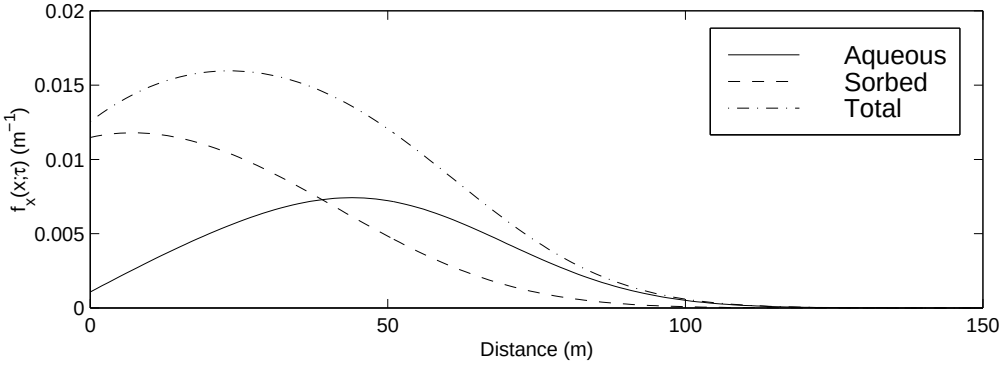

Figure 6.12: Location probability with linear non-equilibrium sorption at $\tau =$ 50 days prior to detection for a detection at $x_w = 0$ in the aqueous phase.

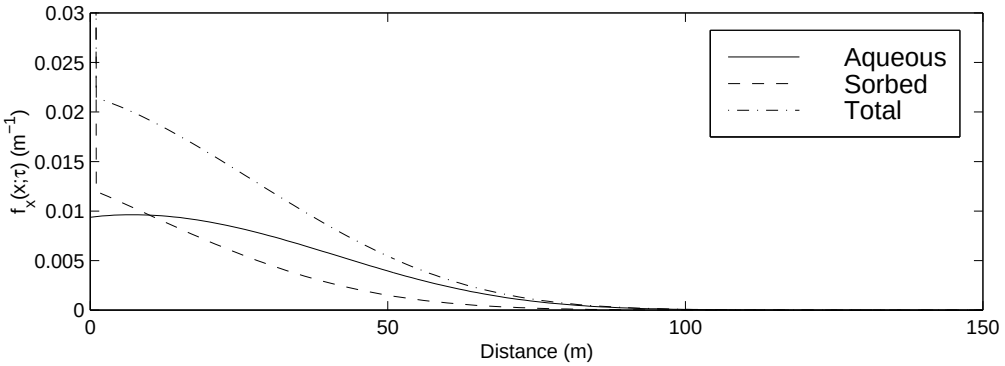

Figure 6.13: Location probability with linear non-equilibrium sorption at $\tau =$ 50 days prior to detection for a detection at $x_w = 0$ in the sorbed phase.

location probabilities at $\tau = 50$ days are plotted in Figure 6.12 for an aqueous detection and in Figure 6.13 for a sorbed-phase detection.

With an aqueous phase detection, the more probable locations at $\tau = 50$ days are well upgradient of the detection location. Since sorption is rate-limited, a particle detected in the aqueous phase is likely to have been in the aqueous phase in the recent past, and therefore could have traveled from upgradient locations. Based on the total location probability, a particle that

was detected in the aqueous phase at the pumping well is most likely to have been at location $x \approx 23$ m at time $\tau = 50$ days in the past.

For a sorbed phase detection, the possible prior locations at $\tau = 50$ days are near the pumping well, with a high probability that the contamination had been in the sorbed phase at the detection location at $\tau = 50$ days. Since sorption is rate-limited, a particle that is detected in the sorbed phase is likely to have been in the sorbed phase in the recent past, and therefore is likely to have been at or near the well. Based on the total probability, the most likely prior location at $\tau = 50$ days is at the detection location, with a high probability that the particle was in the sorbed phase.

For backward travel time probability with a detection at a pumping well, the appropriate performance functional for the adjoint equation is $h = C\delta(x - x_w)\delta(\tau)$. For the linear non-equilibrium sorption case, the adjoint equation is equivalent to (6.53), and the solution is given in (6.54). Using (6.52), $dP/d\alpha = \psi_A^*$ for $\alpha = C_{Ao}$ (aqueous prior phase) and $dP/d\alpha = \psi_A^* + \psi_S^*$ for $\alpha = C_{So}$ (sorbed prior phase). Travel time probability is equivalent to the magnitude of the flux of marginal sensitivity, therefore $g_{\tau_{A|A}} = |v(x)|\psi_A^*$ and $g_{\tau_{A|S}} = |v(x)|(\psi_A^* + \psi_S^*)$.

The backward travel time probabilities are defined in (6.43). They are related to the $g_{\tau_{A|i}}$ by Bayes' theorem, as in (6.44) and (6.45) for f_{τ_A} and f_{τ_S}, respectively. By definition, $f_{\tau_T} = f_{\tau_A} + f_{\tau_S}$.

We calculated the adjoint states by numerically inverting the Laplace transforms using a Stehfest algorithm [*Jury and Roth*, 1990] with the parameter values in Tables 6.1 and 6.3. From the adjoint state and their relationships

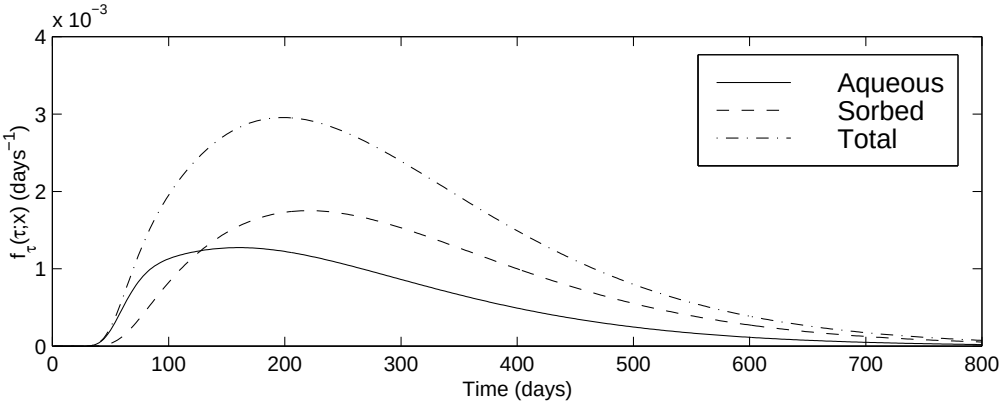

Figure 6.14: Backward travel time probability from the pumping well to $x = 100$ m for the linear non-equilibrium sorption case.

with $g_{x_{j|i}}$, we calculated the backward travel time probabilities using (6.44) and (6.45). The backward aqueous, sorbed, and total travel time probabilities are plotted in Figure 6.14. Based on the total probability, the most likely travel time from $x = 100$ m to the pumping well is $\tau \approx 204$ days. If the detected contamination had been in the aqueous phase at $x = 100$ m, its most likely travel time to the pumping well is $\tau \approx 160$ days. Similarly, if the detected contamination had been in the sorbed phase at $x = 100$ m, its most likely travel time to the pumping well is $\tau \approx 220$ days. At $x = 100$ m, $\int_\tau f_{\tau_A}\, d\tau = 0.40$; $\int_\tau f_{\tau_S}\, d\tau = 0.60$; and $\int_\tau f_{\tau_T}\, d\tau = 1.0$. Thus, a particle detected at the pumping well is most likely to have been at location $x = 100$ m at time $\tau \approx 204$ days in the past, and it was in the aqueous phase 40% of the time and in the sorbed phase 60% of the time at that location.

In his heuristic development of the backward probability model for linear non-equilibrium sorption, *Liu* [1995] did not distinguish between the possible phases of the detection. He obtained one aqueous phase location prob-

ability and one sorbed phase location probability; these are equivalent to $g_{x_{A|A}}$ and $g_{x_{S|A}}$ calculated here. The travel time probabilities obtained heuristically by *Liu* [1995] are equivalent to the $g_{\tau_{A|i}}$ calculated here.

6.4 Practical Considerations

The backward models presented in this paper address transport of reactive contaminants that undergo first order decay, linear equilibrium sorption, or linear non-equilibrium sorption. The governing equations for the first-order decay and linear equilibrium sorption models are similar to the advection-dispersion equation; therefore any code that can solve the forward ADE for those cases can also be used to solve the backward adjoint equation.

For linear non-equilibrium sorption, the governing equations for the backward model (6.51) cannot be solved directly using a code that solves the forward governing equation (6.47). In the example presented here, we used a one-dimensional domain and solve the backward model equations using Laplace transforms. This was reasonable for this simple one-dimensional problem with constant parameters; however, it may become impractical for more complex problems.

6.5 Conclusions

Backward-in-time location and travel time probabilities were developed heuristically by *Liu* [1995] and *Wilson and Liu* [1994] for several cases, including transport of conservative and reactive chemicals, uniform and non-uniform flow fields, homogeneous and heterogeneous systems, and one- and

multi-dimensional domains. *Neupauer and Wilson* [1999, 2000a,b] demonstrated that these backward-in-time probabilities are adjoint states of resident concentration, and used adjoint theory to obtain the governing equations of backward probabilities for conservative tracers in steady, uniform flow fields. The advantage of the adjoint approach over the heuristic approach in obtaining the governing equations is that adjoint theory provides a rigorous mathematical procedure for developing the equations for all aquifer geometries and for all transport processes.

In this paper, we applied adjoint theory to the cases of first-order decay, and linear equilibrium and non-equilibrium sorption. Many of these cases were developed heuristically by *Liu* [1995], and we compare his results to those presented here. In this paper, we presented examples only for a one-dimensional domain; however, the backward model can be extended to multiple detections following the approach of *Neupauer and Wilson* [2000a].

For contamination that is detected in an aquifer, location probability describes the probability of the contaminant's prior position at some time in the past. Travel time probability describes the probability of the travel time of the detected contamination from an upgradient location to the detection location. We have shown that two different interpretations can be made for contaminants that are subject to first-order decay. With one interpretation, probability decays in time, indicating that if the contamination was in the aquifer at a previous time, there is a non-zero probability that the contamination would have decayed prior to reaching the detection location. In the second interpretation, the probability is conditioned on the contamination reaching the well (i.e., it has not decayed), and the probability does not decay.

For sorbing contaminants, backward location probability depends on the phase of the detected contamination and on the phase of interest at the prior location. Since backward travel time probability depends on flux concentration, which is non-zero only in the aqueous phase, travel time probability can only be calculated for an aqueous phase detection. The backward probabilities are not obtained directly from adjoint states of aqueous and sorbed phase resident concentration; however, we demonstrated a simple relationship between the backward probabilities and the adjoint states.

Acknowledgments

This research was supported in part by the Geophysical Research Center at New Mexico Tech and in part by the Environmental Protection Agency's STAR Fellowship program under Fellowship No. U-915324-01-0. This work has not been subjected to the EPA's peer and administrative review and therefore may not necessarily reflect the views of the Agency and no official endorsement should be inferred. The authors acknowledge William D. Stone for his input on operator theory.

References

Bagtzoglou, A.C., D.E. Dougherty, and A.F.B. Thompson, Application of particle methods to reliable identification of groundwater pollution sources, *Water Resources Management*, 6, 15–23, 1992.

Chin, D.A. and P.V.K. Chittaluru, Risk management in wellhead protection, *J. Water Resour. Plan. Manage.*, 120(3), 294–315. 1994.

Dagan, G., Stochastic modeling of groundwater flow by unconditional and conditional probabilities, 2, The solute transport, *Water Resour. Res.*, 18(4), 835–848, 1982.

Dagan, G., Theory of solute transport by groundwater, *Ann. Rev. Fluid Mech.*, 19, 183–215, 1987.

Dagan, G., *Flow and Transport in Porous Formations*, Springer-Verlag, New York, 1989.

Dagan, G., and V. Nguyen, A comparison of travel time and concentration approaches to modeling transport by groundwater, *Journal of Contaminant Hydrology*, 4, 79–91, 1989.

Jury, W.A., Simulation of solute transport using a transfer function model, *Water Resour. Res.*, 18(2), 363–368, 1982.

Jury, W.A., G. Sposito, and R.E. White, A transfer function model of solute transport through soil, 1, Fundamental concepts, *Water Resour. Res.*, 22(2), 243–247, 1986.

Jury, W.A. and K. Roth, *Transfer Functions and Solute Movement through Soil: Theory and Applications*, Birkhauser Verlag, Boston, 1990.

Liu, J., *Travel time and location probabilities for groundwater contaminant sources*, Master's thesis, New Mexico Institute of Mining and Technology, Socorro, 1995.

Neupauer, R.M. and J.L. Wilson, Adjoint method for obtaining backward-in-time location and travel time probabilities of a conservative groundwater contaminant, *Water Resour. Res.*, 35(11), 3389–3398, 1999.

Neupauer, R.M. and J.L. Wilson, Adjoint-derived location and travel time probabilities in a multi-dimensional groundwater flow system, *Water Resour. Res.*, in press, 2000a.

Neupauer, R.M. and J.L. Wilson, Backward location and travel time probabilities for contamination in a one-dimensional infinite aquifer, submitted to *J. Contam. Hydrol.*, 2000b.

Parker, J.C. and M. Th. van Genuchten, Flux-averaged and volume-averaged concentrations in continuum approaches to solute transport, *Water Resour. Res.*, 20(7), 866–872, 1984.

Rubin, Y. and G. Dagan, Conditional estimation of solute travel time in heterogeneous formations: impact of transmissivity measurements, *Water Resour. Res.*, 28(4), 1033–1040, 1992.

Shapiro, A.M. and V.D. Cvetkovic, Stochastic analysis of solute arrival time in heterogeneous porous media, *Water Resour. Res.*, 24(10), 1711–1718, 1988.

Sykes, J.F., J.L. Wilson, and R.W. Andrews, Sensitivity analysis for steady state groundwater flow using adjoint operators, *Water Resour. Res.*, 21(3), 359–371, 1985.

Uffink, G.J.M., Application of Kolmogorov's backward equation in random walk simulations of groundwater contaminant transport, in *Contaminant Transport in Groundwater*, H.E. Kobus and W. Kinzelbach, editors, pp. 283–289, A.A. Balkema, Brookfield, Vt., 1989.

Wilson, J.L. and J. Liu, Backward tracking to find the source of pollution, in *Waste-management: From Risk to Remediation*, edited by R. Bhada *et al.*, ECM Press, Albuquerque, NM, 181–199, 1994.

Wilson, J.L. and J. Liu, Field Validation of the Backward-in-time Advection Dispersion Theory. *Proceedings of the 1996 HSRC/WERC Joint Conf. on the Environment*, Great Plains-Rocky Mountain Hazardous Substance Center, Manhattan, Kansas, http://www.engg.ksu.edu/HSRC/ 96Proceed/wilson.html, 1997.

Zauderer, E., *Partial Differential Equations of Applied Mathematics*, 2nd ed., John Wiley and Sons, New York, 1989.

6.A Derivation of the Solution to the Adjoint Equation with Decay

The governing equation for backward location probability for a decaying chemical in the one-dimensional aquifer shown in Figure 6.1 is given by

$$\frac{\partial \bar{f}_x}{\partial \tau} = \frac{\partial}{\partial x}\left(D\frac{\partial \bar{f}_x}{\partial x}\right) + \frac{\partial}{\partial x}(v\bar{f}_x) - \lambda \bar{f}_x + \delta(x - x_w)\delta(\tau)\ , \tag{6.57}$$

$$\bar{f}_x(x,0) = 0$$

$$D\frac{\partial \bar{f}_x}{\partial x} + v\bar{f}_x = 0 \text{ at } x = 0$$

$$\bar{f}_x = 0 \text{ as } x \to \infty\ ,$$

where $\bar{f}_x$ denotes the location probability for a decaying chemical and we substituted $\bar{f}_x = \psi_x^*/\theta$ and used the fact that porosity is constant. Multiplying both sides of this equation and the boundary and initial conditions by $e^{\lambda\tau}$ results in

$$e^{\lambda\tau}\frac{\partial \bar{f}_x}{\partial \tau} = \frac{\partial}{\partial x}\left(D\frac{\partial f_x}{\partial x}\right) + \frac{\partial}{\partial x}(vf_x) - e^{\lambda\tau}\lambda \bar{f}_x + e^{\lambda\tau}\delta(x - x_w)\delta(\tau)\ , \tag{6.58}$$

$$f_x(x,0) = 0$$

$$D\frac{\partial f_x}{\partial x} + vf_x = 0 \text{ at } x = 0$$

$$f_x = 0 \text{ as } x \to \infty\ ,$$

where we substituted $f_x = e^{\lambda\tau}\bar{f}_x$. Rearranging the partial differential equation yields

$$e^{\lambda\tau}\left[\frac{\partial \bar{f}_x}{\partial \tau} + \lambda \bar{f}_x\right] = \frac{\partial}{\partial x}\left(D\frac{\partial f_x}{\partial x}\right) + \frac{\partial}{\partial x}(vf_x) + e^{\lambda\tau}\delta(x - x_w)\delta(\tau)\ . \tag{6.59}$$

Substituting $f_x = e^{\lambda\tau}\bar{f}_x$ on the left-hand side results in

$$\frac{\partial f_x}{\partial \tau} = \frac{\partial}{\partial x}\left(D\frac{\partial f_x}{\partial x}\right) + \frac{\partial}{\partial x}(v f_x) + e^{\lambda\tau}\delta(x - x_w)\delta(\tau) \; . \tag{6.60}$$

The last term on the right-hand side is non-zero only for $\tau = 0$; therefore, the coefficient, $e^{\lambda\tau}$, must be evaluated at $\tau = 0$, simplifying the equation to

$$\frac{\partial f_x}{\partial \tau} = \frac{\partial}{\partial x}\left(D\frac{\partial f_x}{\partial x}\right) + \frac{\partial}{\partial x}(v f_x) + \delta(x - x_w)\delta(\tau) \; . \tag{6.61}$$

This equation is equivalent to (6.12), for a conservative tracer; therefore, f_x is the location probability for a conservative tracer (6.16). Since $f_x = e^{\lambda\tau}\bar{f}_x$, the solution to (6.57) is $e^{-\lambda\tau}f_x$, where f_x given in (6.16) and $\bar{f}_x$ is equivalent to the expression in (6.22).

6.B Adjoint Equation for Linear Equilibrium Sorption

The sensitivity analysis approach can be used to obtain the adjoint equation for the backward probability model with linear equilibrium sorption, and from it, we can obtain the relationships between the adjoint states and the location and travel time probabilities of interest. We follow the sensitivity analysis approach of *Sykes et al.* [1985]. In sensitivity analysis, we define a performance measure, P, as in (6.8), with $h = h(\alpha, C, C_S)$ for this two-phase system. We determine the marginal sensitivity of the performance measure with respect to a system parameter α as shown in (6.9). For this two-phase system, the equivalent expression is

$$\frac{dP}{d\alpha} = \iint_{x,t} \left[\frac{\partial h}{\partial \alpha} + \frac{\partial h}{\partial C}\psi_A + \frac{\partial h}{C_S}\psi_S \right] \, dx \, dt \, , \tag{6.62}$$

where $dP/d\alpha$ is the marginal sensitivity and $\psi_A = \partial C/\partial \alpha$ is the variation of C, and $\psi_S = \partial C_S/\partial \alpha$ is the variation of C_S.

To eliminate the unknown state sensitivities, ψ_A and ψ_S, from (6.62), we first obtain their governing equations by differentiating each equation term of (6.25) with respect to the parameter α, resulting in

$$\begin{aligned}
\frac{\partial \psi_A}{\partial t} + \frac{\partial \psi_S}{\partial t} &= D\frac{\partial^2 \psi_A}{\partial x^2} - v\frac{\partial \psi_A}{\partial x} + L_{\alpha,A} && (6.63)\\
\psi_S &= \frac{K_d \rho_b}{\theta}\psi_A + C\frac{\partial}{\partial \alpha}\left(\frac{K_d \rho_b}{\theta}\right) && (6.64)\\
\psi_A(x,0) &= \frac{\partial C_{Ao}}{\partial \alpha}\delta(x - x_o)\\
\psi_S(x,0) &= \frac{\partial C_{So}}{\partial \alpha}\delta(x - x_o)\\
\frac{\partial \psi_A}{\partial x} = 0 &\quad \text{at} \quad x = 0\\
\psi_A \to 0 &\quad \text{as} \quad x \to \infty\ ,
\end{aligned}$$

where $L_{\alpha,A}$ contains the remaining terms, all independent of ψ_A and ψ_S, given by

$$L_{\alpha,A} = \frac{\partial D}{\partial \alpha}\frac{\partial^2 C}{\partial x^2} - \frac{\partial v}{\partial \alpha}\frac{\partial C}{\partial x}\ . \qquad (6.65)$$

In (6.63), we replaced the initial conditions from (6.25) with general initial conditions, C_{Ao} for the initial aqueous concentration and C_{So} for the initial sorbed concentration. By the equilibrium assumption, $C_{So} = (K_d \rho_b/\theta)C_{Ao}$. For the problem considered here, α is related to the source strengths (C_{Ao} and C_{So}); therefore $L_{\alpha,A} = 0$ and $\partial\alpha(K_d\rho_b/\theta)/\partial\alpha = 0$.

Next we take the inner product of each term in (6.63) with an arbitrary function, ψ_A^*, and the inner product of each term in (6.64) with a second arbitrary function, ψ_S^*. The functions ψ_A^* and ψ_S^* are adjoint states. The inner product of two real functions f and g is defined as $\langle f, g\rangle = \int_0^T \int_{x_1}^{x_2} f\, g\ dx\ dt$, where the time domain is $0 \le t \le T$. The inner product of (6.63) with ψ_A^*

produces

$$\iint_{x,t}\left[\psi_A^* D\frac{\partial^2\psi_A}{\partial x^2} - \psi_A^* v\frac{\partial\psi_A}{\partial x} - \psi_A^*\frac{\partial\psi_A}{\partial t} - \psi_A^*\frac{\partial\psi_S}{\partial t}\right]dx\ dt = 0, \tag{6.66}$$

and the inner product of (6.64) with ψ_S^* produces

$$\iint_{x,t}\left[-\psi_S^*\psi_S + \psi_S^*\frac{K_d\rho_b}{\theta}\psi_A\right]dx\ dt = 0\ . \tag{6.67}$$

Since the left-hand sides of (6.66) and (6.67) evaluate to zero, they can be added to the right-hand side of (6.62) without changing the equality. Making these additions, using the product rule on each derivative term, and rearranging the terms, (6.62) becomes

$$\begin{aligned}\frac{dP}{d\alpha} \;=\; & \iint_{x,t}\left\{\frac{\partial h(\alpha,C)}{\partial\alpha} + \psi_A\left[\frac{\partial h}{\partial C} + \frac{\partial\psi_A^*}{\partial t} + D\frac{\partial^2\psi_A^*}{\partial x^2} + v\frac{\partial\psi_A^*}{\partial x} + \frac{K_d\rho_b}{\theta}\psi_S^*\right]\right. \\ & +\psi_S\left[\frac{\partial h}{\partial C_S} + \frac{\partial\psi_A^*}{\partial t} - \psi_S^*\right] - \frac{\partial}{\partial t}\left(\psi_A^*\psi_A + \psi_A^*\psi_S\right) \\ & \left.+\frac{\partial}{\partial x}\left(\psi_A^* D\frac{\partial\psi_A}{\partial x} - \psi_A D\frac{\partial\psi_A^*}{\partial x} - \psi_A^* v\psi_A\right)\right\}dx\ dt\ .\end{aligned} \tag{6.68}$$

The last two terms in the integral are divergence terms, containing unknown values of ψ_A and ψ_S. To eliminate these unknown values from the divergence terms, we define boundary and final conditions on the adjoint states so that the divergence terms containing unknown values of ψ_A and ψ_S vanish. After integration over the spatial domain, the divergence terms in space become

$$\int_t\left[\psi_A^* D\frac{\partial\psi_A}{\partial x} - \psi_A D\frac{\partial\psi_A^*}{\partial x} - \psi_A^* v\psi_A\right]\Bigg|_{x_1}^{x_2} dt\ . \tag{6.69}$$

After we substitute the boundary conditions on ψ_A from (6.63), the terms involving unknown values of ψ can be eliminated from (6.69) if we set $D\partial\psi_A^*/\partial x + v\psi_A^* = 0$ at $x = x_1$, and $\psi_A^* = 0$ at $x = x_2$. Similarly, after integration over the time domain, the divergence term in time becomes

$$\int_x [\psi_A^* \psi_A + \psi_A^* \psi_S] \Big|_{t=0}^{t=T} dx \ . \tag{6.70}$$

After we substitute the initial conditions on ψ_A and ψ_S from (6.63), we can eliminate the terms involving $\psi_A(x,T)$ and $\psi_S(x,T)$ by setting $\psi_A^* = 0$ at $t = T$. These are the final and boundary conditions for the adjoint state, ψ_A^*.

The only remaining terms containing ψ_A and ψ_S in (6.68) are the terms in square brackets. To eliminate ψ_A and ψ_S from the expression, we set the quantities inside the square brackets to zero, producing the adjoint equations in (6.31). With these definitions of the adjoint equations and boundary and initial (in τ) conditions, (6.68) reduces to (6.32).

6.C Relationship between Backward Probabilities and Adjoint States for Linear Equilibrium and Non-equilibrium Sorption

We derive the relationship between adjoint states obtained from the linear equilibrium sorption model and the backward location probabilities. The derivation also holds for the linear non-equilibrium sorption case. Consider the backward aqueous phase location probability based on a detection in the sorbed phase, $f_{x_{A|S}}$, defined in (6.39), which is the desired backward probability. This probability can be related to $g_{x_{S|A}}$ and $g_{x_{S|S}}$, which are defined in (6.38), using Bayes' theorem,

$$\mathrm{P}(x_o, A; T|x_w, S; 0) = \frac{\mathrm{P}(x_w, S; 0|x_o, A; T)\mathrm{P}(x_o, A; T)}{\mathrm{P}(x_w, S; 0)} \tag{6.71}$$

where we have dropped random variables from the notation, A and S indicate aqueous and sorbed phase, respectively, x_o is the random variable, and

$$\begin{aligned} \mathrm{P}(x_w, S; 0) \;=\; & \int_{x_o} [\mathrm{P}(x_w, S; 0|x_o, A; T)\mathrm{P}(x_o, A; T) + \\ & \qquad \mathrm{P}(x_w, S; 0|x_o, S; T)\mathrm{P}(x_o, S; T)]\; dx_o \;, \end{aligned} \tag{6.72}$$

The unconditional probabilities $\mathrm{P}(x_o, A; T)$ and $\mathrm{P}(x_o, S; T)$ define the probability that the particle was at x_o at time T in the aqueous and sorbed phases, respectively. These probabilities are independent of the particle's position and phase at time $\tau = 0$. From Bayes' theorem, $\mathrm{P}(A \text{ and } B) = \mathrm{P}(A|B)\mathrm{P}(B)$; therefore the unconditional probabilities can be replaced with

$$\mathrm{P}(x_o, A; T) = \mathrm{P}(x = x_o; \tau = T)\mathrm{P}(p_o = A|x = x_o; \tau = T) \tag{6.73}$$

$$\mathrm{P}(x_o, S; T) = \mathrm{P}(x = x_o; \tau = T)\mathrm{P}(p_o = S | x = x_o; \tau = T) \ , \tag{6.74}$$

where $\mathrm{P}(x = x_o; \tau = T)$ is the unconditional probability that the particle was at x_o and backward time T, independent of its phase, and $\mathrm{P}(p_o = A|x = x_o; \tau = T)$ and $\mathrm{P}(p_o = S|x = x_o; \tau = T)$ are the probabilities that the particle was in the aqueous and sorbed phases, respectively, at $x = x_o$. Making these substitutions in (6.71), we obtain

$$\mathrm{P}(x_o, A; T|x_w, S; 0) = \frac{\mathrm{P}(x_w, S; 0|x_o, A; T)\mathrm{P}(x_o; T)\mathrm{P}(A|x_o; T)}{\mathrm{P}(x_w, S; 0)} \tag{6.75}$$

$$\begin{aligned} \mathrm{P}(x_w, S; 0) = \int_{x_o} [&\mathrm{P}(x_w, S; 0|x_o, A; T)\mathrm{P}(x_o; T)\mathrm{P}(A|x_o; T) + \\ &\mathrm{P}(x_w, S; 0|x_o, S; T)\mathrm{P}(x_o; T)\mathrm{P}(S|x_o; T)] \ dx_o \ . \end{aligned} \tag{6.76}$$

Without any additional information on $\mathrm{P}(x_o; T)$, we assume it is uniformly-distributed. Without any information on prior locations or phases of a particle, $\mathrm{P}(A|x_o; T) = 1/R(x_o)$ is the probability that the particle is in the aqueous phase, and $\mathrm{P}(S|x_o, T) = (R(x_o)-1)/R(x_o)$ is the probability that the particle is in the sorbed phase. Making these substitutions in (6.75) and using (6.38) and (6.39), we obtain (6.40). Following the same approach for the other backward probabilities, and using $g_{x_{T|i}} = g_{x_{A|i}} + g_{x_{S|i}}$, we obtain the remaining equations described by (6.40) and (6.41).

A similar approach can be followed for backward travel time probability; however, in that case, the random variable in (6.71) is T instead of x_o, and integration in (6.72) and (6.76) is over all T.

6.D Adjoint Equation for Linear Non-equilibrium Sorption

We develop the adjoint equations for linear non-equilibrium sorption model, following the approach in Appendix 6.B. The marginal sensitivity equation, (6.62), contains the unknown state sensitivities, ψ_A and ψ_S, which are defined as $\psi_A = \partial C/\partial\alpha$, $\psi_S = \partial C_S/\partial\alpha$, and α is a system parameter.

To eliminate the unknown state sensitivities from (6.62), we first obtain their governing equations by differentiating each equation term of (6.47) with respect to α, resulting in

$$\begin{aligned}
\frac{\partial\psi_A}{\partial t} + \frac{\partial\psi_S}{\partial t} &= D\frac{\partial^2\psi_A}{\partial x^2} - v\frac{\partial\psi_A}{\partial x} + L_{\alpha,A} && (6.77)\\
\frac{\partial\psi_S}{\partial t} &= \frac{\alpha_s K_d \rho_b}{\theta}\psi_A - \alpha_s\psi_S + L_{\alpha,S} && (6.78)\\
\psi_A(x,0) &= \frac{\partial C_{Ao}}{\partial\alpha}\delta(x-x_o)\\
\psi_S(x,0) &= \frac{\partial C_{So}}{\partial\alpha}\delta(x-x_o)\\
\frac{\partial\psi_A}{\partial x} = 0 &\quad \text{at} \quad x = 0\\
\psi_A \to 0 &\quad \text{as} \quad x \to \infty\ ,
\end{aligned}$$

where $L_{\alpha,A}$ and $L_{\alpha,S}$ contain terms independent of ψ_A and ψ_S, given by

$$\begin{aligned}
L_{\alpha,A} &= \frac{\partial D}{\partial\alpha}\frac{\partial^2 C}{\partial x^2} - \frac{\partial v}{\partial\alpha}\frac{\partial C}{\partial x} && (6.79)\\
L_{\alpha,S} &= C\frac{\partial}{\partial\alpha}\left(\frac{\alpha_s K_d\rho_b}{\theta}\right) - C_S\frac{\partial\alpha_s}{\partial\alpha}\ . && (6.80)
\end{aligned}$$

In the problem presented here, α is related to the source strengths, C_{Ao} and C_{So}, therefore $L_{\alpha,A} = L_{\alpha,S} = 0$.

Next we take the inner product of each term in (6.77) with an arbitrary function, ψ_A^*, and the inner product of each term in (6.78) with a second arbitrary function, ψ_S^*, producing (6.66) and

$$\iint_{x,t} \left[-\psi_S^* \frac{\partial \psi_S}{\partial t} + \psi_S^* \frac{\alpha_s K_d \rho_b}{\theta} \psi_A \right] dx\, dt = 0 \,. \tag{6.81}$$

By adding the left-hand sides of (6.66) and (6.81) to (6.62), using the product rule on each derivative term, and rearranging the terms, we replace (6.62) with

$$\begin{aligned} \frac{dP}{d\alpha} \;=\; & \iint_{x,t} \left\{ \frac{\partial h(\alpha, C)}{\partial \alpha} + \psi_A \left[\frac{\partial h}{\partial C} + \frac{\partial \psi_A^*}{\partial t} + D \frac{\partial^2 \psi_A^*}{\partial x^2} + v \frac{\partial \psi_A^*}{\partial x} + \frac{\alpha_s K_d \rho_b}{\theta} \psi_S^* \right] \right. \\ & + \psi_S \left[\frac{\partial h}{\partial C_S} + \frac{\partial \psi_A^*}{\partial t} + \frac{\partial \psi_S^*}{\partial t} - \alpha_s \psi_S^* \right] - \frac{\partial}{\partial t} \left(\psi_A^* \psi_A + \psi_A^* \psi_S + \psi_S^* \psi_S \right) \\ & \left. + \frac{\partial}{\partial x} \left(\psi_A^* D \frac{\partial \psi_A}{\partial x} - \psi_A D \frac{\partial \psi_A^*}{\partial x} - \psi_A^* v \psi_A \right) \right\} dx\, dt \,. \end{aligned} \tag{6.82}$$

The last two terms in the integral are divergence terms, containing unknown values of ψ_A and ψ_S. To eliminate these unknown values from the divergence terms, we define boundary and final conditions on the adjoint states so that the divergence terms containing unknown values of ψ_A and ψ_S vanish. The spatial divergence term is equivalent to the spatial divergence in (6.68); therefore the boundary conditions for this case are equivalent to those for the linear equilibrium sorption case. After integration over the time domain, the divergence term in time becomes

$$\int_x \left[\psi_A^* \psi_A + \psi_A^* \psi_S + \psi_S^* \psi_S \right] \Big|_{t=0}^{t=T} dx \,. \tag{6.83}$$

By substituting the initial conditions on ψ_A and ψ_S from (6.77), we eliminate the terms involving $\psi_A(x,T)$ and $\psi_S(x,T)$ by setting $\psi_A^* = 0$ and $\psi_S^* = 0$ at $t = T$. These are the final conditions for the adjoint states.

The only remaining terms containing ψ_A and ψ_S in (6.82) are the terms in square brackets. To eliminate ψ_A and ψ_S from the expression, we set the quantities inside the square brackets to zero, producing the adjoint equations in (6.51). With these definitions of the adjoint equations and boundary and initial (in τ) conditions, (6.82) reduces to (6.52).

6.E Derivation of Laplace-Transformed Adjoint States for Linear Non-equilibrium Sorption

We verify here that (6.54) and (6.56) are the Laplace-transformed solutions of (6.53) and (6.55), respectively. The Laplace transform in time ($t \rightarrow s$) of (6.53) and its boundary conditions from (6.51) is

$$s\hat{\psi}_A^* = D\frac{d^2\hat{\psi}_A^*}{dx^2} + v\frac{d\hat{\psi}_A^*}{dx} + \frac{\alpha_s K_d \rho_b}{\theta}\hat{\psi}_S^* + g(x) \tag{6.84}$$

$$s\hat{\psi}_A^* + s\hat{\psi}_S^* = -\alpha_s \hat{\psi}_S^* \ , \tag{6.85}$$

where $\hat{\psi}_A^*$ and $\hat{\psi}_S^*$ are the Laplace transforms of ψ_A^* and ψ_S^*, respectively, $g(x) = \delta(x - x_w)$, and we used the fact that $\psi_A^*(x,0) = \psi_S^*(x,0) = 0$. Rearranging (6.85) to solve for $\hat{\psi}_S^*$, we obtain the second equation in (6.54). Substituting this result into (6.84), we obtain

$$s\gamma\hat{\psi}_A^* - g(x) = D\frac{d^2\hat{\psi}_A^*}{dx^2} + v\frac{d\hat{\psi}_A^*}{dx} \ , \tag{6.86}$$

where $\gamma = 1 + \alpha_s K_d \rho_b / (\theta[s + \alpha_s])$.

The Laplace transform in space ($x \rightarrow r$) of (6.86) yields

$$\gamma\bar{\hat{\psi}}_A^* - \bar{g} = Dr^2\bar{\hat{\psi}}_A^* - D\left.\frac{d\hat{\psi}_A^*}{dx}\right|_{x=0} - Dr\hat{\psi}_A^*|_{x=0} + vr\bar{\hat{\psi}}_A^* - v\hat{\psi}_A^*|_{x=0} \ , \tag{6.87}$$

where $\bar{\hat{\psi}}_A^*$ is the double Laplace transform of ψ_A^* and $\bar{g}$ is the Laplace transform in space of $g(x)$. Using the boundary condition at $x = 0$, rearranging terms,

and using partial fractions, we obtain

$$\bar{\hat{\psi}}_A^* = \frac{1}{D(r_1 - r_2)} \left[\frac{Dr_1 \hat{\psi}_A^*|_{x=0} - \bar{g}}{r - r_1} + \frac{\bar{g} - Dr_2 \hat{\psi}_A^*|_{x=0}}{r - r_2} \right] , \tag{6.88}$$

where $r_1 = -v/(2D)(1+\xi)$, $r_2 = -v/(2D)(1-\xi)$, and $\xi = \sqrt{1 + 4\gamma D/v^2}$. Note that $\xi > 1$; therefore, since $v < 0$, $r_1 > 0$ and $r_2 < 0$.

Taking the inverse Laplace transform in r, we obtain

$$\begin{aligned} \hat{\psi}_A^* &= \frac{1}{D(r_1 - r_2)} \Big[Dr_1 \hat{\psi}_A^*|_{x=0} \exp\{r_1 x\} - \int_0^x g(x') \exp\{r_1(x - x')\} dx' \\ &\quad + \int_0^x g(x') \exp\{r_2(x - x')\} dx' - Dr_2 \hat{\psi}_A^*|_{x=0} \exp\{r_2 x\} \Big] . \end{aligned} \tag{6.89}$$

Next we use the boundary condition that $\hat{\psi}_A^* \to 0$ as $x \to \infty$. As $x \to \infty$, $\exp\{r_2 x\} \to 0$ because $r_2 < 0$; therefore the last two terms inside the square brackets in (6.89) vanish. To ensure that the boundary condition holds as $x \to \infty$, the first two terms inside the square brackets in (6.89) must sum to zero, which occurs if

$$\hat{\psi}_A^*|_{x=0} = \frac{1}{Dr_1} \int_0^\infty g(x') \exp\{-r_1 x'\} dx' . \tag{6.90}$$

Substituting (6.90) into (6.89), we obtain

$$\begin{aligned} \hat{\psi}_A^* &= \frac{1}{D(r_1 - r_2)} \Big[\int_x^\infty g(x') \exp\{r_1(x - x')\} dx' \\ &\quad + \int_0^x g(x') \exp\{r_2(x - x')\} dx' - \frac{r_2}{r_1} \int_0^\infty g(x') \exp\{r_2 x - r_1 x')\} dx' \Big] . \end{aligned} \tag{6.91}$$

At $x_w = 0$, $g(x') = \delta(x')$. Making this substitution in (6.91), evaluating the

integrals (note that the first integral vanishes because the Dirac delta function is acting outside of the limits of integration), and rearranging, we obtain the first equation in (6.54).

The Laplace transform in time ($t \to s$) of (6.55) is

$$s\hat{\psi}_A^* = D\frac{d^2\hat{\psi}_A^*}{dx^2} + v\frac{d\hat{\psi}_A^*}{dx} + \frac{\alpha_s K_d \rho_b}{\theta}\hat{\psi}_S^* \tag{6.92}$$

$$s\hat{\psi}_A^* + s\hat{\psi}_S^* = -\alpha_s\hat{\psi}_S^* + g(x)\ . \tag{6.93}$$

Rearranging (6.93) to solve for $\hat{\psi}_S^*$, we obtain the second equation in (6.56). Substituting this result into (6.92), we obtain

$$s\gamma\hat{\psi}_A^* - \frac{\alpha_s K_d \rho_b}{\theta(s+\alpha_s)}g(x) = D\frac{d^2\hat{\psi}_A^*}{dx^2} + v\frac{d\hat{\psi}_A^*}{dx}\ . \tag{6.94}$$

This equation is similar to (6.86), with a new coefficient on $g(x)$. Therefore, the solution to this equation is the solution to (6.86), scaled by this new coefficient, which is equivalent to the first equation in (6.56).

CHAPTER 7

NUMERICAL IMPLEMENTATION OF THE BACKWARD PROBABILITY MODEL

Abstract

Backward location and travel time probabilities can be used to characterize known and unknown sources of groundwater contamination. Backward location probability describes the probability distribution for the position of the detected contamination at some time in the past; backward travel time probability describes the probability distribution for the amount of time prior to detection that the contamination was released from its source or was at an upgradient location. The governing equation for backward probabilities is the adjoint of the governing equation for contaminant transport. Many numerical codes have been written to solve the advection-dispersion equation for contaminant transport in an aquifer. These codes can also be used to solve the adjoint equation for location and travel time probabilities; however, the interpretation of the results is different and some approximations must be made for the probability load terms. We present the governing equations for backward location and travel time probability for several situations. We then provide appropriate numerical approximations for these equations using general cell-centered finite difference models, and finite element models with linear triangular elements in two dimensions and linear triangular prism elements in three dimensions. Finally, we show one- and two-dimensional implementations of the backward probability model using MODFLOW-96 [*Harbaugh and McDonald*, 1996] and MT3DMS [*Zheng and Wang*, 1999].

7.1 Introduction

When contamination is detected in an aquifer, the source of contamination is often unknown. To remediate the aquifer or to assign responsibility we might need to identify the source of contamination or the time of release of contamination from the source. In conventional contaminant transport modeling, the source of contamination is known or assumed to be known, and the future positions of the contaminant plume is simulated. If the source of contamination is unknown, this conventional transport modeling approach is difficult to use. Backward modeling of groundwater contamination is an efficient approach for characterizing sources of groundwater contamination [*Wilson and Liu*, 1994, 1997; *Neupauer and Wilson*, 1999, 2000a].

Backward modeling is based on backward location and travel time probabilities. The results show the probability of the former position of the contamination (location probability) or the probability of the contaminant's travel time from some upgradient location to the sampling location (travel time probability). Not only can the backward probability model be used to improve characterization of known sources of groundwater contamination or to identify previously unknown contamination sources, but it can also be used to delineate capture zones.

Location and travel time probabilities are often used in forward modeling to describe solute transport in groundwater [e.g., *Dagan*, 1982, 1987; *Jury*, 1982; *Jury and Roth*, 1990; *Chin and Chittaluru*, 1994]. Forward location probability describes the position of a solute parcel at a fixed time after its release from the source [*Dagan*, 1982, 1987, 1989; *Jury and Roth*, 1990; *Chin and Chit-*

taluru, 1994] and is related to resident concentration [*Dagan*, 1987; *Jury and Roth*, 1990]. Forward travel time probability describes the time required for a solute parcel to travel from its source to a location of interest [*Jury*, 1982; *Jury et al.*, 1986; *Dagan*, 1989; *Dagan and Nguyen*, 1989], and is related to flux concentration [*Shapiro and Cvetkovic*, 1988; *Rubin and Dagan*, 1992].

In forward modeling we model the movement of solute (or probability) downgradient away from the contamination source and obtain information about the future position of the contamination. With backward modeling we treat the sampling location as a source of probability (there is a probability of one that the contamination was at the sampling location at the time of sampling) and allow the probability to advect upgradient in backward time and to spread out by dispersion. The result is a plume of backward probability that provides information about the former position of contamination. For a solute parcel that was detected in the groundwater, backward location probability describes its position at some time prior to sampling, and travel time probability describes the amount of time required for the solute parcel to travel to the sampling location from some upgradient position, such as a known or suspected contamination source.

The mathematical model governing backward probabilities is similar to the model for forward contaminant transport with some modifications to account for the upgradient movement of probability. By reversing the flow field in a random walk method, *Bagtzoglou et al.* [1992] obtained backward location probabilities for identifying sources of contamination. *Uffink* [1989] and *Chin and Chittaluru* [1994] used a similar random walk approach to delineate capture zones around pumping wells. *Wilson and Liu* [1994, 1997] used a heuristic

method to obtain a backward probabilistic continuum model from the forward advection-dispersion equation. The approach was validated using data from a field-scale tracer experiment at the Borden site [*Wilson and Liu*, 1997]; however, no formal justification was given for the model. *Neupauer and Wilson* [1999] showed that backward location and travel time probabilities are adjoint states of resident concentration. They illustrated the formal adjoint approach for obtaining the governing equations of the backward model for a conservative chemical in a steady, uniform flow field in a one-dimensional domain [*Neupauer and Wilson*, 1999, 2000b] and in a multi-dimensional domain [*Neupauer and Wilson*, 2000a]. The backward model for reactive transport (first-order decay, and linear equilibrium and non-equilibrium sorption) and non-uniform and transient flow has been developed heuristically by *Liu* [1995] and formally in Chapters 5 and 6 using adjoint theory.

Because backward probabilities are related to adjoint states of concentration, the governing equation for the backward model is the adjoint of the forward governing equations. The adjoint has a similar form as the forward equation, with some modifications to the boundary conditions, reversal of sign on the first derivative terms, and a new load term. Because the backward equations are similar to the forward equations, any numerical model that can simulate contaminant transport (forward model) should also be capable of simulating backward probabilities. Some modifications must be made to account for the differences between the forward and adjoint equations; and approximations to the load term are necessary.

We present an overview of backward probability theory and show the resulting governing equations of the backward probability models. We dis-

cuss the implementation of the backward model using conventional transport codes, including the approximations to the load terms. We show general load term approximations for the cell-centered finite difference method and for the finite element method with linear triangular elements in two dimensions and linear triangular prism elements in three dimensions. Finally, we illustrate the numerical implementation of the backward model using MODFLOW-96 [*Harbaugh and McDonald*, 1996] and MT3DMS [*Zheng and Wang*, 1999]. These commonly-used codes are cell-centered finite-difference models for groundwater flow and contaminant transport, respectively. We present simulations for location and travel time probability of a conservative solute in both one- and two-dimensional domains, and for observations made with either a pumping well or a monitoring well. Analytical solutions can be obtained for the one-dimensional domain, and for these cases, we compare the numerical results to the analytical solution.

7.2 Backward Probability Theory

Transport of a conservative chemical in groundwater can be modeled using the advection-dispersion equation (ADE):

$$\frac{\partial}{\partial t}(\theta C) = \frac{\partial}{\partial x_i}\left(\theta D_{ij}\frac{\partial C}{\partial x_j}\right) - \frac{\partial}{\partial x_i}(\theta v_i C) + q_I C_I - q_O C \ , \tag{7.1}$$

$$C(\mathbf{x},0) = C_i(\mathbf{x})$$

$$C(\mathbf{x},t) = g_1(t) \text{ on } \Gamma_1$$

$$\left[D_{ij}\frac{\partial C}{\partial x_j}\right] \mathrm{n}_i = g_2(t) \text{ on } \Gamma_2$$

$$\left[v_i C - D_{ij}\frac{\partial C}{\partial x_j}\right] \mathrm{n}_i = g_3(t) \text{ on } \Gamma_3$$

where $C(\mathbf{x},t)$ is resident concentration, t is time, x_i are the spatial directions ($i = 1,2,3$), $\mathbf{x} = (x_1, x_2, x_3)$, D_{ij} is the i,j^{th} entry of the dispersion tensor, v_i is the groundwater velocity in the direction of x_i, q_I is the source flow rate per unit volume, C_I is the source strength, θ is porosity, q_O is the sink flow rate per unit volume, C_i is the initial concentration, g_1, g_2, and g_3 are known functions, Γ_1, Γ_2, and Γ_3 are the domain boundaries, and n_i is the outward unit normal vector in the x_i direction.

Resident concentration, C, measures the mass of solute per unit volume of water. Concentration is also reported as mass flux of solute per unit water flux, or flux concentration, C^f. The relationship between flux and resident concentration is [*Sposito and Barry*, 1987]

$$C^f = C - \frac{1}{|v|}\left[\left(D_{ij}\frac{\partial C}{\partial x_j}\right)\frac{v_i}{|v|}\right] \ , \tag{7.2}$$

where $|v|$ is the magnitude of the velocity vector. In one dimension, this sim-

plifies to [*Parker and van Genuchten*, 1984]

$$C^f = C - \frac{D}{v}\frac{\partial C}{\partial x} \; . \tag{7.3}$$

The backward probability model is the adjoint of (7.1), and can be obtained from the forward ADE using adjoint theory. The adjoint equation for (7.1) is given by [Chapter 5]

$$\frac{\partial}{\partial \tau}\left(\theta \psi^*\right) = \frac{\partial}{\partial x_i}\left(\theta D_{ij}\frac{\partial \psi^*}{\partial x_j}\right) + \frac{\partial}{\partial x_i}(\theta v_i \psi^*) - q_I \psi^* + \frac{\partial h}{\partial C} \tag{7.4}$$

$$\psi^*(\mathbf{x}, 0) = 0$$

$$\psi^*(\mathbf{x}, \tau) = 0 \text{ on } \Gamma_1$$

$$\left[D_{ij}\frac{\partial \psi^*}{\partial x_j} + v_i \psi^*\right] \mathrm{n}_i = 0 \text{ on } \Gamma_2$$

$$\left[D_{ij}\frac{\partial \psi^*}{\partial x_j}\right] \mathrm{n}_i = 0 \text{ on } \Gamma_3 \; .$$

where ψ^* is the adjoint state (related to either location or travel time probability), τ is backward time or time prior to sampling ($\tau = T - t$, where $t = T$ is the detection time), and h is a performance functional that depends on the type of probability and the detection mechanism (e.g., pumping well, monitoring well). This adjoint equation has the same form as (7.1), except that the flow field is reversed (compare signs on v_i terms and q_I terms), time is reversed, and the boundary conditions are modified. If the adjoint equation is solved numerically, the form of the adjoint equation must be consistent with the form of the ADE in the numerical code. Appendix 7.A shows a second form for the adjoint equation.

In (7.4), the term $\partial h/\partial C$ is called the load term. It is a Fréchet derivative of the performance functional, h, with respect to concentration, C. The adjoint equation describes a family of adjoint states; a particular adjoint state is defined by the load term, through the choice of the performance functional, h. We are interested in the two adjoint states that are related to location and travel time probability.

For location probability, the appropriate performance functional is related to the resident concentration at the detection location at the time of sampling [*Neupauer and Wilson*, 2000a]:

$$h(\mathbf{x},\tau) = C\delta(x_1 - x_{1_w})\delta(x_2 - x_{2_w})\frac{B_{x_3}(x_{3_{wt}}, x_{3_{wb}})}{x_{3_{wt}} - x_{3_w b}}\delta(\tau) \ , \tag{7.5}$$

where $\delta(x)$ is a Dirac delta function and (x_{1_w}, x_{2_w}) are the coordinates of the center of the well (detection location), $x_{3_{wt}}$ and $x_{3_{wb}}$ are the elevations of the top and bottom of the well, respectively, and $B_{x_i}(a,b)$ is a boxcar function defined as

$$B_{x_i}(a,b) = \begin{cases} 1 & a < x_i < b \\ 0 & \text{otherwise} \ . \end{cases} \tag{7.6}$$

The integral of (7.5) over space and time evaluates to the average resident concentration in the well at the time of sampling. With the performance functional defined in (7.5), the appropriate load term in (7.4) is

$$\frac{\partial h}{\partial C} = \delta(x_1 - x_{1_w})\delta(x_2 - x_{2_w})\frac{B_{x_3}(x_{3_{wt}}, x_{3_{wb}})}{x_{3_{wt}} - x_{3_{wb}}}\delta(\tau) \ . \tag{7.7}$$

This load term represents an instantaneous (at $\tau = 0$) source of probability, acting at a point in the x_1, x_2-plane (x_{1_w}, x_{2_w}), over a finite length in the x_3-direction $(x_{3_{wt}} - x_{3_{wb}})$. With this load term in (7.4), location probability, $f_x(\mathbf{x};\tau)$ is given by [Chapter 5]

$$f_x(\mathbf{x};\tau) = \theta(\mathbf{x})\psi^*(\mathbf{x},\tau) \; . \tag{7.8}$$

For travel time probability with a monitoring well detection, the appropriate performance functional is related to flux concentration, C^f, at the sampling location, given by

$$h(\mathbf{x},\tau) = C^f \delta(x_1 - x_{1_w})\delta(x_2 - x_{2_w})\frac{B_{x_3}(x_{3_{wt}}, x_{3_{wb}})}{x_{3_{wt}} - x_{3_wb}}\delta(\tau) \; . \tag{7.9}$$

With this expression for h and the relationship between flux and resident concentration from (7.2), the load term for travel time probability is [*Neupauer and Wilson*, 2000a]

$$\begin{aligned} \frac{\partial h}{\partial C} \;=\; & \Big[\delta(x_1 - x_{1_w})\delta(x_2 - x_{2_w}) + a_L\frac{v_1}{|v|}\delta'_{x_1}(x_1 - x_{1_w})\delta(x_2 - x_{2_w}) \\ & + a_L\frac{v_2}{|v|}\delta(x_1 - x_{1_w})\delta'_{x_2}(x_2 - x_{2_w})\Big]\frac{B_{x_3}(x_{3_{wb}}, x_{3_{wt}})}{x_{3_{wt}} - x_{3_{wb}}}\delta(\tau) \; , \end{aligned} \tag{7.10}$$

where $\delta'_{x_i}(x_i - x_{i_w})$ is the derivative of the Dirac delta function with respect to x_i, we assumed flow is essentially horizontal in the vicinity of the well, and the dispersion coefficient is given by [*Bear*, 1972]

$$D_{ij} = a_T v\delta_{ij} + (a_L - a_T)\frac{v_i v_j}{|v|} \tag{7.11}$$

where a_L and a_T are the longitudinal and transverse dispersivities, and δ_{ij} is the Kronecker delta function. This load term represents an instantaneous source of probability, acting at a point in the x_1, x_2-plane over a finite length in the x_3-direction, representing the screened interval of the well. Travel time probability is related to the adjoint state through the relationship [*Neupauer and Wilson*, 2000b]

$$f_\tau(\tau; \mathbf{x}) = |v(\mathbf{x})| w(\mathbf{x}) B(\mathbf{x}) \psi^*(\mathbf{x}, \tau) \ , \tag{7.12}$$

where w is the flow width at $\mathbf{x}$ in the x_1, x_2-plane, and $B(\mathbf{x})$ is the aquifer thickness at $\mathbf{x}$. At a pumping well, we often assume that $\partial C / \partial x_i = 0$; therefore, from (7.2), $C^f = C$ at a pumping well, and the load term in the adjoint equation is defined as in (7.7).

The complete governing equation for backward location and travel time probabilities is (7.4), with the appropriate load term defined in (7.7) or (7.10). The load terms were specified for a three-dimensional domain. If the domain is not three-dimensional, the correct load term can be obtained by integrating (7.7) or (7.10) over the dimension or dimensions that are excluded (examples can be found in *Neupauer and Wilson*, [2000a]).

7.3 Numerical Considerations

The governing equation for the backward model (7.4) is similar in form to the governing equation for the forward model (7.1); therefore, any numerical code that solves the forward governing equation can also be used to solve the backward governing equation. The differences between the two equations are

the reversed flow field in the backward model and the boundary conditions. These differences must be accounted for in the numerical solution. In addition, the load terms in the backward model contain special functions that must be approximated for use in a numerical model. Finally, special interpretation of the backward model results must be made to account for probability as the state variable and backward time as the time variable. In this section, we address these numerical considerations.

7.3.1 Flow Field

In forward contaminant transport modeling, the advective transport of contamination is controlled by the velocity field. We assume that the concentration of the contaminant is sufficiently low so that the mass does not affect flow. The flow field for a forward model can be obtained by running a forward flow simulation, and the resulting velocity field is used in the transport model.

The flow terms in the backward governing equation (7.4) have opposite signs as those in the forward governing equation (7.1). To account for these changes, the flow model obtained from the forward flow simulation must be reversed in direction for all flow processes including specific discharges, source and sink flow rates, change in storage, well fluxes, flow at prescribed head boundaries, recharge, evapotranspiration, and gains and losses to rivers and streams. If the flow field is transient, it must also be reversed in time so that the last time interval in the forward model becomes the first time interval in the backward model.

7.3.2 Boundary Conditions

The boundary conditions on the backward governing equation (7.4) are slightly different than those on the forward governing equation (7.1). The first-type boundary in the forward model (on Γ_1) remains a first-type boundary in the backward model, but the second-type boundary in the forward model (on Γ_2) becomes a third-type boundary in the backward model, and vice versa. The boundary conditions in the backward transport model must account for these modifications. Since all three types of boundary conditions are possible in the forward model, most codes can handle or approximate all three types of boundary conditions.

7.3.3 Interpretation of Results

Conventional contaminant transport codes are written for the forward model with concentration as the state variable and with forward time as the time variable. When a conventional transport code is used to simulate the backward probability model, the time variable in the simulation must be interpreted at backward time, τ, and the state variable represents the adjoint state. To obtain the appropriate probability from these adjoint states, the results must be post-processed using (7.8) or (7.12). The units of the adjoint state are per unit aquifer length for one-dimensional simulations, per unit aquifer area for two-dimensional problems, and per unit aquifer volume for three-dimensional problems. These units are not consistent with the normal units of the state variable in contaminant transport problems (e.g., mass per unit volume of water for concentration).

7.3.4 Load Terms

All load terms, $\partial h/\partial C$, for the backward model contain special functions including the Dirac delta function, the spatial derivative of the Dirac delta function, and the boxcar function. Since these functions cannot be used explicitly in numerical models, they must be approximated.

The Dirac delta function in time can be treated in two ways. To model an instantaneous source of probability, we can specify a positive mass loading rate for a short, but non-zero, duration. For example, the function $c\delta(\tau)$, where c is a constant, can be approximated as a mass loading of $c/\Delta t$ over a duration of Δt. If Δt is small relative to the duration of the simulation, then the load is essentially instantaneous.

The Dirac delta function in time can also be treated as an initial condition. Since the load term is non-zero only at $\tau = 0$, (7.4) and its initial condition can be rewritten as

$$\begin{aligned} \frac{\partial}{\partial \tau}(\theta\psi^*) &= \frac{\partial}{\partial x_i}\left(\theta D_{ij}\frac{\partial \psi^*}{\partial x_j}\right) + \frac{\partial}{\partial x_i}(\theta v_i \psi^*) - q_I\psi^* \\ \psi^*(\mathbf{x},0) &= \frac{\delta(x_1 - x_{1_w})\delta(x_2 - x_{2_w})}{\theta}\frac{B_{x_3}(x_{3_{wt}}, x_{3_{wb}})}{x_{3_{wt}} - x_{3_{wb}}}\ , \end{aligned} \tag{7.13}$$

for location probability. Similar initial conditions can be written for travel time probability. With the load term as an initial condition, we avoid any numerical approximation of the Dirac delta function in time.

The approximations for the boxcar function, the Dirac delta function in space, and the spatial derivative of the Dirac delta function depend on the numerical method used to solve the equation. We present the approximations

needed for the cell-centered finite difference method and for the finite element method with linear triangular elements.

Numerical Approximations for the Cell-Centered Finite Difference Method

In cell-centered finite difference models (e.g. MODFLOW [*McDonald and Harbaugh*, 1988] and MT3D [*Zheng*, 1990]), the domain is discretized into an array of rectangular elements. A section of a typical two-dimensional finite difference grid is shown in Figure 7.1. We first show the numerical approximations for a two-dimensional (x_1, x_2) domain, and then generalize the results to three dimensions.

All of the load terms contain Dirac delta functions in space. The finite difference approximation of a Dirac delta is a spatially-distributed source over the cell that contains the well. For example, the function $c\delta(x_1-x_{1_w})\delta(x_2-x_{2_w})$, where c is a constant, can be approximated as a distributed source of strength $c/[(\Delta x_1)_k(\Delta x_2)_k]$ over cell k, where $(\Delta x_1)_k$ and $(\Delta x_2)_k$ are the lengths of the k^{th} cell in the x_1- and x_2-directions, respectively, and the k^{th} cell contains the well center (x_{1_w}, x_{2_w}). If the discretization is fine relative to the size of the domain, this load is essentially a point source in x_1, x_2-space.

The load term for travel time probability with a monitoring well detection contains the spatial derivative of a Dirac delta function. It can be approximated using a central difference as

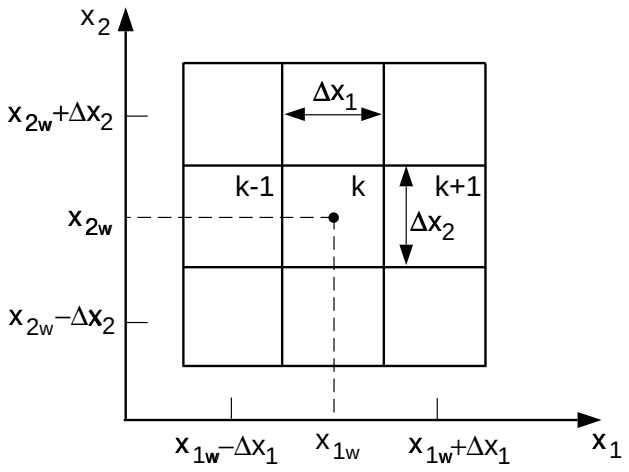

Figure 7.1: Cell-centered finite difference grid.

$$\begin{aligned} \delta'_{x_i}(x_i - x_{i_w}) &\approx \frac{\delta(x_i + \Delta x_i - x_{i_w}) - \delta(x_i - \Delta x_i - x_{i_w})}{2\Delta x_i} \\ &\approx \frac{\delta[x_i - (x_{i_w} - \Delta x_i)] - \delta[x_i - (x_{i_w} + \Delta x_i)]}{2\Delta x_i} , \end{aligned} \tag{7.14}$$

assuming uniform spatial discretization in direction i. Thus, the spatial derivative is approximated as two Dirac delta functions with one acting at the cell immediately upgradient of the well and one acting at the cell immediately downgradient of the well. The Dirac delta functions are approximated as distributed loads over an cell, as described above. Note that one of these Dirac delta functions is negative; therefore, at early times, the adjoint state (and probability) is negative near the monitoring well, and the numerical code must allow negative values of the state variable (concentrations). The negative probability is an artifact of the dispersion model (7.1), which uses a constant dispersion coefficient (Gaussian plume). A constant dispersion coefficient is a reasonable approxima-

tion in the forward model when contamination has traveled a distance much greater than the length scale of the aquifer heterogeneity. Similarly, it is a reasonable approximation in the backward model at distances sufficiently far from the detection. In regions where probability is negative, a constant dispersion coefficient model is not necessarily valid; however, if these negative values persist only for early backward times, the model is reasonably valid at the locations and times of interest.

For a three-dimensional domain, the boxcar function in x_3-space in (7.7) and (7.10) must be included in the load term. It causes the load to act only over the well length. To model this numerically, the domain must be discretized so that the well length corresponds exactly to an integer number of cells in the vertical direction. Consider the load

$$\frac{\partial h}{\partial C} = c\frac{B_{x_3}(x_{3_{wt}} - x_{3_{wb}})}{(x_{3_{wt}} - x_{3_{wb}})} \,, \tag{7.15}$$

where c is a constant that represents the approximations for the other factors as described above. If this load is acting at cell k, then the top of cell k must be at elevation $x_{3_{wt}}$ and the bottom must be at $x_{3_{wb}}$. The total mass contributed by this load is c, so it can be approximated as a distributed load of $c/(x_{3_{wt}} - x_{3_{wb}})$ over cell k. Note that c already contains the approximation in the x_1 and x_2 directions, so the load is distributed over the entire volume of cell k.

Numerical Approximations for Linear Triangular Finite Elements

In finite element models, the domain is discretized into elements of specified shapes such as triangles (e.g. AQUIFEM-N [*Townley*, 1990]) or quadri-

laterals (e.g. FEMWATER [*Yeh and Ward*, 1980] and SUTRA [*Voss*, 1984]). In this section, we demonstrate the numerical approximations for the load terms for triangular finite elements, assuming concentration varies linearly across the element. We first show the approximations for a two-dimensional (x_1, x_2) domain with triangular elements, and then generalize the results to a three-dimensional domain with triangular prism elements.

We assume that the finite elements are triangular in x_1, x_2-space, as shown in Figure 7.2, and that the state variable varies linearly across the elements. The linear weighting functions are [*Segerlind*, 1984]

$$[N]^T = \begin{bmatrix} N_i \\ N_j \\ N_k \end{bmatrix} = \frac{1}{2A} \begin{bmatrix} a_i + b_i x_1 + c_i x_2 \\ a_j + b_j x_1 + c_j x_2 \\ a_k + b_k x_1 + c_k x_2 \end{bmatrix} , \tag{7.16}$$

where the superscript T denotes the vector transpose, A is the elemental area, N_i, N_j, and N_k are the weighting functions for nodes i, j, and k, respectively, the coefficients are defined as

$$\begin{aligned} a_i &= x_{1j}x_{2k} - x_{1k}x_{2j} \quad b_i = x_{2j} - x_{2k} \quad c_i = x_{1k} - x_{1j} , \\ a_j &= x_{1k}x_{2i} - x_{1i}x_{2k} \quad b_j = x_{2k} - x_{2i} \quad c_j = x_{1i} - x_{1k} , \\ a_k &= x_{1i}x_{2j} - x_{1j}x_{2i} \quad b_k = x_{2i} - x_{2j} \quad c_k = x_{1j} - x_{1i} , \end{aligned}$$

where x_{ml} is the x_m-coordinate of node l, and $a_i + a_j + a_k = 2A$. From this, we can see that $N_l = 1$ at node l and $N_l = 0$ at the other two nodes.

In the finite element method, each element has a stiffness matrix and

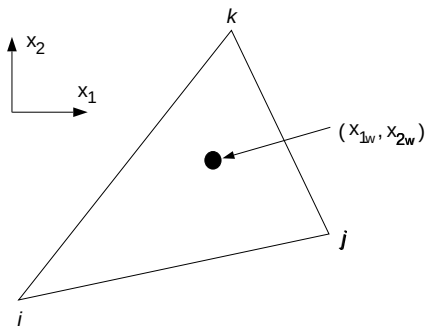

Figure 7.2: Two-dimensional finite element grid.

a force vector. For linear triangular elements, the element stiffness matrix is a 3×3 matrix (one row and one column for each node) whose values represent the material properties and shape properties of the element. The element force vector has length 3 (one entry for each node) whose values represent the loads applied to that element. The stiffness matrix for each element is combined to form a global stiffness matrix of size $N_n \times N_n$, where N_n is the number of nodes, and the element force vectors are combined to form a global force vector of length N_n.

The load term in (7.4) becomes part of the element force vector, $\left[f^{(e)}\right]$, for the element or elements at which the load is acting, where the superscript (e) denotes the element number. Using Galerkin's method, the entries in the element force vector are obtained from

$$\left[f^{(e)}\right] = \int_A \frac{\partial h}{\partial C}[N]^T \, dA \, , \tag{7.17}$$

where $[N]$ is the vector of weighting functions from (7.16) and $\partial h/\partial C$ is the load term containing Dirac delta functions in space and its spatial derivative.

The form of the element force vector depends on whether the load is acting on the interior of an element or on the boundary.

A load acting in the interior of an element is shown in Figure 7.2. For a point source, the load is represented by a Dirac delta function as $\partial h/\partial C = c\delta(x_1 - x_{1_w})\delta(x_2 - x_{2_w})$, where c is the magnitude of the point source. From (7.16) and (7.17), the element force vector for this load is

$$\begin{aligned}\left[f^{(e)}\right] &= c\int_A \delta(x_1 - x_{1_w})\delta(x_2 - x_{2_w}) \begin{bmatrix} N_i(x_1, x_2) \\ N_j(x_1, x_2) \\ N_k(x_1, x_2) \end{bmatrix} dA \\ &= c\begin{bmatrix} N_i(x_{1_w}, x_{2_w}) \\ N_j(x_{1_w}, x_{2_w}) \\ N_k(x_{1_w}, x_{2_w}) \end{bmatrix} . \end{aligned} \tag{7.18}$$

For a point source acting on the interior of an element, the entries of the element force vector are simply the weighting functions evaluated at the point, multiplied by the source magnitude, c.

For travel time probability, the load term (7.10) contains three terms. The first term is the product of Dirac delta functions and can be approximated as (7.18); the remaining terms contain the product of a Dirac delta function and the derivative of a Dirac delta function. Consider the term from (7.10) given by

$$\frac{\partial h}{\partial C} = a_L \frac{v_1}{|v|}\delta'_{x_1}(x_1 - x_{1_w})\delta(x_2 - x_{2_w})\delta(\tau) . \tag{7.19}$$

By substituting this expression into (7.17) and evaluating the integral, we obtain the element force vector for this term, given by (Appendix 7.B)

$$\left[f^{(e)}\right] = \frac{-a_L v_1}{2A|v|} \begin{bmatrix} b_i \\ b_j \\ b_k \end{bmatrix} \delta(\tau) \; . \tag{7.20}$$

By inspection, we see that the element force vector for the third term in (7.10) is

$$\left[f^{(e)}\right] = \frac{-a_L v_2}{2A|v|} \begin{bmatrix} c_i \\ c_j \\ c_k \end{bmatrix} \delta(\tau) \; . \tag{7.21}$$

The total element force vector for the load term representing travel time probability (7.10) is

$$\left[f^{(e)}\right] = \delta(\tau) \begin{bmatrix} N_i(x_{1_w}, x_{2_w}) \\ N_j(x_{1_w}, x_{2_w}) \\ N_k(x_{1_w}, x_{2_w}) \end{bmatrix} - \frac{a_L \delta(\tau)}{2A|v|} \left\{ v_1 \begin{bmatrix} b_i \\ b_j \\ b_k \end{bmatrix} + v_1 \begin{bmatrix} c_i \\ c_j \\ c_k \end{bmatrix} \right\} \tag{7.22}$$

Note that some of the components of the force vector may be negative, an artifact of the constant dispersion coefficient, as discussed above; therefore, the numerical code must allow negative values of the state variable (concentration). The Dirac delta function in time can be approximated using one of the methods described above.

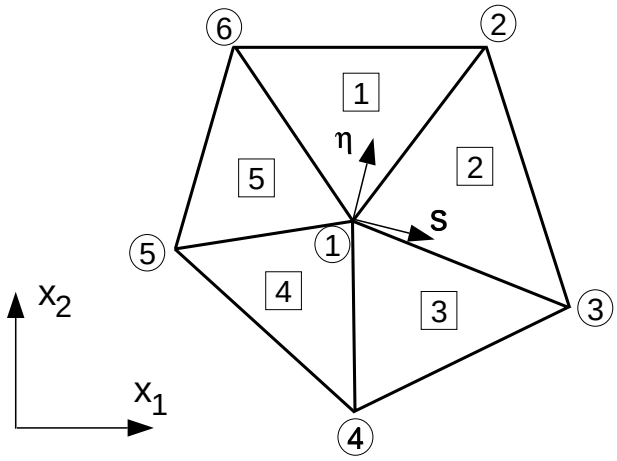

Figure 7.3: Two-dimensional finite element grid with a load at a node. Numbers surrounded by circles are node numbers; numbers surrounded by squares are element numbers. The groundwater flow direction is s, the direction perpendicular to flow is η, and the coordinates of node "1" are $(s, \eta) = (0, 0)$.

The element force vectors are different if the load is acting at a node as shown in Figure 7.3. For a point source, the load is represented by a Dirac delta function as $\partial h/\partial C = c\delta(x_1 - x_{1_w})\delta(x_2 - x_{2_w})$, where c is the magnitude of the point source. The load is acting on node "1", therefore it can be applied directly to the global force vector at the entry representing node "1". For the entry in the global force vector that represents node "1", the value is c.

For travel time probability at a monitoring well detection, the load term is (7.10). The first term in (7.10) is a point load, applied to the global force vector as described above. The remaining terms can be written in local streamline-based coordinates as

$$\frac{\partial h}{\partial C} = a_L \frac{v}{|v|} \delta_s'(s)\delta(\eta)\delta(\tau) \ , \tag{7.23}$$

where s is the direction of groundwater flow at the well, η is the direction perpendicular to groundwater flow, and the center of the well is at $(s, \eta) = (0, 0)$ (see Figure 7.3). In a linear triangular finite element model, velocity is constant within an element and discontinuous at element boundaries. Therefore, if the center of the well lies on a node (at node "1" in Figure 7.3), the groundwater velocity is undefined at the well. An approximate velocity can be calculated by areally-averaging the velocities of the adjacent elements (elements 1–5 in Figure 7.3). The direction s in Figure 7.3 represents the direction of this average flow.

Substituting (7.23) into (7.17) and integrating, we obtain (Appendix 7.B)

$$\left[f^{(2)}\right] = \frac{-a_L \delta(\tau)}{4Av} \begin{bmatrix} (b_i v_1 + c_i v_2) \\ (b_j v_1 + c_j v_2) \\ (b_k v_1 + c_k v_2) \end{bmatrix} \tag{7.24}$$

$$\left[f^{(5)}\right] = -\left[f^{(2)}\right] \tag{7.25}$$

$$\left[f^{(1)}\right] = \left[f^{(3)}\right] = \left[f^{(4)}\right] = 0 \; . \tag{7.26}$$

The appropriate velocity to use in these force vectors is the areally-averaged velocity described above.

For a three-dimensional domain, the boxcar function in x_3-space in (7.7) and (7.10) must be included in the load term. It causes the load to act only over the well length. To model this numerically, the domain must be discretized so that the well length corresponds exactly to an integer number of

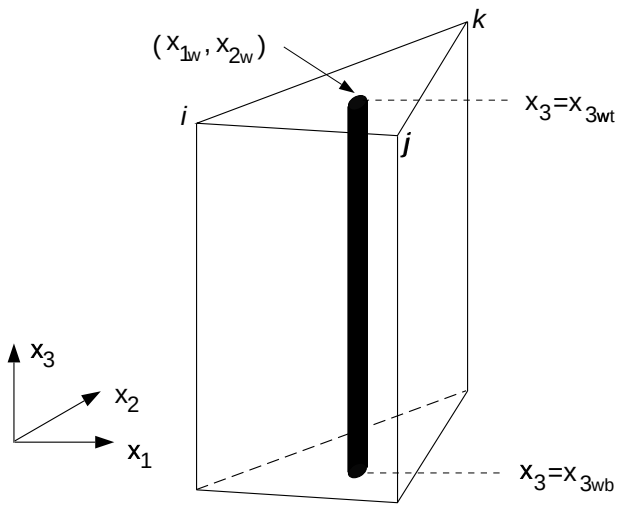

Figure 7.4: A three-dimensional finite element linear triangular prism element.

elements in the vertical direction. Consider the

$$\frac{\partial h}{\partial C} = c\frac{B_{x_3}(x_{3_{wt}} - x_{3_{wb}})}{(x_{3_{wt}} - x_{3_{wb}})}\,, \tag{7.27}$$

where c represents the approximations for the other factors as described above. If this load is acting at (x_{1_w}, x_{2_w}) and distributed over the well length, then the top of the element must be at elevation $x_{3_{wt}}$ and the bottom must be at $x_{3_{wb}}$ (See Figure 7.4). The contribution from this load is c. With linear elements, this distributed load can be approximated as point loads of strength $c/2$ at the top of the element at $(x_1, x_2, x_3) = (x_{1_w}, x_{2_w}, x_{3_{wt}})$ and at the bottom of the element at $(x_1, x_2, x_3) = (x_{1_w}, x_{2_w}, x_{3_{wb}})$. The element force vectors for these two point loads can be obtained through the method described above.

7.4 Numerical Implementation of the Backward Model using MODFLOW and MT3D

MODFLOW [*McDonald and Harbaugh*, 1988; *Harbaugh and McDonald*, 1996] and MT3D [*Zheng*, 1990; *Zheng and Wang*, 1999] are numerical codes commonly used to model groundwater flow and contaminant transport, respectively. MODFLOW creates an output file containing flow information that can be used to specify the flow field in MT3D. In this section, we present examples of numerical implementation of the backward probability model using these two codes. For all flow simulations, we used MODFLOW-96 [*Harbaugh and McDonald*, 1996]; and for all transport simulations, we used MT3DMS with the total variation diminishing (TVD) solver for advection and the generalized conjugate gradient solver (fully implicit) for the finite difference solution [*Zheng and Wang*, 1999]. With the TVD scheme, if a negative concentration is calculated, MT3DMS sets the concentration to zero. Some load terms in the backward model are approximated with negative loads, leading to negative probabilities (concentration) near the detection location. Since negative probabilities are necessary in the backward model, we commented out the statement in MT3DMS that sets negative concentrations to zero (in MT3DMS Release DoD_3.50.A, Line 380 of the function `cface.for`: `IF(CFACE.LT.0.) CFACE=0.0` [*Zheng and Wang*, 1999]).

We present both one- and two-dimensional simulations for a homogeneous, isotropic, confined aquifer of uniform thickness. In all cases presented here, we assume steady flow and we treat the adjoint load terms as initial conditions (Section 7.3.4). For the one-dimensional simulation, we use a monitoring

well detection; and for the two-dimensional simulation, we use a pumping well detection.

7.4.1 Simulations in One Dimension

For simple aquifer geometries, we can obtain analytical solutions to the adjoint equations. In this section, we present results of numerical simulations of location and travel time probabilities in a one-dimensional, homogeneous aquifer, and verify that the numerical results agree well with the analytical solutions. We consider only the case of a monitoring well detection.

Forward Model

The one-dimensional domain used in the simulations is a confined aquifer of length 600 m shown in Figure 7.5. The domain is discretized into 120 evenly-spaced cells ($\Delta x_1 = 5$ m). The problem is one-dimensional, but the code requires a width and thickness, so we use a uniform width of $\Delta x_2 = 1$ m and an aquifer thickness of $B = 1$ m. We use first-type boundary conditions for the flow model, with $h = 95$ m at $x = 2.5$ m and $h = 100$ m at $x = 597.5$ m. MODFLOW is a cell-centered finite difference model; therefore the heads are specified at the centers of the first and last cells. The aquifer bottom is at 65 m and the transmissivity is $T = 0.0001$ m^2/s. The aquifer properties are summarized in Table 7.1. The resulting head profile decreases linearly across the domain, and the velocity is $v_1 = -2.80 \times 10^{-6}$ m/s.

We used MT3DMS to run a forward contaminant transport simulation for a conservative chemical, subject to advection and dispersion only. The

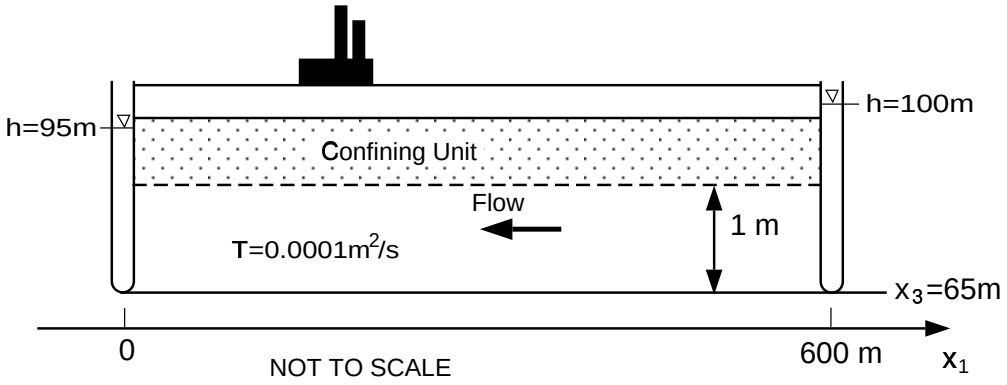

Figure 7.5: Aquifer geometry for numerical example.

Table 7.1: Aquifer properties for the one-dimensional model.

Parameter	Value
Length	600 m
Spatial discretization, Δx_1	5 m
Bottom elevation	65 m
Aquifer thickness, B	1 m
Transmissivity, T	0.0001 m^2/s

contamination is assumed to enter through an instantaneous point source at $x_{1_o} = 397.5$ m at $t = 0$. The source mass is $M = 300$ g per unit cross-sectional area of aquifer. The initial condition for this case is

$$C(x_1, 0) = \frac{M}{\theta}\delta(x_1 - x_{1_o}) \ , \tag{7.28}$$

where $\theta = 0.3$ is the porosity. The initial condition can be approximated as a distributed mass of strength $M/(\theta\Delta x_1)$ over the cell containing x_{1_o}, giving

$$C(x_1, 0) = \begin{cases} 200 \text{ g/m}^3 & \text{at the cell containing } x_{1_o} \\ 0 & \text{otherwise} \end{cases} \ . \tag{7.29}$$

We use a dispersivity, a_L, of 10 m, and $D = a_L|v|$. The boundary conditions are zero-gradient (second-type) at $x_1 = 0$ and no-flux (third-type) at $x_1 = 600$ m; however, MT3DMS approximates a third-type boundary condition as first-type (specified concentration), so the actual boundary condition is $C = 0$ at $x_1 = 597.5$ m (since MT3D is a cell-centered model, the concentration must be specified at the center of the last cell). The maximum allowable time step is calculated internally in MT3DMS; for these simulations, the time step was $\Delta t = 1.785 \times 10^6$ s over the entire simulation period. The transport model parameters are shown in Table 7.2. The plume after 800 days is shown in Figure 7.6. With the velocity of -2.80×10^{-6} m/s, the plume centroid travels almost 200 m in 800 days.

Table 7.2: Transport parameters for the one-dimensional model.

Parameter	Value
Source mass, M	300 g/m^2
Source location, x_{1_o}	397.5 m
Dispersivity, a_L	10 m
Porosity, θ	0.3
Time step, Δt	1.785×10^6 s

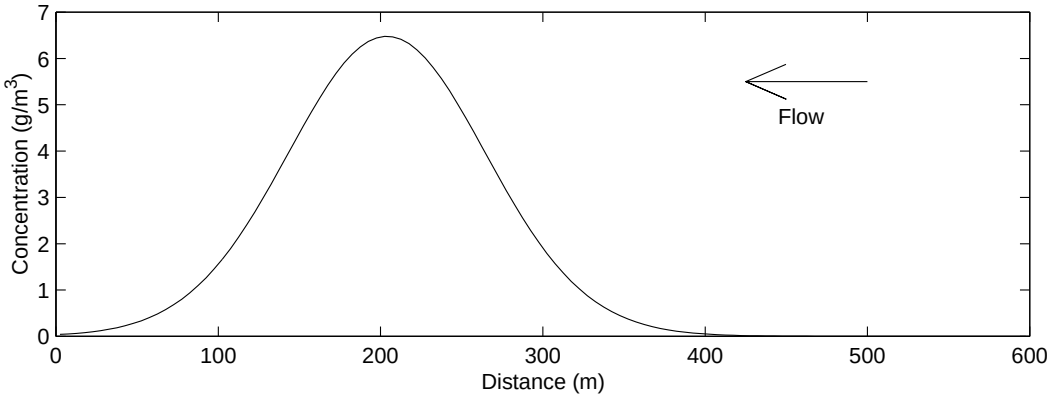

Figure 7.6: Concentration at $t = 800$ days for the one-dimensional simulation.

Backward Model

Suppose contamination is detected in a monitoring well at location $x_1 = 197.5$ m at time $t = 800$ days. We can run a simulation for backward location probability to determine the likely location of the detected contamination at some time in the past. We can also run a simulation for backward travel time probability to determine when the detected contamination was at a specific location.

MODFLOW creates a binary output file that contains all of the flow information needed by MT3D. After running a flow simulation to obtain the forward flow field, the binary file must be modified to include the reversed flow field. A Fortran code that reverses the flow field in this binary output file is described in Appendix A.

The boundary conditions for the backward model are modifications of the boundary conditions in the forward transport model. For this one-dimensional problem, the transport model boundary conditions are second-type at $x_1 = 0$ and third-type at $x_1 = 600$ m; therefore, the appropriate boundary conditions in the backward model are third-type at $x_1 = 0$ and second-type at $x_1 = 600$ m. Recall that with MT3DMS the third-type boundary condition must be approximated as a first-type boundary, so the actual backward boundary condition at $x_1 = 2.5$ m is $\psi^* = 0$.

Location Probability The appropriate governing equation for the backward location probability model is (7.4) with the load term in (7.7). Since this is a one-dimensional simulation in the x_1-direction only, the load term reduces to

$\partial h/\partial C = \delta(x_1 - x_{1_w})\delta(\tau)$. We treat this load as an initial condition with

$$\psi_x^*(x_1;0) = \frac{\delta(x_1 - x_{1_w})}{\theta} \ , \tag{7.30}$$

where ψ_x^* is adjoint state for location probability and $x_{1_w} = 197.5$ m. The initial condition is approximated as a distributed source over the cell containing $x_{1_w} = 197.5$ m. Since the spatial discretization is $\Delta x_1 = 5$ m, the initial condition is approximated as

$$\psi_x^*(x;0) = \begin{cases} 0.667 \text{ m}^{-1} & \text{at the cell containing } x_{1_w} \\ 0 & \text{otherwise} \end{cases} \ . \tag{7.31}$$

Using the resulting adjoint state in (7.8), we calculated the backward location probability at $\tau = 800$ days prior to detection, which is shown in Figure 7.7. The curve shows that the detected particle was most likely near $x_1 = 397.5$ m at $\tau = 800$ days prior to detection. The analytical solution for the infinite domain version of this problem is [*Neupauer and Wilson*, 2000b]

$$f_x(x_1;t) = \frac{1}{\sqrt{4\pi D\tau}} \exp\left\{-\frac{(x_1 - x_{1_w} + v\tau)^2}{4D\tau}\right\} \ , \tag{7.32}$$

and is also shown in Figure 7.7. The numerical solution matches well with the analytical solution. The minor differences are due to spatial discretization of the load (initial condition), with almost no contribution from the different boundary conditions between the analytical solution (infinite domain) and numerical model (finite domain).

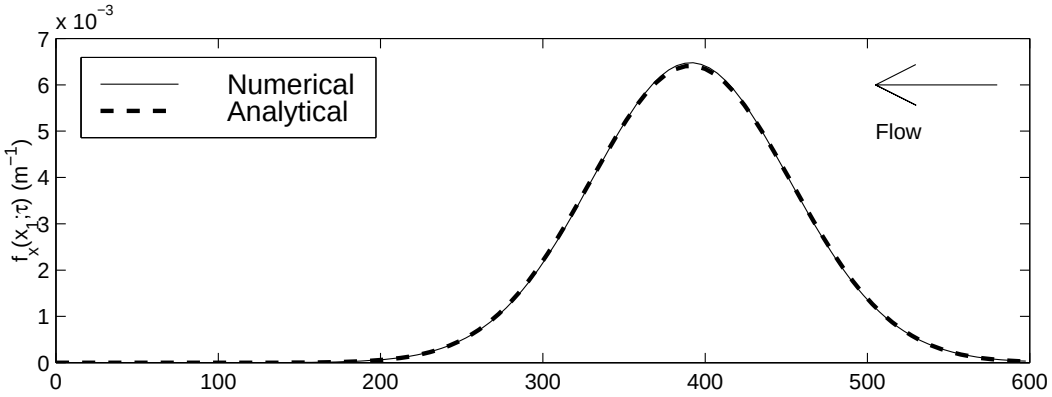

Figure 7.7: Backward location probability at $\tau = 800$ days prior to detection for the one-dimensional simulation.

Travel Time Probability The appropriate governing equation for the backward travel time probability model is (7.4) with the load term in (7.10). Since this is a one-dimensional simulation in the x_1-direction only, the load term reduces to $\partial h/\partial C = [\delta(x_1 - x_{1_w}) + (a_L v_1/(|v_1|)\delta'_{x_1}(x_1 - x_{1_w})]\delta(\tau)$. We treat this load as an initial condition with

$$\psi^*_\tau(0; x_1) = \frac{\delta(x_1 - x_{1_w})}{\theta} + \frac{a_L v_1}{|v_1|\theta}\delta'_{x_1}(x_1 - x_{1_w}) \,, \tag{7.33}$$

where ψ^*_τ is the adjoint state for travel time probability and $x_{1_w} = 197.5$ m. The first term in the initial condition is approximated as a distributed mass over the cell containing $x_{1_w} = 197.5$ m. The second term is approximated as the difference of two Dirac delta functions acting at the cells immediately upgradient and downgradient of the well. With a spatial discretization of $\Delta x_1 = 5$ m,

the initial condition is approximated as

$$f_\tau(0;x_1) = \begin{cases} 0.667 \text{ s}^{-1} & \text{at cells containing } x_{1_w} \text{ and } x_{1_w} + \Delta x_1 \\ -0.667 \text{ s}^{-1} & \text{at the cell containing } x_{1_w} - \Delta x_1 \\ 0 & \text{otherwise} \end{cases} , \quad (7.34)$$

since $v_1 < 0$, $a_L = 10$ m, and $\theta = 0.3$.

Using the resulting adjoint state in (7.12), we calculated the backward travel time probability from $x_1 = x_{1_o} = 397.5$ m to the detection location, shown in Figure 7.8. The curve shows that the detected particle was most likely at $x_{1_o} = 397.5$ m at $\tau \approx 740$ days prior to detection. The analytical solution for the infinite domain version this problem is [*Neupauer and Wilson*, 2000b]

$$f_\tau(\tau;x_1) = \frac{-v(x_1 - x_{1_w} - v\tau)}{4|v|\sqrt{\pi D\tau^3}} \exp\left\{-\frac{(x_1 - x_{1_w} + v\tau)^2}{4D\tau}\right\} , \quad (7.35)$$

and is also shown in Figure 7.8. The numerical solution matches well with the analytical solution.

7.4.2 Simulations in Two Dimensions

In this section, we present numerical results for location and travel time probabilities in a two-dimensional, homogeneous, isotropic aquifer. We present results for a pumping well detection in the interior of the model domain. The flow field is spatially non-uniform because of pumping.

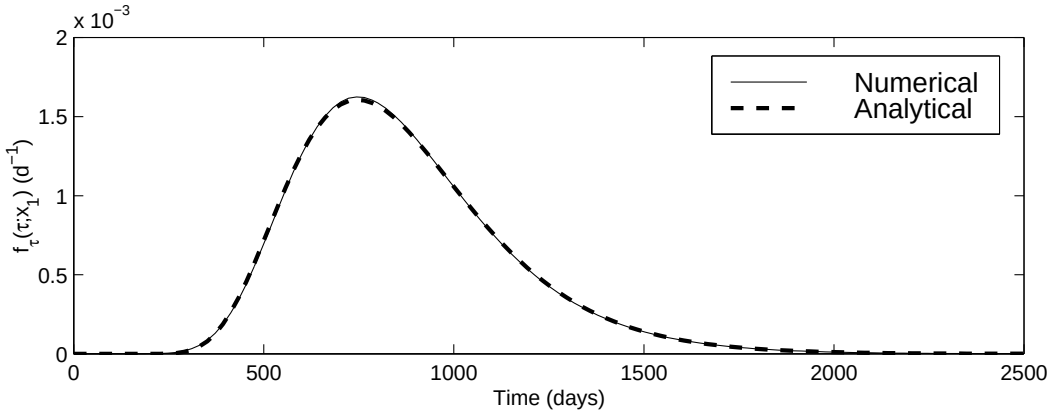

Figure 7.8: Backward travel time probability from $x_1 = 397.5$ m to the detection at $x_{1_w} = 197.5$ m for the one-dimensional simulation.

Forward Model

The two-dimensional domain used in the simulations is a confined aquifer of length 600 m and width 350 m shown in Figure 7.9. The domain is discretized into 5 m $\times$ 5 m cells ($\Delta x_1 = \Delta x_2 = 5$ m). The problem is two-dimensional, but the code requires a thickness, so we use a uniform aquifer thickness of $B = 1$ m. For the flow model, we use first-type boundary conditions on the west and east sides, with $h = 95$ m at $x_1 = 2.5$ m and $h = 100$ m at $x_1 = 597.5$ m; and we use no-flow boundaries on the north and south sides. MODFLOW is a cell-centered model; therefore the heads are specified at the cell centers. A pumping well is located at $(x_{1_w}, x_{2_w}) = (197.5 \text{ m}, 177.5 \text{ m})$, and pumps at a rate of $Q = 1 \times 10^{-4}$ m^3/s. The aquifer bottom is at 65 m and the transmissivity is $T = 0.0001$ m^2/s. The aquifer properties are summarized in Table 7.3. The resulting head profile is shown in Figure 7.10.

We used MT3DMS to run a forward contaminant transport simulation for a conservative chemical, subject to advection and dispersion only. The

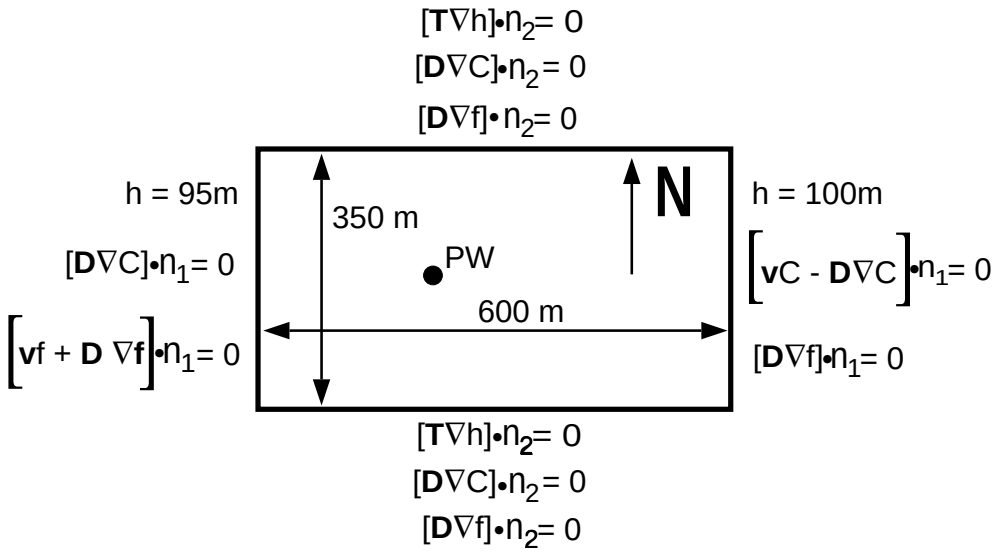

Figure 7.9: Aquifer geometry and boundary conditions for the two-dimensional numerical example. The filled circle denotes the pumping well (PW) location.

Table 7.3: Aquifer properties for the two-dimensional model.

Parameter	Value
Length	600 m
Width	350 m
Spatial discretization, Δx_1	5 m
Spatial discretization, Δx_2	5 m
Bottom elevation	65 m
Aquifer thickness, B	1 m
Transmissivity, T	0.0001 m^2/s
Well location, (x_{1_w}, x_{2_w})	(197.5 m, 177.5 m)
Pumping rate, Q	1×10^{-4} m^3/s

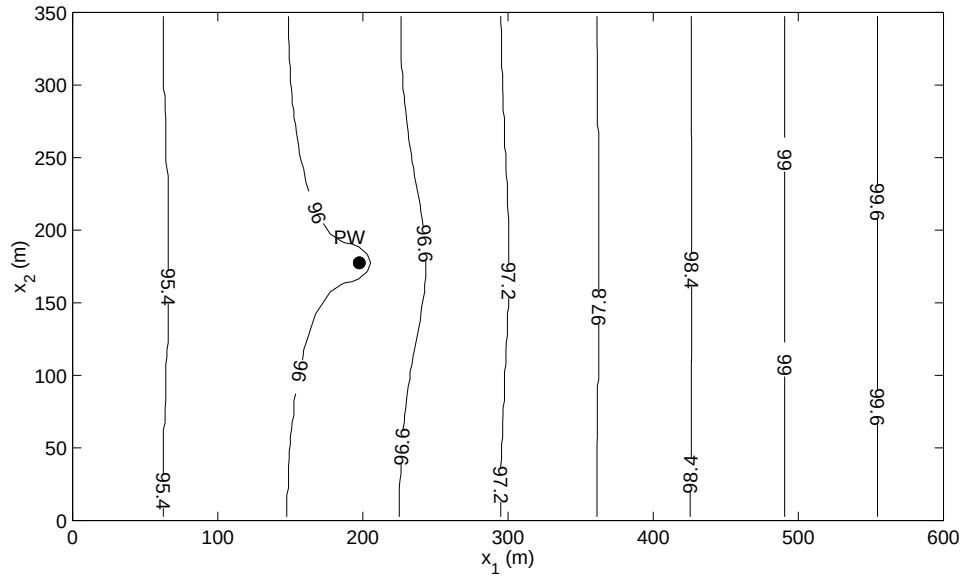

Figure 7.10: Head profile for the two-dimensional simulation (units are m). The filled circle denotes the pumping well (PW) location.

contamination was assumed to enter through an instantaneous point source at $(x_{1_o}, x_{2_o}) = (397.5 \text{ m}, 177.5 \text{ m})$ at $t = 0$. The source mass was $M = 300$ g per unit thickness of aquifer. The initial condition for this case is

$$C(x_1, x_2, 0) = \frac{M}{\theta}\delta(x_1 - x_{1_o})\delta(x_2 - x_{2_o}) \,, \tag{7.36}$$

where $\theta = 0.3$ is the porosity. The initial condition can be approximated as a distributed mass of strength $M/(\theta\Delta x_1 \Delta x_2)$ over the cell containing (x_{1_o}, x_{2_o}), giving

$$C(x_1, x_2, 0) = \begin{cases} 40 \text{ g/m}^3 & \text{at the cell containing } (x_{1_w}, x_{2_w}) \\ 0 & \text{otherwise} \end{cases} \,. \tag{7.37}$$

Table 7.4: Transport parameters for the two-dimensional model.

Parameter	Value
Source mass, M	300 g/m
Source location, (x_{1_o}, x_{2_o})	(397.5 m, 177.5 m)
Longitudinal dispersivity, a_L	10 m
Transverse dispersivity, a_T	2 m
Porosity, θ	0.3
Time step, Δt	1.3899×10^5 s

We used longitudinal and transverse dispersivities of $a_L = 10$ m and $a_T = 2$ m, and D_{ij} defined in (7.11). The boundary conditions were no-flux (third-type) at the eastern boundary and zero-gradient (second-type) at the other three boundaries. The boundary conditions are shown in Figure 7.9. MT3DMS approximates a third-type boundary condition as a first-type (specified concentration), so the actual boundary condition at the eastern boundary is $C(x_1 = 597.5 \text{ m}, x_2, t) = 0$. The time step (calculated internally by MT3DMS) was $\Delta t = 1.3899 \times 10^5$ s. The transport model parameters are shown in Table 7.4. The plume after 800 days is shown in Figure 7.11. The plume centroid travels almost 200 m in 800 days, and the plume is captured by the well.

Backward Model

Suppose contamination is detected at the pumping well at time $t =$ 800 days. We can run a simulation to obtain the backward location probability describing the likely location of the detected contamination at some time in the past. We can also run a simulation for backward travel time probability to

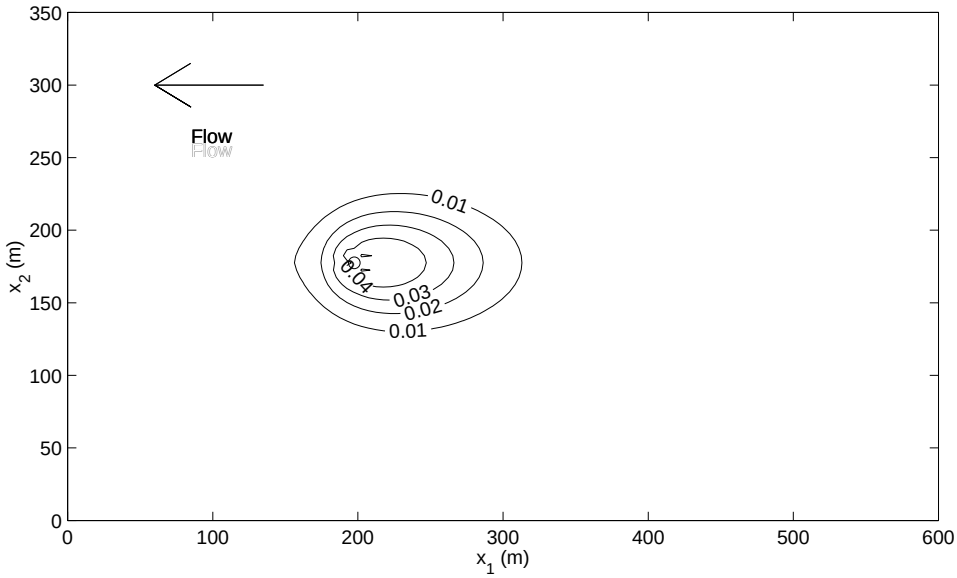

Figure 7.11: Concentration at $t = 800$ days for the two-dimensional simulation (units are g/m^3).

determine when the detected contamination was at a specific location.

The MODFLOW binary output file containing all of the flow information from the forward model above was modified to contain the reversed flow field. The boundary conditions from the forward model were modified for the backward simulations. For this two-dimensional problem, the forward model boundary conditions are third-type at the eastern boundary and second-type at all other boundaries (see Figure 7.9). The third-type boundary in the forward model becomes a second type boundary in the backward model, and vice versa. However, since the northern and southern boundaries are no-flow boundaries (i.e., $v_2 = 0$ at these boundaries), the third-type boundary reduces to a second-type boundary. Because MT3DMS approximates a third-type boundary as a first-type boundary, the appropriate boundary condition for the western

boundary in the backward model is $\psi^* = 0$ at $x_1 = 2.5$ m.

Location Probability The appropriate governing equation for the backward location probability model is (7.4) with the load term in (7.7). Since this is a two-dimensional simulation in the x_1- and x_2-directions only, the load term reduces to $\partial h/\partial C = \delta(x_1 - x_{1_w})\delta(x_2 - x_{2_w})\delta(\tau)$. We treat this load as an initial condition with

$$\psi_x^*(x_1, x_2; 0) = \frac{\delta(x_1 - x_{1_w})\delta(x_2 - x_{2_w})}{\theta} \ , \tag{7.38}$$

where ψ_x^* is the adjoint state for location probability and the pumping well location is $(x_{1_w}, x_{2_w}) = (197.5 \text{ m}, 177.5 \text{ m})$. The initial condition is approximated as a distributed source over the cell containing the pumping well. Since the spatial discretization is $\Delta x_1 = \Delta x_2 = 5$ m, the initial condition is approximated as

$$\psi_x^*(x_1, x_2; 0) = \begin{cases} 0.133 \text{ m}^{-1} & \text{at the cell containing } (x_{1_w}, x_{2_w}) \\ 0 & \text{otherwise} \end{cases} \ . \tag{7.39}$$

Using the resulting adjoint state in (7.8), we calculated the backward location probability at $\tau = 800$ days prior to detection at the pumping well, shown in Figure 7.12. The plot shows that the detected particle was most likely near $(x_1, x_2) \approx (437.5 \text{ m}, 177.5 \text{ m})$ at $\tau = 800$ days prior to detection.

Travel Time Probability For travel time probability with a pumping well detection, the governing equation is equivalent to the governing equation for

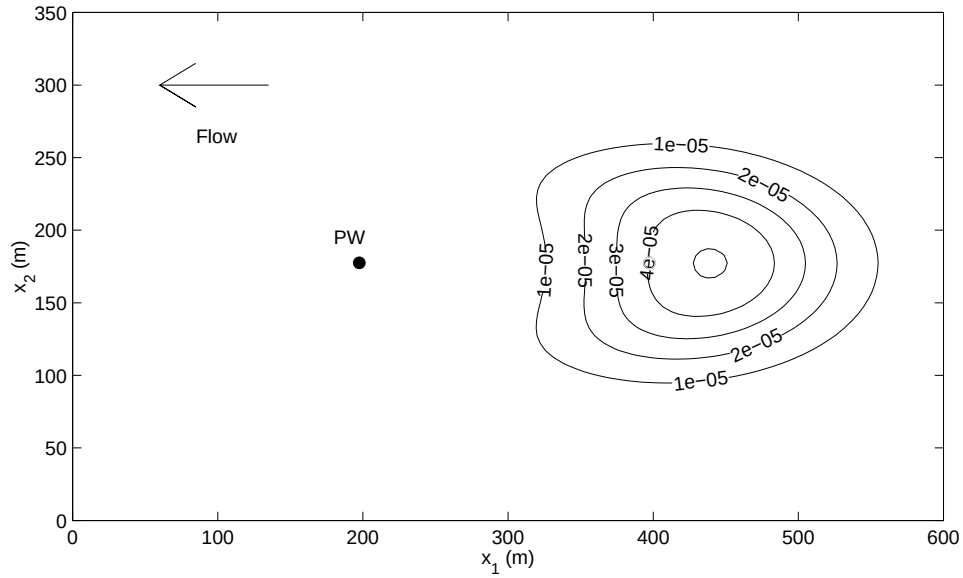

Figure 7.12: Backward location probability at $\tau = 800$ days prior to detection for the two-dimensional simulation (units are m^{-2}).

location probability; therefore $\psi_\tau^* = \psi_x^*$, where ψ_τ^* is the adjoint state for travel time probability. Using $\psi_\tau^* = \psi_x^*$ in (7.12), we calculated the backward travel time probability to the pumping well from from $(x_{1_o}, x_{2_o}) = (397.5\ \mathrm{m}, 177.5\ \mathrm{m})$, which is shown in Figure 7.13. The curve shows that the detected particle was most likely at the source at $\tau \approx 600$ days prior to detection at the pumping well. The area under the travel time probability distribution shows the probability that the detected particle was ever at the location of interest. The area under the curve in Figure 7.13 is 0.04, indicating a 4% probability that the detected particle was ever at $(x_{1_o}, x_{2_o}) = (397.5\ \mathrm{m}, 177.5\ \mathrm{m})$.

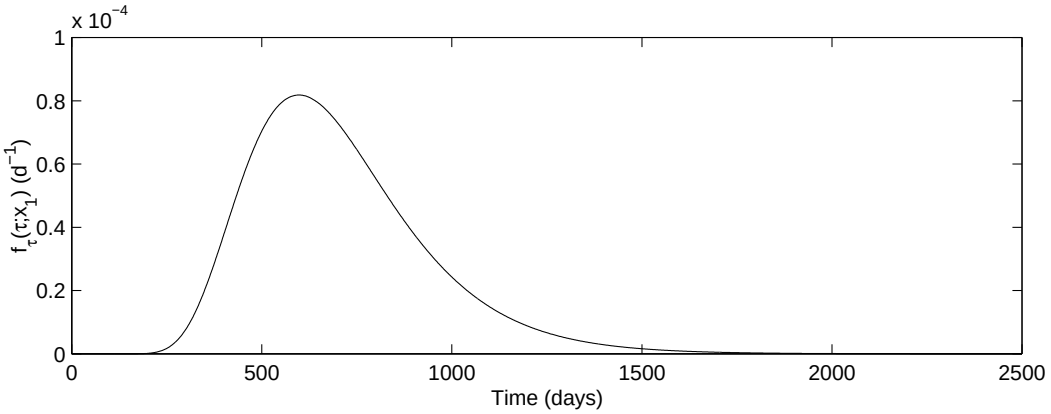

Figure 7.13: Backward travel time probability from the source area to the pumping well for the two-dimensional simulation.

7.5 Conclusions

The governing equation for the backward probability model is similar to the governing equation of contaminant transport; therefore, any numerical code that can be used to model contaminant transport should be capable of modeling backward location and travel time probabilities. Some adjustments must be made in the numerical implementation to account for the differences between the forward and backward models. The main differences are that the flow field is reversed, the boundary conditions are modified, and the backward model contains a new load term. The load term is an instantaneous source of probability, representing the sampling location and time. The load term acts at a point or line in space, and contains one or more Dirac delta functions, the derivative of a Dirac delta function, or a boxcar function.

We discussed the numerical approximations of the load terms for cell-centered finite difference models and finite element models with linear triangular and prism elements. The procedure can be extended to node-centered finite

difference models and to finite element models with other types of elements.

We used MODFLOW-96 and MT3DMS to illustrate the numerical implementation approach. Using these codes with a one-dimensional domain, we modeled location and travel time probability for a monitoring well detection. The results matched well with analytical solutions for the same problem. We also used these codes to model location and travel time probability in a two-dimensional domain with a pumping well detection.

Acknowledgments

This research was supported in part by the Geophysical Research Center at New Mexico Tech and in part by the Environmental Protection Agency's STAR Fellowship program under Fellowship No. U-915324-01-0. This work has not been subjected to the EPA's peer and administrative review and therefore may not necessarily reflect the views of the Agency and no official endorsement should be inferred. William D. Stone provided input on generalized functions.

References

Bagtzoglou, A.C., D.E. Dougherty, and A.F.B. Thompson, Application of particle methods to reliable identification of groundwater pollution sources, *Water Resources Management*, 6, 15–23, 1992.

Chin, D.A. and P.V.K. Chittaluru, Risk management in wellhead protection, *J. Water Resour. Plan. Manage.*, 120(3), 294–315. 1994.

Dagan, G., Stochastic modeling of groundwater flow by unconditional and conditional probabilities, 2, The solute transport, *Water Resour. Res.*, 18(4), 835–848, 1982.

Dagan, G., Theory of solute transport by groundwater, *Ann. Rev. Fluid Mech.*, 19, 183–215, 1987.

Dagan, G., *Flow and Transport in Porous Formations*, Springer-Verlag, New York, 1989.

Dagan, G., and V. Nguyen, A comparison of travel time and concentration approaches to modeling transport by groundwater, *Journal of Contaminant Hydrology*, 4, 79–91, 1989.

Harbaugh A.W. and M.G. McDonald, *User's Documentation for MODFLOW-96, an update to the U.S. Geological Survey Modular Finite-Difference Ground-Water Flow Model*, U.S. Geological Survey, Open-File Report 96-485, 1996.

Jury, W.A., Simulation of solute transport using a transfer function model, *Water Resour. Res.*, 18(2), 363–368, 1982.

Jury, W.A., G. Sposito, and R.E. White, A transfer function model of solute transport through soil, 1, Fundamental concepts, *Water Resour. Res.*, 22(2), 243–247, 1986.

Jury, W.A. and K. Roth, *Transfer Functions and Solute Movement through Soil: Theory and Applications*, Birkhauser Verlag, Boston, 1990.

Liu, J., *Travel time and location probabilities for groundwater contaminant sources*, Master's thesis, New Mexico Institute of Mining and Technology, Socorro, 1995.

McDonald, M.G. and A.W. Harbaugh, *A Modular Three-Dimensional Finite-Difference Groundwater Flow Model*, U.S. Geological Survey Techniques of Water-Resources Investigations, Book 6, Chapter A1, 1988.

Neupauer, R.M. and J.L. Wilson, Adjoint method for obtaining backward-in-time location and travel time probabilities of a conservative groundwater contaminant, *Water Resour. Res.*, 35(11), 3389–3398, 1999.

Neupauer, R.M. and J.L. Wilson, Adjoint-derived location and travel time probabilities in a multi-dimensional groundwater flow system, *Water Resour. Res.*, in press, 2000a.

Neupauer, R.M. and J.L. Wilson, Backward location and travel time probabilities for contamination in a one-dimensional infinite aquifer, submitted to *J. Contam. Hydrol.*, 2000b.

Parker, J.C. and M. Th. van Genuchten, Flux-averaged and volume-averaged concentrations in continuum approaches to solute transport, *Water Resour. Res.*, 20(7), 866–872, 1984.

Rubin, Y. and G. Dagan, Conditional estimation of solute travel time in heterogeneous formations: impact of transmissivity measurements, *Water Resour. Res.*, 28(4), 1033–1040, 1992.

Segerlind, L.J., *Applied Finite Element Analysis*, 2nd ed., John Wiley and Sons, New York, 1984.

Shapiro, A.M. and V.D. Cvetkovic, Stochastic analysis of solute arrival time in heterogeneous porous media, *Water Resour. Res.*, 24(10), 1711–1718, 1988.

Sposito, G. and D.A. Barry, On the Dagan model of solute transport in ground water: Foundational aspects, *Water Resour. Res.*, 23(10), 1867–1875, 1987.

Townley, L.R., *AQUIFEM-N: A Multi-layer Finite Element Aquifer Flow Model, User's Manual and Description*, CSIRO Division of Water Resources, Perth, Western Australia, 1990.

Uffink, G.J.M., Application of Kolmogorov's backward equation in random walk simulations of groundwater contaminant transport, in *Contaminant Transport in Groundwater*, H.E. Kobus and W. Kinzelbach, editors, pp. 283–289, A.A. Balkema, Brookfield, Vt., 1989.

Voss, C.I., *A Finite-element Simulation Model for Saturated-unsaturated, Fluid-density-dependent Groundwater-water Flow with Energy Transport or Chemically-reactive Single-species Solute Transport*, U.S. Geological Survey Water-Resources Investigations Report 84-4369, 1984.

Wilson, J.L. and J. Liu, Backward tracking to find the source of pollution, in

Waste-management: From Risk to Remediation, edited by R. Bhada *et al.*, ECM Press, Albuquerque, NM, 181–199, 1994.

Wilson, J.L. and J. Liu, Field Validation of the Backward-in-time Advection Dispersion Theory. *Proceedings of the 1996 HSRC/WERC Joint Conf. on the Environment*, Great Plains-Rocky Mountain Hazardous Substance Center, Manhattan, Kansas, http://www.engg.ksu.edu/HSRC/ 96Proceed/wilson.html, 1997.

Yeh, G.T. and D.S. Ward, *FEMWATER: A Finite-element Model of Water Flow through Saturated-unsaturated Porous Media*, Environmental Sciences Division, Oak Ridge National Laboratory, 1980.

Zheng, C., *MT3D: A Modular Three-Dimensional Transport Model for Simulation of Advection, Dispersion and Chemical Reactions of Contaminants in Groundwater Systems*, Report to the U.S. Environmental Protection Agency, Ada, Oklahoma, 170 pp., 1990.

Zheng, C. and P.P. Wang, *MT3DMS: Documentation and User's Guide*, U.S. Army Corps of Engineers, Washington, DC, November, 1999.

7.A Form of the Adjoint Equation

The adjoint of the advection-dispersion equation (ADE) can be solved numerically to obtain backward location and travel time probabilities. The numerical code chosen for the numerical simulations dictates the necessary form of the adjoint equation. Some numerical codes solve the ADE in the form shown in (7.1). Other codes solve the ADE in a modified form that can be obtained by expanding the advection term as

$$-\frac{\partial}{\partial x_i}\left(q_i C\right) = -q_i \frac{\partial C}{\partial x_i} - C\frac{\partial q_i}{\partial x_i}\ , \tag{7.40}$$

where $q_i = \theta v_i$. The new form of the ADE is

$$\frac{\partial}{\partial t}\left(\theta C\right) = \frac{\partial}{\partial x_i}\left(\theta D_{ij}\frac{\partial C}{\partial x_j}\right) - q_i\frac{\partial C}{\partial x_i} + q_I(C_I - C) - q_O C\ . \tag{7.41}$$

The adjoint equation shown in (7.4) is consistent with the ADE in (7.1) and should be used if the numerical code solves that form of the ADE. If the code solves the form of the ADE in (7.41), the adjoint equation in (7.4) must be modified using the velocity expansion above, resulting in

$$\frac{\partial}{\partial \tau}\left(\theta \psi^*\right) = \frac{\partial}{\partial x_i}\left(\theta D_{ij}\frac{\partial \psi^*}{\partial x_j}\right) + q_i\frac{\partial \psi^*}{\partial x_i} + \frac{\partial h}{\partial C}\ , \tag{7.42}$$

where we used the continuity equation for steady flow ($\partial q_i/\partial x_i = q_I - q_O$). This form of the adjoint equation is consistent with the ADE in (7.41). The main difference between (7.4) and (7.42) are the source and sink terms. The source term (containing q_I) from (7.1) becomes a sink term in (7.4), and the

sink term (containing q_O) in (7.1) does not appear in (7.4). In contrast, the source and sink terms from (7.41) do not appear in (7.42).

7.B Derivation of Element Force Vectors

We derive the element force vectors for the load term for travel time probability. The element force vector depends on whether the load acts on the interior of an element or at node. We treat each case separately.

7.B.1 Load on the Interior of an Element

Consider the load term given by (7.19) for a load acting on the interior of an element. From (7.17), the element force vector for this term is given by

$$\left[f^{(e)}\right] = a_L \delta(\tau) \frac{v_1}{|v|} \int_A \delta'_{x_1}(x_1 - x_{1_w}) \delta(x_2 - x_{2_w}) \begin{bmatrix} N_i(x_1, x_2) \\ N_j(x_1, x_2) \\ N_k(x_1, x_2) \end{bmatrix} dA \; . \quad (7.43)$$

Considering only the N_i entry, separating the integral into x_1 and x_2 components, and substituting (7.16) for N_i, we replace the previous equation with

$$\begin{aligned} f_i^{(e)} \;\; = \;\; & \frac{a_L v_1 \delta(\tau)}{2A|v|} \int_{x_1} \delta'_{x_1}(x_1 - x_{1_w}) \cdot \\ & \left[\int_{x_2} \delta(x_2 - x_{2_w}) \left(a_i + b_i x_1 + c_i x_2\right) dx_2 \right] dx_1 \; . \end{aligned} \quad (7.44)$$

Evaluating the integral over x_2 results in

$$f_i^{(e)} = \frac{a_L v_1 \delta(\tau)}{2A|v|} \int_{x_1} \delta'_{x_1}(x_1 - x_{1_w}) \left[a_i + b_i x_1 + c_i x_{2_w}\right] dx_1 \; . \quad (7.45)$$

To evaluate the integral over x_1, we use integration by parts with $u = a_i + b_i x_1 + c_i x_{2_w}$ and $dw = \delta'(x_1 - x_{1_w}) dx_1$, so that the integral in (7.45) is defined

as $\int_{x_1} u dw$. By definition,

$$\int_{x_1} u dw = uw|_{\text{limits}} - \int_{x_1} w du \ . \tag{7.46}$$

With u and dw defined as above, we have $w = \delta(x_1 - x_{1_w})$ and $du = b_i dx_1$; therefore (7.45) becomes

$$f_i^{(e)} = \frac{a_L v_1 \delta(\tau)}{2A|v|} \left[(a_i + b_i x_1 + c_i x_{2_w}) \delta(x_1 - x_{1_w}) \Big|_{\text{limits}} - b_i \int_{x_1} \delta(x_1 - x_{1_w}) dx_1 \right] \ . \tag{7.47}$$

Since x_{1_w} is on the interior of an element and integration is over the element, $\delta(x_1 - x_{1_w}) = 0$ at the limits integration and the first term in the square brackets vanishes. Evaluating the integral in the second term over x_1 produces the final result

$$f_i^{(e)} = \frac{-a_L v_1 \delta(\tau)}{2A|v|} b_i \ . \tag{7.48}$$

Following the same approach for the N_j and N_k entries results in the final form of the element force vector shown in (7.20).

7.B.2 Load at a Node

Consider the load term given by (7.23) for a load acting on the interior of an element. From (7.17), the element force vector for this term is given by

$$\left[f^{(e)}\right] = \frac{a_L v \delta(\tau)}{|v|} \int_A \delta'_s(s)\delta_\eta \begin{bmatrix} N_i(s,\eta) \\ N_j(s,\eta) \\ N_k(s,\eta) \end{bmatrix} dA \, . \tag{7.49}$$

Since this expression is written in the (s,η) coordinate system, the weighting functions, $[N]$, must also be written in this coordinate system. For the configuration shown in Figure 7.3, the relationship between (x_1, x_2)-space and (s,η)-space is

$$x_1 = x_{1_w} + \frac{v_1}{|v|}s - \frac{v_2}{|v|}\eta \tag{7.50}$$

$$x_2 = x_{2_w} + \frac{v_2}{|v|}s + \frac{v_1}{|v|}\eta \, , \tag{7.51}$$

where $(x_1, x_2) = (x_{1_w}, x_{2_w})$ is the well location (coordinates for the node at which the load is applied) in x_1, x_2-space and $(s,\eta) = (0,0)$ is the well location in s,η-space.

Substituting these expressions for x_1 and x_2 in $[N]$ gives

$$\begin{bmatrix} N_i(s,\eta) \\ N_j(s,\eta) \\ N_k(s,\eta) \end{bmatrix} = \frac{1}{2A|v|} \begin{bmatrix} 2A|v| + (b_i v_1 + c_i v_2)s - (b_i v_2 - c_i v_1)\eta \\ (b_j v_1 + c_j v_2)s - (b_j v_2 - c_j v_1)\eta \\ (b_k v_1 + c_k v_2)s - (b_k v_2 - c_k v_1)\eta \end{bmatrix} , \tag{7.52}$$

where we have used the fact the $N_i = 1$ at node i, and $N_j = N_k = 0$ at node i, and node i is at $(s, \eta) = (0, 0)$. Considering only the N_i entry of (7.49), separating the integral into s and η components, and substituting the first row of (7.52) for N_i, the i^{th} entry in the element force vector is

$$f_i^{(e)} = \frac{a_L \delta(\tau)}{2Av} \int_s \delta_s'(s) \left\{ \int_\eta \delta(\eta) \left[2A|v| + (b_i v_1 + c_i v_2)s - (b_i v_2 - c_i v_1)\eta \right] d\eta \right\} ds \, . \tag{7.53}$$

Evaluating the integral over η results in

$$f_i^{(e)} = \frac{a_L \delta(\tau)}{2Av} \int_s \delta_s'(s) \left[2A|v| + (b_i v_1 + c_i v_2)s \right] ds \, . \tag{7.54}$$

We can define $\delta_s'(s)$ as a limit, given by

$$\delta_s'(s) = \lim_{\Delta s \to 0} \frac{\delta(s + \Delta s) - \delta(s - \Delta s)}{2\Delta s} \, . \tag{7.55}$$

Substituting this limit into (7.54), we obtain

$$f_i^{(e)} = \lim_{\Delta s \to 0} \frac{a_L \delta(\tau)}{4Av\Delta s} \int_s \left(\delta(s+\Delta s) - \delta(s-\Delta s) \right) \left[2A|v| + (b_i v_1 + c_i v_2)s \right] ds \, . \tag{7.56}$$

The function $\delta(s + \Delta s)$ is non-zero only in element "5", and function $\delta(s - \Delta s)$ is non-zero only in element "2"; therefore $f_i^{(e)} = 0$ for $e = 1, 3$, and 4.

Evaluating the integral in (7.56) for element "5" and taking the limit

on the second term yields

$$f_i^{(5)} = \frac{a_L \delta(\tau)}{4Av} \left(b_i v_1 + c_i v_2 - \lim_{\Delta s \to 0} \frac{2A|v|}{\Delta s} \right) \tag{7.57}$$

Following the same procedure on the j^{th} and k^{th} entries, we obtain

$$\left[f^{(5)} \right] = \frac{a_L \delta(\tau)}{4Av} \left\{ \begin{bmatrix} b_i v_1 + c_i v_2 \\ b_j v_1 + c_j v_2 \\ b_k v_1 + c_k v_2 \end{bmatrix} + \lim_{\Delta s \to 0} \frac{2A|v|}{\Delta s} \begin{bmatrix} 1 \\ 0 \\ 0 \end{bmatrix} \right\}, \tag{7.58}$$

where i corresponds to node "1", j to node "6", and k to node "7". Evaluating the integral in (7.56) for element "2" and taking the limit, we obtain

$$\left[f^{(2)} \right] = \frac{-a_L \delta(\tau)}{4Av} \left\{ \begin{bmatrix} b_i v_1 + c_i v_2 \\ b_j v_1 + c_j v_2 \\ b_k v_1 + c_k v_2 \end{bmatrix} + \lim_{\Delta s \to 0} \frac{2A|v|}{\Delta s} \begin{bmatrix} 1 \\ 0 \\ 0 \end{bmatrix} \right\}, \tag{7.59}$$

where i corresponds to node "1", j to node "3", and k to node "2". The terms containing the limit as $\Delta s \to 0$ are both acting at node "1", and are equal in magnitude with opposite signs; therefore, they cancel and the element force vectors reduce to those shown in (7.24)–(7.26).

CHAPTER 8

DEVELOPMENT OF THE BACKWARD PROBABILITY MODEL USING MULTIPLE DETECTIONS OF CONTAMINATION

Abstract

Backward location and travel time probabilities can be used to determine the former location of contamination in an aquifer. For a contaminant parcel that was detected in an aquifer, the backward location probability describes its position at some time prior to sampling and the backward travel time probability describes the amount of time required for it to travel to the sampling location from some upgradient position. The backward probability model has been developed for a single detection of contamination [e.g., *Wilson and Liu*, 1994; *Neupauer and Wilson*, 1999]. In practical situations contamination is sampled at multiple locations and times, and these additional data provide more information that can be used to characterize the prior position of contamination. We present an approach for incorporating multiple detections of contamination into the backward probability model. The additional information available from multiple detections reduces the variances for the location and travel time probability distributions and improves the characterization of the contamination source.

8.1 Introduction

When contamination is detected in an aquifer, the source of contamination is often unknown. To remediate the aquifer or to assign responsibility,

we might need to identify the source of contamination or the time of release of contamination from the source. In conventional contaminant transport modeling, the source of contamination is known or assumed to be known, and the future positions of the contaminant plume are simulated. If the source of contamination is unknown, this conventional transport modeling approach can be cumbersome to use. A more efficient approach for characterizing sources of groundwater contamination is backward modeling [*Wilson and Liu*, 1994, 1997; *Neupauer and Wilson*, 1999, 2000a].

Backward modeling is based on backward location and travel time probabilities. The results of a backward model show the probability of the former position of the contamination (location probability) or the probability of the contaminant's travel time from some upgradient location to the sampling location (travel time probability). Not only can the backward probability model be used to improve characterization of known sources of groundwater contamination or to identify previously unknown contamination sources, but it can also be used to delineate capture zones.

Backward location and travel time probability models have been developed for a single detection of contamination. By reversing the flow field in a random walk method, *Bagtzoglou et al.* [1992] obtained backward location probabilities that were used for identifying sources of contamination. *Uffink* [1989] and *Chin and Chittaluru* [1994] used a similar random walk approach to delineate capture zones around pumping wells. *Wilson and Liu* [1994, 1997] used a heuristic method to obtain a backward probabilistic continuum model from the forward advection-dispersion equation. The approach was validated using data from a field-scale tracer experiment at the Borden site [*Wilson and*

Liu, 1997]; however, no formal justification was given for the model. *Neupauer and Wilson* [1999, 2000a] showed that backward probabilities are related to adjoint states of concentration, and they presented a formal framework for obtaining the governing equation of the backward probability model using adjoint theory. The backward model for reactive transport (first-order decay, and linear equilibrium and non-equilibrium sorption) and non-uniform and transient flow has been developed heuristically by *Liu* [1995] and formally in Chapters 5 and 6 using adjoint theory.

In practical situations, multiple samples of contamination will be taken. For example, in determining the extent of a plume, samples will be taken at many locations in space. Also, once a well is in place, it will be sampled periodically over time. Thus we will have multiple detections of contamination in space and time. This additional information should improve the characterization of the prior position of the detected contamination, resulting in a variance reduction of the probability distributions. The purpose of this paper is to extend the single-detection backward probability model to multiple detections of contamination.

When multiple detections of contamination are made, the existence of the contamination is known at two or more points (here, "point" refers to a coordinate in the space-time domain). In general, we also know the concentration of the detected contamination. The concentration measurements can be used to further reduce the uncertainty (variance) of the probability distributions. For example, if concentrations of 1000 mg/L and 1 mg/L are sampled at different locations, the 1000-mg/L-sample presumably contains more information about the contamination source. Thus, using concentration measurements is more

informative than just considering the presence or absence of contamination at the two locations. In this paper, we deal only with the presence or absence of contamination and we treat each detection as a contaminant "particle" of uniform mass that remains intact as it travels through the aquifer. The use of concentration measurements will be addressed in a later paper.

The multiple-detection probability model is related to the two-particle stochastic model of forward contaminant transport, which uses a stochastic representation of the heterogeneous aquifer properties that affect flow and transport. Hydraulic conductivity is spatially heterogeneous, causing the local velocity field to deviate from the mean groundwater flow. Since the conductivity field cannot be quantified exactly, the true velocity field is unknown. Contaminant particles will follow the general direction of the mean groundwater flow; however, the velocity fluctuations will force the position of the contaminant particles to deviate from the mean flow path. If two particles originate near each other (e.g., from the same source), they will initially follow similar travel paths, resulting in a small separation distance between the particles. However, as the particles sample more heterogeneities, each will experience different velocity fluctuations, and their separation distance will grow. The particle positions will initially be correlated, but the velocity fluctuations will cause their positions to eventually become uncorrelated. The two-particle forward contaminant transport problem treats the hydraulic conductivity as a random field, providing a stochastic representation of the conductivity field, the velocity fluctuations, and the resulting contaminant particle paths and separation distances.

The spread of a contaminant plume is based on the travel paths of

many particle pairs and is quantified by the dispersion coefficient. The early time behavior of a pair of particles, characterized by a small separation distance, is analogous to a compact contaminant plume with a small dispersion coefficient. After particles sample more heterogeneities, their separation distance becomes larger, leading to more spread in the plume and a growing dispersion coefficient. Eventually, the particle positions are uncorrelated, and the dispersion coefficient approaches an asymptotic value. Two-particle transport theory has been used to develop expressions for this scale-dependent dispersion coefficient, based on velocity variations and covariances between particle pairs [e.g. *Kitanidis*, 1988; *Dagan*, 1990, 1991; *Salandin et al.*, 1991; *Rajaram and Gelhar*, 1993a, 1993b; *Zhang et al.*, 1996]. Although it is well-known that dispersion is scale-dependent, most standard contaminant transport codes, such as MT3D [*Zheng*, 1990], assume that the asymptotic approximation to the dispersion coefficient is strictly valid, and use a non-scale-dependent value. In other words, they assume that a sufficient amount of time has passed such that the particle positions are uncorrelated.

The multiple-detection probability model presented in this paper uses the asymptotic (non-scale-dependent) approximation to the dispersion coefficient. We assume that the positions of the two (or more) detected contamination particles are uncorrelated, with the exception that they originated from the same source. This backward probability model can be modified to also account for scale-dependent dispersion, if desired.

In the next section, we review the background on contaminant transport modeling and the forward location and travel time probability model, including its application to multiple sources. We then review the backward

probability model for a single detection of contamination. Finally, we present the procedure for using multiple detections of contamination to obtain location and travel time probabilities, and show that the variance of the resulting distributions are smaller than the variance of the single-detection distributions.

8.2 Contaminant Transport and Forward Probability Models

In this section, we present background on contaminant transport in groundwater (forward model) and forward location and travel time probabilities. We illustrate the concepts with a simple one-dimensional example.

8.2.1 Contaminant Transport

Transport of a conservative chemical in groundwater can be modeled using the advection-dispersion equation (ADE)

$$\begin{gathered}\frac{\partial C}{\partial t} = \frac{\partial}{\partial x_i}\left(D_{ij}\frac{\partial C}{\partial x_j}\right) - \frac{\partial}{\partial x_i}\left(v_i C\right) + \frac{q_I}{\theta}C_I - \frac{q_O}{\theta}C\ , \qquad (8.1)\\ C(\mathbf{x},0) = C_i(\mathbf{x})\\ C(\mathbf{x},t) = g_1(t) \text{ on } \Gamma_1\\ \left[D_{ij}\frac{\partial C}{\partial x_j}\right]\mathrm{n}_i = g_2(t) \text{ on } \Gamma_2\\ \left[v_i C - D_{ij}\frac{\partial C}{\partial x_j}\right]\mathrm{n}_i = g_3(t) \text{ on } \Gamma_3\end{gathered}$$

where $C(\mathbf{x},t)$ is resident concentration, t is time, x_i are the spatial directions $(i = 1,2,3)$, $\mathbf{x} = (x_1, x_2, x_3)$, D_{ij} is the i,j^{th} entry of the dispersion tensor, v_i is the groundwater velocity in the direction of x_i, q_I is the source flow rate per

unit volume, C_I is the source strength, θ is porosity, q_O is the sink flow rate per unit volume, C_i is the initial concentration, g_1, g_2, and g_3 are known functions, Γ_1, Γ_2, and Γ_3 are the domain boundaries, and n_i is the outward unit normal vector in the x_i direction. Resident concentration is a measure of the mass of solute per unit volume of water, or a volume-averaged concentration.

As an example, consider the one-dimensional, confined aquifer shown in Figure 8.1. The aquifer is infinite in extent with water flowing from right to left, and no internal sources or sinks of water. There is a contamination source at x_{1_o} and a monitoring well at x_{1_w}. For an instantaneous input of a conservative chemical at the source at x_{1_o}, the governing equation for contaminant transport is (8.1), with $q_I = q_O = 0$ and $C_i(x_1) = M'\delta(x_1 - x_{1_o})$, where M' is the source mass per unit cross-sectional area of water in the aquifer. For this model, the boundary conditions are $C \to 0$ as $x_1 \to \pm\infty$. The solution of this equation for constant v and D is [*Bear*, 1972; *Carslaw and Jaeger*, 1959]

$$C(x_1, t) = \frac{M'}{\sqrt{4\pi D t}} \exp\left\{ -\frac{(x_1 - x_{1_o} - vt)^2}{4Dt} \right\} , \tag{8.2}$$

and is plotted in Figure 8.2 for $M' = 2.0$ g/m^2, $D = 3$ m^2/d, $t = 100$ days, $x_{1_o} = 200$ m, and $v = -1$ m/d. The parameter values are also listed in Table 8.1. The solid line shows the concentration distribution at 100 days after release from the source.

For constant v and D, (8.1) can also be solved for flux concentration [*Kreft and Zuber*, 1978; *Parker and van Genuchten*, 1984]. Flux concentration is a measure of the solute mass flux per unit water flux, or a flux-averaged concentration. In one dimension, the relationship between flux and resident

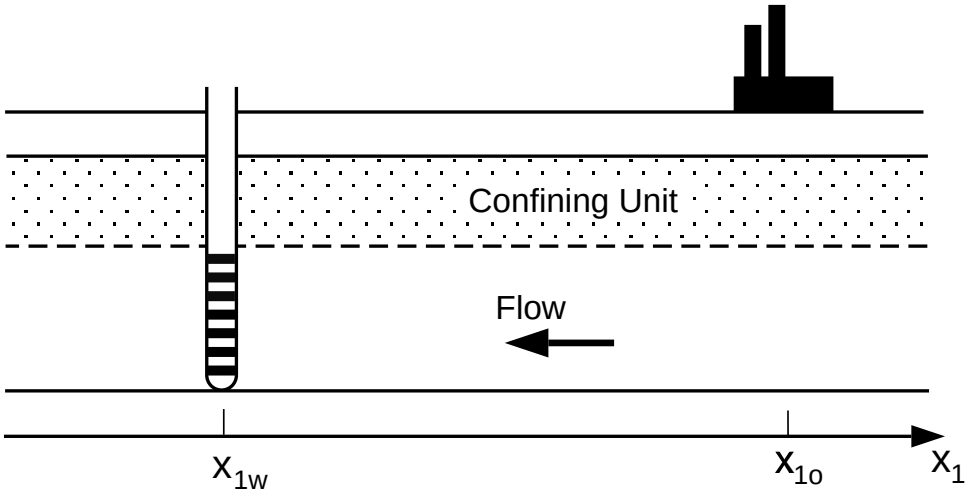

Figure 8.1: Sample one-dimensional aquifer.

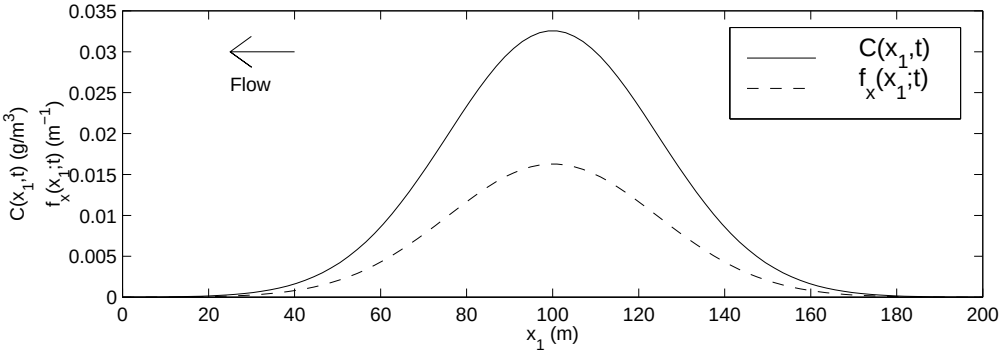

Figure 8.2: Resident concentration and forward location probability at $t = 100$ days after release from an instantaneous point source of contamination at $x_{1_o} = 200$ m. ($M' = 2.0$ g/m^2, $D = 3$ m^2/d, $v = -1$ m/d).

Table 8.1: Transport parameter values.

Parameter	Value
Source mass, M'	2.0 g/m^2
Dispersion coefficient , D	3 m^2/d
Velocity, v	-1 m/d
Porosity, θ	0.3
Well location, x_{1_w}	100 m
Source location (single detection), x_{1_o}	200 m
Source location (particle A), X_{Ao}	200 m
Source location (particle B), X_{Bo}	190 m
Release time (particle A), T_{o_A}	0
Release time (particle B), T_{o_B}	20 days
Detection location (particle A), X_{Aw}	20 m
Detection location (particle B), X_{Bw}	35 m
Detection time (particle A), τ_{w_A}	0
Detection time (particle B), τ_{w_B}	20 days

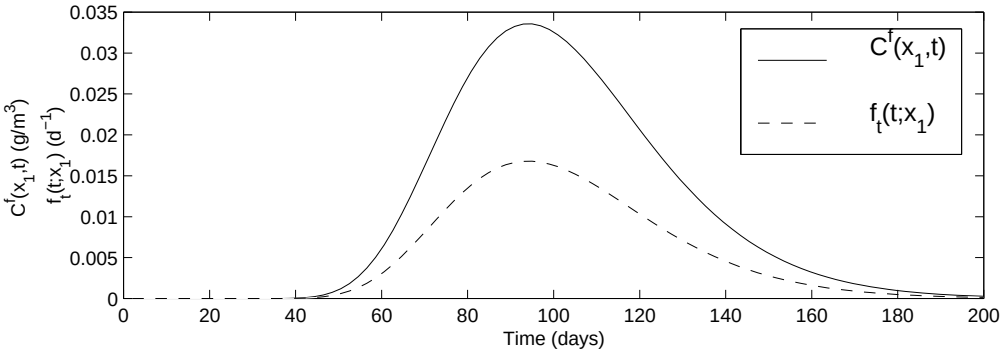

Figure 8.3: Flux concentration and forward travel time probability at $x_{1_w} = 100$ m due to release from an instantaneous point source of contamination at $x_{1_o} = 200$ m. ($M' = 2.0$ g/m^2, $D = 3$ m^2/d, $v = -1$ m/d).

concentration is [*Parker and van Genuchten*, 1984]

$$C^f = C - \frac{D}{v}\frac{\partial C}{\partial x} \,, \tag{8.3}$$

where C^f is flux concentration. Using (8.2) in (8.3), we obtain an expression for flux concentration at location x_1

$$C^f(x_1, t) = \frac{M'(x_1 - x_{1_o} + vt)}{4v\sqrt{\pi D t^3}} \exp\left\{-\frac{(x_1 - x_{1_o} - vt)^2}{4Dt}\right\} \,, \tag{8.4}$$

which is plotted in Figure 8.3 for $M' = 2.0$ g/m^2, $D = 3$ m^2/d, $x_1 = x_{1_w} = 100$ m, $x_{1_o} = 200$ m, and $v = -1$ m/d. The parameter values are also listed in Table 8.1. The solid line shows the flux concentration at $x_{1_w} = 100$ m for a release at $x_{1_o} = 200$ m.

8.2.2 Forward Probability Model for a Single Contamination Source

Location and travel time probabilities are often used in forward modeling to describe solute transport in groundwater [e.g., *Dagan*, 1982, 1987; *Jury*, 1982; *Jury and Roth*, 1990; *Chin and Chittaluru*, 1994]. In this section, we show the relationship between concentration and forward probabilities for a single source of contamination (single-particle probabilities).

Forward location probability describes the position of a solute parcel at a fixed time after its release from the source [*Dagan*, 1982, 1987, 1989; *Jury and Roth*, 1990; *Chin and Chittaluru*, 1994] and is related to resident concentration [*Dagan*, 1987; *Jury and Roth*, 1990]. The normalized concentration distribution at some time t after release from an instantaneous point source is equivalent to the location probability density function at time t, given by

$$f_{\mathbf{x}}(\mathbf{x};t) = \frac{C(\mathbf{x},t)}{\int_{\Omega} C(\mathbf{x},0^+)\, d\Omega}, \tag{8.5}$$

where $f_{\mathbf{x}}(\mathbf{x};t)$ is location probability at time t, $\mathbf{x}$ is the position vector, $C(\mathbf{x},t)$ is the resident concentration distribution from an instantaneous point source, Ω is the spatial domain, and $\int_{\Omega} C(\mathbf{x},0^+)\, d\Omega = M'$, where M' is a measure of the total mass that entered the system. For the one-dimensional domain in Figure 8.1, the location probability can be obtained from (8.5) and (8.2) and is given by

$$f_x(x_1;t) = \frac{1}{\sqrt{4\pi D t}} \exp\left\{ -\frac{(x_1 - x_{1_o} - vt)^2}{4Dt} \right\}, \tag{8.6}$$

Figure 8.2 shows the location probability of a contaminant particle at $t =$ 100 days after release from a source at $x_{1_o} = 200$ m. This curve represents the probability that the particle is at location x_1 (random variable) at $t = 100$ days after release from the source. The most likely location of the particle at $t =$ 100 days is $x_1 = 100$ m. The location probability in (8.6) could also be obtained from (8.1), by replacing C with f_x as the state variable, and with $q_I = q_O = 0$, $f_x(x_1; 0) = \delta(x - x_{1_o})$, and $f_x \rightarrow 0$ as $x \rightarrow \pm\infty$. The initial condition is this case is an instantaneous point source of probability at the contamination source, indicating that for a contaminant particle released at the source at time $t = 0$, there is a probability of one that it exists at the source location at $t = 0$ and a probability of zero that it is at any other location.

Forward travel time probability describes the time required for a solute parcel to travel from its source to a location of interest [*Jury*, 1982; *Jury et al.*, 1986; *Dagan*, 1989; *Dagan and Nguyen*, 1989], and is related to flux concentration [*Shapiro and Cvetkovic*, 1988; *Rubin and Dagan*, 1992]. For an instantaneous point source of contamination, the normalized flux concentration at a downgradient location, $\mathbf{x}$, is equivalent to the travel time probability density function for that location, given by

$$f_t(t; \mathbf{x}) = \frac{C^f(\mathbf{x}, t)}{\int_0^\infty C^f(\mathbf{x}, t)dt} = \frac{|v|AC^f(\mathbf{x}, t)}{M'} \tag{8.7}$$

where $f_t(t; \mathbf{x})$ is travel time probability from the source to $\mathbf{x}$, v is the groundwater velocity, $C^f(\mathbf{x}, t)$ is flux concentration, M' is a measure of the total amount of mass that entered at the source, and A is a flow area. We consider travel time probability across a plane perpendicular to flow, and A is the cross-sectional

area of this plane. For the one-dimensional domain in Figure 8.1, $A = 1$ and the forward travel time probability can be obtained from (8.7) and (8.4) as is given by

$$f_t(t; x_1) = \frac{|v|(x_1 - x_{1_o} + vt)}{4v\sqrt{\pi D t^3}} \exp\left\{-\frac{(x_1 - x_{1_o} - vt)^2}{4Dt}\right\} . \tag{8.8}$$

The forward travel time probability at $x_{1_w} = 100$ m for a source release at $x_{1_o} = 200$ m is shown by the dashed line in Figure 8.3. For a single contaminant particle that entered the source at $x_{1_o} = 200$ m, this curve represents the probability that the particle arrives at the monitoring well at $x_{1_w} = 100$ m at time t (random variable). The most likely arrival time for the particle is $t \approx 95$ days. This curve can also be obtained from (8.1), by replacing C with f_t as the state variable, and with $q_I = q_O = 0$, $f_t(0; x_1) = \delta(x - x_{1_o}) - (D/v)\delta'(x - x_{1_o})$,where δ' is the derivative of the Dirac delta function, and $f_t \to 0$ as $x \to \pm\infty$.

8.2.3 Forward Probability Model for Multiple Sources of Contamination

The forward location and travel time probabilities just described consider the future position or arrival time of a single particle released from one source. Next we consider the forward location and travel time probabilities of two particles released into the aquifer (two-particle probabilities). The approach can easily be extended to releases of more than two particles (multiple-particle probabilities).

For the aquifer shown in Figure 8.1, consider two particles (A and B)

released into the aquifer at locations $x_{1_{oA}} = X_{Ao}$ and $x_{1_{oB}} = X_{Bo}$, and at time $t_{o_A} = T_{o_A}$ and $t_{o_B} = T_{o_B}$, respectively, where t_o represents the release time. The two-particle location probability, $f_{x_A,x_B}(x_{1_A}, x_{1_B}; t, x_{1_oA} = X_{Ao}, x_{1_oB} = X_{Bo}, t_{o_A} = T_{o_A}, t_{o_B} = T_{o_B})$, is the probability that particle A is at location $x_1 = x_{1_A}$ and particle B is at location $x_1 = x_{1_B}$ at time t, given that they were released at X_{Ao} and X_{Bo} at times T_{o_A} and T_{o_B}, respectively. We assume that the travel paths of the two particles are uncorrelated (a necessary condition for (8.1) to apply with a non-scale-dependent dispersion coefficient). Therefore, the two-particle locations probability is the product of the two single-particle probabilities:

$$f_{x_A,x_B}(x_{1_A}, x_{1_B}; t, x_{1_oA} = X_{Ao}, x_{1_oB} = X_{Bo}, t_{o_A} = T_{o_A}, t_{o_B} = T_{o_B}) = \tag{8.9}$$
$$f_x(x_1 = x_{1_A}; t, x_{1_oA} = X_{Ao}, t_{o_A} = T_{o_A})$$
$$f_x(x_1 = x_{1_B}; t, x_{1_oB} = X_{Bo}, t_{o_B} = T_{o_B}) \ ,$$

where $f_x(x_1 = x_{1_A}; t, x_{1_oA} = X_{Ao}, t_{o_A} = T_{o_A})$ is the single-particle location probability for particle A and $f_x(x_1 = x_{1_B}; t, x_{1_oB} = X_{Bo}, t_{o_B} = T_{o_B})$ is the single-particle location probability for particle B. Let $X_{Ao} = 200$ m, $X_{Bo} = 190$ m, $T_{o_A} = 0$ and $T_{o_B} = 20$ days. The two single-particle location probabilities (from (8.6)) at $t = 100$ days are shown in Figure 8.4, using the transport parameters in Table 8.1. Note that (8.6) assumes that the source release time is $t = 0$. Since the release time of particle B is $t_{o_B} = 20$ days, t in (8.6) must be replaced by $(t - t_{o_B})$ for particle B. The plot shows that particle A is likely to be farther downgradient than particle B because it entered the aquifer earlier. The most likely locations for the particles at $t = 100$ days are $x_1 = 100$ m for particle A

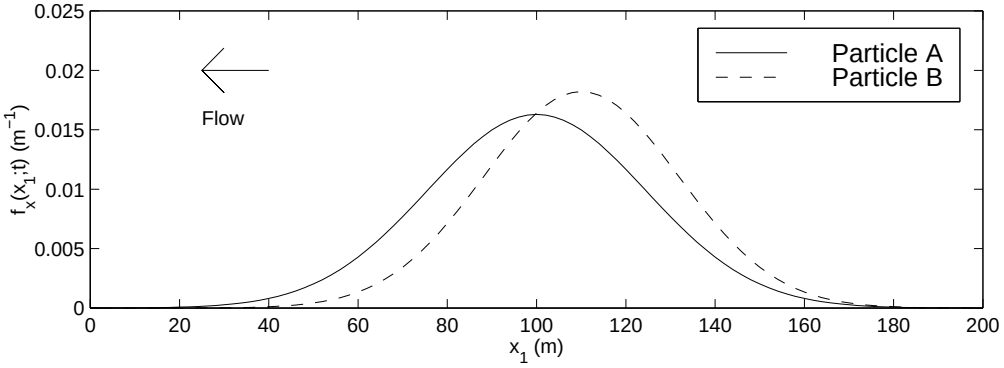

Figure 8.4: Single-particle forward location probability at $t = 100$ days for two particles. Particle A was released at location $X_{Ao} = 200$ m at time $T_{o_A} = 0$, and particle B was released at location $X_{Bo} = 190$ m at time $T_{o_B} = 20$ days. ($D = 3$ m^2/d, $v = -1$ m/d).

and $x_1 = 110$ m for particle B. The two-particle location probability, which is the product of these two one-particle probabilities, is shown in Figure 8.5 for the same case. The figure shows the probability that particle A is at x_{1_A} and particle B is at x_{1_B} at time $t = 100$ days.

Suppose we somehow know that the positions of the two particles coincide at time $t = 100$ days, but we do not know the where this position is in the domain. A new location probability can be calculated to determine the likely position of the two particles, given that their positions coincide. We can express this single-location two-particle probability as $f_x(x_{1_A} = x_1, x_{1_B} = x_1, t | x_{1_A} - x_{1_B} = 0)$, where the source locations and release times were omitted to simplify the notation. From Bayes' theorem, this single-location probability is related to the two single-particle probabilities for particles A and B by

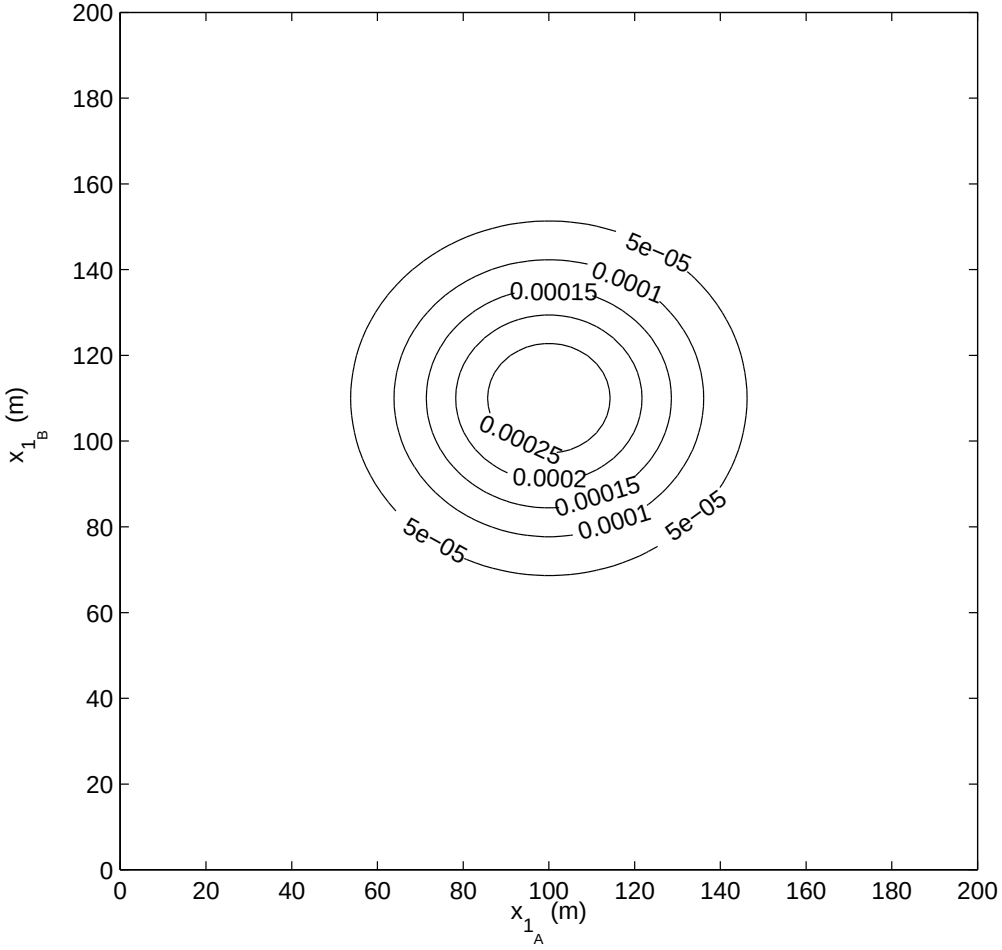

Figure 8.5: Two-particle forward location probability at $t = 100$ days. Particle A was released at location $X_{Ao} = 200$ m at time $T_{o_A} = 0$, and particle B was released at location $X_{Bo} = 190$ m at time $T_{o_B} = 20$ days. ($D = 3$ m^2/d, $v = -1$ m/d).

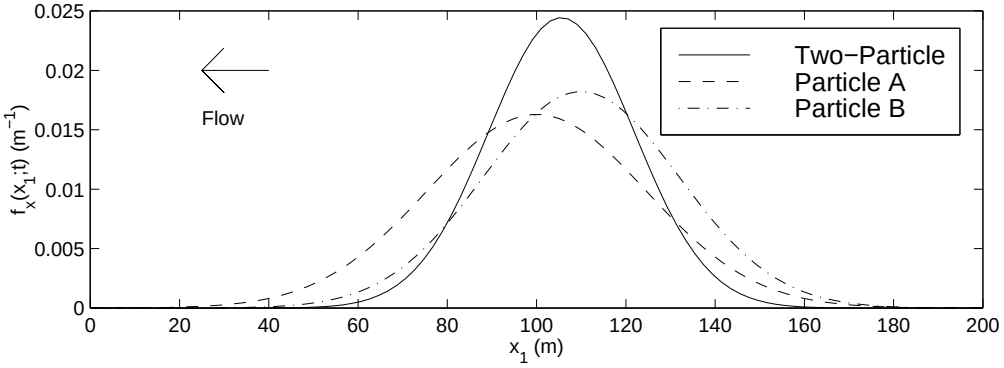

Figure 8.6: Single-location two-particle forward location probability at $t = 100$ days. Particle A was released at location $X_{Ao} = 200$ m at time $T_{o_A} = 0$, and particle B was released at location $X_{Bo} = 190$ m at time $T_{o_B} = 20$ days. ($D = 3$ m^2/d, $v = -1$ m/d).

(Appendix 8.A)

$$f_x(x_{1_A} = x_1, x_{1_B} = x_1, t | x_{1_A} - x_{1_B} = 0) = \frac{f_x(x_{1_A}; t) f_x(x_{1_B}; t)}{f_{A-B}(x_{1_A} - x_{1_B} = 0; t)} , \quad (8.10)$$

where f_{A-B} is the separation distance probability of the two particles at time t. This probability depends on the relative position of the two particles, not on their absolute locations, and can be related to the two single-particle probabilities by (Appendix 8.A)

$$f_{A-B}(x_{1_A} - x_{1_B} = 0; t) = \int_{x_1} f_x(x_{1_A} = x_1; t) f_x(x_{1_B} = x_1; t)\, dx_1 . \quad (8.11)$$

For the aquifer in Figure 8.1 and with $X_{Ao} = 200$ m, $X_{Bo} = 190$ m, $T_{o_A} = 0$ and $T_{o_B} = 20$ days, the single-location two-particle location probability from (8.10) with (8.11) is shown in Figure 8.6 at $t = 100$ days, along with the two single-particle location probabilities for each detection. The solid line shows

the probability that the two particles are located at x_1 at time t, given that their positions coincide. The most likely location of the two particles at $t = 100$ days is $x_1 \approx 105$ m. This single-location two-particle location probability can easily be extended to multiple particles. This probability is the forward analog of the backward multiple-detection location probability.

The two particle travel time probability, $f_{t_A,t_B}(t_A, t_B; x_{1_w}, x_{1_{oA}} = X_{Ao}, x_{1_{oB}} = X_{Bo}, t_{o_A} = T_{o_A}, t_{o_B} = T_{o_B})$, is the probability that particle A reaches location x_{1_w} at time t_A and particle B reaches x_{1_w} at time t_B, given that they were released at locations X_{Ao} and X_{Bo} at times T_{o_A} and T_{o_B}, respectively. Since we assume that the travel paths of the two particles are uncorrelated, the two-particle probability of their arrival times is the product of the two one-particle probabilities:

$$f_{t_A,t_B}(t_A, t_B; x_{1_w}, x_{1_{oA}} = X_{Ao}, x_{1_{oB}} = X_{Bo}, t_{o_A} = T_{o_A}, t_{o_B} = T_{o_B}) = \tag{8.12}$$
$$f_t(t = t_A; x_{1_w}, x_{1_{oA}} = X_{Ao}, t_{o_A} = T_{o_A})$$
$$f_t(t = t_B; x_{1_w}, x_{1_{oB}} = X_{Bo}, t_{o_B} = T_{o_B}) \ ,$$

where $f_t(t = t_A; x_{1_w}, x_{1_{oA}} = X_{Ao}, t_{o_A} = T_{o_A})$ is the single-particle travel probability for particle A and $f_t(t = t_B; x_{1_w}, x_{1_{oB}} = X_{Bo}, t_{o_B} = T_{o_B})$ is the single-particle travel probability for particle B. Let $X_{Ao} = 200$ m, $X_{Bo} = 190$ m, $T_{o_A} = 0$ and $T_{o_B} = 20$ days. The two single-particle travel time probabilities (from (8.8)) at $x_{1_w} = 100$ m are shown in Figure 8.7, for the transport parameters in Table 8.1. Because (8.8) assumes that the release time was $t = 0$ but particle B was released at $t_{o_B} = 20$ days, t in (8.8) must be replaced by $(t - t_{o_B})$ for particle B, and $f_t(t_B = t; x_{1_w}) = 0$ for $t < 20$ days. The plot shows

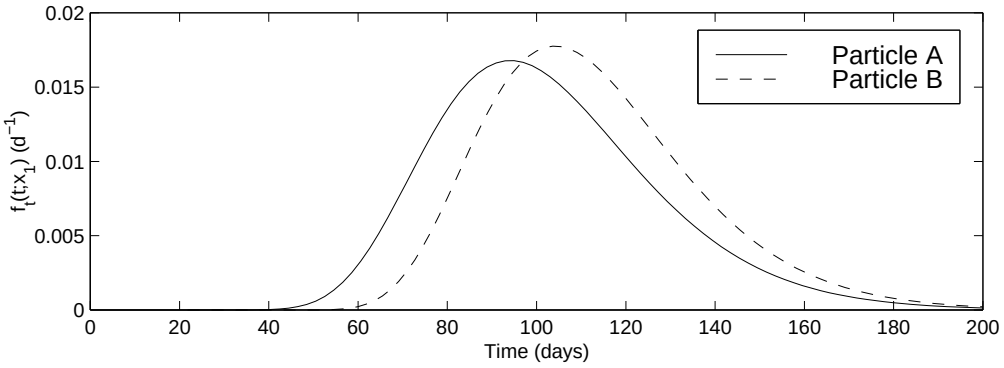

Figure 8.7: Single-particle forward travel time probability at $x_{1_w} = 100$ m for two particles. Particle A was released at location $X_{Ao} = 200$ m at time $T_{o_A} = 0$, and particle B was released at location $X_{Bo} = 190$ m at time $T_{o_B} = 20$ days. ($D = 3$ m^2/d, $v = -1$ m/d).

that particle A is likely to reach the monitoring well sooner than particle B because it was released from the source earlier. The most likely arrival time for the two particles are $t_A \approx 95$ days for particle A and $t_B \approx 104$ days for particle B. The two-particle travel time probability, which is the product of the two one-particle probabilities, is shown in Figure 8.8 for the same case. The figure shows the probability that particle A reaches the well at t_A and particle B reaches the well at t_B.

Suppose we know that both particles reach the well at x_{1_w} at the same time. A new travel time probability can be calculated to determine the likely arrival time of the two particles, given that the arrival times coincide. This single-time two-particle travel time probability is given by (Appendix 8.A)

$$f_t(t_A = t, t_B = t, x_{1_w} | t_A - t_B = 0) = \frac{f_t(t_A; x_{1_w}) f_t(t_B; x_{1_w})}{f_{t_A - t_B}(t_A - t_B = 0; x_{1_w})} , \qquad (8.13)$$

where $f_t(t_A; x_{1_w})$ and $f_t(t_B; x_{1_w})$ are the single-particle travel time probabilities

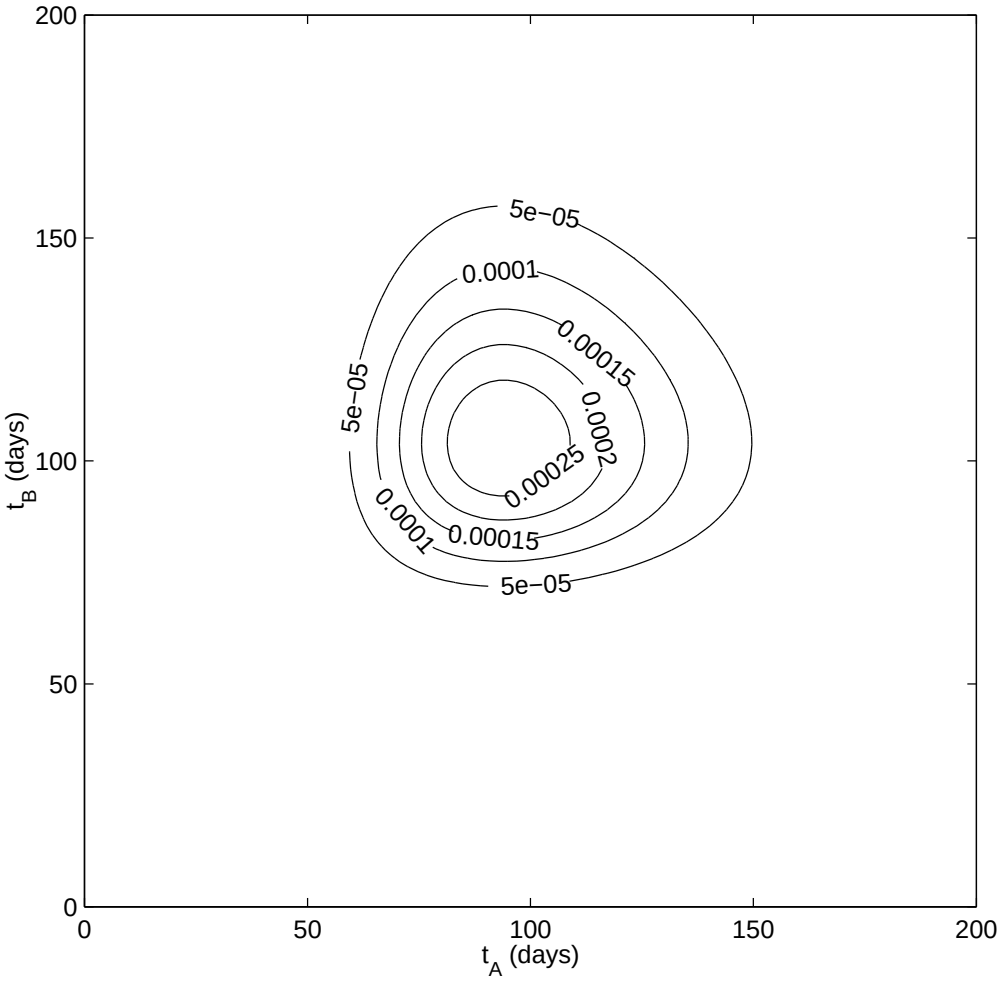

Figure 8.8: Two-particle forward travel time probability at $x_{1_w} = 100$ m. Particle A was released at location $X_{Ao} = 200$ m at time $T_{o_A} = 0$, and particle B was released at location $X_{Bo} = 190$ m at time $T_{o_B} = 20$ days. ($D = 3$ m^2/d, $v = -1$ m/d).

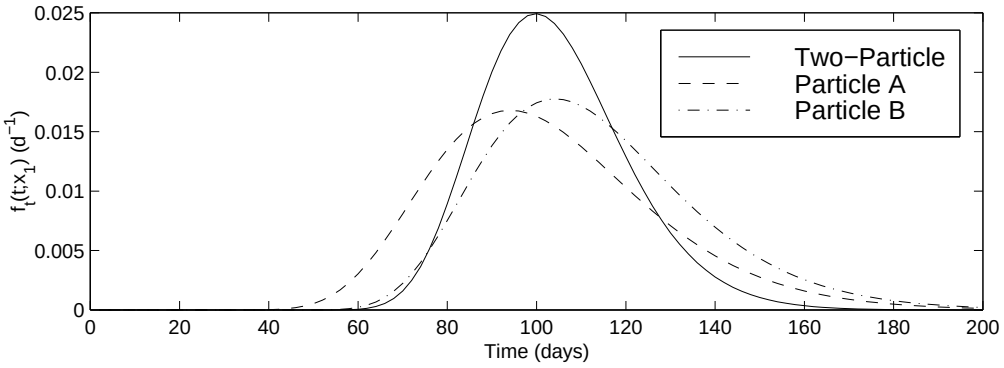

Figure 8.9: Single-time two-particle forward travel time probability at $x_{1_w} = 100$ m. Particle A was released at location $X_{Ao} = 200$ m at time $T_{o_A} = 0$, and particle B was released at location $X_{Bo} = 190$ m at time $T_{o_B} = 20$ days. ($D = 3$ m^2/d, $v = -1$ m/d).

for particles A and B, respectively, and $f_{t_A - t_B}$ is the separation time probability of the two particles at x_{1_w}, expressed as (Appendix 8.A)

$$f_{t_A - t_B}(t_A - t_B = 0; x_{1_w}) = \int_t f_t(t_A = t; x_{1_w}) f_t(t_B = t; x_{1_w})\, dt\ . \qquad (8.14)$$

For the aquifer in Figure 8.1 and with $X_{Ao} = 200$ m, $X_{Bo} = 190$ m, $T_{o_A} = 0$ and $T_{o_B} = 20$ days, the single-time two-particle travel time probability from (8.13) with (8.14) is shown in Figure 8.9 at $x_{1_w} = 100$ m, along with the single-particle travel time probabilities for the two detections. The solid line shows the probability that the two particles arrive at x_{1_w} at time t, given that their arrival times coincide. The most likely arrival time of the two particles at $x_{1_w} = 100$ m is $t \approx 100$ days. This single-time two-particle travel time probability can easily be extended to multiple particles. This probability is the forward analog of the backward multiple-detection travel time probability.

8.3 Backward Probability Model for a Single Detection of Contamination

In forward modeling we model the movement of solute (or probability) downgradient away from the contamination source and obtain information about the future position of the contamination. With backward modeling we treat the sampling location as a source of probability and allow the probability to advect upgradient in backward time and to spread out by dispersion. The resulting plume of backward probability gives information about the former position of contamination. For a solute parcel that was detected in an aquifer, backward location probability describes its position at some time prior to sampling, and backward travel time probability describes the amount of time required for the solute parcel to travel to the sampling location from some upgradient position, such as a known or suspected contamination source.

For the forward model governed by (8.1), the mathematical model for backward probabilities for a single detection of contamination is the adjoint of (8.1), given by [*Neupauer and Wilson*, 2000a]

$$\frac{\partial \psi^*}{\partial \tau} = \frac{\partial}{\partial x_i}\left(D_{ij}\frac{\partial \psi^*}{\partial x_j}\right) + \frac{\partial}{\partial x_i}(v_i\psi^*) - \frac{q_I}{\theta}\psi^* + \frac{\partial h}{\partial C} \tag{8.15}$$

$$\psi^*(\mathbf{x}, 0) = 0$$

$$\psi^*(\mathbf{x}, \tau) = 0 \text{ on } \Gamma_1$$

$$\left[D_{ij}\frac{\partial \psi^*}{\partial x_j} + v_i\psi^*\right] \mathrm{n}_i = 0 \text{ on } \Gamma_2$$

$$\left[D_{ij}\frac{\partial \psi^*}{\partial x_j}\right] \mathrm{n}_i = 0 \text{ on } \Gamma_3 \, .$$

where ψ^* is the adjoint state (related to either location or travel time probabil-

ity), τ is backward time or time prior to sampling ($\tau = T - t$, where $t = T$ is the sampling time), and h is a performance functional that depends on the type of probability and the detection mechanism (e.g., pumping well, monitoring well). The term $\partial h / \partial C$, called the load term, is a Fréchet derivative of the performance functional, h, with respect to concentration, C [*Neupauer and Wilson*, 1999]. The adjoint equation describes a family of adjoint states; a particular adjoint state is defined by the load term, through the choice of the performance functional. *Neupauer and Wilson* [2000a] suggest performance functionals for several different cases.

Although the basic form of the advection-dispersion equation (8.1) and its adjoint (8.15) are similar, several differences between the two equations are evident. First, the flow field in the adjoint equation is reversed. This can be observed by noting that the sign on the advection term is reversed and that the sources in (8.1) become sinks in (8.15), and vice versa. This flow field reversal in the adjoint equation allows the backward probability to travel upgradient, away from the detection and toward the possible contamination sources. Another difference between the two equations is that the backward equation is written in terms of backward time, τ, while the forward equation is written in terms of forward time, t. Thus, the forward model predicts the future position of contamination; while the backward model identifies the prior positions of contamination. A final difference between the two equations is that the boundary conditions on Γ_2 and Γ_3 are different. The second type boundary condition in the forward model (on Γ_2) becomes a third boundary condition in the backward model, and the third type boundary in the forward model (on Γ_3) becomes second type in the backward model.

Suppose contamination is detected at one location in an aquifer, but the source of contamination is unknown. We denote backward location probability for this single detection as $f_{\mathbf{x}}(\mathbf{x};\tau,\mathbf{x}_w)$, where $\mathbf{x}$ is the particle position (random variable), τ is the time of interest prior to detection (deterministic parameter), and $\mathbf{x}_w$ is the detection location (deterministic parameter). This probability can be calculated using (8.15), with the appropriate load term described in *Neupauer and Wilson* [1999, 2000a]. For a detection at the monitoring well in the one-dimensional domain shown in Figure 8.1, the governing equation for backward location probability is [*Neupauer and Wilson*, 2000b]

$$\frac{\partial f_x}{\partial \tau} = D\frac{\partial^2 f_x}{\partial x_1^2} + v\frac{\partial f_x}{\partial x_1} + \delta(x_1 - x_{1_w})\delta(\tau) \tag{8.16}$$

$$f_x \rightarrow 0 \text{ as } x \rightarrow \pm\infty$$

$$f_x(x_1;0,x_{1_w}) = 0$$

where D is the dispersion coefficient, v is the groundwater velocity, and x_{1_w} is the location of the monitoring well. The load term, $\delta(x_1 - x_{1_w})\delta(\tau)$, produces an instantaneous point source of probability at the time and place of detection. The solution of (8.16) is [*Neupauer and Wilson*, 2000b]

$$f_x(x_1;\tau,x_{1_w}) = \frac{1}{\sqrt{4\pi D\tau}}\exp\left\{-\frac{(x_1 - x_{1_w} + v\tau)^2}{4D\tau}\right\} . \tag{8.17}$$

Here, the random variable, x_1, represents the prior location of the contamination at time τ prior to detection. If the source release was known to be at time τ, then x_1 would represent the source location x_{1_o} (still a random variable). Figure 8.10 shows plot of backward location probability (8.17) at time

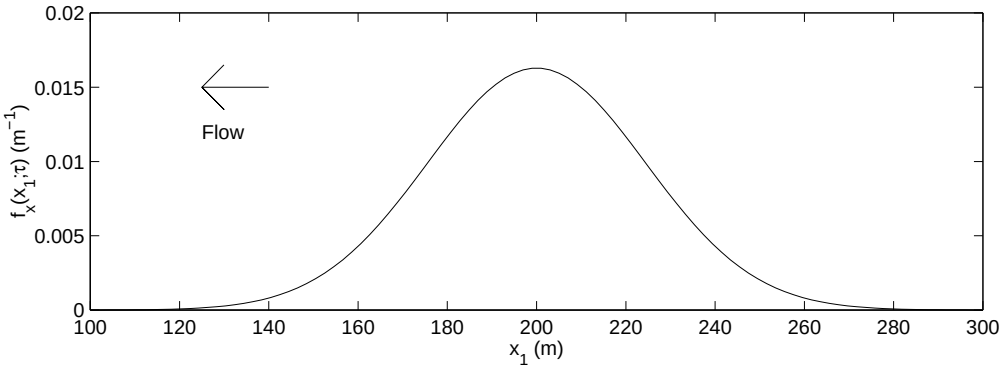

Figure 8.10: Single-detection backward location probability for $\tau = 100$ days prior to detection at $x_{1_w} = 100$ m. ($D = 3$ m^2/d, $v = -1$ m/d).

$\tau = 100$ days prior to detection at $x_{1_w} = 100$ m. The transport parameters are shown in Table 8.1. At $\tau = 100$ days, the most likely location of the detected particle is $x_1 = 200$ m.

Backward travel time probability for a single detection of contamination is denoted by $f_\tau(\tau; \mathbf{x}, \mathbf{x}_w)$, where τ is the particle's travel time in backward time (random variable), $\mathbf{x}$ is the location of interest (deterministic parameter), and $\mathbf{x}_w$ is the detection location (deterministic parameter). We assume that the detection occurred at $\tau = 0$. This probability can be calculated from the adjoint of the advection-dispersion operator (8.15), with an appropriate load term described in *Neupauer and Wilson* [1999, 2000b]. For a detection at the monitoring well in the domain shown in Figure 8.1, the governing equation for backward travel time probability is [*Neupauer and Wilson*, 2000a]

$$\frac{\partial \psi^*}{\partial \tau} = D\frac{\partial^2 \psi^*}{\partial x_1^2} + v\frac{\partial \psi^*}{\partial x_1} + \delta(x_1 - x_{1_w})\delta(\tau) + \frac{D}{v}\delta'_{x_1}(x_1 - x_{1_w})\delta(\tau) \qquad (8.18)$$

$$\psi^* \to 0 \text{ as } x \to \pm\infty$$

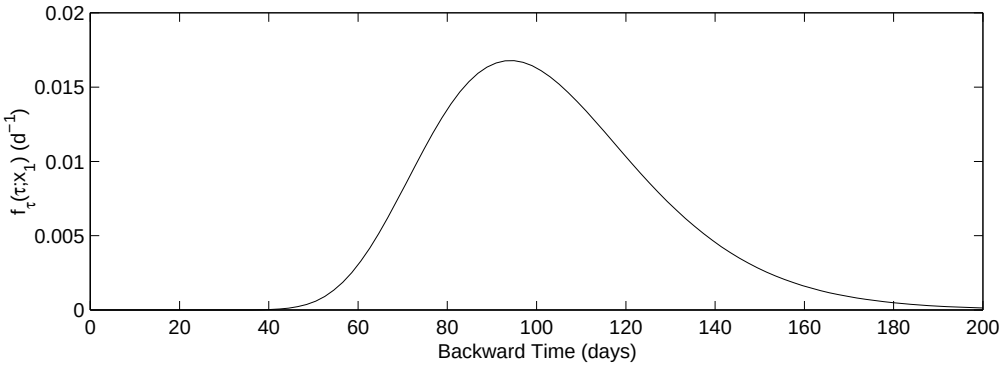

Figure 8.11: Single-detection backward travel time probability at $x_1 = 200$ m for a detection at $x_{1_w} = 100$ m. ($D = 3$ m^2/d, $v = -1$ m/d).

$$\psi^*(0; x_1, x_{1_w}) = 0 \ ,$$

where $\delta'_{x_1}(x_1 - x_{1_w})$ denotes the derivative of the Dirac delta function with respect to x_1, and travel time probability is a function of the adjoint state, ψ^*, given by $f_\tau(\tau; x_1, x_{1_w}) = |v(x_1)|\psi^*(x_1, \tau)$, for this one-dimensional problem. The solution of (8.18) is [*Neupauer and Wilson*, 2000b]

$$f_\tau(\tau; x_1, x_{1_w}) = \frac{-|v|(x_1 - x_{1_w} - v\tau)}{4v\sqrt{\pi D\tau^3}} \exp\left\{-\frac{(x_1 - x_{1_w} + v\tau)^2}{4D\tau}\right\} \ . \qquad (8.19)$$

Here, the random variable, τ, is the backward travel time of the contaminant parcel, i.e., the time prior to sampling when the contaminant parcel was at location x_1. Figure 8.11 is a plot of backward travel time probability at $x_1 = 200$ m for a detection at $x_{1_w} = 100$ m. The transport parameters are summarized in Table 8.1. For the particle detected at $x_{1_w} = 100$ m at $\tau = 0$, its most likely travel time from $x_1 = 200$ m to the detection is $\tau \approx 95$ days.

8.4 Backward Probability Model for Multiple Detections of Contamination

The backward probabilities described in the previous section address a single detection of contamination. In most practical situations, however, multiple detections of contamination are made. The multiple detections could be made at many locations in space and at many different times. Each detection provides additional information that can be used to characterize the prior position of contamination, thus reducing the uncertainty. In a probabilistic context, uncertainty is quantified by the variance of the probability distribution. The additional information available from multiple detections should reduce the variance of the probability distribution. In this section, we show the approach for using information from multiple detections in the backward probability model.

Multiple-detection backward probabilities are similar to the single-location and single-time multiple-particle forward probabilities described in Section 8.2.3. With those forward probability models, we had two (or more) sources of contamination, with a contaminant particle released from each. For location probability, we were interested in the future location of the particles at time t; and for travel time probability we were interested in the arrival time at x_{1_w}. In both cases, we assumed that the particle positions coincided at the time or location of interest. In other words, there were two or more contamination sources, and we wanted to find the location at which the two particles could be detected simultaneously at time t. The backward multiple-detection location probability is similar, with the sources and detections interchanged. In the backward model, we have two (or more) detections of contamination. If the

detected contamination originated from the same source at backward time τ, the prior positions of the detected contamination will coincide at time τ. Thus, the multiple-detection backward probability describes the probability that the two (or more) detected contamination particles were at location $\mathbf{x}$ at time τ in the past, given that their positions coincided. For location probability, the backward time, τ, is fixed and the particle position, $\mathbf{x}$, is random; for travel time probability, $\mathbf{x}$ is fixed and τ is random.

This approach assumes that the two (or more) detected particles originated from the same source, and that the source was an instantaneous point source, although these conditions can be relaxed. We ignore the concentrations of the detections and consider only that the contamination exists at the detection locations. We present the approach here for two detections in a one-dimensional domain, then state the results for multiple detections in a multi-dimensional domain.

8.4.1 Multiple-Detection Location Probability

Let us define the two-detection backward location probability for a one-dimensional domain as $f_x(x_{1_A} = x_1, x_{1_B} = x_1; \tau, x_{1_{w_A}} = X_{Aw}, x_{1_{w_B}} = X_{Bw}, \tau_{w_A} = T_{w_A}, \tau_{w_B} = T_{w_B})$, representing the probability that particles A and B were both at location x_1 (random variable) at backward time τ, given that particle A was detected at location X_{Aw} at backward time T_{w_A} and particle B was detected at location X_{Bw} at backward time T_{w_B}. From Bayes' theorem, this two-detection location probability is related to the two single-detection

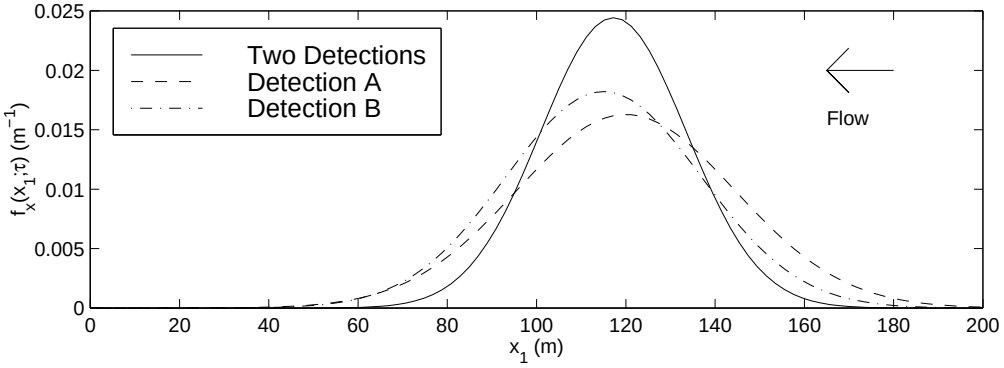

Figure 8.12: Two-particle backward location probability at $\tau = 100$ days. Particle A was detected at location $X_{Aw} = 20$ m at time $\tau_{w_A} = 0$, and particle B was detected at location $X_{Bw} = 35$ m at time $\tau_{w_B} = 20$ days. ($D = 3$ m^2/d, $v = -1$ m/d).

location probabilities for each of the two detections by (Appendix 8.A)

$$f_x(x_{1_A} = x_1, x_{1_B} = x_1; \tau) = \frac{f_x(x_{1_A} = x_1; \tau) f_x(x_{1_B} = x_1; \tau)}{\int_{x_1} f_x(x_{1_A} = x_1; \tau) f_x(x_{1_B} = x_1; \tau)\, dx_1} \ , \quad (8.20)$$

where $f_x(x_{1_A} = x_1; \tau)$ is the single-detection location probability for detection A, $f_x(x_{1_B} = x_1; \tau)$ is the single-detection location probability for detection B, and the detection locations and times have been omitted from the notation.

For the aquifer in Figure 8.1 and with $X_{Aw} = 20$ m, $X_{Bw} = 35$ m, $\tau_{w_A} = 0$ and $\tau_{w_B} = 20$ days, the two-particle backward location probability from (8.20) is shown in Figure 8.12 at $\tau = 100$ days, along with the single-particle location probabilities for each detection. The values of the transport parameters are shown in Table 8.1. The solid line shows the probability that the two particles were located at x_1 at backward time τ, given that their positions coincide. This distribution assumes that the particles did exist in the system at time τ and that they were at the same location. Thus, if both particles were

Table 8.2: Variances of the location probability distributions at $\tau = 100$ days.

Distribution	Variance (m^2)
Detection A	600
Detection B	480
Two Detections	267

released from the source at time $\tau = 100$ days, the most likely source location is $x_1 \approx 117$ m.

By inspection of Figure 8.12, we see that the spread (variance) of the two-particle distribution is smaller than the spread of either of the two single-detection distributions. The actual variances are listed in Table 8.2. This shows that the additional information obtained from the multiple detections reduces the uncertainty of the results, and this is quantified by a variance reduction.

The two-particle location probability in (8.20) can be generalized to account for multiple detections of contamination in a multi-dimensional domain, given by

$$f_{\mathbf{x}}(\mathbf{x}_1 = \mathbf{x}_2 = \ldots = \mathbf{x}_N = \mathbf{x}; \tau) = \frac{\prod_{k=1}^{N} f_{\mathbf{x}}(\mathbf{x}_k; \tau)}{\int_{\mathbf{x}} \prod_{k=1}^{N} f_{\mathbf{x}}(\mathbf{x}_k; \tau)\, d\mathbf{x}}\,, \tag{8.21}$$

where N is the number of detections, $f_{\mathbf{x}}(\mathbf{x}_k; \tau)$ is the single-detection location probability for detection k, $\mathbf{x}_k$ denotes the prior position of the particle from detection k, and the integral is evaluated over all spatial dimensions.

The procedure for numerically calculating the multiple-detection location probability is to first run one backward simulation for each of the N

detections to obtain $f_{\mathbf{x}}(\mathbf{x}_k;\tau)$, for $k = 1, 2, \ldots, N$. The spatial discretization should be consistent for all the simulations. Next, the product of these single-detection location probabilities must be obtained numerically by multiplying the N values at each cell on the numerical grid. This product is then normalized by its integral over the spatial domain, which can be calculated numerically. This normalized product is the multiple-detection location probability. The numerical implementation of the single-detection backward probability model is described in Chapter 7.

Since it is necessary, in general, to run one backward simulation for each detection, the procedure may become computationally inefficient if a large number of detections are considered. The advantage of the backward model over a conventional contaminant transport model is that the backward model is more efficient if the number of possible sources is large relative to the number of considered observations. As the number of considered detections increases, the user must decide whether or not it is advantageous to use the backward model.

For the special case of a steady, uniform flow field, we can solve directly for the multiple-detection location probability using only one simulation of the backward model. For the one-dimensional infinite aquifer in Figure 8.1, the backward location probability for a single detection is given by (8.17). Substituting this expression into (8.21), we obtain

$$f_{\mathbf{x}}(\mathbf{x}_1 = \mathbf{x}_2 = \ldots = \mathbf{x}_N = x_1;\tau) = \frac{1}{\sqrt{4\pi D\tau_h/N}} \exp\left\{-\frac{(x_1 - \bar{x}_{1_w} + v\tau_h)^2}{4D\tau_h/N}\right\}, \quad (8.22)$$

where N is the number of detections, $\bar{x}_{1_w}$ is the arithmetic mean of the N

detection locations, and τ_h is the harmonic mean of the N detection times. This is a normal distribution whose variance is $\sigma^2 = 2D\tau_h/N$. Thus, each additional detection reduces the variance of the distribution, and for N detections the variance is $\approx 1/N$ of the variance of the single-detection distribution. By inspection of (8.16), (8.17), and (8.22), we see that the governing equation for the multiple-detection location probability in a steady uniform flow field is

$$\frac{\partial f_x}{\partial \tau_h} = \frac{D}{N}\frac{\partial^2 f_x}{\partial x_1^2} + v\frac{\partial f_x}{\partial x_1} + \delta(x_1 - \bar{x}_{1_w})\delta(\tau_h) \; , \tag{8.23}$$

with appropriate initial and boundary conditions. With this equation, the multiple-detection location probability can be obtained with only one simulation of the backward model by reducing the dispersion coefficient by a factor of N, treating the arithmetic mean of the detection locations, $\bar{x}_{1_w}$, as an instantaneous point source of probability, and defining $\tau_h = 0$ to be the harmonic mean of the detection times. This result can be extended to multi-dimensional domains with steady uniform flow.

8.4.2 Multiple-Detection Travel Time Probability

In a one-dimensional domain, the two-detection backward travel time probability can be defined as $f_\tau(\tau_A = \tau, \tau_B = \tau; x_1, x_{1_{wA}} = X_{Aw}, x_{1_{wB}} = X_{Bw}, \tau_{w_A} = T_{w_A}, \tau_{w_B} = T_{w_B})$, representing the probability that particles A and B were both at location x_1 at backward time τ (random variable), given that particle A was detected at location X_{Aw} at backward time T_{w_A} and particle B was detected at location X_{Bw} at backward time T_{w_B}. This two-detection travel time probability is related to the single-detection travel time probabilities for

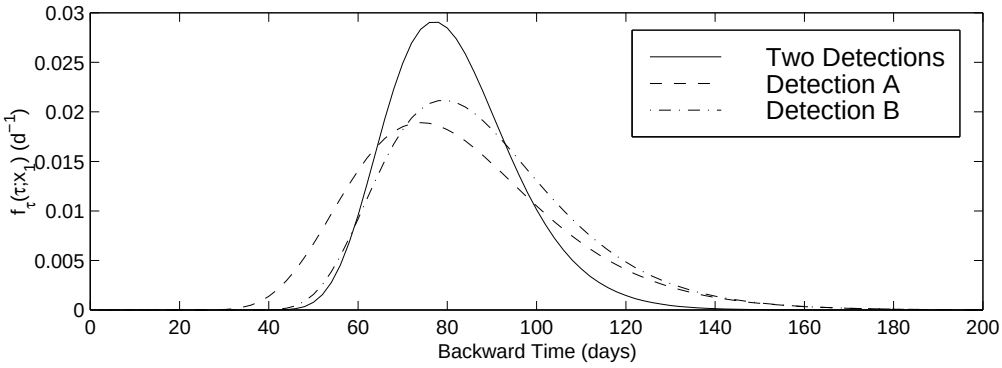

Figure 8.13: Two-particle backward travel time probability at $x_1 = 100$ m. Particle A was detected at location $X_{Aw} = 20$ m at time $\tau_{w_A} = 0$, and particle B was detected at location $X_{Bw} = 35$ m at time $\tau_{w_B} = 20$ days. ($D = 3$ m^2/d, $v = -1$ m/d).

each detection by (Appendix 8.A)

$$f_\tau(\tau_A = \tau, \tau_B = \tau; x_1) = \frac{f_\tau(\tau; x_{1_A} = x_1) f_\tau(\tau; x_{1_B} = x_1)}{\int_\tau f_\tau(\tau_A = \tau; x_1) f_\tau(\tau_B = \tau; x_1)\, dx_1}\,, \qquad (8.24)$$

where $f_\tau(\tau_A = \tau; x_1)$ is the single-detection travel time probability for detection A, $f_\tau(\tau_B = \tau; x_1)$ is the single-detection travel time probability for detection B, and the detection locations and times have been omitted from the notation.

For the aquifer in Figure 8.1 and with $X_{Aw} = 20$ m, $X_{Bw} = 35$ m, $T_{w_A} = 0$ and $T_{w_B} = 20$ days, the two-particle travel time probability from (8.24) is shown in Figure 8.13 at $x_1 = 100$ m, along with the single-particle travel time probabilities for the two detections. The values of the transport parameters are shown in Table 8.1. The solid line shows the probability that the two particles were at x_1 at time τ, given that their arrivals coincide. This distribution assumes that the particles did exist at x_1 and that both particles were at that location at the same time. Thus, if the source location is at

Table 8.3: Variances of the travel time probability distributions from a source at $x_1 = 100$ m.

Distribution	Variance (d^2)
Detection A	521
Detection B	432
Two Detections	208

$x_1 = 100$ m, the most likely release time from the source is $\tau \approx 78$ days. The spread (variance) of the two-particle distribution is smaller than the spread of either of the two single-detection distributions. The actual variances are listed in Table 8.3. This shows that the additional information obtained from the multiple detections reduces the uncertainty of the results, and this is quantified by a variance reduction.

The two-particle travel time probability in (8.24) can be generalized to account for multiple detections of contamination in a multi-dimensional domain, given by

$$f_\tau(\tau_1 = \tau_2 = \ldots = \tau_N = \tau; \mathbf{x}) = \frac{\prod_{k=1}^{N} f_\tau(\tau_k; \mathbf{x})}{\int_{\mathbf{x}} \prod_{k=1}^{N} f_\tau(\tau_k; \mathbf{x})\, d\tau} \ , \tag{8.25}$$

where N is the number of detections and $f_\tau(\tau_k; \mathbf{x})$ is the single-detection location probability for detection k.

For a conservative solute in a one-dimensional domain, all mass that was released at the source must eventually pass all downgradient points provided there are no intermediate sinks; for this case $\int_t f(t; x)\ dt = 1$ for all x downgradient of the source. Similarly, for backward travel time probability in

a one-dimensional domain $\int_\tau f(\tau; x)\ d\tau = 1$ for all x upgradient of the detection. This is not the case for multi-dimensional domains. In multi-dimensional domains, a particle that is released from the source will not pass through all downgradient locations; it will only pass through the locations along its travel path, and $\int_t f(t; \mathbf{x})\ dt < 1$. Similarly, a particle that was detected in a multi-dimensional domain has not passed through all upgradient locations; it has only passed through the locations along its travel path. Therefore, for a single-detection backward travel time probability, $\int_\tau f(\tau; \mathbf{x})\ d\tau < 1$ because the particle might never have been at the location of interest. This integral is equivalent to $F(\tau \rightarrow \infty)$, the limiting value of the cumulative distribution of travel time probability. Since the cumulative distribution function describes the probability that the particle was at location $\mathbf{x}$ at any time less than τ, $F(\tau \rightarrow \infty)$ represents the probability that the detected particle was ever at location $\mathbf{x}$.

In defining the multiple-detection travel time probability we assumed that the two (or more) particles did pass through the upgradient location of interest and that they passed through that location at the same time. With this definition, the multiple-detection travel time probability will always integrate to one over time. Therefore, it does not provide any information about the probability that the two (or more) particles ever existed at the location of interest. It does, however, identify the most likely travel times.

The procedure for numerically calculating the multiple-detection travel time probability is similar to that described above for location probability. The only difference is that the product of the single-detection probabilities is normalized by its integral over the time domain. To obtain an accurate integral, the simulations must be of sufficient duration so that the tails of the

travel time probability distributions completely pass the location of interest. Again, it is necessary to run one backward simulation for each detection, and the procedure may become computationally inefficient if a large number of detections are considered. Furthermore, the special case of steady uniform flow does not result in a simplified expression for travel time probability as it did for location probability.

8.5 Conclusions

If contamination is detected in an aquifer, but the source of contamination is unknown, backward location and travel time probabilities can be used to identify the prior locations of the detected contamination. The backward probability model has been developed for a single detection of contamination [*Wilson and Liu*, 1994; *Liu*, 1995; *Neupauer and Wilson*, 1999]. In most practical situations, contamination is detected at more than one location or time. This additional information can improve the characterization of the prior position of contamination by reducing the variance of the probability distributions. In this paper, we presented the development of the backward probability model for multiple detections of contamination. The multiple-detection probability distributions are related to the single-detection probability distributions for each of the detections, and the relationships are based on Bayes' theorem and the law of total probability.

The multiple-detection location probability assumes that all particles were at the same location at time τ in the past, and the probability distribution describes the particles' position at time τ. If the contamination was known

to have been released at time τ, then this distribution describes the source location probability. The multiple-detection travel time probability assumes that all particles were at location $\mathbf{x}$ at the same time in the past, and the probability distribution describes the time at which the particles were at that location. If we know that $\mathbf{x}$ is the contamination source, then this distribution describes the probability of the source release time.

The multiple-detection probability is the product of the single-detection probabilities for each detection, normalized by the integral of this product. The integral is evaluated over the spatial domain for location probability and over the time domain for travel time probability. By illustration with a one-dimensional example, we showed that the variance of the multiple-detection location probability is smaller than the variances of the single-detection probabilities.

In general, to calculate the multiple-detection location probability, it is necessary to run a simulation of the backward probability model for each detection. Thus, the procedure may become computationally inefficient if a large number of detections are considered. The user must decide whether it is more efficient to use the backward model or a conventional contaminant transport model.

Acknowledgments

This research was supported in part by the Geophysical Research Center at New Mexico Tech and in part by the Environmental Protection Agency's

STAR Fellowship program under Fellowship No. U-915324-01-0. This work has not been subjected to the EPA's peer and administrative review and therefore may not necessarily reflect the views of the Agency and no official endorsement should be inferred.

References

Bagtzoglou, A.C., D.E. Dougherty, and A.F.B. Thompson, Application of particle methods to reliable identification of groundwater pollution sources, *Water Resources Management*, 6, 15–23, 1992.

Bear, J., *Dynamics of Fluids in Porous Media*, American Elsevier Publishing Company, New York, 1972.

Carslaw, H.S. and J.C. Jaeger, *Conduction of Heat in Solids*, 2nd ed., Clarendon Press, Oxford, 1959.

Chin, D.A. and P.V.K. Chittaluru, Risk management in wellhead protection, *J. Water Resour. Plan. Manage.*, 120(3), 294–315. 1994.

Dagan, G., Stochastic modeling of groundwater flow by unconditional and conditional probabilities, 2, The solute transport, *Water Resour. Res.*, 18(4), 835–848, 1982.

Dagan, G., Theory of solute transport by groundwater, *Ann. Rev. Fluid Mech.*, 19, 183–215, 1987.

Dagan, G., *Flow and Transport in Porous Formations*, Springer-Verlag, New York, 1989.

Dagan, G., Transport in heterogeneous porous formations: spatial moments, ergodicity, and effective dispersion, *Water Resour. Res.*, 26(6), 1281–1290, 1990.

Dagan, G., Dispersion of a passive solute in non-ergodic transport by steady velocity fields in heterogeneous formation, *J. Fluid Mech.*, 233, 197–210, 1991.

Dagan, G., and V. Nguyen, A comparison of travel time and concentration approaches to modeling transport by groundwater, *Journal of Contaminant Hydrology*, 4, 79–91, 1989.

Jury, W.A., Simulation of solute transport using a transfer function model, *Water Resour. Res.*, 18(2), 363–368, 1982.

Jury, W.A., G. Sposito, and R.E. White, A transfer function model of solute transport through soil, 1, Fundamental concepts, *Water Resour. Res.*, 22(2), 243–247, 1986.

Jury, W.A. and K. Roth, *Transfer Functions and Solute Movement through Soil: Theory and Applications*, Birkhauser Verlag, Boston, 1990.

Kitanidis, P.K., Prediction by the method of moments of transport in a heterogeneous formation, *J. Hydrol.*, 102, 453–473, 1988.

Kreft, A. and A. Zuber, On the physical meaning of the dispersion equation and its solutions for different initial and boundary conditions, *Chemical Engineering Science*, 33, 1471–1480, 1978.

Liu, J., *Travel time and location probabilities for groundwater contaminant sources*, Master's thesis, New Mexico Institute of Mining and Technology, Socorro, 1995.

Liu, J. and J.L. Wilson, Modeling travel time and source location probabilities in two-dimensional heterogeneous aquifer. *Proceedings 5th Annual WERC Technology Development Conference*, New Mexico State University, Las Cruces, New Mexico, 59–67, 1995.

Neupauer, R.M. and J.L. Wilson, Adjoint method for obtaining backward-

in-time location and travel time probabilities of a conservative groundwater contaminant, *Water Resour. Res.*, 35(11), 3389–3398, 1999.

Neupauer, R.M. and J.L. Wilson, Adjoint-derived location and travel time probabilities in a multi-dimensional groundwater flow system, *Water Resour. Res.*, in press, 2000a.

Neupauer, R.M. and J.L. Wilson, Backward location and travel time probabilities for contamination in a one-dimensional infinite aquifer, submitted to *J. Contam. Hydrol.*, 2000b.

Parker, J.C. and M. Th. van Genuchten, Flux-averaged and volume-averaged concentrations in continuum approaches to solute transport, *Water Resour. Res.*, 20(7), 866–872, 1984.

Rajaram, H. and L.W. Gelhar, Plume scale-dependent dispersion in heterogeneous aquifers, 1, Lagrangian analysis in a stratified aquifer, *Water Resour. Res.*, 29(9), 3249–3260, 1993a.

Rajaram, H. and L.W. Gelhar, Plume scale-dependent dispersion in heterogeneous aquifers, 2, Eulerian analysis and three-dimensional aquifers, *Water Resour. Res.*, 29(9), 3261–3276, 1993b.

Rubin, Y. and G. Dagan, Conditional estimation of solute travel time in heterogeneous formations: impact of transmissivity measurements, *Water Resour. Res.*, 28(4), 1033–1040, 1992.

Salandin, P., A. Rinaldo, and G. Dagan, A note on transport in stratified formations by flow tilted with respect to bedding, *Water Resour. Res.*, 27(11), 3009–3017, 1991.

Shapiro, A.M. and V.D. Cvetkovic, Stochastic analysis of solute arrival time in heterogeneous porous media, *Water Resour. Res.*, 24(10), 1711–1718, 1988.

Uffink, G.J.M., Application of Kolmogorov's backward equation in random walk simulations of groundwater contaminant transport, in *Contaminant Transport in Groundwater*, H.E. Kobus and W. Kinzelbach, editors, pp. 283–289, A.A. Balkema, Brookfield, Vt., 1989.

Wilson, J.L. and J. Liu, Backward tracking to find the source of pollution, in *Waste-management: From Risk to Remediation*, edited by R. Bhada *et al.*, ECM Press, Albuquerque, NM, 181–199, 1994.

Wilson, J.L. and J. Liu, Field Validation of the Backward-in-time Advection Dispersion Theory. *Proceedings of the 1996 HSRC/WERC Joint Conf. on the Environment*, Great Plains-Rocky Mountain Hazardous Substance Center, Manhattan, Kansas, http://www.engg.ksu.edu/HSRC/ 96Proceed/wilson.html, 1997.

Zhang, Y.-K., D. Zhang, and J. Lin, Nonergodic solute transport in three-dimensional heterogeneous isotropic aquifers, *Water Resour. Res.*, 32(9), 2955-2963, 1996.

Zheng, C., *MT3D: A Modular Three-Dimensional Transport Model for Simulation of Advection, Dispersion and Chemical Reactions of Contaminants in Groundwater Systems*, Report to the U.S. Environmental Protection Agency, Ada, Oklahoma, 170 pp., 1990.

8.A Probability Relationships

The single-location two-particle location probability is the probability that particles A and B are at location x_1 at time t, given that they are at the same location. In probability notation, this can be written as $P(x_{1_A} = x_1, x_{1_B} = x_1; t | x_{1_A} - x_{1_B} = 0)$. The two-particle probability is related to the two single-particle probabilities for particles A and B, and this relationship is based on Bayes' theorem and the law of total probability. From Bayes' theorem, the probability of event C conditioned on the occurrence of event D, $P(C|D)$, is related to $P(D|C)$ by

$$P(C|D) = \frac{P(D|C)P(C)}{P(D)} \,, \tag{8.26}$$

where P denotes probability. Substituting the expression for the single-location two-particle probability into (8.26) yields

$$P(x_{1_A} = x_1, x_{1_B} = x_1; t | x_{1_A} - x_{1_B} = 0) = \frac{P(x_{1_A} - x_{1_B} = 0; t | x_{1_A} = x_1, x_{1_B} = x_1) P(x_{1_A} = x_1, x_{1_B} = x_1; t)}{P(x_{1_A} - x_{1_B} = 0; t)} \,. \tag{8.27}$$

By definition, if $x_{1_A} = x_1$ and $x_{1_B} = x_1$, then $x_{1_A} - x_{1_B} = 0$, so $P(x_{1_A} - x_{1_B} = 0 | x_{1_A} = x_1, x_{1_B} = x_1) = 1$. Making this substitution and accounting for the fact that the particle positions are uncorrelated, the single-location two-particle probability in terms of probability density functions becomes

$$f_x(x_{1_A} = x_1, x_{1_B} = x_1; t | x_{1_A} - x_{1_B} = 0) = \frac{f_x(x_{1_A}; t) f_x(x_{1_B}; t)}{f_{A-B}(x_{1_A} - x_{1_B} = 0; t)} \,, \tag{8.28}$$

where f_{A-B} is the separation distance probability of the two particles at time t. This probability depends on the relative position of the two particles, not their absolute locations.

The law of total probability states that

$$P(C) = \int_{\eta} P(C|D=\eta)P(D=\eta)d\eta \; . \tag{8.29}$$

Using this expression, the separation distance probability can be written as

$$P(x_{1_A} - x_{1_B} = 0) = \int_{x_1} P(x_{1_A} - x_{1_B} = 0 | x_{1_A} = x_1) P(x_{1_A} = x_1) \; dx_1 \; . \tag{8.30}$$

In the first factor inside the integral, $P(x_{1_A} - x_{1_B} = 0)$ is conditioned on $x_{1_A} = x_1$, implying that $x_{1_A} = x_{1_B} = x_1$, so the first factor can be rewritten as $P(x_{1_A} - x_{1_B} = 0 | x_{1_A} = x_1) = P(x_{1_A} = x_1, x_{1_B} = x_1 | x_{1_A} = x_1)$. Using this substitution, and replacing the conditional probability with an equivalent expression of joint probability, (8.30) becomes

$$\begin{aligned} P(x_{1_A} - x_{1_B} = 0) &= \int_{x_1} \frac{P(x_{1_A} = x_1, x_{1_B} = x_1)}{P(x_{1_A} = x_1)} P(x_{1_A} = x_1) \; dx_1 \\ &= \int_{x_1} P(x_{1_A} = x_1, x_{1_B} = x_1) \; dx_1 \; . \end{aligned} \tag{8.31}$$

Thus the separation distance probability is

$$f_{A-B}(x_{1_A} - x_{1_B} = 0; t) = \int_{x_1} f_x(x_{1_A} = x_1; t) f_x(x_{1_B} = x_1; t) \; dx_1 \; . \tag{8.32}$$

Using the same approach for travel time probability, we find that

$$f_t(t_A = t, t_B = t, x_{1_w} | t_A - t_B = 0) = \frac{f_t(t_A; x_{1_w}) f_t(t_B; x_{1_w})}{f_{t_A - t_B}(t_A - t_B = 0; x_{1_w})} \, , \qquad (8.33)$$

where $f_t(t_A; x_{1_w})$ and $f_t(t_B; x_{1_w})$ are the one-particle travel time probabilities for particles A and B, respectively, $f_{t_A - t_B}$ is the separation time probability of the two particles at x_{1_w}, and

$$f_{t_A - t_B}(t_A - t_B = 0; x_{1_w}) = \int_t f_t(t_A = t; x_{1_w}) f_t(t_B = t; x_{1_w}) \, dt \, . \qquad (8.34)$$

CHAPTER 9

DEVELOPMENT OF THE BACKWARD PROBABILITY MODEL USING CONCENTRATION MEASUREMENTS

Abstract

Backward location and travel time probabilities can be used to determine the former location of contamination in an aquifer. For a contaminant parcel that was detected in an aquifer, the backward location probability describes its position at some time prior to sampling and the backward travel time probability describes the amount of time required for it to travel to the sampling location from some upgradient position. The backward probability model has been developed for one or more detections of contamination [e.g., *Wilson and Liu*, 1994; *Neupauer and Wilson*, 1999; Chapter 8]; however, these models only accounted for the presence of contamination, and did not use the measured concentration. In practical situations concentration measurements are taken, and they provide additional information that can be used to characterize the prior position of contamination. We present an approach for incorporating concentration measurements into the backward probability model. If the source mass is known or fairly well-constrained, the additional information reduces the variances of the location and travel time probability distributions and improves the characterization of the contamination source.

9.1 Introduction

When contamination is detected in an aquifer, the source of contamination is often unknown. To remediate the aquifer or to assign responsibility, we might need to identify the source of contamination or the time of release of contamination from the source. In conventional contaminant transport modeling, the source of contamination is known or assumed to be known, and the future positions of the contaminant plume are simulated. If the source of contamination is unknown, this conventional transport modeling approach can be cumbersome to use. A more efficient approach for characterizing sources of groundwater contamination is backward modeling [*Wilson and Liu*, 1994, 1997; *Neupauer and Wilson*, 1999].

Backward modeling is based on backward location and travel time probabilities. For a solute parcel that was detected in an aquifer, backward location probability describes its position at some time prior to sampling, and backward travel time probability describes the amount of time required for the solute parcel to travel to the sampling location from some upgradient position, such as a known or suspected contamination source. In backward modeling, the sampling location is treated as a source of probability, and probability is transported upgradient in backward time to obtain information about the prior position of the detected contamination.

Backward location and travel time probability models have been used to characterize sources of groundwater contamination, to delineate pumping well capture zones, and to identify the prior position of contamination in groundwater. By reversing the flow field in a random walk method, *Bagt-*

zoglou et al. [1992] obtained backward location probabilities that were used for identifying sources of contamination. *Uffink* [1989] and *Chin and Chittaluru* [1994] used a similar random walk approach to delineate capture zones around pumping wells. *Wilson and Liu* [1994, 1997] used a heuristic method to obtain a backward probabilistic continuum model from the forward advection-dispersion equation using a single detection of contamination. The approach was validated using data from a field-scale tracer experiment at the Borden site [*Wilson and Liu*, 1997]; however, no formal justification was given for the model. *Neupauer and Wilson* [1999, 2000a] showed that backward probabilities are related to adjoint states of concentration and presented a formal framework for obtaining the governing equation of the backward probability model using adjoint theory. The backward model for reactive transport (first-order decay, and linear equilibrium and non-equilibrium sorption) and non-uniform and transient flow has been developed heuristically by *Liu* [1995] and formally in Chapters 5 and 6 using adjoint theory. In Chapter 8, we extended the model to multiple detections of contamination. Each detection provides additional information about the prior location of contamination, resulting in a variance reduction of the probability distributions.

Previous work on backward modeling dealt only with the location and time of the detection. In practical situations we also know the concentration of the detected contamination. Concentration measurements provide additional information that can be used to characterize the source. For example, if we made two detections with concentrations of 1000 mg/L and 1 mg/L, the 1000-mg/L-detection presumably can provide more information about the contamination source. Thus, it is more informative to use concentration mea-

surements than to simply consider the presence of contamination at the two locations, and the additional information can reduce the variance of the probability distributions.

In this paper, we incorporate the use of concentration measurements into the backward probability model and show that the additional information reduces the variance of the distributions. In the next section, we review the background on contaminant transport modeling and the forward probability model. We then review the backward probability model for single and multiple detections of contamination. Finally, we present the procedure for using concentration measurements to obtain location and travel time probabilities, first for a single detection and then for multiple detections. The results show that if the source mass is well-constrained, the variance of the resulting distributions are smaller than the variance of the distributions obtained without using concentration measurements. We develop the procedure for a conservative chemical in a steady, uniform, one-dimensional flow field. It can be extended to multiple dimensions, complex flow fields, and reactive chemicals using the approaches in *Neupauer and Wilson* [2000a] and Chapters 5 and 6.

9.2 Contaminant Transport and Probability Models

In this section, we present background on contaminant transport in groundwater (forward model) and forward and backward location and travel time probabilities. We illustrate the concepts with a simple one-dimensional example.

9.2.1 Contaminant Transport

Transport of a conservative chemical in groundwater can be modeled using the advection-dispersion equation (ADE)

$$\frac{\partial C}{\partial t} = \frac{\partial}{\partial x_i}\left(D_{ij}\frac{\partial C}{\partial x_j}\right) - \frac{\partial}{\partial x_i}\left(v_i C\right) + \frac{q_I}{\theta}C_I - \frac{q_O}{\theta}C \ , \tag{9.1}$$

$$C(\mathbf{x}, t_o) = C_i(\mathbf{x})$$

$$C(\mathbf{x}, t) = g_1(t) \text{ on } \Gamma_1$$

$$\left[D_{ij}\frac{\partial C}{\partial x_j}\right] \mathrm{n}_i = g_2(t) \text{ on } \Gamma_2$$

$$\left[v_i C - D_{ij}\frac{\partial C}{\partial x_j}\right] \mathrm{n}_i = g_3(t) \text{ on } \Gamma_3 \ \ ,$$

where $C(\mathbf{x}, t)$ is resident concentration, t is time, x_i are the spatial directions $(i = 1, 2, 3)$, $\mathbf{x} = (x_1, x_2, x_3)$, D_{ij} is the i, j^{th} entry of the dispersion tensor, v_i is the groundwater velocity in the direction of x_i, q_I is the source flow rate per unit volume, C_I is the source strength, θ is porosity, q_O is the sink flow rate per unit volume, t_o is the initial time, C_i is the initial concentration, g_1, g_2, and g_3 are known functions, Γ_1, Γ_2, and Γ_3 are the domain boundaries, and n_i is the outward unit normal vector in the x_i direction. Resident concentration is a measure of the mass of solute per unit volume of water, or a volume-averaged concentration.

As an example, consider the one-dimensional, confined aquifer shown in Figure 9.1. It is infinite in extent with water flowing from right to left, and no internal sources or sinks of water. A contamination source is present at x_{1_o} and a monitoring well is located at x_{1_w}. For an instantaneous input of a conservative chemical at the source at x_{1_o} at time t_o, the governing equation for

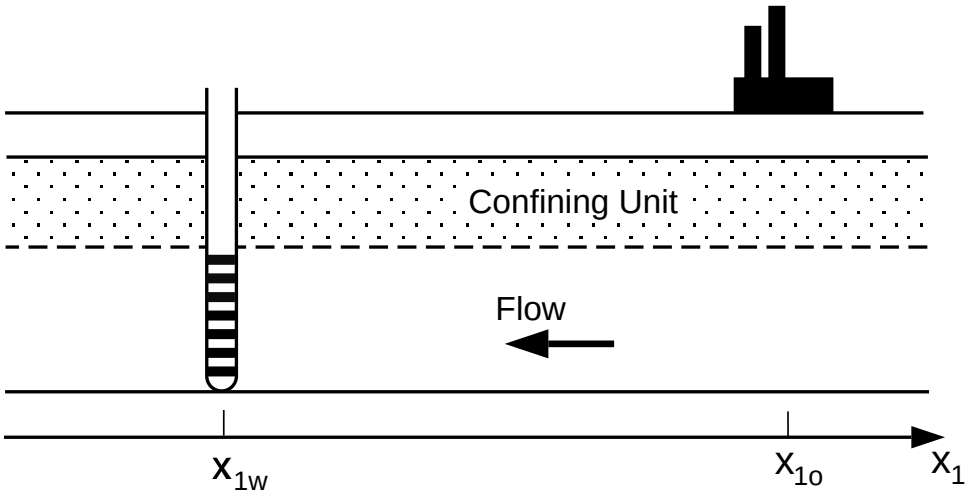

Figure 9.1: Sample one-dimensional aquifer.

contaminant transport is (9.1), with $q_I = q_O = 0$ and $C_i(x_1) = M'\delta(x_1 - x_{1_o})$, where M' is the source mass per unit cross-sectional area of water in the aquifer. For this model, the boundary conditions are $C \to 0$ as $x_1 \to \pm\infty$. The solution of this equation for constant v and D is [*Carslaw and Jaeger*, 1959; *Bear*, 1972]

$$C(x_1, t) = \frac{M'}{\sqrt{4\pi D(t - t_o)}} \exp\left\{-\frac{[x_1 - x_{1_o} - v(t - t_o)]^2}{4D(t - t_o)}\right\} , \tag{9.2}$$

and is plotted in Figure 9.2 for $M' = 2.0$ g/m^2, $D = 3$ m^2/d, $x_{1_o} = 200$ m, $v = -1$ m/d, and $t_o = 0$. The parameter values, listed in Table 9.1, are used throughout this paper unless otherwise stated. The solid line shows the concentration distribution at $t = 100$ days after release from the source.

For constant v and D, (9.1) can also be solved for flux concentration [*Kreft and Zuber*, 1978; *Parker and van Genuchten*, 1984]. Flux concentration is a measure of the solute mass flux per unit water flux, or a flux-averaged

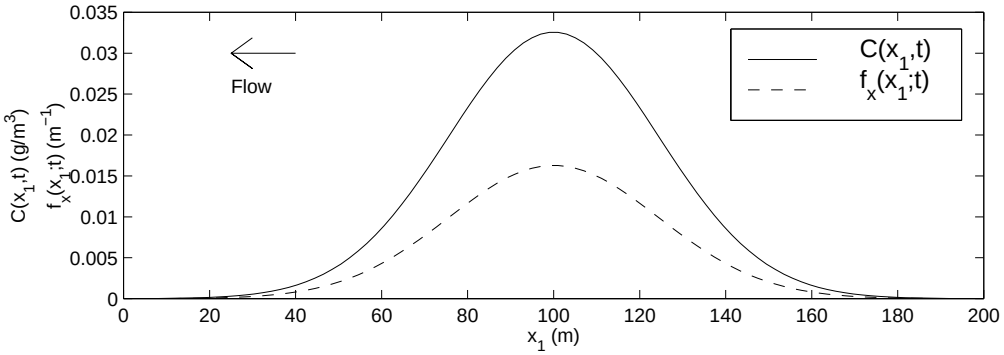

Figure 9.2: Resident concentration and forward location probability at $t = 100$ days after release from an instantaneous point source of contamination at $x_{1_o} = 200$ m. ($M' = 2.0$ g/m^2, $D = 3$ m^2/d, $v = -1$ m/d).

Table 9.1: Transport parameter values.

Parameter	Value
Source mass, M'	2.0 g/m^2
Dispersion coefficient , D	3 m^2/d
Velocity, v	-1 m/d
Porosity, θ	0.3
Well location, x_{1_w}	100 m
Source location, x_{1_o}	200 m
Release time, t_o	0

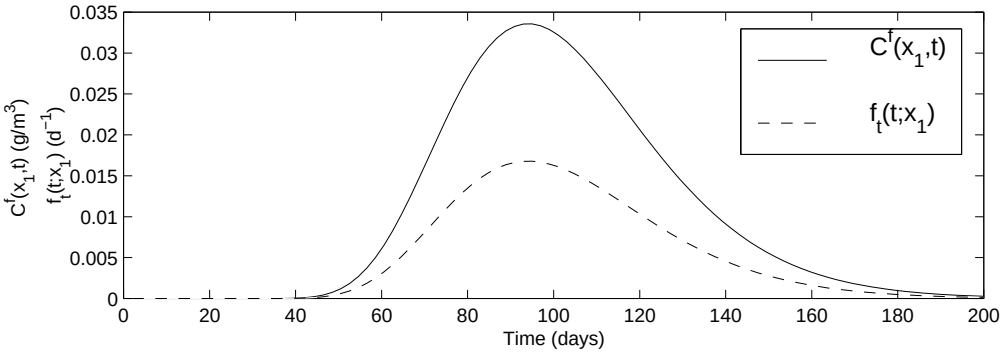

Figure 9.3: Flux concentration and forward travel time probability at $x_{1_w} = 100$ m due to release from an instantaneous point source of contamination at $x_{1_o} = 200$ m. ($M' = 2.0$ g/m^2, $D = 3$ m^2/d, $v = -1$ m/d, $\theta = 0.3$, $t_o = 0$).

concentration. In one dimension, the relationship between flux and resident concentration is [*Parker and van Genuchten*, 1984]

$$C^f = C - \frac{D}{v}\frac{\partial C}{\partial x} \;, \tag{9.3}$$

where C^f is flux concentration. Using (9.2) in (9.3), we obtain an expression for flux concentration at location x_1

$$C^f(x_1, t) = \frac{M'(x_1 - x_{1_o} + vt)}{4v\sqrt{\pi D t^3}} \exp\left\{-\frac{(x_1 - x_{1_o} - vt)^2}{4Dt}\right\} \;, \tag{9.4}$$

which is plotted in Figure 9.3 using the parameter values in Table 9.1. The solid line shows the flux concentration at $x_{1_w} = 100$ m for a release at $x_{1_o} = 200$ m.

9.2.2 Forward Probability Model

Location and travel time probabilities are often used in forward modeling to describe solute transport in groundwater [e.g., *Dagan*, 1982, 1987; *Jury*,

1982; *Jury and Roth*, 1990; *Chin and Chittaluru*, 1994]. In this section, we show the relationship between concentration and forward probabilities.

Forward location probability describes the position of a solute parcel at a fixed time after its release from the source [*Dagan*, 1982, 1987, 1989; *Jury and Roth*, 1990; *Chin and Chittaluru*, 1994] and is related to resident concentration [*Dagan*, 1987; *Jury and Roth*, 1990]. The normalized concentration distribution at some time t after release from an instantaneous point source is equivalent to the location probability density function at time t, given by

$$f_{\mathbf{x}}(\mathbf{x};t) = \frac{C(\mathbf{x},t)}{\int_\Omega C(\mathbf{x},t_o^+)\, d\Omega}, \tag{9.5}$$

where $f_{\mathbf{x}}(\mathbf{x};t)$ is location probability at time t, $\mathbf{x}$ is the position vector, $C(\mathbf{x},t)$ is the resident concentration distribution from an instantaneous point source, Ω is the spatial domain, and $\int_\Omega C(\mathbf{x},t_o^+)\, d\Omega = M'$, where M' is a measure of the total mass that entered the system. For the one-dimensional domain in Figure 9.1, the location probability obtained from (9.5) and (9.2) is

$$f_x(x_1;t) = \frac{1}{\sqrt{4\pi D(t-t_o)}} \exp\left\{-\frac{[x_1 - x_{1_o} - v(t-t_o)]^2}{4D(t-t_o)}\right\}. \tag{9.6}$$

Figure 9.2 shows the location probability of a contaminant particle at $t =$ 100 days due to a release from a source at $x_{1_o} = 200$ m at time $t_o = 0$. This curve represents the probability that the particle is at location x_1 (random variable) at $t = 100$ days, and the most likely location is $x_1 = 100$ m. The location probability in (9.6) could also be obtained from (9.1), by replacing C with f_x as the state variable, and with $q_I = q_O = 0$, $f_x(x_1;t_o) = \delta(x - x_{1_o})$,

and $f_x \to 0$ as $x \to \pm\infty$. The initial condition is this case is an instantaneous point source of probability at the contamination source, indicating that for a contaminant particle released at the source at time $t = t_o$, there is a probability of one that it exists at the source location at $t = t_o$ and a probability of zero that it is at any other location.

Forward travel time probability describes the time required for a solute parcel to travel from its source to a location of interest [*Jury*, 1982; *Jury et al.*, 1986; *Dagan*, 1989; *Dagan and Nguyen*, 1989], and is related to flux concentration [*Shapiro and Cvetkovic*, 1988; *Rubin and Dagan*, 1992]. For an instantaneous point source of contamination, the normalized flux concentration at a downgradient location, $\mathbf{x}$, is equivalent to the travel time probability density function for that location, given by

$$f_t(t;\mathbf{x}) = \frac{C^f(\mathbf{x},t)}{\int_0^\infty C^f(\mathbf{x},t)dt} = \frac{|v|AC^f(\mathbf{x},t)}{M'} \,, \tag{9.7}$$

where $f_t(t;\mathbf{x})$ is travel time probability from the source to $\mathbf{x}$, v is the groundwater velocity, $C^f(\mathbf{x},t)$ is flux concentration, M' is a measure of the total amount of mass that entered at the source, and A is a flow area. We consider travel time probability across a plane perpendicular to flow, and A is the cross-sectional area of this plane. For the one-dimensional domain in Figure 9.1, the forward travel time probability can be obtained from (9.7) and (9.4) and is given by

$$f_t(t;x_1) = \frac{|v|\left[x_1 - x_{1_o} + v(t-t_o)\right]}{4v\sqrt{\pi D(t-t_o)^3}} \exp\left\{-\frac{\left[x_1 - x_{1_o} - v(t-t_o)\right]^2}{4D(t-t_o)}\right\} \,. \tag{9.8}$$

The forward travel time probability at $x_{1_w} = 100$ m for a source release at

$x_{1_o} = 200$ m is shown by the dashed line in Figure 9.3. For a single contaminant particle that entered the source at $x_{1_o} = 200$ m, this curve represents the probability that the particle arrives at the monitoring well ($x_{1_w} = 100$ m) at time t (random variable). The most likely arrival time for the particle is $t \approx 95$ days. For constant v and D, this curve can also be obtained from (9.1), by replacing C with f_t as the state variable, and with $q_I = q_O = 0$, $f_t(0; x_1) = \delta(x - x_{1_o}) - (D/v)\delta'(x - x_{1_o})$,where δ' is the derivative of the Dirac delta function, and $f_t \to 0$ as $x \to \pm\infty$.

9.2.3 Backward Probability Model

In forward modeling we model the movement of solute (or probability) downgradient away from the contamination source and obtain information about the future position of the contamination. With backward modeling we treat the sampling location as a source of probability and allow the probability to advect upgradient in backward time and to spread out by dispersion. The resulting plume of backward probability gives information about the former position of contamination. For a solute parcel that was detected in an aquifer, backward location probability describes its position at some time prior to sampling, and backward travel time probability describes the amount of time required for the solute parcel to travel to the sampling location from some upgradient position, such as a known or suspected contamination source.

The mathematical model for backward probabilities for a single detection of contamination is the adjoint of (9.1), given by [*Neupauer and Wilson*,

2000a]

$$\frac{\partial \psi^*}{\partial \tau} = \frac{\partial}{\partial x_i}\left(D_{ij}\frac{\partial \psi^*}{\partial x_j}\right) + \frac{\partial}{\partial x_i}(v_i \psi^*) - \frac{q_I}{\theta}\psi^* + \frac{\partial h}{\partial C} \tag{9.9}$$

$$\psi^*(\mathbf{x}, 0) = 0$$

$$\psi^*(\mathbf{x}, \tau) = 0 \text{ on } \Gamma_1$$

$$\left[D_{ij}\frac{\partial \psi^*}{\partial x_j} + v_i \psi^*\right] \mathrm{n}_i = 0 \text{ on } \Gamma_2$$

$$\left[D_{ij}\frac{\partial \psi^*}{\partial x_j}\right] \mathrm{n}_i = 0 \text{ on } \Gamma_3 \ ,$$

where ψ^* is the adjoint state (related to either location or travel time probability), τ is backward time or time prior to sampling ($\tau = T - t$, where $t = T$ is the sampling time), and h is a performance functional that depends on the type of probability and the detection mechanism (e.g., pumping well, monitoring well). The term $\partial h / \partial C$, called the load term, is a Fréchet derivative of the performance functional, h, with respect to concentration, C [*Neupauer and Wilson*, 1999]. The adjoint equation describes a family of adjoint states; a particular adjoint state is defined by the load term, through the choice of the performance functional. *Neupauer and Wilson* [2000a] suggest performance functionals for several different cases.

Although the basic form of the advection-dispersion equation (9.1) and its adjoint (9.9) are similar, several differences between the two equations are evident. First, the flow field in the adjoint equation is reversed. This can be observed by noting that the sign on the advection term is reversed and that the sources in (9.1) become sinks in (9.9), and vice versa. This flow field reversal in the adjoint equation allows the backward probability to travel

upgradient, away from the detection and toward the possible contamination sources. Another difference between the two equations is that the backward equation is written in terms of backward time, τ, while the forward equation is written in terms of forward time, t. Thus, the forward model predicts the future position of contamination; while the backward model identifies the prior positions of contamination. A final difference between the two equations is that the boundary conditions on Γ_2 and Γ_3 are different. The second type boundary condition in the forward model (on Γ_2) becomes a third boundary condition in the backward model, and the third type boundary in the forward model (on Γ_3) becomes second type in the backward model.

Suppose contamination is detected at one location in an aquifer, but the source of contamination is unknown. We denote backward location probability for this single detection as $f_{\mathbf{x}}(\mathbf{x};\tau,\mathbf{x}_w)$, where $\mathbf{x}$ is the particle position (random variable), τ is the time of interest prior to detection (deterministic parameter), and $\mathbf{x}_w$ is the detection location (deterministic parameter). This probability can be calculated using (9.9), with the appropriate load term described in *Neupauer and Wilson* [1999, 2000a]. For a detection at the monitoring well in the one-dimensional domain shown in Figure 8.1, the governing equation for backward location probability is [*Neupauer and Wilson*, 1999]

$$\frac{\partial f_x}{\partial \tau} = D\frac{\partial^2 f_x}{\partial x_1^2} + v\frac{\partial f_x}{\partial x_1} + \delta(x_1 - x_{1_w})\delta(\tau) \tag{9.10}$$

$$f_x \rightarrow 0 \text{ as } x \rightarrow \pm\infty$$

$$f_x(x_1;0,x_{1_w}) = 0$$

where D is the dispersion coefficient, v is the groundwater velocity, and x_{1_w} is

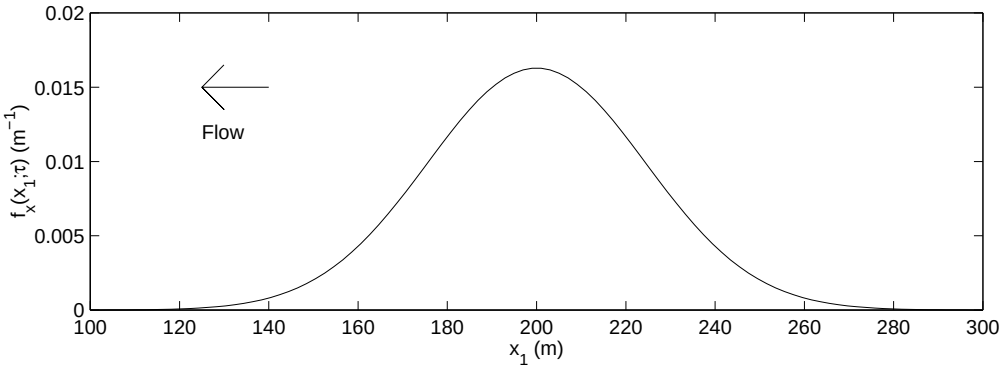

Figure 9.4: Single-detection backward location probability for $\tau = 100$ days prior to detection at $x_{1_w} = 100$ m. ($D = 3$ m^2/d, $v = -1$ m/d).

the location of the monitoring well. The load term, $\delta(x_1 - x_{1_w})\delta(\tau)$, produces an instantaneous point source of probability at the time and place of detection. The solution of (9.10) is [*Neupauer and Wilson*, 2000b]

$$f_x(x_1;\tau,x_{1_w}) = \frac{1}{\sqrt{4\pi D\tau}}\exp\left\{-\frac{(x_1 - x_{1_w} + v\tau)^2}{4D\tau}\right\} . \tag{9.11}$$

Here, the random variable, x_1, represents the prior location of the contamination at time τ prior to detection. If the source release was known to be at time τ, then x_1 would represent the source location x_{1_o} (still a random variable). Figure 9.4 shows plot of backward location probability (9.11) at time $\tau = 100$ days prior to detection at $x_{1_w} = 100$ m. The transport parameters are shown in Table 9.1. At $\tau = 100$ days, the most likely location of the detected particle is $x_1 = 200$ m.

The single-detection backward location probability can be generalized to account for multiple detections of contamination. The multiple-detection location probability for N detections is related to the single-detection location

probabilities for each of the N detections, given by [Chapter 8]

$$f_{\mathbf{x}}(\mathbf{x}_1 = \mathbf{x}_2 = \ldots = \mathbf{x}_N = \mathbf{x}; \tau) = \frac{\prod_{k=1}^{N} f_{\mathbf{x}}(\mathbf{x}_k; \tau)}{\int_{\mathbf{x}} \prod_{k=1}^{N} f_{\mathbf{x}}(\mathbf{x}_k; \tau)\, d\mathbf{x}} \,, \tag{9.12}$$

where N is the number of detections, $f_{\mathbf{x}}(\mathbf{x}_k; \tau)$ is the single-detection location probability for detection k, $\mathbf{x}_k$ denotes the prior position of the particle from detection k, and the integral is evaluated over all spatial dimensions.

Backward travel time probability for a single detection of contamination is denoted by $f_\tau(\tau; \mathbf{x}, \mathbf{x}_w)$, where τ is the particle's travel time in backward time (random variable), $\mathbf{x}$ is the location of interest (deterministic parameter), and $\mathbf{x}_w$ is the detection location (deterministic parameter). We assume that the detection occurred at $\tau = 0$. This probability can be calculated from the adjoint of the advection-dispersion operator (9.9), with an appropriate load term, described in *Neupauer and Wilson* [2000a]. For a detection at the monitoring well in the domain shown in Figure 8.1, the governing equation for backward travel time probability is [*Neupauer and Wilson*, 2000a]

$$\frac{\partial \psi^*}{\partial \tau} = D\frac{\partial^2 \psi^*}{\partial x_1^2} + v\frac{\partial \psi^*}{\partial x_1} + \delta(x_1 - x_{1_w})\delta(\tau) + \frac{D}{v}\delta'_{x_1}(x_1 - x_{1_w})\delta(\tau) \tag{9.13}$$

$$\psi^* \to 0 \text{ as } x \to \pm\infty$$

$$\psi^*(0; x_1, x_{1_w}) = 0 \,,$$

where $\delta'_{x_1}(x_1 - x_{1_w})$ denotes the derivative of the Dirac delta function with respect to x_1, and travel time probability is a function of the adjoint state, ψ^*, given by $f_\tau(\tau; x_1, x_{1_w}) = |v(x_1)|\psi^*(x_1, \tau)$, for the one-dimensional problem

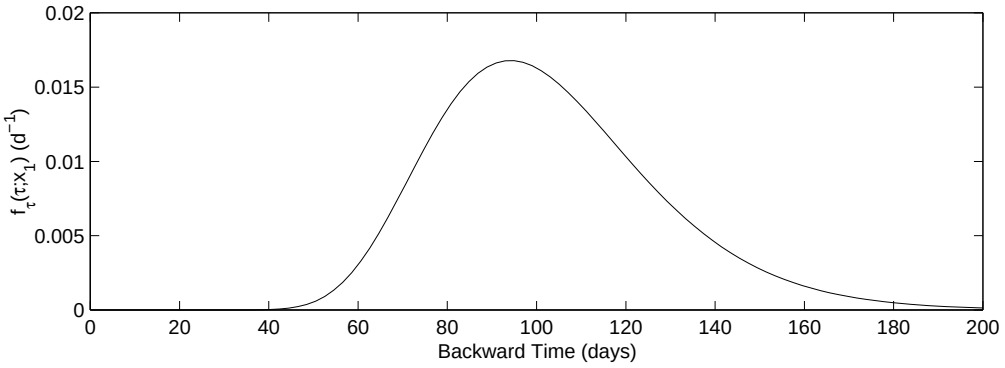

Figure 9.5: Single-detection backward travel time probability at $x_1 = 200$ m for a detection at $x_{1_w} = 100$ m. ($D = 3$ m^2/d, $v = -1$ m/d).

shown here. The solution of (9.13) is [*Neupauer and Wilson*, 2000b]

$$f_\tau(\tau; x_1, x_{1_w}) = \frac{-|v|(x_1 - x_{1_w} - v\tau)}{4v\sqrt{\pi D\tau^3}} \exp\left\{-\frac{(x_1 - x_{1_w} + v\tau)^2}{4D\tau}\right\} . \quad (9.14)$$

Here, the random variable, τ, is the backward travel time of the contaminant parcel, i.e., the time prior to sampling when the contaminant parcel was at location x_1. Figure 9.5 shows a plot of backward travel time probability at $x_1 = 200$ m for a detection at $x_{1_w} = 100$ m. The transport parameters are shown in Table 9.1. For the particle detected at $x_{1_w} = 100$ m at $\tau = 0$, its most likely travel time from $x_1 = 200$ m to the detection is $\tau \approx 95$ days.

The single-detection backward travel time probability can be generalized to account for multiple detections of contamination. The multiple-detection travel time probability for N detections is related to the single-detection travel time probabilities for each of the N detections, given by [Chap-

ter 8]

$$f_\tau(\tau_1 = \tau_2 = \ldots = \tau_N = \tau; \mathbf{x}) = \frac{\prod_{k=1}^{N} f_\tau(\tau_k; \mathbf{x})}{\int_\tau \prod_{k=1}^{N} f_\tau(\tau_k; \mathbf{x})\ d\tau}\ , \tag{9.15}$$

where N is the number of detections and $f_\tau(\tau_k; \mathbf{x})$ is the single-detection location probability for detection k.

9.3 Single-Detection Probabilities Using Concentration Measurements

If contamination is detected in an aquifer, the concentration of the sample is usually measured. The sampled concentration depends on the source mass, source history, distance from the source, travel time, transport parameter values, and measurement error. In this paper, we assume that the transport parameters are known exactly and that the source of contamination is an instantaneous point source. The remaining unknown parameters are the total source mass and the source location or release time.

For an instantaneous release of a conservative solute from a point source, the plume centroid travels at approximately the same velocity as the groundwater, assuming flow is unaffected by concentration. The plume concentrations are higher near its center of mass, and lower away from the center. By comparing the concentrations of two (or more) detections, we can obtain some information about the relative position of the two detections within the plume. For example, the larger of the two detections is more likely to have been sampled near the plume centroid. Since the plume centroid travels with the velocity of the groundwater, the larger detection provides more informa-

tion about the source location. The absolute concentration of either or both detections is useful if we have some knowledge of the source mass.

If we have only one detection, the concentration provides no additional information, unless the source mass is known or can be described by a probability distribution. In this section, we first develop the backward location and travel time probabilities for a known source mass. Then we generalize the results by replacing the known source mass with a probability distribution of possible source masses. A reasonable upper limit of the source mass is the mass that would produce the solubility limit of the chemical in the aquifer, and a reasonable lower limit is zero.

9.3.1 Known Source Mass and Exact Sampling

Suppose we are interested in the concentration at the monitoring well in the one-dimensional domain in Figure 9.1. If the source mass and transport parameters are known exactly, then the concentration distribution is given by (9.2). The concentration distribution is plotted in Figure 9.6 for $M' = 2.0$ g/m^2, $D = 3$ m^2/d, $t = 100$ days, $v = -1$ m/d, and $t_o = 0$ for three different values of x_{1_o}. The concentration at the monitoring well at time $t = 100$ days after release from one of the three sources is shown in Table 9.2. For these parameters, we see from Figure 9.6 and Table 9.2 that the maximum possible concentration at x_{1_w} at $t = 100$ days is $C(x_{1_w}, t) \approx 0.033$ g/m^3, and this occurs if the source location is at $x_{1_o} = 200$ m. For all other source locations, $C(x_{1_w}, t) < 0.033$ g/m^3; and $C(x_{1_w}, t) > 0.033$ g/m^3 is impossible. We also see that the maximum concentration anywhere in the aquifer is independent of

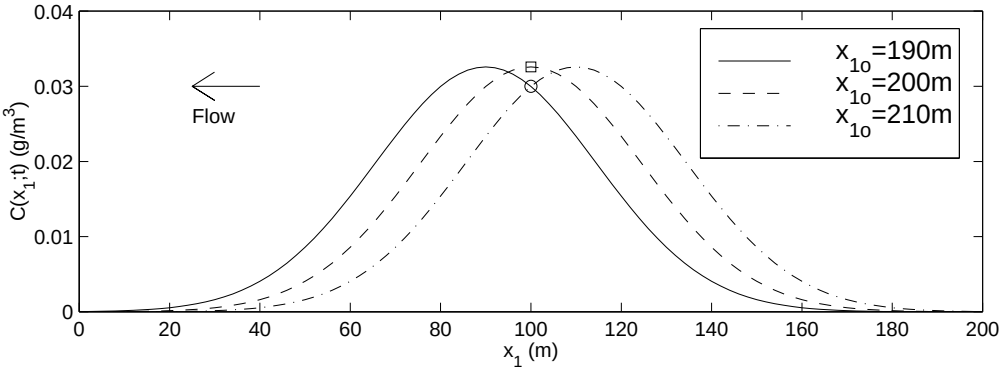

Figure 9.6: Concentration distribution at $t = 100$ days after release for three different source locations. The concentrations at the monitoring well ($x_{1_w} = 100$ m) are shown with the square for $x_{1_o} = 200$ m and by the circle for $x_{1_o} = 190$ m and $x_{1_o} = 210$ m. ($M' = 2.0$ g/m^2, $D = 3$ m^2/d, $v = -1$ m/d).

Table 9.2: Concentration at the monitoring well at $t = 100$ days after release from three different sources.

Source Location	$C(x_{1_w}, t)$
190 m	0.030 g/m^3
200 m	0.033 g/m^3
210 m	0.030 g/m^3

the source location. We define $C_{\max}(t)$ to be the maximum concentration that can be achieved at time t for the given transport parameters, source mass, and source release time. For this example, $C_{\max}(t = 100 \text{ days}) \approx 0.033$ g/m^3.

Suppose the source location is unknown, but the concentration at the monitoring well is known and the sample contains no measurement error. We can rearrange (9.2) to obtain an expression for the source location as a function

of the measured concentration, $C(x_{1_w}, t)$, given by

$$x_{1_o} = x_{1_w} - v(t - t_o) \pm \sqrt{-4D(t - t_o)\left\{\ln\left[\sqrt{4\pi D(t - t_o)}\frac{C(x_{1_w}, t)}{M'}\right]\right\}} \quad (9.16)$$

Depending on the values of the parameters in this equation, we obtain either zero, one, or two possible values of x_{1_o}. If the source location is known, but the release time is unknown, a similar process can be followed. As with source location, there could be zero, one, or two possible release times. An iterative procedure would be needed to obtain t from (9.2). We do not show this case here.

9.3.2 Known Source Mass and Inexact Sampling

In practical situations the sampled concentration contains measurement error, ϵ. We show the procedure for obtaining backward location probability based on a concentration measurement that contains additive error. For the aquifer in Figure 9.1, the measured concentration, $\hat{C}$, is

$$\hat{C} = \frac{M'}{\sqrt{4\pi D(t - t_o)}} \exp\left\{-\frac{[x_{1_w} - x_{1_o} - v(t - t_o)]^2}{4D(t - t_o)}\right\} + \epsilon \ , \quad (9.17)$$

where the first term on the right-hand side is C from (9.2), M' is a measure of the source mass which we assume is known, and $\epsilon = \hat{C} - C$ is the measurement error. We assume that resident concentration is measured and that the measurement error is normally distributed with mean zero and variance σ_ϵ^2,

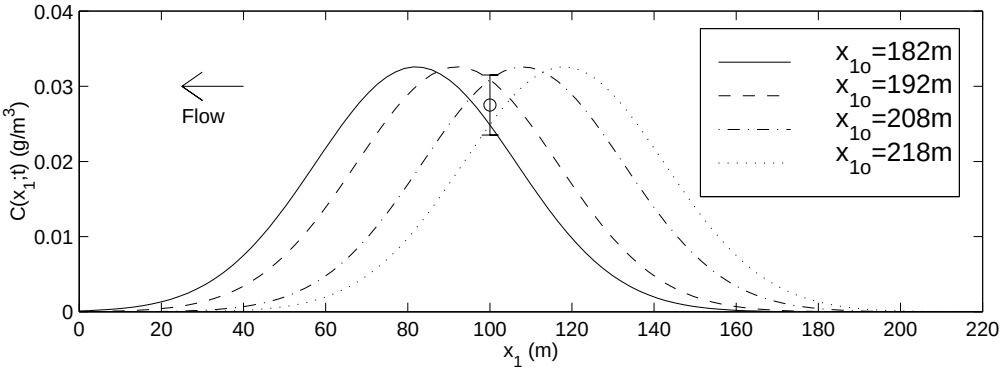

Figure 9.7: Sampled concentration ($\circ$) and contaminant plumes from four possible source locations. Error bars represent two standard deviations. (t = 100 days, x_{1_w} = 100 m, $\hat{C}$ = 0.0275 g/m^3, M' = 2.0 g/m^2, D = 3 m^2/d, $v = -1$ m/d, $t_o = 0$).

$N(0, \sigma_\epsilon^2)$, according to the probability density function

$$f_\epsilon(\epsilon) = \frac{1}{\sqrt{2\pi}\sigma_\epsilon} \exp\left\{-\frac{\epsilon^2}{2\sigma_\epsilon^2}\right\} . \tag{9.18}$$

Suppose contamination is sampled at the monitoring well at x_{1_w} = 100 m at time t = 100 days, with $\hat{C}(x_{1_w}, t)$ = 0.0275 g/m^3, and the measurement error has a standard deviation of σ_ϵ = 0.002 g/m^3. The sample is plotted in Figure 9.7, along with errors bars representing two standard deviations. The plot also shows contaminant plumes at t = 100 days after release from four different source locations. Note that all of these source locations are possible since the concentration at x_{1_w} from each of those sources falls within the error bars on the measurement. Many other source locations would also result in a value of $C(x_{1_w}, t)$ that falls within the error bars. Thus, with measurement error, the number of possible source locations increases substantially.

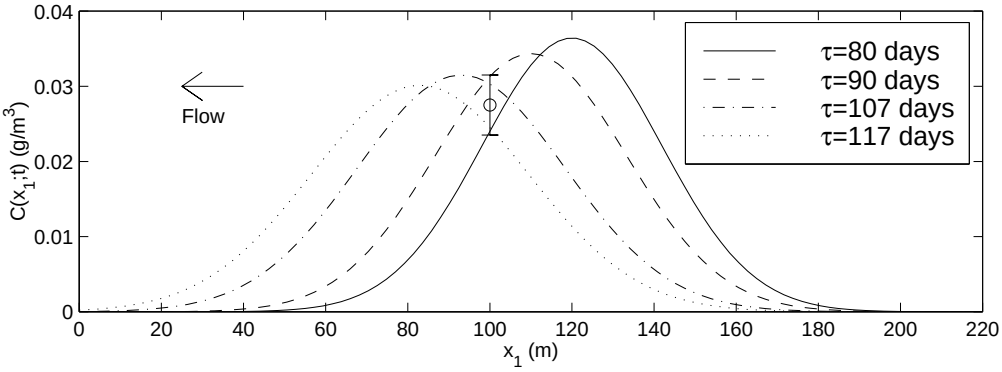

Figure 9.8: Sampled concentration ($\circ$) and contaminant plumes from four possible source release times. Error bars represent two standard deviations. ($t = 100$ days, $x_{1_w} = 100$ m, $M' = 2.0$ g/m^2, $D = 3$ m^2/d, $v = -1$ m/d, $x_{1_o} = 200$ m, $\tau = 100$ days $- t_o$).

The same sample and error bars are also plotted in Figure 9.8, with contaminant plumes from $x_{1_o} = 200$ m at four different release times, t_o, identified as backward time τ, or time prior to detection, $\tau = 100$ days $- t_o$. Note that all of these release times are possible since the concentration at x_{1_w} falls within the error bars on the measurement, and many others also would be possible.

The backward location probability, $f(x_{1_o}|\hat{C};\tau)$, is the probability that the contamination originated at location x_{1_o} (random variable) at $\tau = T$ (fixed parameter), given that a concentration of $\hat{C}$ was measured at the monitoring well at $\tau = 0$. We can define $f(\hat{C}|x_{1_o};t_o)$, as the forward probability of measuring $\hat{C}$ at the monitoring well given a source release at location x_{1_o} at time t_o. From (9.17) and (9.18), we see that for a given source location, x_{1_o}, $\hat{C}$ is a normally-distributed random variable with with mean $C(x_1, t)$ and variance

σ_ϵ^2, $N(C(x_1,t),\sigma_\epsilon^2)$, and $f(\hat{C}|x_{1_o};t_o)$ is given by

$$f(\hat{C}|x_{1_o};t_o) = \frac{1}{\sqrt{2\pi\sigma_\epsilon^2}} \exp\left[-\frac{(\hat{C}-C)^2}{2\sigma_\epsilon^2}\right] , \tag{9.19}$$

where C is defined in (9.2), and all other variables are known. Backward location probability is related to $f(\hat{C}|x_{1_o};t_o)$ through Bayes' theorem,

$$f(x_{1_o}|\hat{C};\tau) = \frac{f(\hat{C}|x_{1_o};t_o) f_{x_{1_o}}(x_{1_o})}{\int_{x_{1_o}} f(\hat{C}|x_{1_o};t_o) f_{x_{1_o}}(x_{1_o})\, dx_{1_o}} , \tag{9.20}$$

where $f_{x_{1_o}}(x_{1_o})$ is a prior distribution on x_{1_o}. A reasonable choice for this prior distribution is (9.11), with $f_{x_{1_o}} = f_x$, the location probability in the absence of any concentration information (i.e., the "no-concentration" probability). We must still calculate $f(\hat{C}|x_{1_o};t_o)$, which, from (9.19), is a function of σ_ϵ, $\hat{C}$, and $C(x_{1_w},t)$. Both σ_ϵ and $\hat{C}$ are known constants, but $C(x_{1_w},t)$ depends on x_{1_o} and t_o and therefore its value changes for each x_{1_o}. *Neupauer and Wilson* [2000a] show that

$$C(x_{1_w}, t = T - t_o; x_{1_o}) = M' f_x(x_{1_w}; \tau = T - t_o, x_1) , \tag{9.21}$$

where $f_x(x_{1_w};\tau = T - t_o, x_1)$ is the no-concentration forward location probability for a detection at x_{1_w}. The forward and backward location probabilities are related by [Chapter 5]

$$\frac{f_x(x_{1_w};\tau = T - t_o, x_1)}{\theta(x_{1_w})} = \frac{f_x(x_1;\tau = T - t_o, x_{1_w})}{\theta(x_1)} ; \tag{9.22}$$

Table 9.3: Variances of single-detection location probability distributions with known source mass.

Distribution	Variance
$\sigma_\epsilon = 0.002$ g/m^3	182 m^2
$\sigma_\epsilon = 0.006$ g/m^3	202 m^2
$\sigma_\epsilon = 0.018$ g/m^3	441 m^2
$\sigma_\epsilon \to \infty$	600 m^2

therefore, we run one simulation of the backward probability model to obtain f_x, and using these results, we obtain C from (9.21), $f(\hat{C}|x_{1_o}; t_o)$ from (9.19), and $f(x_{1_o}|\hat{C}; \tau)$ from (9.20).

A plot of $f(x_{1_o}|\hat{C}; \tau)$ at $\tau = 100$ days is shown in Figure 9.9 for the parameters shown in Table 9.1, and with $\hat{C} = 0.0275$ g/m^3, and three different values of σ_ϵ ($\sigma_\epsilon = 0.002$ g/m^3, 0.006 g/m^3, and 0.018 g/m^3). The plot shows a two-peaked probability distribution with $\sigma_\epsilon = 0.002$ g/m^3 and 0.006 g/m^3, with the left peak representing possible sources if the sample was taken on the trailing edge of the plume, and the right peak representing possible sources if the sample was taken on the leading edge of the plume. For comparison, the no-concentration location probability distribution is also shown on the plot; this is equivalent to $f(x_{1_o}|\hat{C}; \tau)$ with $\sigma_\epsilon \to \infty$. Notice that the spread (variance) of the distributions increases with increasing σ_ϵ, as summarized in Table 9.3. If measurement error is sufficiently small, the probability distribution obtained using the measured concentration has a significantly lower variance than the no-concentration distribution.

The backward travel time probability, $f(\tau|\hat{C}; x_{1_o})$, is the probability

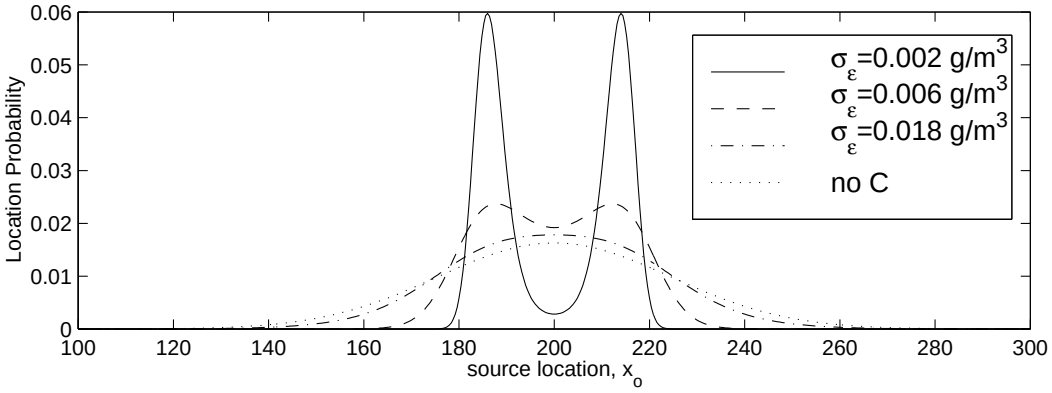

Figure 9.9: Source location probability for one detection of contamination with a known source mass. (τ = 100 days, x_{1_w} = 100 m, M' = 2.0 g/m^2, D = 3 m^2/d, $v = -1$ m/d, $\hat{C} = 0.0275$ g/m^3).

that the contamination originated at x_{1_o} (fixed parameter) at $\tau = T$ (random variable), given that a concentration of $\hat{C}$ was measured at the monitoring well at $\tau = 0$. This probability is related to $f(\hat{C}|x_{1_o}; t_o)$ through Bayes' theorem,

$$f(\tau|\hat{C}; x_{1_o}) = \frac{f(\hat{C}|x_{1_o}; t_o) f_\tau(\tau)}{\int_\tau f(\hat{C}|x_{1_o}; t_o) f_\tau(\tau)\, d\tau}\,, \tag{9.23}$$

where $f_\tau(\tau)$ is a prior distribution on τ, the travel time from x_{1_o} to the monitoring well. A reasonable choice for this prior distribution is (9.14), the no-concentration travel time probability. As stated above, $C(x_{1_w}, t = T - t_o; x_{1_o})$ can be obtained from the no-concentration backward location probability, f_x. Therefore, we can run two simulations of backward location probability, one each for f_x and f_τ, and we can use the results to obtain C from (9.21), $f(\hat{C}|x_{1_o}; t_o)$ from (9.19), and $f(\tau|\hat{C}; x_{1_o})$ from (9.23).

A plot of $f(\tau|\hat{C}; x_{1_o})$ is shown in Figure 9.10 for the parameters shown in Table 9.1, and with $\hat{C} = 0.0275$ g/m^3, and three different values of σ_ϵ

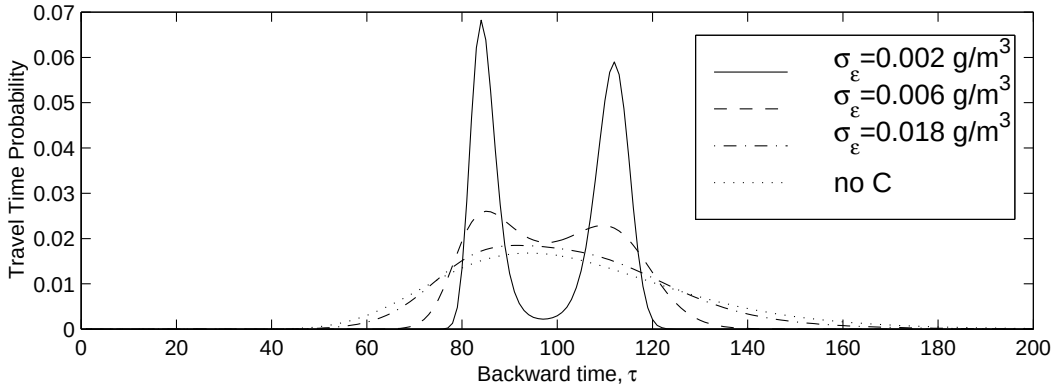

Figure 9.10: Travel time probability for one detection of contamination with a known source mass. ($x_{1_w} = 100$ m, $x_{1_o} = 100$ m, $M' = 2.0$ g/m^2, $D = 3$ m^2/d, $v = -1$ m/d, $\hat{C} = 0.0275$ g/m^3).

($\sigma_\epsilon = 0.002$ g/m^3, 0.006 g/m^3, and 0.018 g/m^3). The plot shows a two-peaked probability distribution for $\sigma_\epsilon = 0.002$ g/m^3 and 0.006 g/m^3, with the left peak representing possible release times if the sample was taken on the leading edge of the plume, and the right peak representing possible release times if the sample was taken on the trailing edge of the plume. For comparison, the no-concentration travel time probability distribution is also shown on the plot; this is equivalent to $f(\tau|\hat{C}; x_{1_o})$ with $\sigma_\epsilon \to \infty$. Notice that the spread of the distributions increases with increasing σ_ϵ, as summarized in Table 9.4. If measurement error is sufficiently small, the probability distribution obtained using the measured concentration has a significantly lower variance than the no-concentration distribution.

Table 9.4: Variances of single-detection travel time probability distributions with known source mass.

Distribution	Variance
$\sigma_\epsilon = 0.002$ g/m^3	182 days^2
$\sigma_\epsilon = 0.006$ g/m^3	199 days^2
$\sigma_\epsilon = 0.018$ g/m^3	452 days^2
$\sigma_\epsilon \to \infty$	621 days^2

9.3.3 Unknown Source Mass and Inexact Sampling

Since the source mass is generally unknown, the source mass in the backward probability model can be treated as a random variable with a specified probability distribution. In the absence of any other information, the probability distribution can be a uniform distribution with an upper limit related to the solubility limit of the chemical and a lower limit of zero. Since the source mass has a random value, (9.19) now represents $f(\hat{C}|M';x_{1_o};t_o)$. To obtain $f(\hat{C}|x_{1_o};t_o)$ for use in (9.20) and (9.23), we use the law of total probability, given by

$$f(\hat{C}|x_{1_o};t_o) = \int_{M'} f(\hat{C}|M';x_{1_o};t_o) f_{M'}(M')\, dM' \,, \tag{9.24}$$

where $f_{M'}(M')$ is the probability distribution for the unknown source mass.

Let M' be a uniform random variable with distribution

$$f_{M'}(M') = \begin{cases} \frac{1}{M_{\mathrm{u}} - M_{\mathrm{l}}} & M_{\mathrm{l}} < M' < M_{\mathrm{u}} \\ 0 & \text{otherwise} \end{cases} \,, \tag{9.25}$$

where M_{u} and M_{l} are the upper and lower bounds of M'. Substituting (9.19), (9.21), and (9.25) into (9.24) and integrating over M', we obtain

$$f(\hat{C}|x_{1_o};t_o) = \frac{1}{2f_x(M_{\mathrm{u}}-M_{\mathrm{l}})}\left[\mathrm{erf}\left(\frac{M_{\mathrm{u}}f_x-\hat{C}}{\sqrt{2\sigma_\epsilon^2}}\right)-\mathrm{erf}\left(\frac{M_{\mathrm{l}}f_x-\hat{C}}{\sqrt{2\sigma_\epsilon^2}}\right)\right]. \quad (9.26)$$

This expression can be used in (9.20) and (9.23) to obtain location and travel time probabilities, respectively.

Figures 9.11 and 9.12 show plots of $f(x_{1_o}|\hat{C};\tau)$ and $f(\tau|\hat{C};x_{1_o})$, respectively, for three different values of M_{u} and three different values of σ_ϵ, along with the no-concentration location probability. In all cases, $M_{\mathrm{l}}=0$. With the range of possible values for M', several source locations are equally likely, indicated by the plateau in each location probability plot. As M_{u} increases, the number of possible source locations increases, thereby increasing the width of the plateau. In the limit as $M_{\mathrm{u}}\to\infty$, all source locations are equally likely. With a small value of σ_ϵ, there is a distinct cutoff between the equally-likely sources and the unlikely sources ($f(x_{1_o}|\hat{(}C)) \approx 0$). As σ_ϵ increases, there is a smoother transition between these two regions because of the measurement error.

The travel time probability plots show a similar plateau-like feature; however, the earlier times are more likely than the later times. As with location probability, as M_{u} increases, the number of possible travel times increases, thereby increasing the width of the plateau. In the limit as $M_{\mathrm{u}}\to\infty$, early times are still more likely than later times. As with location probability, the travel time probability distributions becomes smoother as σ_ϵ increases.

Table 9.5: Variances of single-detection location probability distributions with unknown source mass.

σ_ϵ (g/m^3)	M_u (g/m^2)	Variance (m^2)
0.002	5	436
0.002	50	1355
0.002	500	2289
0.02	5	592
0.02	50	1446
0.02	500	2356
0.2	5	600
0.2	50	902
0.2	500	1762

For small σ_ϵ and small M_u, the variance of the distributions is smaller than the variance of the no-concentration distribution (see Tables 9.5 and 9.6); however, for a fixed σ_ϵ, increasing uncertainty in the initial mass results in a larger variance, often larger than that of the no-concentration distribution.

9.4 Multiple-Detection Probabilities Using Concentration Measurements

Multiple detections of contamination provide additional information about the prior positions of contamination. Here we consider two samples, denoted by A and B; however, the approach can be extended to three or more samples of contamination. For a sampled concentration of $\hat{C}_A = 0.0275$ g/m^3 at $x_{1_A} = 100$ m at $t = 100$ days, Figure 9.7 showed four possible source locations that were likely to have resulted in the measured concentration. If

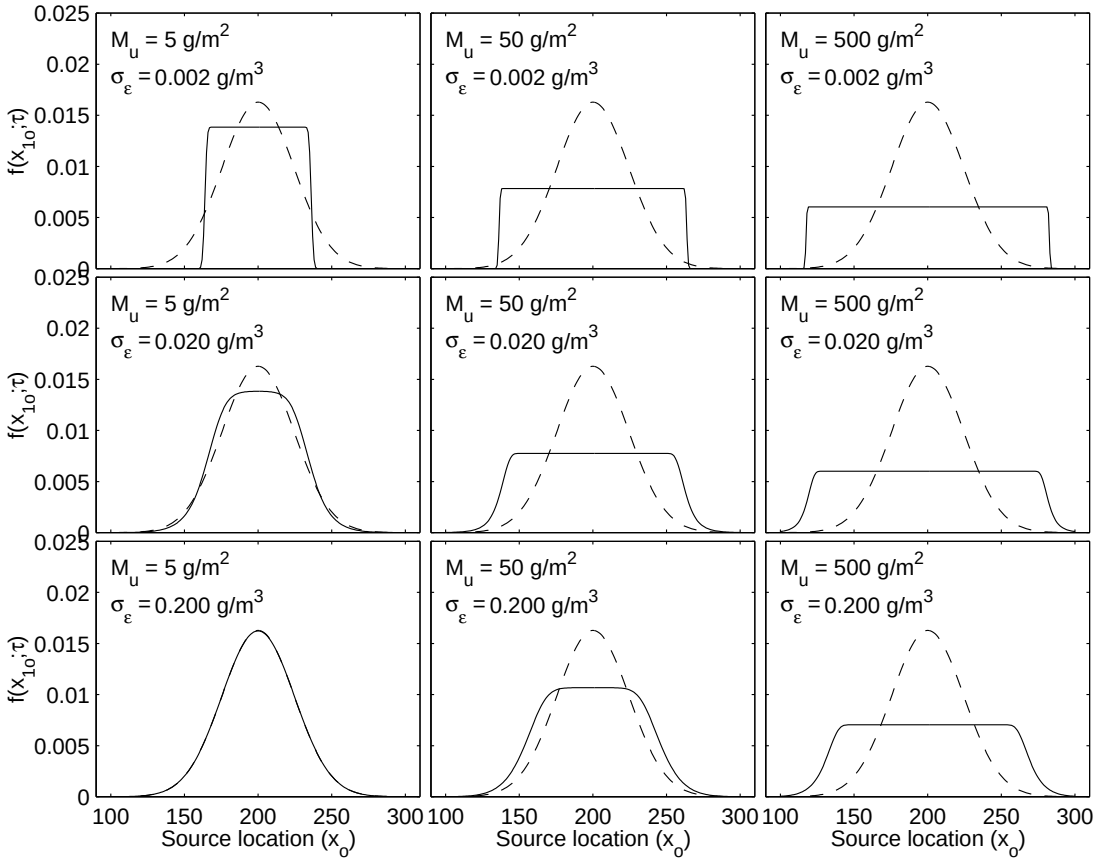

Figure 9.11: Location probability for one detection of contamination with an unknown source mass (solid line) and no-concentration location probability (dashed line). (τ = 100 days, x_{1_w} = 100 m, D = 3 m^2/d, v = -1 m/d, $\hat{C}$ = 0.0275 g/m^3, $M_{\rm l} = 0$, $M_{\rm u}$ varies, σ_ϵ varies).

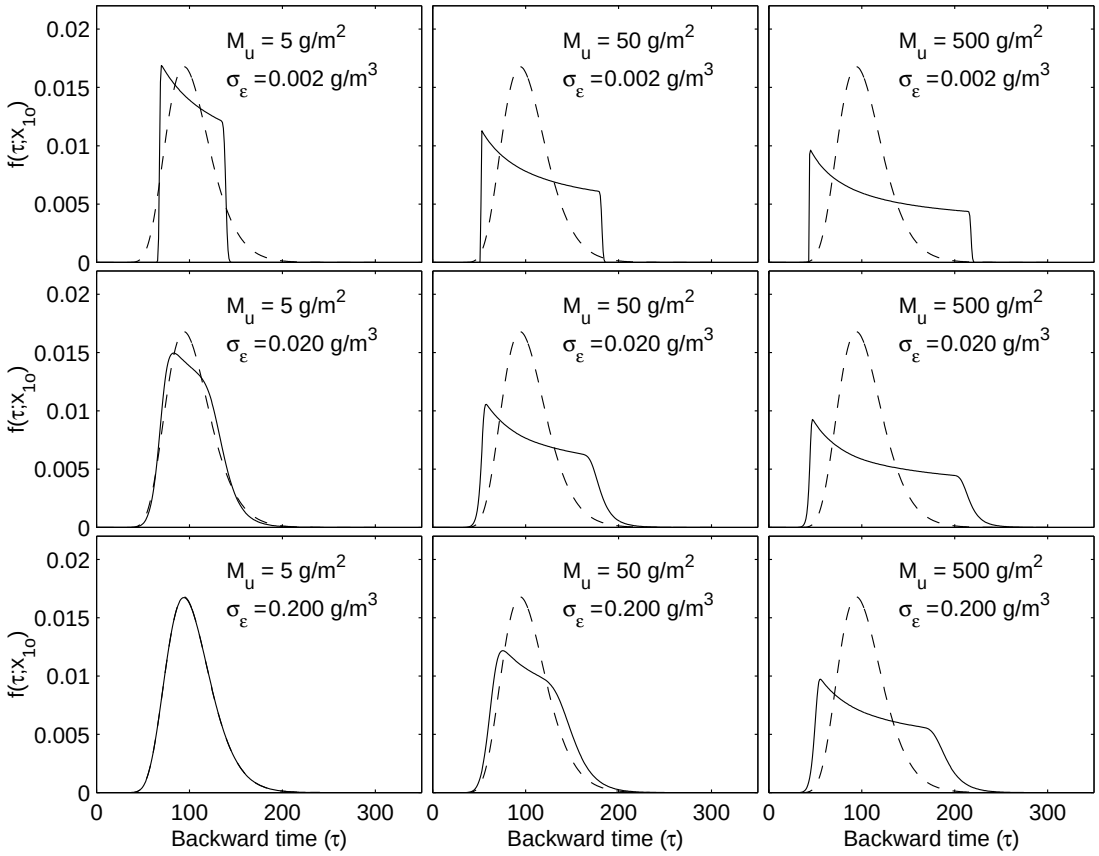

Figure 9.12: Travel time probability for one detection of contamination with an unknown source mass (solid line) and no-concentration travel time probability (dashed line). ($x_{1_w} = 100$ m, $x_{1_o} = 200$ m, $D = 3$ m^2/d, $v = -1$ m/d, $\hat{C} = 0.0275$ g/m^3, $M_\mathrm{l} = 0$, M_u varies, σ_ϵ varies).

Table 9.6: Variances of single-detection travel time probability distributions with unknown source mass.

σ_ϵ (g/m^3)	M_u (g/m^2)	Variance (m^2)
0.002	5	431
0.002	50	1442
0.002	500	2609
0.02	5	622
0.02	50	1575
0.02	500	2734
0.2	5	645
0.2	50	972
0.2	500	1980

an additional measurement of $\hat{C}_B = 0.0135$ g/m^3 is taken at $x_{1_B} = 120$ m at $t = 100$ days, Figure 9.13 show that only two of those source locations could have produced both measured concentration values. Thus, the second sample reduced the number of possible source locations. In this section, we develop the location and travel time probability distributions for multiple measurements of concentration.

For two samples, denoted by A and B, (9.19) can be modified as

$$f(\hat{C}_\beta | x_{1_o}; t_o) = \frac{1}{\sqrt{2\pi\sigma_\epsilon^2}} \exp\left[-\frac{(\hat{C} - C_\beta)^2}{2\sigma_\epsilon^2}\right] , \tag{9.27}$$

where

$$C_\beta(x_1, t) = \frac{M'}{\sqrt{4\pi D(t_\beta - t_o)}} \exp\left\{-\frac{[x_{1_\beta} - x_{1_o} - v(t_\beta - t_o)]^2}{4D(t_\beta - t_o)}\right\} , \tag{9.28}$$

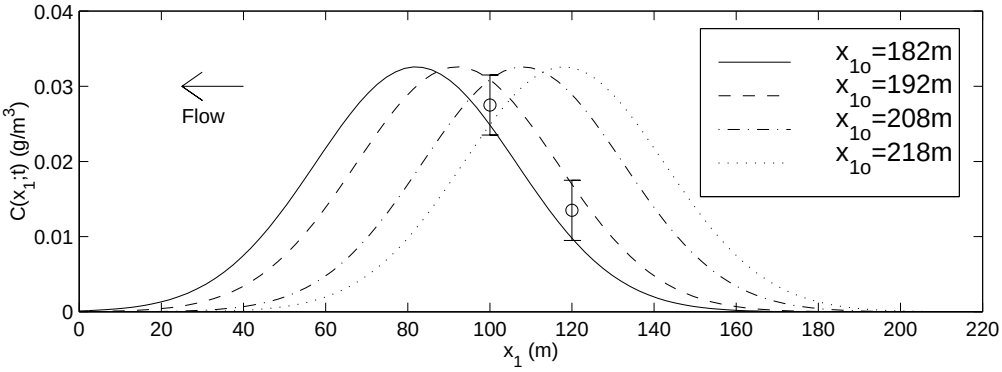

Figure 9.13: Sampled concentration ($\circ$) at two locations and contaminant plumes from four possible source locations. Error bars represent two standard deviations. ($t = 100$ days, $x_{1_A} = 100$ m, $x_{1_B} = 120$ m, $\hat{C}_A = 0.0275$ g/m^3, $\hat{C}_B = 0.0135$ g/m^3, $M' = 2.0$ g/m^2, $D = 3$ m^2/d, $v = -1$ m/d, $t_o = 0$).

with $\beta = A, B$, and all variables are known. Since the two samples are uncorrelated,

$$f(\hat{C}_A, \hat{C}_B | x_{1_o}; t_o) = f(\hat{C}_A | x_{1_o}; t_o) f(\hat{C}_B | x_{1_o}; t_o) \; . \tag{9.29}$$

From Bayes' theorem and (9.29), the two-detection location probability is

$$f(x_{1_o} | \hat{C}_A, \hat{C}_B; \tau) = \frac{f(\hat{C}_A | x_{1_o}; t_o) f(\hat{C}_B | x_{1_o}; t_o) f_{x_{1_o}}(x_{1_o})}{\int_{x_{1_o}} f(\hat{C}_A | x_{1_o}; t_o) f(\hat{C}_B | x_{1_o}; t_o) f_{x_{1_o}}(x_{1_o}) \, dx_{1_o}} \; , \tag{9.30}$$

where $f_{x_{1_o}}(x_{1_o})$ is a prior distribution on x_{1_o}, given by (9.12) with $N = 2$, the two-detection location probability in the absence of any concentration information. Similarly, the two-detection travel time probability is

$$f(\tau | \hat{C}_A, \hat{C}_B; x_{1_o}) = \frac{f(\hat{C}_A | x_{1_o}; t_o) f(\hat{C}_B | x_{1_o}; t_o) f_\tau(\tau)}{\int_\tau f(\hat{C}_A | x_{1_o}; t_o) f(\hat{C}_B | x_{1_o}; t_o) f_\tau(\tau) \, dx_\tau} \; , \tag{9.31}$$

where $f_\tau(\tau)$ is a prior distribution on τ, given by (9.15) with $N = 2$.

Figures 9.14 and 9.15 are plots of location and travel time probability, respectively, for two detections of contamination. We used the parameters shown in Table 9.1, with $\hat{C}_A = 0.0275$ g/m^3 at $x_{1_A} = 100$ m, $\hat{C}_B = 0.0135$ g/m^3 at $x_{1_B} = 120$ m, and three different values of σ_ϵ ($\sigma_\epsilon = 0.002$ g/m^3, 0.006 g/m^3, and 0.018 g/m^3). Both plots show single-peaked probability distributions. The most likely source location is at $x_{1_o} = 210$ m, and the most likely release time in the range of 85 days $\leq \tau \leq$ 91 days, depending on the value of σ_ϵ. For comparison, the no-concentration location and travel time probability distributions are also shown on the plots; these are equivalent to the limiting distributions of $f(x_{1_o}|\hat{C}_A, \hat{C}_B; \tau)$ and $f(\tau|\hat{C}_A, \hat{C}_B; x_{1_o})$ as $\sigma_\epsilon \to \infty$. Notice that the spread of the distributions increases with increasing σ_ϵ, as summarized in Tables 9.7 and 9.8, for location and travel time probabilities, respectively.

By comparing Tables 9.3 and 9.7 and Tables 9.4 and 9.8, we see that the variances of the two-detection distributions are smaller than the variances of the single-detection distributions. This can also be seen by comparing Figures 9.9 and 9.14, and Figures 9.10 and 9.15. With the additional detection at $x_{1_B} = 120$ m, the left peak from Figure 9.9 is eliminated in the two-detection location probability distribution, and the right peak from Figure 9.10 is eliminated in the travel time probability distribution. The variances of the distributions would decrease even further for additional detections, although we do not show this here. Thus, with each additional detection, the variance of the distributions decreases, and the uncertainty in the source location or release time is reduced.

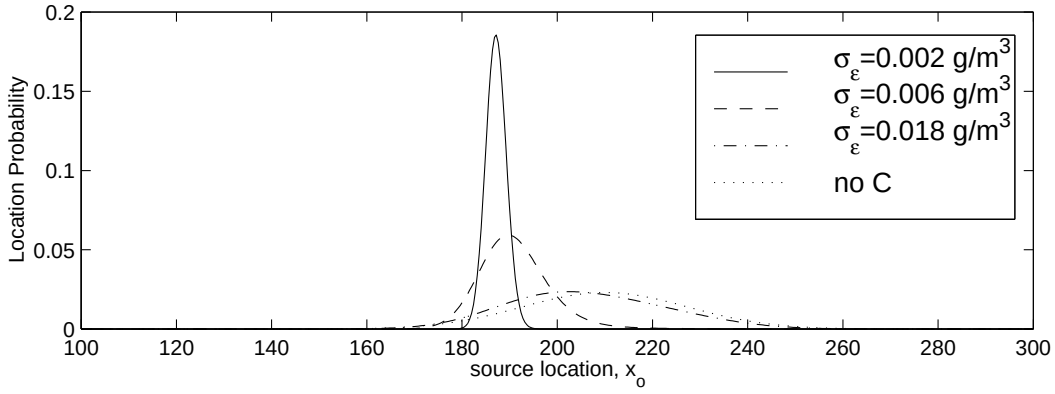

Figure 9.14: Source location probability for two detections of contamination with a known source mass. ($\tau = 100$ days, $M' = 2.0$ g/m^2, $D = 3$ m^2/d, $v = -1$ m/d, $\hat{C}_A = 0.0275$ g/m^3, $x_{1_A} = 100$ m, $\hat{C}_B = 0.0135$ g/m^3, $x_{1_B} = 120$ m).

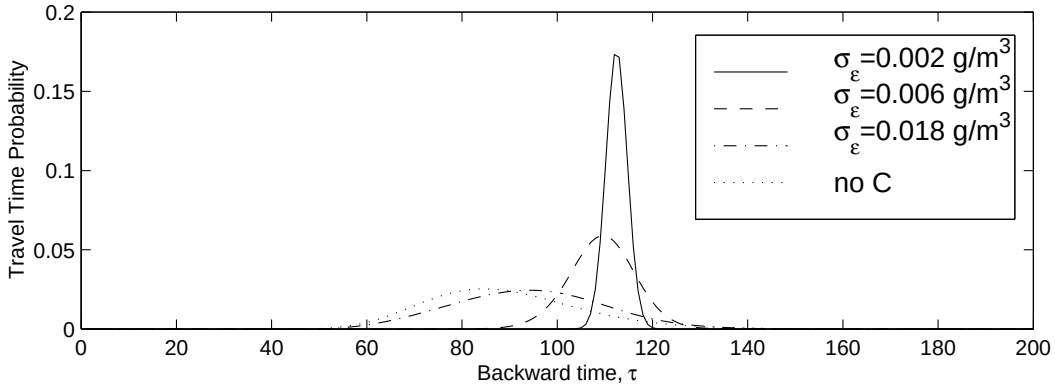

Figure 9.15: Travel time probability for two detections of contamination with a known source mass. ($\tau = 100$ days, $M' = 2.0$ g/m^2, $D = 3$ m^2/d, $v = -1$ m/d, $\hat{C}_A = 0.0275$ g/m^3, $x_{1_A} = 100$ m, $\hat{C}_B = 0.0135$ g/m^3, $x_{1_B} = 120$ m).

Table 9.7: Variances of two-detection location probability distributions with known source mass.

Distribution	Variance
$\sigma_\epsilon = 0.002$ g/m^3	5 m^2
$\sigma_\epsilon = 0.006$ g/m^3	59 m^2
$\sigma_\epsilon = 0.018$ g/m^3	278 m^2
$\sigma_\epsilon \to \infty$	300 m^2

Table 9.8: Variances of two-detection travel time probability distributions with known source mass.

Distribution	Variance
$\sigma_\epsilon = 0.002$ g/m^3	5 days^2
$\sigma_\epsilon = 0.006$ g/m^3	50 days^2
$\sigma_\epsilon = 0.018$ g/m^3	256 days^2
$\sigma_\epsilon \to \infty$	267 days^2

If the source mass is unknown, we can follow a similar procedure as in Section 9.3.3. Figures 9.16 and 9.17 show plots of two-detection location and travel time probability, respectively, using measured concentrations and a uniform distribution for the source mass. We used three different values of M_{u} and three different values of σ_ϵ, and also show the no-concentration two-detection probabilities. In all cases, $M_{\mathrm{l}} = 0$.

The two-detection probabilities with unknown source mass follows the same trends as the single-detection probabilities in (Figures 9.11 and 9.12). For location probability, several source locations are equally likely, indicated by the plateau in each plot. For travel time probability, a similar plateau-like feature is observed, but earlier times are more likely than later times. For both types of probability, the width of the plateau increases as M_{u} increases.

The two-detection location probability distributions are not symmetric about the no-concentration two-detection distribution; they are shifted in the direction of the larger sample. In Figure 9.16, the larger sample is taken at $x_{1_A} = 100$ m and the lower at $x_{1_B} = 120$ m. The two-detection location probability is shifted towards $-x_1$, indicating a heavier weighting of the detection with the larger sample. For a fixed M_{u}, the degree of weighting (shifting) decreases as σ_ϵ increases, because with a larger measurement error, the true concentration at x_{1_A} need not be higher than the true concentration at x_{1_B}. This shifting is not observed in the travel time probability plots because both samples were taken at the same time; however, if the samples were taken at different times, the two-detection probability distribution would be shifted toward the time of the larger sample.

Table 9.9: Variances of two-detection location probability distributions with unknown source mass.

σ_ϵ (g/m^3)	M_u (g/m^2)	Variance (m^2)
0.002	5	330
0.002	50	1084
0.002	500	1885
0.02	5	378
0.02	50	1113
0.02	500	1917
0.2	5	302
0.2	50	553
0.2	500	1301

For small σ_ϵ and small M_u, the variance of the distributions is smaller than the variance of the no-concentration distribution (see Table 9.9); however, for a fixed σ_ϵ, increasing uncertainty in the initial mass results in a larger variance, often larger than that of the no-concentration distribution. For each combination of M_u and σ_ϵ, the variance of the two-detection distribution is less than the variance of the single-detection distribution, indicating that multiple detections provide more information and reduce the uncertainty of the distributions.

9.5 Conclusions

Backward-in-time location and travel time probabilities can be used to obtain information about the prior position of contamination that was detected in an aquifer. The backward probability model has been developed for

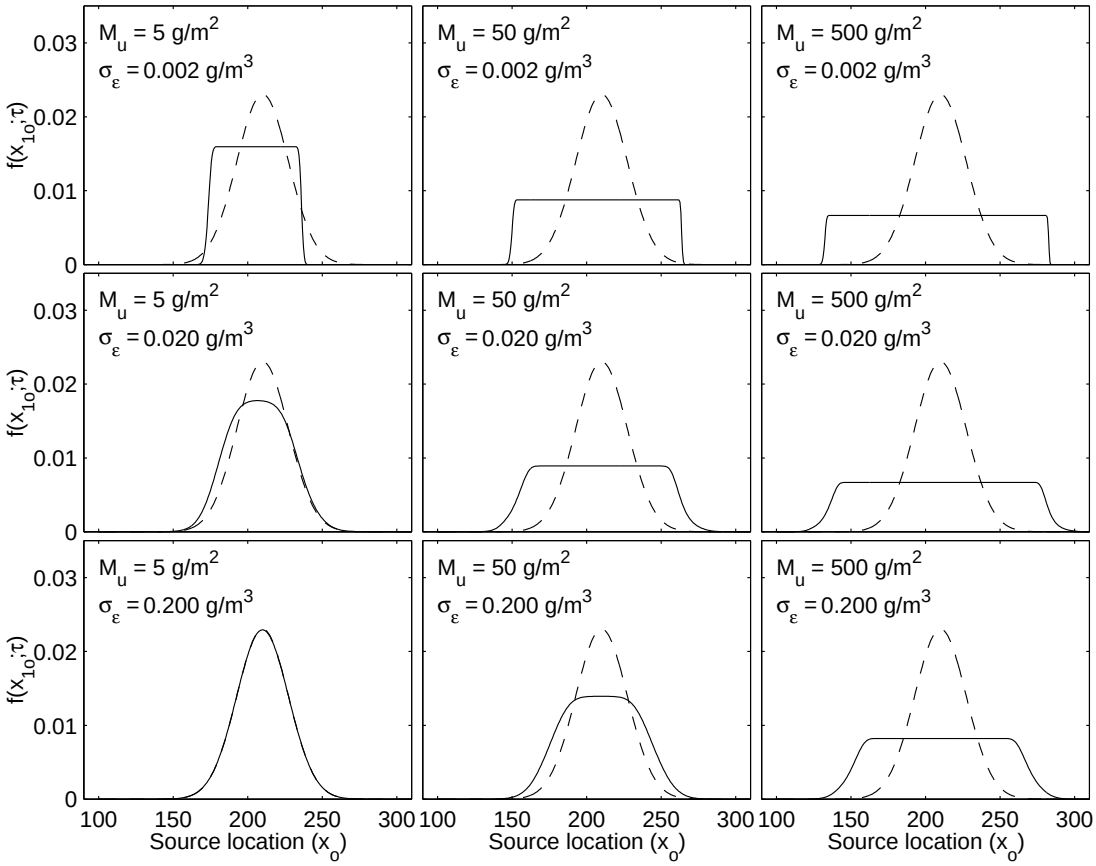

Figure 9.16: Location probability for two detections of contamination with an unknown source mass (solid line) and no-concentration two-detection location probability (dashed line). (x_{1_w} = 100 m, τ = 100 days, D = 3 m^2/d, v = -1 m/d, $\hat{C}_A$ = 0.0275 g/m^3, x_{1_A} = 100 m, $\hat{C}_B$ = 0.0135 g/m^3, x_{1_B} = 120 m, M_{u} varies, σ_ϵ varies).

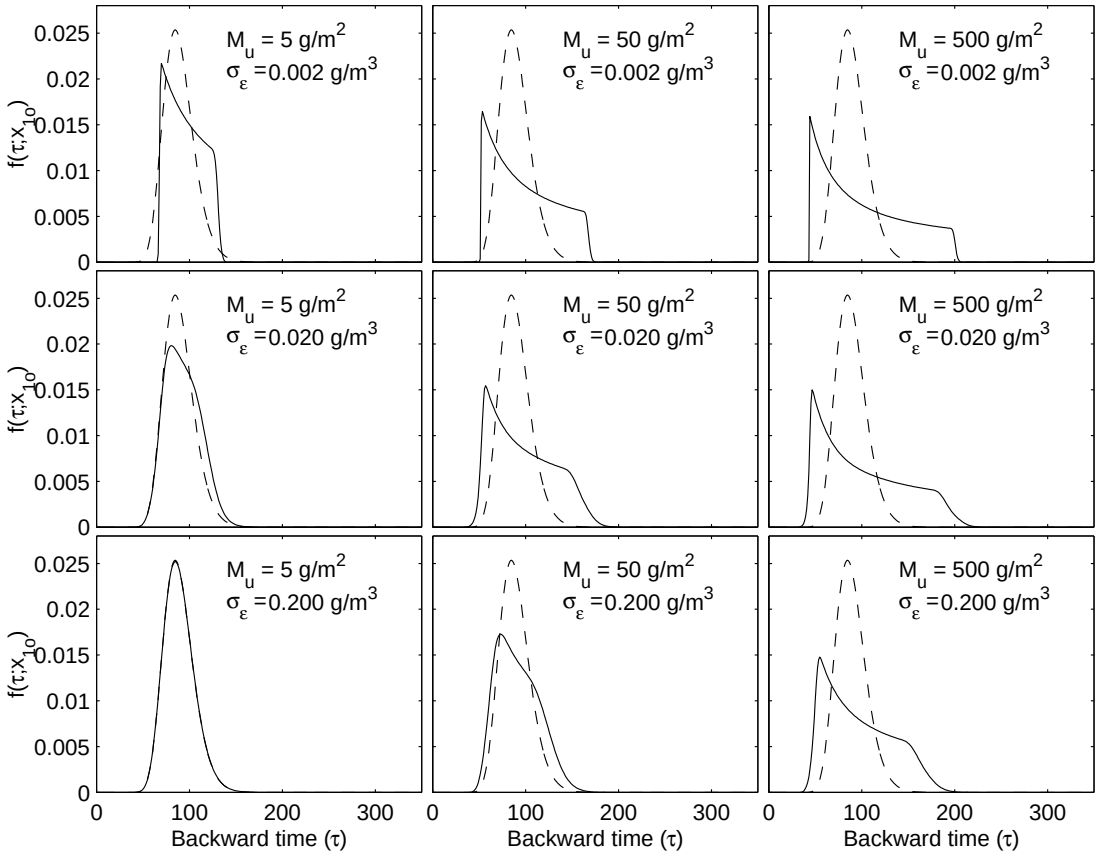

Figure 9.17: Travel time probability for two detections of contamination with an unknown source mass (solid line) and no-concentration two-detection travel time probability (dashed line). ($x_{1_w} = 100$ m, $x_{1_o} = 200$ m, $D = 3$ m^2/d, $v = -1$ m/d, $\hat{C}_A = 0.0275$ g/m^3, $x_{1_A} = 100$ m, $\hat{C}_B = 0.0135$ g/m^3, $x_{1_B} = 120$ m, M_{u} varies, σ_ϵ varies).

Table 9.10: Variances of two-detection travel time probability distributions with unknown source mass.

σ_ϵ (g/m^3)	M_u (g/m^2)	Variance (m^2)
0.002	5	340
0.002	50	1132
0.002	500	2074
0.02	5	351
0.02	50	1109
0.02	500	2048
0.2	5	269
0.2	50	513
0.2	500	1284

a single detection of contamination [e.g., *Wilson and Liu*, 1994; *Neupauer and Wilson*, 1999] and for multiple detections of contamination [Chapter 8]; however, they only accounted for the presence of detected contamination and did not consider the sampled concentration. In this paper, we incorporated the use of concentration measurements into the backward probability model. The additional information available from the concentration measurements can be used to better characterize the source of contamination, quantified by a variance reduction of the probability distributions.

In this paper, we assumed that the contamination source was an instantaneous point source of unknown location, and we assumed that measured concentrations contain random measurement error that is normally-distributed with mean zero and known variance. We considered both single- and two-detection problems, and the cases of known and unknown source mass. If the

source mass was unknown, it was treated as a random variable with a uniform distribution between a prescribed upper bound and a lower bound of zero.

With a known source mass, the location and travel time probability distributions have a smaller variance than the no-concentration distributions. The variance increases as measurement error increases, and in the limit as measurement error becomes extremely large, the probability distributions approach the no-concentration distributions. These features were observed for both the single- and two-detection results.

With an unknown source mass, the location and travel time probability distributions show a region of high probability, represented by a plateau-like feature. With location probability, there are several equally-likely source locations. With travel time probability, earlier times are always more likely than later times. The width of the plateau increases as the upper bound on the source mass increases. For small measurement error, the variances of the distributions are smaller than the variances of the no-concentration distributions, but for larger measurement uncertainty, the variances of the probability distributions with concentration are larger than the no-concentration distributions.

Acknowledgments

This research was supported in part by the Geophysical Research Center at New Mexico Tech and in part by the Environmental Protection Agency's STAR Fellowship program under Fellowship No. U-915324-01-0. This work has not been subjected to the EPA's peer and administrative review and therefore

may not necessarily reflect the views of the Agency and no official endorsement should be inferred.

References

Bagtzoglou, A.C., D.E. Dougherty, and A.F.B. Thompson, Application of particle methods to reliable identification of groundwater pollution sources, *Water Resources Management*, 6, 15–23, 1992.

Bear, J., *Dynamics of Fluids in Porous Media*, American Elsevier Publishing Company, New York, 1972.

Carslaw, H.S. and J.C. Jaeger, *Conduction of Heat in Solids*, 2nd ed., Clarendon Press, Oxford, 1959.

Chin, D.A. and P.V.K. Chittaluru, Risk management in wellhead protection, *J. Water Resour. Plan. Manage.*, 120(3), 294–315. 1994.

Dagan, G., Stochastic modeling of groundwater flow by unconditional and conditional probabilities, 2, The solute transport, *Water Resour. Res.*, 18(4), 835–848, 1982.

Dagan, G., Theory of solute transport by groundwater, *Ann. Rev. Fluid Mech.*, 19, 183–215, 1987.

Dagan, G., *Flow and Transport in Porous Formations*, Springer-Verlag, New York, 1989.

Dagan, G., and V. Nguyen, A comparison of travel time and concentration approaches to modeling transport by groundwater, *Journal of Contaminant Hydrology*, 4, 79–91, 1989.

Jury, W.A., Simulation of solute transport using a transfer function model, *Water Resour. Res.*, 18(2), 363–368, 1982.

Jury, W.A., G. Sposito, and R.E. White, A transfer function model of solute transport through soil, 1, Fundamental concepts, *Water Resour. Res.*, 22(2), 243–247, 1986.

Jury, W.A. and K. Roth, *Transfer Functions and Solute Movement through Soil: Theory and Applications*, Birkhauser Verlag, Boston, 1990.

Kreft, A. and A. Zuber, On the physical meaning of the dispersion equation and its solutions for different initial and boundary conditions, *Chemical Engineering Science*, 33, 1471–1480, 1978.

Liu, J., *Travel time and location probabilities for groundwater contaminant sources*, Master's thesis, New Mexico Institute of Mining and Technology, Socorro, 1995.

Neupauer, R.M. and J.L. Wilson, Adjoint method for obtaining backward-in-time location and travel time probabilities of a conservative groundwater contaminant, *Water Resour. Res.*, 35(11), 3389–3398, 1999.

Neupauer, R.M. and J.L. Wilson, Adjoint-derived location and travel time probabilities in a multi-dimensional groundwater flow system, *Water Resour. Res.*, in press, 2000a.

Neupauer, R.M. and J.L. Wilson, Backward location and travel time probabilities for contamination in a one-dimensional infinite aquifer, submitted to *J. Contam. Hydrol.*, 2000b.

Parker, J.C. and M. Th. van Genuchten, Flux-averaged and volume-averaged concentrations in continuum approaches to solute transport, *Water Resour. Res.*, 20(7), 866–872, 1984.

Rubin, Y. and G. Dagan, Conditional estimation of solute travel time in heterogeneous formations: impact of transmissivity measurements, *Water Resour. Res.*, 28(4), 1033–1040, 1992.

Shapiro, A.M. and V.D. Cvetkovic, Stochastic analysis of solute arrival time in heterogeneous porous media, *Water Resour. Res.*, 24(10), 1711–1718, 1988.

Uffink, G.J.M., Application of Kolmogorov's backward equation in random walk simulations of groundwater contaminant transport, in *Contaminant Transport in Groundwater*, H.E. Kobus and W. Kinzelbach, editors, pp. 283–289, A.A. Balkema, Brookfield, Vt., 1989.

Wilson, J.L. and J. Liu, Backward tracking to find the source of pollution, in *Waste-management: From Risk to Remediation*, edited by R. Bhada *et al.*, ECM Press, Albuquerque, NM, 181–199, 1994.

Wilson, J.L. and J. Liu, Field Validation of the Backward-in-time Advection Dispersion Theory. *Proceedings of the 1996 HSRC/WERC Joint Conf. on the Environment*, Great Plains-Rocky Mountain Hazardous Substance Center, Manhattan, Kansas, http://www.engg.ksu.edu/HSRC/ 96Proceed/wilson.html, 1997.

CHAPTER 10

APPLICATION OF THE BACKWARD PROBABILITY MODEL

Abstract

Backward location and travel time probabilities can be used to determine the possible former locations of contamination in an aquifer. For a contaminant parcel that was detected in an aquifer, the backward location probability describes its position at some time prior to sampling and the backward travel time probability describes the amount of time required for it to travel to the sampling location from some upgradient position. The backward probability model has been developed for conservative and reactive solutes. We apply it to a trichloroethylene (TCE) plume at Massachusetts Military Reservation. We use four TCE samples distributed throughout the plume to obtain single-detection and multiple-detection location and travel time probabilities in three dimensions. These probabilities provide information about the possible sources of contamination.

10.1 Introduction

When contamination is detected in an aquifer, the source of contamination is often unknown. To remediate the aquifer or to assign responsibility, we might need to identify the source of contamination or the time of release of contamination from the source. In conventional contaminant transport modeling, the source of contamination is known or assumed to be known, and

the future positions of the contaminant plume are simulated. If the source of contamination is unknown, this conventional transport modeling approach can be cumbersome to use. A more efficient approach for characterizing sources of groundwater contamination is backward modeling [*Wilson and Liu*, 1994, 1997; *Neupauer and Wilson*, 1999].

Backward modeling is based on backward location and travel time probabilities. For a solute parcel that was detected in an aquifer, backward location probability describes its position at some time prior to sampling, and backward travel time probability describes the amount of time required for the solute parcel to travel to the sampling location from some upgradient position, such as a known or suspected contamination source. In backward modeling, the sampling location is treated as a source of probability, and probability is transported upgradient in backward time to obtain information about the prior position of the detected contamination.

Backward location and travel time probability models have been used to characterize sources of groundwater contamination, to delineate pumping well capture zones, and to identify the prior position of contamination in groundwater. By reversing the flow field in a random walk method, *Bagtzoglou et al.* [1992] obtained backward location probabilities that were used for identifying sources of contamination. *Uffink* [1989] and *Chin and Chittaluru* [1994] used a similar random walk approach to delineate capture zones around pumping wells. *Wilson and Liu* [1994, 1997] used a heuristic method to obtain a backward probabilistic continuum model from the forward advection-dispersion equation using a single detection of contamination. The approach was validated using data from a field-scale tracer experiment at the Borden

site [*Wilson and Liu*, 1997]; however, no formal justification was given for the model. *Neupauer and Wilson* [1999, 2000] showed that backward probabilities are related to adjoint states of concentration and presented a formal framework for obtaining the governing equation of the backward probability model using adjoint theory.

In this paper, we use data from a trichloroethylene (TCE) plume at the Massachusetts Military Reservation (MMR) on Cape Cod as a test case for applying the backward probability model, which we use to obtain information about the prior positions of the observed TCE. In the next section, we present background on the MMR site and the TCE plume. Then we provide a brief description of the backward probability model, followed by the application of the model to the MMR TCE plume.

10.2 Site Background

Massachusetts Military Reservation (MMR) is a military training facility covering approximately 30 square miles on the western edge of Cape Cod in Massachusetts (see Figure 10.1). MMR is situated over the recharge area of the Sagamore Lens, a 300-foot-thick aquifer comprised mainly of permeable sand. The Sagamore Lens is the sole-source aquifer supplying drinking water for western Cape Cod, and is recharged by rainwater [*MMR IRP*, 2000d].

In 1989 the U.S. Environmental Protection Agency added MMR to the National Priorities List because of several groundwater plumes and soil contamination that could potentially contaminate the drinking water supply [*USEPA*, 1991]. Chemical Spill 10 (CS-10) is one of the groundwater plumes,

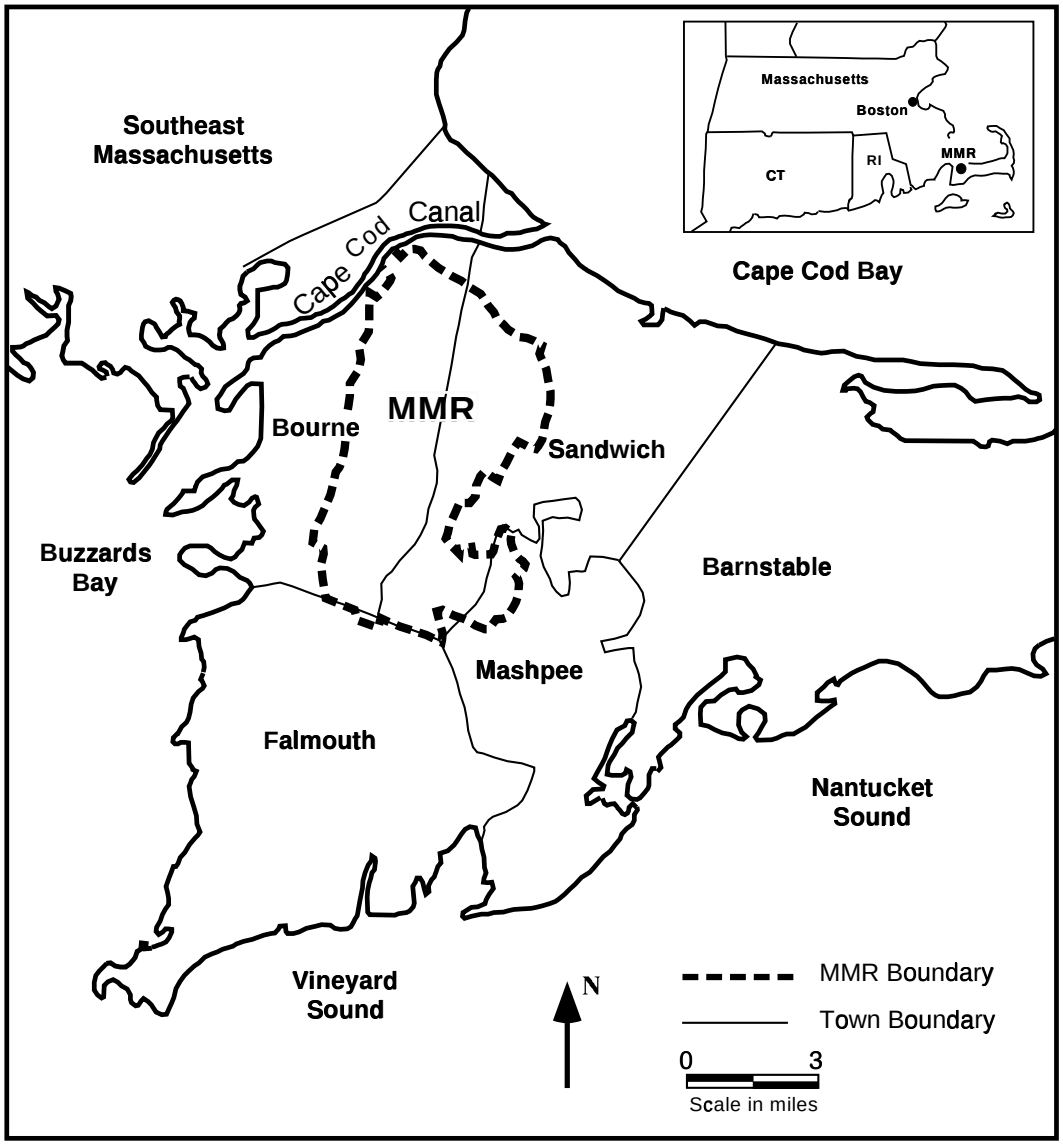

Figure 10.1: Location of Massachusetts Military Reservation (MMR) (adapted from *MMR IRP*, [2000d]).

and encompasses approximately 38 acres in the southeast corner of the MMR (see Figure 10.2). The primary contaminants in the plume are trichloroethylene (TCE) and perchloroethylene (PCE), common solvents used for equipment maintenance and degreasing. TCE concentrations have been measured as high as 5000 μg/L in the plume, which is significantly higher than the primary drinking water standard of 0.005 ppm ($\approx$ 5 μg/L) [*USEPA*, 1999]. Ethylene dibromide (EDB) has been sporadically detected in the plume area in concentrations below safe drinking water standards. The plume is approximately 17,000 ft long, has a maximum width of 4,000 ft, and a thickness of up to 140 ft. It is over 120 feet below ground surface and 60 feet below the water table along most of its length. It has separated into two lobes and the eastern lobe has migrated offsite. In 1998 TCE upwelling was observed in the western portion of Johns Pond (see Figure 10.2); this may be the leading edge of the CS-10 plume. In 1999 TCE upwelling from the CS-10 plume was observed in the northwest corner of Ashumet Pond [*MMR IRP*, 1999, 2000a; *Kavanaugh et al.*, 2000].

A suspected source area for CS-10 is the former Boeing Michigan Aerospace Research Center (BOMARC) Missile Site and current Unit Training Equipment Site (UTES), near the eastern boundary of the MMR (see Figure 10.2). The BOMARC Missile Site was in operation between 1962 and 1973, and UTES has been in operation since 1978. The area is presently used for maintenance and storage of vehicles. Spills and releases of chemicals occurred in these areas in the past. Eleven other potential source areas have been identified in the western and central portions of the plume. In addition, waste storage and disposal structures in the vicinity of the plume may have

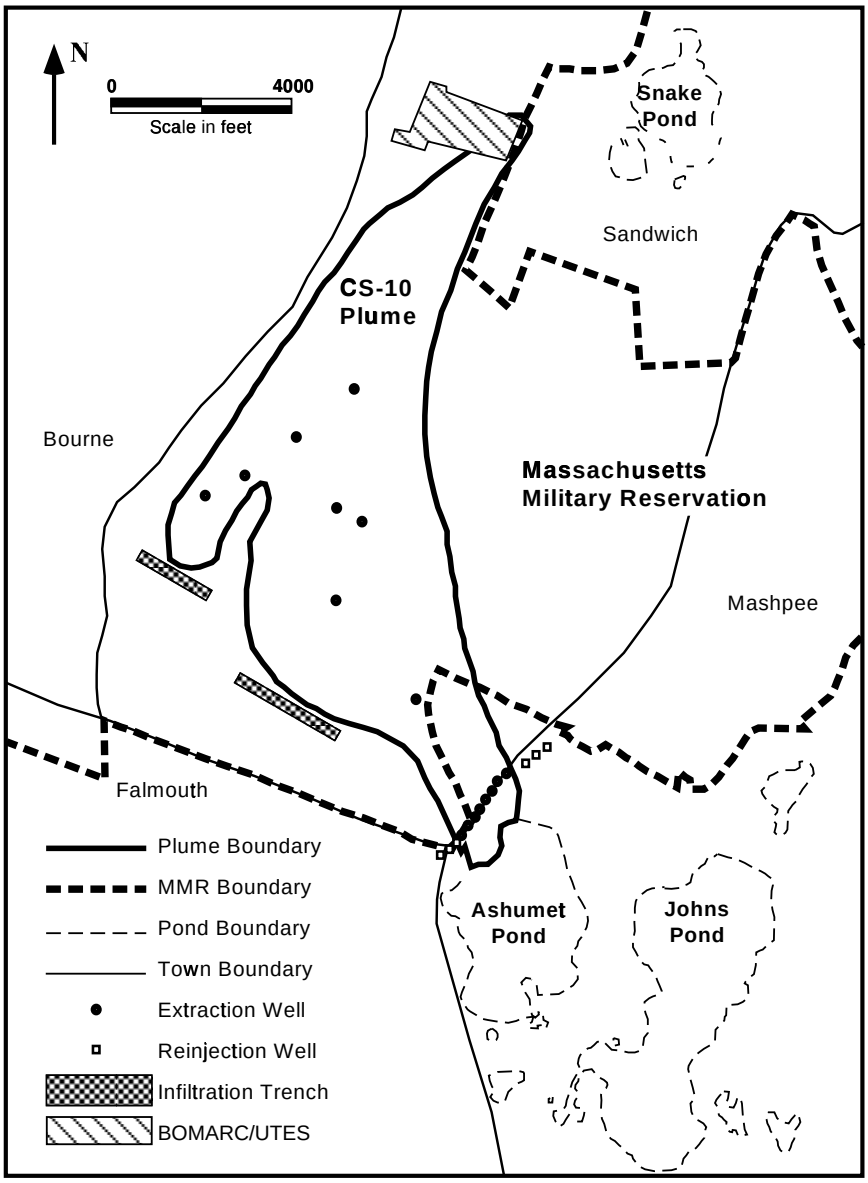

Figure 10.2: Location of inferred CS-10 plume, BOMARC/UTES area, and remediation system. (adapted from *MMR IRP*, [1997, 1998, 2000a]).

contributed to the contamination. Some additional sources of TCE are shown in Figure 10.3. The plume from LF-1 flows toward the west, and plumes from FTA-1 and FS-5 flow south; therefore it is believed that they do not contribute to the CS-10 plume [*MMR IRP*, 1997, 2000a]. A recent press release (Sept. 26, 2000) stated that CS-22 has been identified as a possible source contamination based on anonymous reports of disposal of unspecified wastes, possibly from the BOMARC facility. [*MMR IRP*, 2000c].

The CS-10 plume has been monitored for TCE and other chemicals. Figures 10.4–10.8 show TCE samples taken annually from 1996 through 2000. Some locations were sampled at multiple depths. The maximum TCE concentration sampled during this period was 5110 μg/L, sampled near Ashumet Pond in June 1997.

Remediation of the CS-10 plume began in June 1999, using an extraction, treatment, and reinjection (ETR) technology. Contaminated groundwater is extracted through 16 extraction wells, is treated, and reenters the aquifer through six reinjection wells and two infiltration trenches (see Figure 10.2). The system is expected to be in operation for 35 years. The total extraction and reinjection rate for the CS-10 ETR remediation system is 5.2 million gallons per day, and it is expected to capture 98% of the contamination [*MMR IRP*, 1999, 2000a,b; *Kavanaugh et al.*, 2000].

10.3 Backward Probability Model

Since the source area of the CS-10 plume is not well-characterized, it is a good test case for using the backward probability model to obtain in-

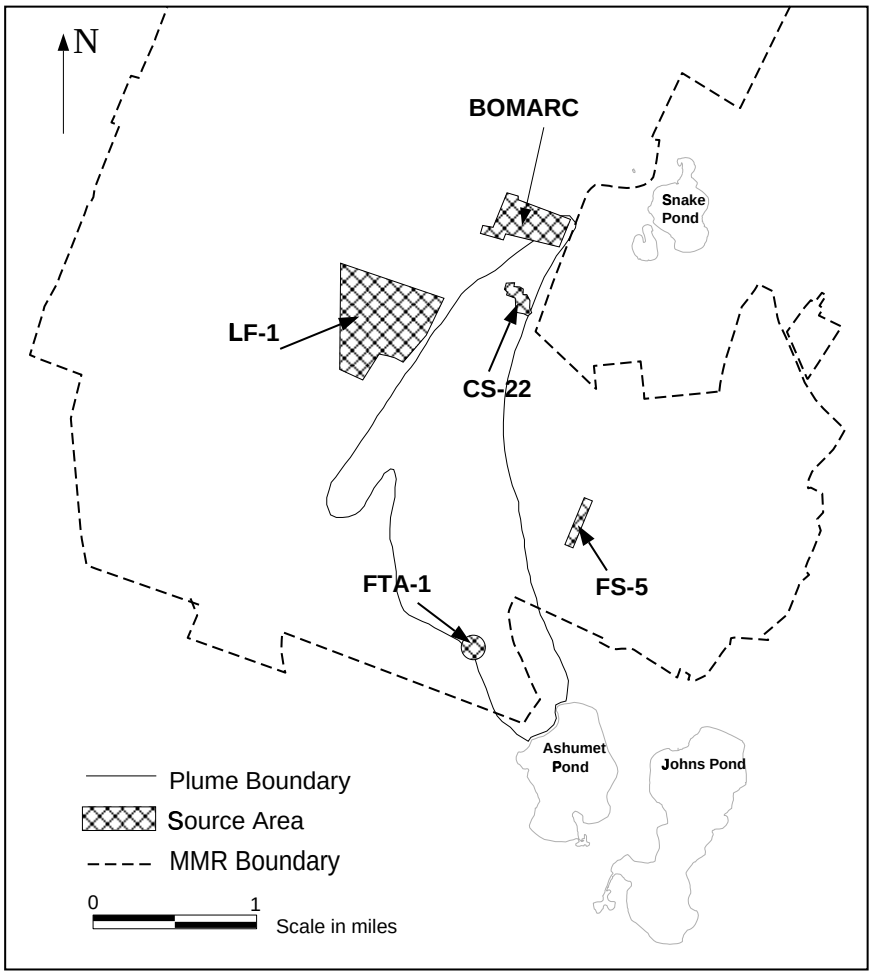

Figure 10.3: Suspected TCE source areas near CS-10 plume. (adapted from *MMR IRP*, 2000e).

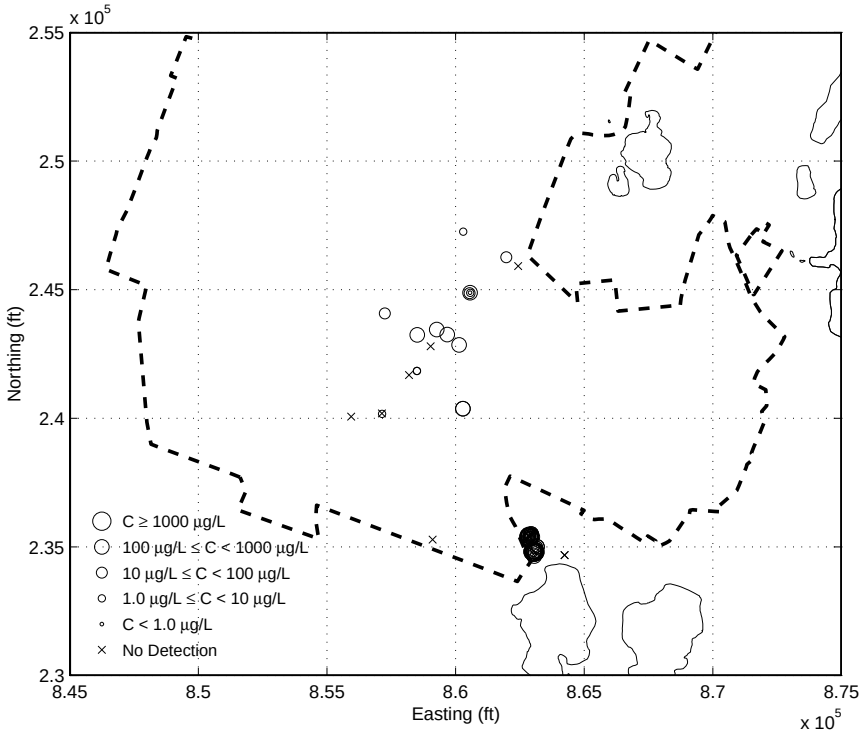

Figure 10.4: Sampled TCE concentrations in CS-10 plume during 1996.

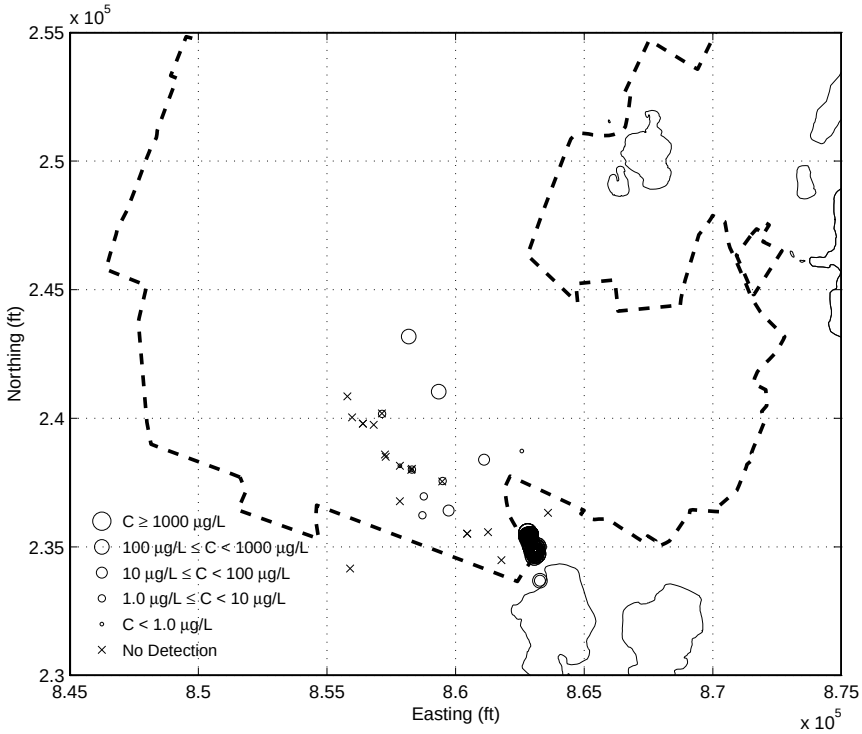

Figure 10.5: Sampled TCE concentrations in CS-10 plume during 1997.

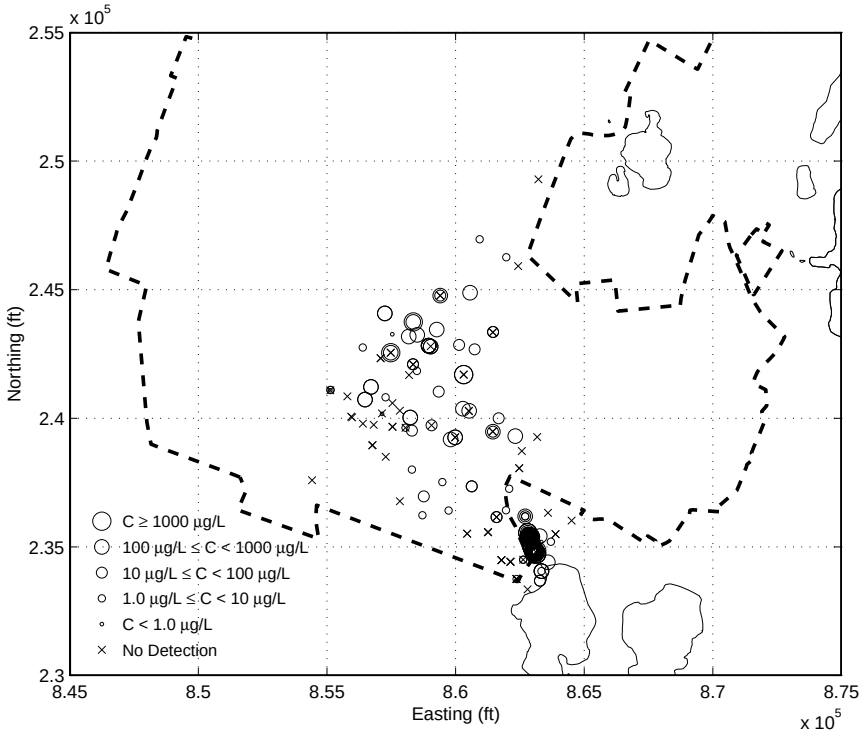

Figure 10.6: Sampled TCE concentrations in CS-10 plume during 1998.

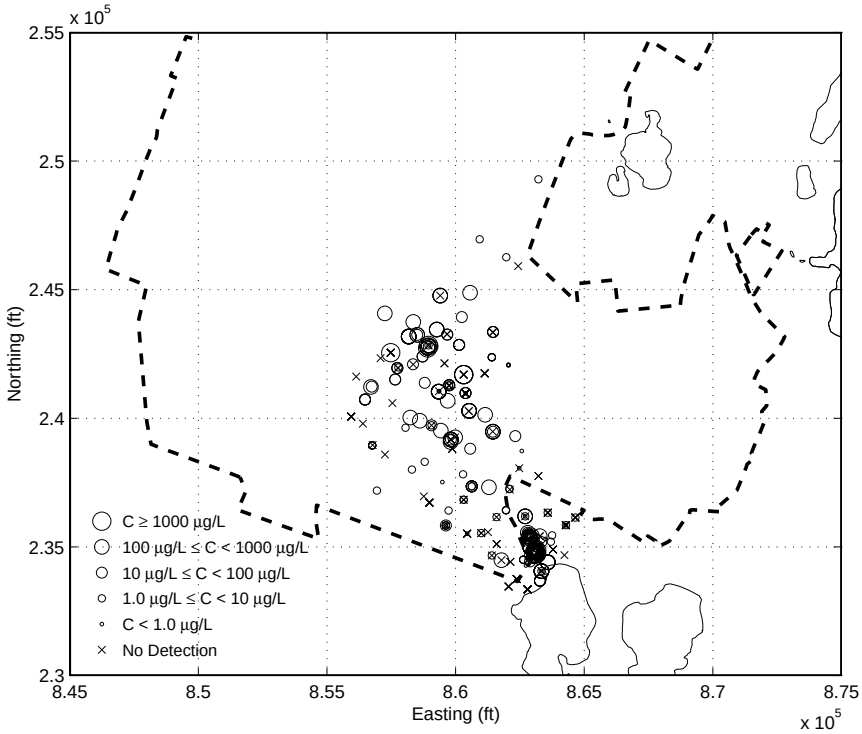

Figure 10.7: Sampled TCE concentrations in CS-10 plume during 1999.

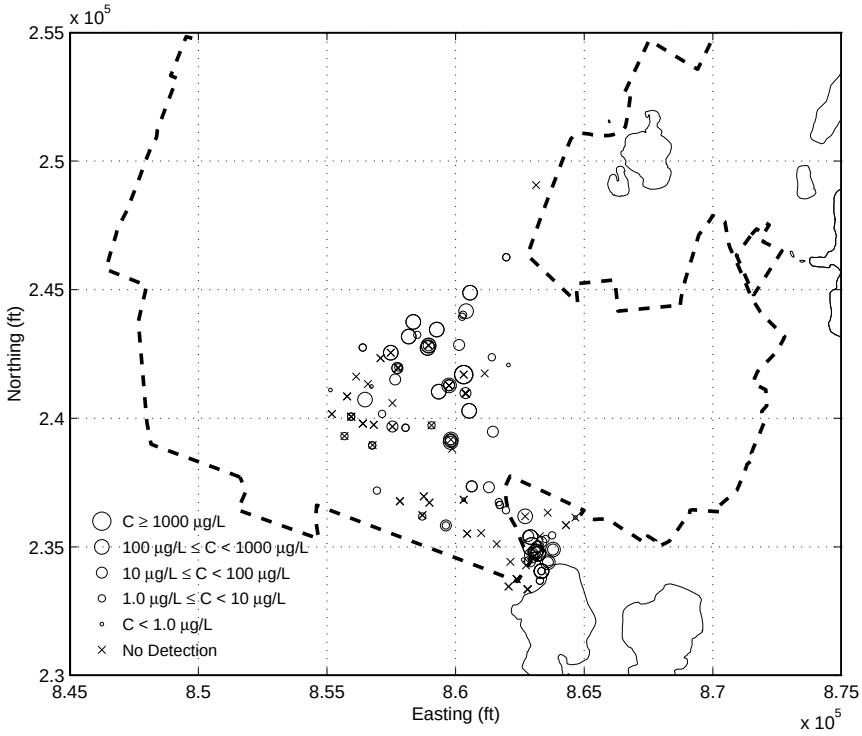

Figure 10.8: Sampled TCE concentrations in CS-10 plume during 2000.

formation about the prior position of detected contamination. The backward probability model produces two types of probabilities–backward location probability and backward travel time probability. For contamination that is detected in an aquifer, backward location probability describes the position of the contamination at some time prior to sampling, and backward travel time probability describes the amount of time required for the contamination to travel to the sampling location from some upgradient position. For a sorbing solute, the backward probabilities can be further subdivided into aqueous and sorbed phases for the detection phase, and aqueous and sorbed phases for the prior phase. In the example presented here, TCE is observed in the aqueous phase only.

With backward modeling we treat the sampling location as a source of probability (there is a probability of one that the contamination was at the sampling location at the time of sampling) and allow the probability to advect upgradient in backward time and to spread out by dispersion, resulting in a plume of backward probability that provides information about the former position of contamination. The mathematical model governing backward probabilities is similar to the model for forward solute transport with modifications to account for the upgradient movement of probability. It is obtained from a forward contaminant transport model by using adjoint theory.

10.3.1 Backward Probability Theory

Solute transport in groundwater at MMR has been modeled using the advection-dispersion equation (ADE) [*Zheng*, 1999]:

$$R\frac{\partial}{\partial t}(\theta C) = \frac{\partial}{\partial x_i}\left(\theta D_{ij}\frac{\partial C}{\partial x_j}\right) - \frac{\partial}{\partial x_i}(\theta v_i C) + q_I C_I - q_O C - \lambda\theta R C \qquad (10.1)$$

$$C_S = (R-1)C$$

$$C(\mathbf{x},0) = C_i(\mathbf{x})$$

$$C_S(\mathbf{x},0) = C_{Si}(\mathbf{x})$$

$$C(\mathbf{x},t) = g_1(t) \text{ on } \Gamma_1$$

$$\left[D_{ij}\frac{\partial C}{\partial x_j}\right] \mathrm{n}_i = g_2(t) \text{ on } \Gamma_2$$

$$\left[v_i C - D_{ij}\frac{\partial C}{\partial x_j}\right] \mathrm{n}_i = g_3(t) \text{ on } \Gamma_3 \ ,$$

where $C(\mathbf{x},t)$ is the aqueous-phase resident concentration, t is time, x_i are the spatial directions ($i = 1,2,3$), $\mathbf{x} = (x_1, x_2, x_3)$, R is the retardation coefficient for linear equilibrium sorption, D_{ij} is the i,j^{th} entry of the dispersion tensor, v_i is the groundwater velocity in the direction of x_i, q_I is the source flow rate per unit volume, C_I is the source strength, θ is porosity, q_O is the sink flow rate per unit volume, λ is the first order decay rate, C_S is the sorbed-phase concentration (in units of mass of solute per volume of water), C_i is the initial concentration in the aqueous phase, $C_{Si} = (R-1)C_i$ is the initial sorbed-phase concentration, g_1, g_2, and g_3 are known functions, Γ_1, Γ_2, and Γ_3 are the domain boundaries, and n_i is the outward unit normal vector in the x_i direction.

The governing equation for the backward model is the adjoint of this equation, given by [*Neupauer and Wilson*, 2000; and Chapters 5 and 6]

$$R\frac{\partial}{\partial\tau}(\theta\psi^*) = \frac{\partial}{\partial x_i}\left(\theta D_{ij}\frac{\partial\psi^*}{\partial x_j}\right) + \frac{\partial}{\partial x_i}(\theta v_i\psi^*) - q_I\psi^* - \lambda\theta R\psi^* + \frac{\partial h}{\partial C} \quad (10.2)$$

$$\psi^*(\mathbf{x},0) = 0$$

$$\psi^*(\mathbf{x},\tau) = 0 \text{ on } \Gamma_1$$

$$\left[D_{ij}\frac{\partial\psi^*}{\partial x_j} + v_i\psi^*\right]\mathrm{n}_i = 0 \text{ on } \Gamma_2$$

$$\left[D_{ij}\frac{\partial\psi^*}{\partial x_j}\right]\mathrm{n}_i = 0 \text{ on } \Gamma_3 \ ,$$

where ψ^* is the adjoint state (related to either location or travel time probability), τ is backward time or time prior to sampling ($\tau = T - t$, where $t = T$ is the detection time), $\partial h/\partial C$ is the load term, and h is a performance functional that depends on the type of probability, the detection mechanism (e.g., pumping well, monitoring well), and the phase of the observed contamination (aqueous or sorbed).

The adjoint equation (10.2) has the same form as the forward contaminant transport model (10.1), except that the flow field is reversed (compare signs on v_i terms and q_I terms), time is reversed, and the boundary conditions are modified (compare the boundary conditions on Γ_2 and Γ_3). With these modifications, probability travels upgradient in backward time. Many numerical codes, such as MT3DMS [*Zheng and Wang*, 1999], solve the advection-dispersion equation (10.1). With a different interpretation of input and output, these codes can also be used to solve the adjoint equation (10.2), as we discussed in Chapter 7.

The modeler can choose to make other modifications to the backward

model, depending on the desired interpretation of the results. For example, the source term in (10.1), $q_I C_I$, accounts for natural recharge; however, if the contamination does not enter the aquifer through recharge, $C_I = 0$ and the source term vanishes. Natural recharge becomes a sink in the backward model with the term $-q_I \psi^*$. Since the flow field is reversed in the backward model, probability can exit the aquifer through reversed natural recharge. This indicates a finite probability that the detected contamination entered the system through the natural recharge and therefore was not in the system at the time of interest. If it is known that the contamination did not enter through natural recharge (i.e., $C_I = 0$ in the forward model), then natural recharge should not be a sink of probability in the backward model. This can be handled by setting $q_I = 0$ in the backward transport model. Since recharge is used in the flow model, the backward probabilities would still be influenced by recharge through the flow field (see Chapter 5).

The modeler may also choose to eliminate the decay term from the adjoint equation (10.2). In the adjoint equation, the first-order decay term, $-\lambda \theta R \psi^*$, causes the adjoint state, and therefore probability, to decay. In Chapter 6, we discussed two different interpretations for handling backward probabilities of decaying solutes. With the first interpretation, the decay term as shown in (10.2) is used, allowing probability to decay. The decaying probability indicates that if the contamination was in the aquifer at a previous time, there is a non-zero probability that it would have decayed prior to reaching the detection location. In other words, more distant prior locations and longer travel times are less likely. In the second interpretation, the probability is conditioned on the contamination reaching the detection location. If a

contaminant parcel reaches the detection location, it obviously did not decay; therefore, with this interpretation, the decay term is eliminated from (10.2).

The adjoint equation (10.2) is solved for the adjoint state, ψ^*. With an appropriate definition of the load term, $\partial h/\partial C$, in (10.2), the adjoint state represents location or travel time probability. For location probability, the appropriate load term for an aqueous-phase observation is [*Neupauer and Wilson*, 2000; Chapter 6]

$$\frac{\partial h}{\partial C} = \delta(x_1 - x_{1_w})\delta(x_2 - x_{2_w})\frac{B_{x_3}(x_{3_{wt}}, x_{3_{wb}})}{x_{3_{wt}} - x_{3_{wb}}}\delta(\tau) \ , \tag{10.3}$$

where $\delta(x)$ is a Dirac delta function and (x_{1_w}, x_{2_w}) are the coordinates of the center of the well (detection location), $x_{3_{wt}}$ and $x_{3_{wb}}$ are the elevations of the top and bottom of the well screen, respectively, and $B_{x_i}(a,b)$ is a boxcar function defined as

$$B_{x_i}(a,b) = \begin{cases} 1 & a < x_i < b \\ 0 & \text{otherwise} \ . \end{cases} \tag{10.4}$$

With this load term in (10.2) and with R constant, aqueous phase location probability, $f_{\mathbf{x}_A}(\mathbf{x};\tau,\mathbf{x}_w)$, is given by [Chapters 5 and 6]

$$f_{\mathbf{x}_A}(\mathbf{x};\tau,\mathbf{x}_w) = \theta(\mathbf{x})\psi^*(\mathbf{x},\tau) \ , \tag{10.5}$$

and sorbed phase location probability, $f_{\mathbf{x}_S}(\mathbf{x};\tau,\mathbf{x}_w)$, is given by [Chapters 5

and 6]

$$f_{\mathbf{x}_S}(\mathbf{x};\tau,\mathbf{x}_w) = (R-1)\theta(\mathbf{x})\psi^*(\mathbf{x},\tau)\ . \tag{10.6}$$

The aqueous phase location probability, $f_{\mathbf{x}_A}(\mathbf{x};\tau,\mathbf{x}_w)$, describes the probability that the detected contamination (detected at $\mathbf{x}_w$) was at location $\mathbf{x}$ (random variable) in the aqueous phase (random variable) at time τ in the past (deterministic parameter); and the sorbed phase location probability, $f_{\mathbf{x}_S}(\mathbf{x};\tau,\mathbf{x}_w)$, describes the probability that the detected contamination was in the sorbed phase at $\mathbf{x}$.

For travel time probability with a monitoring well detection, the appropriate load term for an aqueous-phase detection is [*Neupauer and Wilson*, 2000; Chapter 6]

$$\begin{aligned}\frac{\partial h}{\partial C} &= \Bigg[\delta(x_1-x_{1_w})\delta(x_2-x_{2_w}) + a_L\frac{v_1}{|v|}\delta'_{x_1}(x_1-x_{1_w})\delta(x_2-x_{2_w}) \\ &\quad + a_L\frac{v_2}{|v|}\delta(x_1-x_{1_w})\delta'_{x_2}(x_2-x_{2_w})\Bigg]\frac{B_{x_3}(x_{3_{wb}},x_{3_{wt}})}{x_{3_{wt}}-x_{3_{wb}}}\delta(\tau)\ ,\end{aligned} \tag{10.7}$$

where $\delta'_{x_i}(x_i-x_{i_w})$ is the derivative of the Dirac delta function with respect to x_i, we assumed flow is essentially horizontal in the vicinity of the well, and the dispersion coefficient is given by [*Bear*, 1972]

$$D_{ij} = a_T v\delta_{ij} + (a_L - a_T)\frac{v_i v_j}{|v|}\ , \tag{10.8}$$

where a_L and a_T are the longitudinal and transverse dispersivities, and δ_{ij} is the Kronecker delta function. Using this load term in (10.2), we obtain the adjoint

state, ψ^*_τ. The aqueous and sorbed phase travel time probabilities are functions of this adjoint state. The aqueous phase travel time probability, $f_{\tau_A}(\tau; \mathbf{x}, \mathbf{x}_w)$, describes the probability that the detected contamination (detected at $\mathbf{x}_w$) was at location $\mathbf{x}$ (deterministic parameter) in the aqueous phase (random variable) at time τ in the past (random variable); and the sorbed phase location probability, $f_{\tau_S}(\tau; \mathbf{x}, \mathbf{x}_w)$, describes the probability that the detected contamination was in the sorbed phase at time τ.

The adjoint state ψ^*_τ is related to these backward travel time probabilities through the relationship [*Neupauer and Wilson*, 2000; Chapter 6]

$$f_{\tau_A}(\tau; \mathbf{x}, \mathbf{x}_w) = |v(\mathbf{x})| w(\mathbf{x}) B(\mathbf{x}) \theta(\mathbf{x}) \psi^*_\tau(\mathbf{x}, \tau) \tag{10.9}$$

for aqueous phase travel time probability and

$$f_{\tau_S}(\tau; \mathbf{x}, \mathbf{x}_w) = (R-1)|v(\mathbf{x})| w(\mathbf{x}) B(\mathbf{x}) \theta(\mathbf{x}) \psi^*_\tau(\mathbf{x}, \tau) \tag{10.10}$$

for sorbed phase travel time probability, where w is the flow width at $\mathbf{x}$ in the x_1, x_2-plane (described below), $B(\mathbf{x})$ is the thickness of the aquifer at $\mathbf{x}$, and R is the retardation coefficient, which is assumed to be spatially uniform. Travel time probability is essentially a flux of ψ^*_τ. This flux must be defined across a control plane, which is represented by the product of the flow width, $w(\mathbf{x})$, and the aquifer thickness, $B(\mathbf{x})$, in (10.9) and (10.10). The flow width is the projection of the control plane onto a line in the x_1, x_2-plane that is perpendicular to groundwater flow (assuming groundwater flow is essentially horizontal), and the aquifer thickness is the height of the control plane.

In most situations, contamination is sampled at multiple locations and times. If multiple detections of contamination are used in the backward model, the location and travel time probabilities can incorporate the information of all detections by relating the single-detection probabilities using [Chapter 8]

$$f_{\mathbf{x}_j}(\mathbf{x};\tau) = \frac{\prod_{k=1}^{N} f_{\mathbf{x}_j}(\mathbf{x};\tau_k,\mathbf{x}_{w_k})}{\int_{\mathbf{x}} \prod_{k=1}^{N} f_{\mathbf{x}_j}(\mathbf{x};\tau_k,\mathbf{x}_{w_k})\, d\mathbf{x}} \tag{10.11}$$

for location probability and

$$f_{\tau_j}(\tau;\mathbf{x}) = \frac{\prod_{k=1}^{N} f_{\tau_j}(\tau;\mathbf{x}_k,\mathbf{x}_{w_k})}{\int_{\tau} \prod_{k=1}^{N} f_{\tau_j}(\tau;\mathbf{x}_k,\mathbf{x}_{w_k})\, d\tau} \tag{10.12}$$

for travel time probability, where j is the phase (aqueous or sorbed), N is the number of detections, $f_{\mathbf{x}_j}(\mathbf{x};\tau_k,\mathbf{x}_{w_k})$ is the single-detection location probability for detection k (from (10.5) or (10.6)), $f_{\tau_j}(\tau;\mathbf{x}_k,\mathbf{x}_{w_k})$ is the single-detection travel time probability for detection k (from (10.9) or (10.10)), $\mathbf{x}_k$ denotes the prior position of the particle from detection k, τ_k is the backward time for detection k, and the integral in (10.11) is evaluated over all spatial dimensions, and the integral in (10.12) is evaluated over the time domain. The multiple-detection location probability is conditioned on the fact that the detected contaminant parcels coexisted at some location at time τ, and the multiple-detection travel time probability is conditioned on the parcels having coexisted at location $\mathbf{x}$ at some time in the past. Because of this conditioning, the multiple-detection location and travel time probabilities integrate to one over the space and time domains, respectively. To calculate the multiple-detection probabilities, we run one simulation for each detection to obtain the single-

detection probabilities, then we combine the results using the equations above.

10.3.2 Flow Model

The flow field for the backward model can be obtained by reversing the flow field in a forward model. *Zheng* [1999] simulated flow and transport of the CS-10 TCE plume under remediation conditions using MODFLOW-96 [*Harbaugh and McDonald*, 1996] and MT3DMS [*Zheng and Wang*, 1999]. We used his model as the foundation for our backward model. The purpose of *Zheng*'s [1999] model was to simulate the performance of the ETR remediation system. Since the backward model simulates transport of TCE in the past, we modified the flow model of *Zheng* [1999] to simulate flow conditions in the vicinity of the CS-10 plume prior to remediation by eliminating the ETR extraction wells, injection wells, and infiltration trenches from the simulation (see Figure 10.2).

The model domain is a 22440 ft $\times$ 27720 ft rectangular region, discretized into 159 columns, 161 rows, and 21 layers (see Figure 10.9). The lower left-hand corner of the domain corresponds to an easting of 852413.6 and a northing of 222347.0, with a rotation of 11 degrees. The horizontal spatial discretization ranges from 110 ft near the plume to 660 ft near the boundaries. Vertical thickness of layers ranges from less than 5 ft to over 50 ft. The flow model boundaries are specified flux at the top boundary with recharge rates ranging from 16 to 34 in/yr, no-flow at the bottom boundary, and specified head at the side boundaries. The hydraulic head values along the side boundaries were interpolated from a regional flow model created by Jacobs Engineering

Group [*Zheng*, 1999].

Hydraulic conductivity in the model domain ranges from 10 ft/day for silts to over 300 ft/day for coarse sands. The average hydraulic gradient is approximately 0.001. Groundwater velocity ranges from 1 ft/day to more than 4 ft/day, generally in the south-southwest direction, and flow is essentially horizontal [*Zheng*, 1999]. We assume that flow can be modeled as steady state. By simulating forward groundwater flow using MODFLOW-96, we obtained the flow field illustrated by the water table elevations in Figure 10.10. The hydraulic head distribution is essentially unchanged over the depth of the model. For the backward probability model, we reverse this flow field.

10.3.3 Transport Model

The backward transport model (10.2) is the adjoint of a forward model (10.1). We used the forward model of *Zheng* [1999] as the basis for our adjoint model. Since the backward model simulates the same transport processes as the forward model, we used the same transport parameters in the backward model as were used in the forward model. However, we chose to eliminate both first-order decay and recharge. By eliminating first-order decay, we are essentially conditioning the probabilities on the fact that the detected solute has not decayed. We eliminate recharge because *Zheng* [1999] used $C_I = 0$ for TCE in his forward transport model, therefore, it is assumed that TCE did not enter the aquifer through natural recharge. The transport parameters are listed in Table 10.1. Note that the MMR forward model assumes equilibrium sorption of TCE (retardation coefficient of 1.56) and first-order decay of TCE,

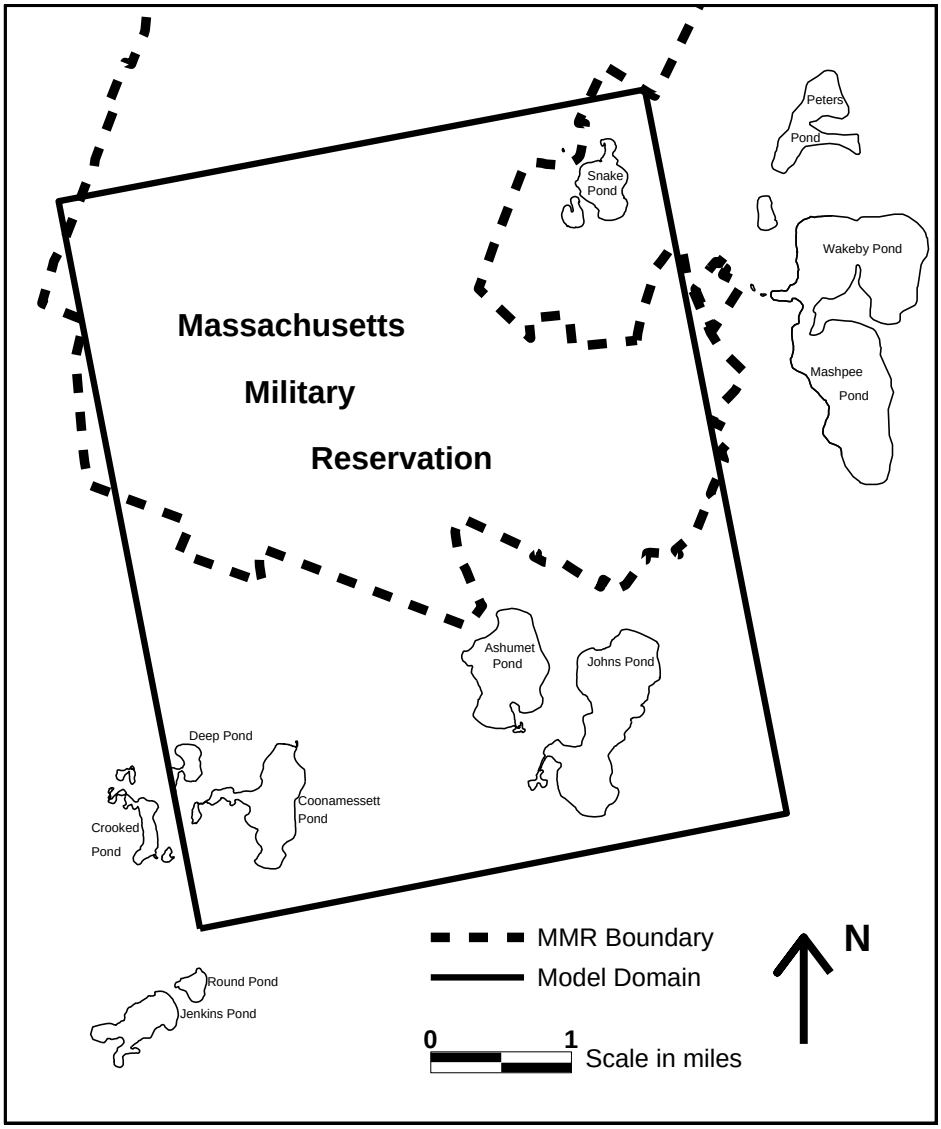

Figure 10.9: Domain for the CS-10 flow and transport model.

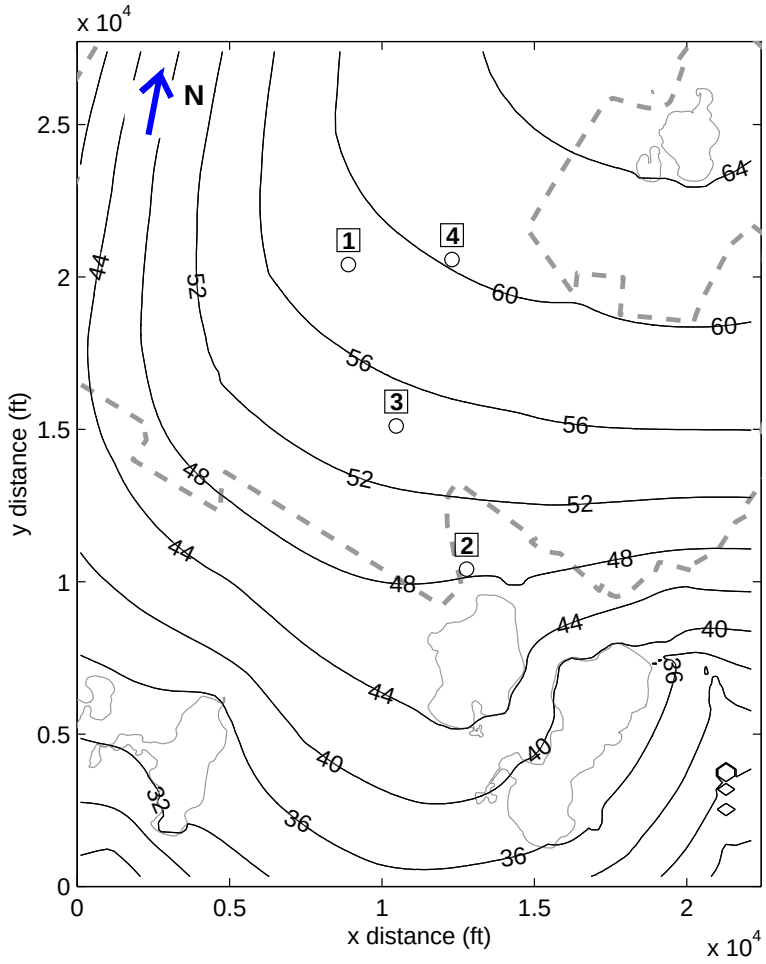

Figure 10.10: Water table elevations from forward flow simulation (units are ft). The four circles denote sample locations that we use later. The boxed numbers denote the sample number.

Table 10.1: Transport parameter values for the MMR TCE simulations (from *Zheng* [1999]).

Parameter	Value
Porosity	0.3
Longitudinal dispersivity (ft)	35
Horizontal transverse dispersivity (ft)	3.5
Vertical transverse dispersivity (ft)	0.35
Retardation coefficient	1.56
First-order decay rate (day^{-1})	3.16×10^{-5}

presumably due to biotic and abiotic dechlorination processes.

The differences between the forward and backward models are the reversal of the velocity field, modification of the boundary and initial conditions, and, if desired, elimination of the first-order decay and recharge terms, as described above. The initial condition of the backward model is homogeneous everywhere, and the boundary conditions depend on the boundary conditions used in the forward model. The transport model boundary conditions used by *Zheng* [1999] in the forward model are zero-gradient at all boundaries (i.e., no dispersive flux); therefore, from (10.2) we see that the boundary conditions for the backward model are third-type (zero flux) everywhere.

We solved the backward model using MT3DMS, using the implicit finite difference method with upstream weighting of the advective term, and using the generalized conjugate gradient matrix solver with the SSOR preconditioner. MT3DMS does not allow third-type boundary conditions; therefore, we used second-type boundary conditions on all boundaries.

Table 10.2: TCE samples used in the backward model.

Sample No.	Easting (ft)	Northing (ft)	Elevation (ft m.s.l.)	Screen Length (ft)	Sample Date	Conc. (μg/L)
1	857251	244076	2.99	5	9/11/1996	58
2	862970.8	235003.4	-124.72	5	6/13/1997	5110
3	859806.3	239178.9	-48.05	40	10/26/1998	203.1
4	860560	244884	-52.1	5	6/21/2000	150

Of the data presented in Figures 10.4–10.8, we arbitrarily selected the four samples listed in Table 10.2 to use in the backward model. The sample locations are shown in Figure 10.11, along with the inferred plume boundary, and in Figure 10.10 for reference. Sample 1, from a shallow monitoring well, is the earliest sample we have; Sample 2 is from a deep monitoring well and has the highest concentration of the samples taken between 1996 and 2000; Sample 3 is in the center of the plume at an intermediate depth, and Sample 4 is the most recent sample we have, and is taken from an intermediate depth near the center of the plume. Samples 1–3 were taken before implementation of the remediation scheme.

In the backward simulations, the sample locations are treated as sources of probability, described in the load term, $\partial h/\partial C$. The load is distributed over the screened interval of the well (implemented with the normalized boxcar function). In Chapter 7, we explain that the model domain should be vertically discretized so that the screened interval corresponds to a model layer. Because we used a model that was developed for a different purpose, the vertical discretization did not correspond to the screened intervals. Therefore,

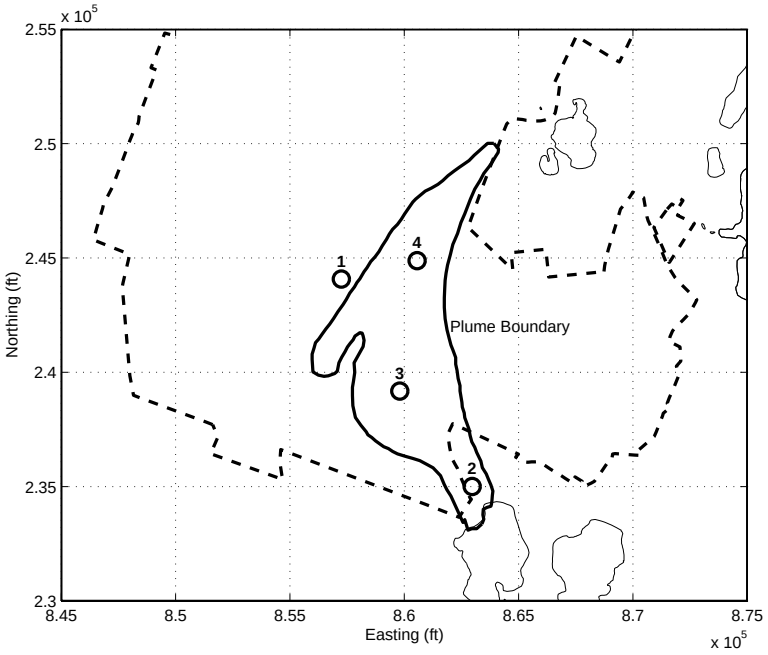

Figure 10.11: Location of samples used in the backward model.

in our implementation of the load terms, within the model cell containing the sample location, we distributed the load over the entire layer thickness. The screen length for Sample 3 was 40 ft, which was larger than the layer thickness; therefore, the load for Sample 3 was distributed over three layers to better approximate a 40-ft screen length.

10.4 Results and Discussion

We ran backward simulations to obtain backward location and travel time probabilities for the four samples in Table 10.2 using MT3DMS, following the numerical implementation discussed in Chapter 7. We present the single-detection and multiple-detection probability distributions resulting from these

simulations.

10.4.1 Backward Location Probability Results

For each sample, we calculated the single-detection backward location probability for five times in the past:

- January 1, 1962–the approximate start of operations at the BOMARC Missile Site,
- January 1, 1968–approximately midway through the BOMARC Missile Site operations,
- January 1, 1973–the approximate end of BOMARC Missile Site operations,
- January 1, 1978– the approximate start of UTES operation,
- January 1, 1988–approximately midway between the start of UTES operation and the sampling dates.

The results can be presented in several ways. For example, if we believe that contamination entered the aquifer through recharge, we could look at the location probability at the water table, i.e., in the top layer of the model. Alternatively, for a dense non-aqueous phase liquid (DNAPL), we could assume that the contamination entered the aquifer in the non-aqueous liquid phase, and because it is more dense than water, became distributed vertically throughout the aquifer. In this case, the source is distributed vertically in the aquifer; therefore, we look at the vertically-averaged location probability over the depth

of the aquifer. For the numerical model, these results can be calculated for each cell in the x_1, x_2-plane. In this example, we assume TCE entered by the second process; therefore, we present the vertically-integrated probabilities.

The vertically-integrated aqueous-phase backward location probabilities for the five times are shown in Figures 10.12–10.16. The vertically-integrated probabilities represent the probability that the sampled contamination was at location (x_1, x_2) at any depth. The sorbed phase location probability distributions (not shown) have the same shape as these, but are scaled by $R - 1 = 0.56$. The location probability distributions indicate that the detected contamination is not likely to have originated at the BOMARC Missile Site. For example, the location probability plume for Sample 2 never reaches the BOMARC Site, and the location probability plume for Sample 3 reaches the BOMARC Site only at very low probabilities and only in 1962, the year that operations began. The location probability plumes for Samples 1 and 4 reach the BOMARC Site, but even in 1962 their centroids are still downgradient of the Site. These plumes could indicate that the BOMARC facility may not have been the source of contamination, but that the actual source was southwest of the BOMARC facility. However, if the BOMARC facility is the source of contamination, the results can be diagnostic of errors in the conceptualization of the model. For example, since the model was calibrated for the remediation conditions, the parameters used in the model may not be accurate for this scenario, or the mathematical conceptualization of the geology, boundary conditions, or transport processes (e.g., linear equilibrium sorption) may be inaccurate. Also, we assumed that the TCE source was vertically-distributed over the entire aquifer depth and that there was only one source; this may be

incorrect. Finally, multiple sources of TCE may be present.

Using the four single-detection aqueous-phase location probability distributions, we calculated the multiple-detection location probability using (10.11). The results, which assume that all four samples share a common prior location, are plotted in Figure 10.17 for 1962, 1968, 1973, and 1978. The results show the likely positions of detected contamination from the four samples assuming their positions coincided at the time of interest. Notice that the spread of the multiple-detection probability distributions is smaller than the spread of the single-detection distributions, indicating that the uncertainty in the prior position is reduced as the number of detections increases. For all four times, if the contaminant parcels coexisted at those times, it is most likely that their position was at a location southwest of the BOMARC Missile Site. However, we cannot say with any certainty that the particles did coexist. Figure 10.18 shows the outlines of the single- and multiple-detection aqueous phase backward location probability plumes for 1962, along with the possible TCE source areas from Figure 10.3. From the backward model results, it appears that a likely source of TCE is CS-22, an area that was recently reported to be a possible source location [*MMR IRP*, 2000c].

For comparison, we also calculated the multiple-detection aqueous phase backward location probability with recharge and decay included in the adjoint equation. The results are plotted in Figure 10.19 for 1962, 1968, 1973, and 1978. The single-detection probabilities (not shown) are not conservative (i.e., do not integrate to one over the spatial domain) because probability is lost through decay and through reversed natural recharge; however, the multiple-detection distribution does integrate to one because it is conditioned on the

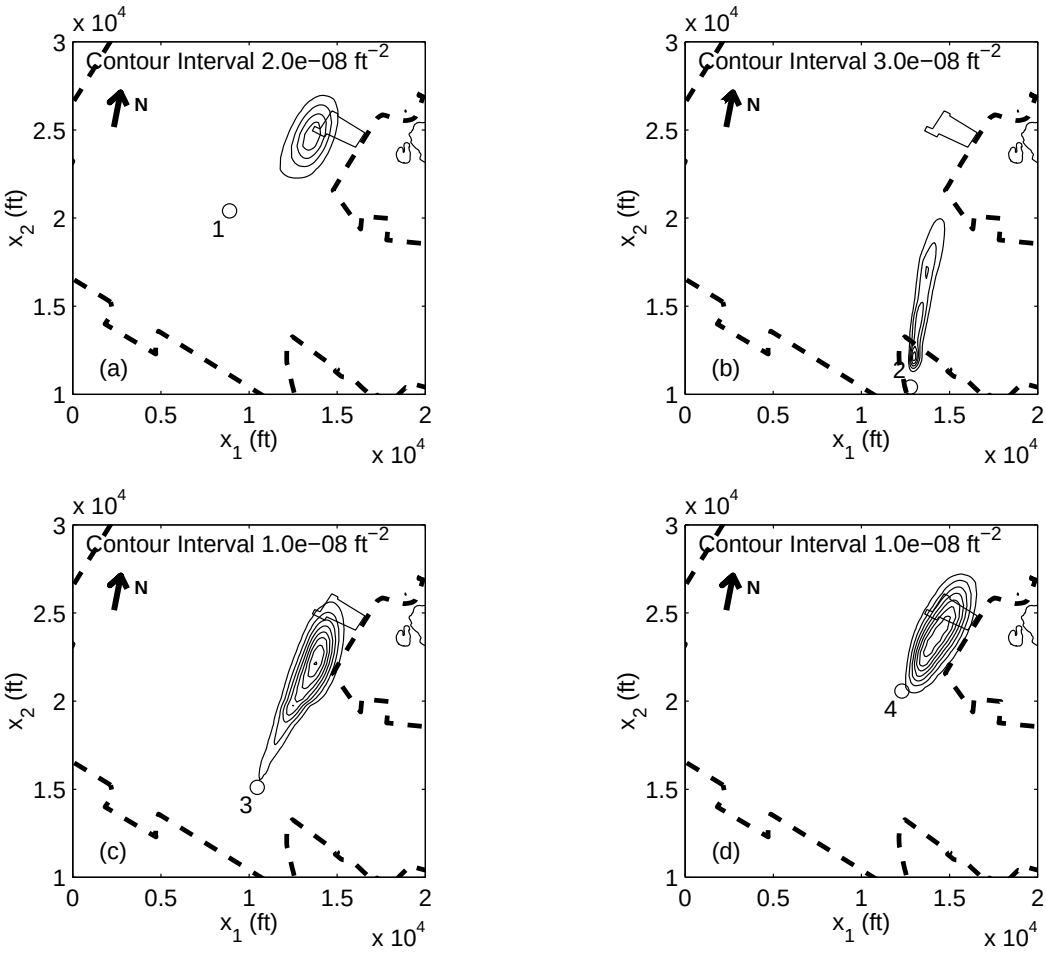

Figure 10.12: Single-detection aqueous-phase backward location probability for four samples on January 1, 1962. (a) Sample 1. (b) Sample 2. (c) Sample 3. (d) Sample 4. Sample locations are marked with a circle.

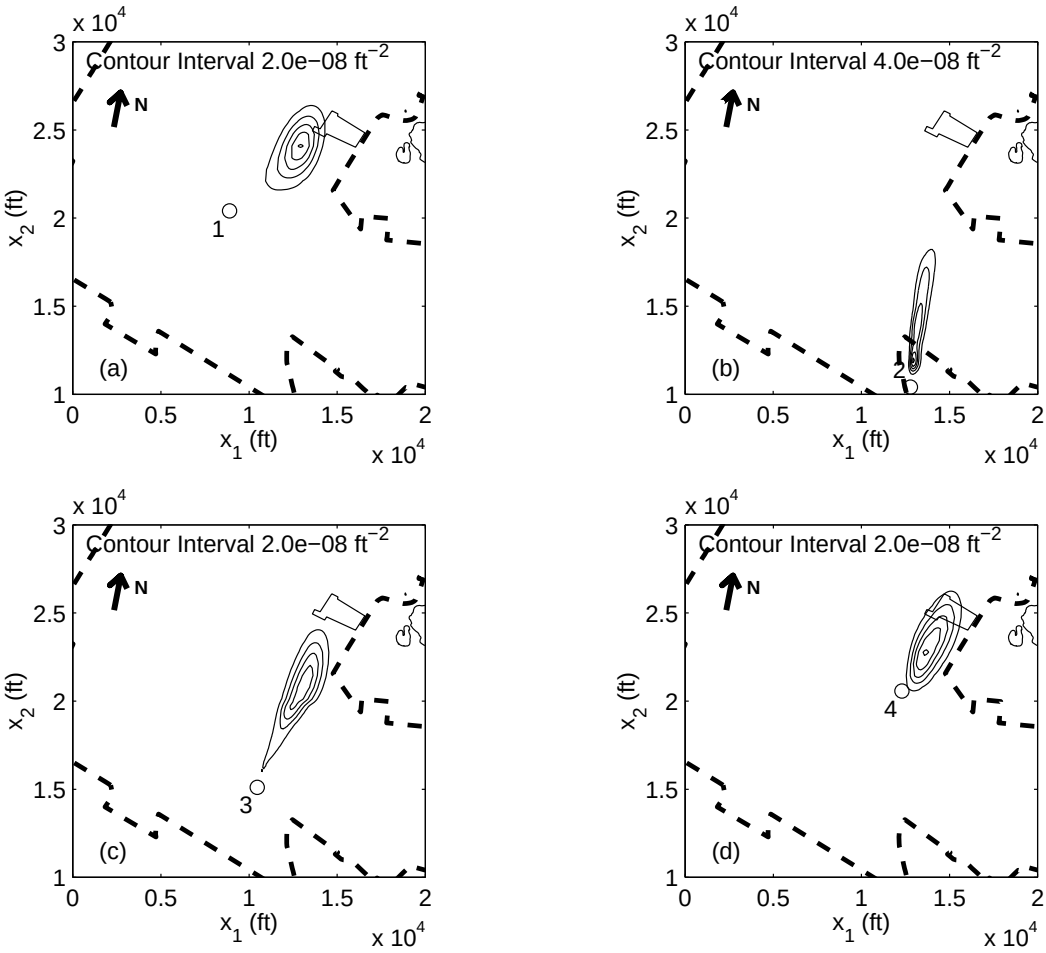

Figure 10.13: Single-detection aqueous phase backward location probability for four samples on January 1, 1968. (a) Sample 1. (b) Sample 2. (c) Sample 3. (d) Sample 4. Sample locations are marked with a circle.

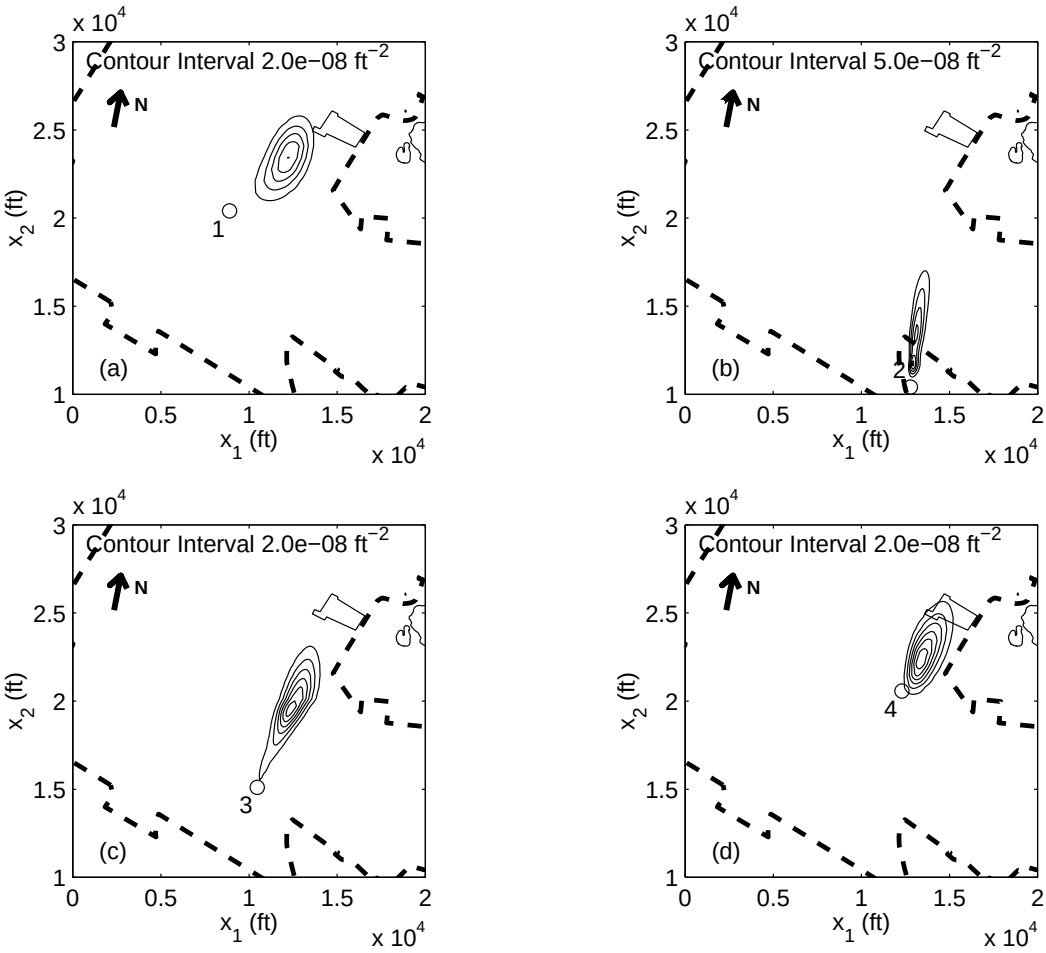

Figure 10.14: Single-detection aqueous phase backward location probability for four samples on January 1, 1973. (a) Sample 1. (b) Sample 2. (c) Sample 3. (d) Sample 4. Sample locations are marked with a circle.

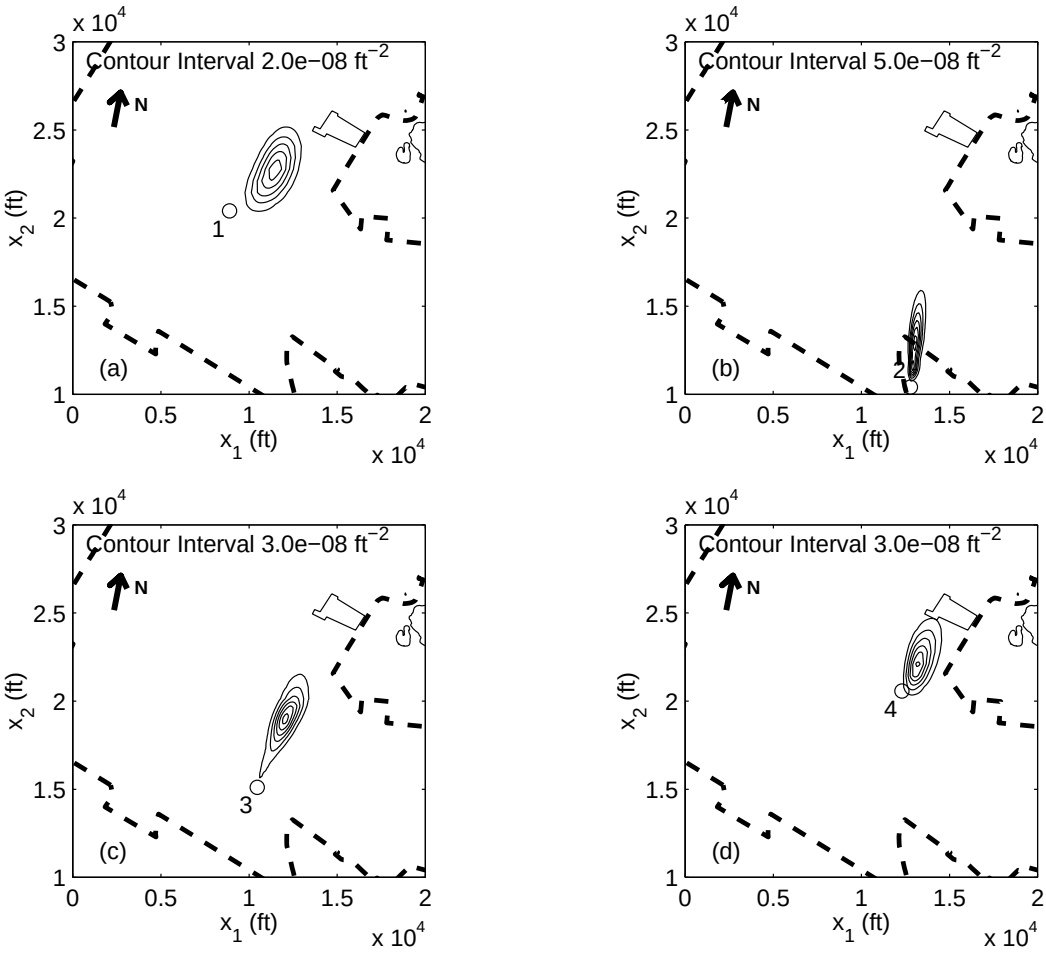

Figure 10.15: Single-detection aqueous phase backward location probability for four samples on January 1, 1978. (a) Sample 1. (b) Sample 2. (c) Sample 3. (d) Sample 4. Sample locations are marked with a circle.

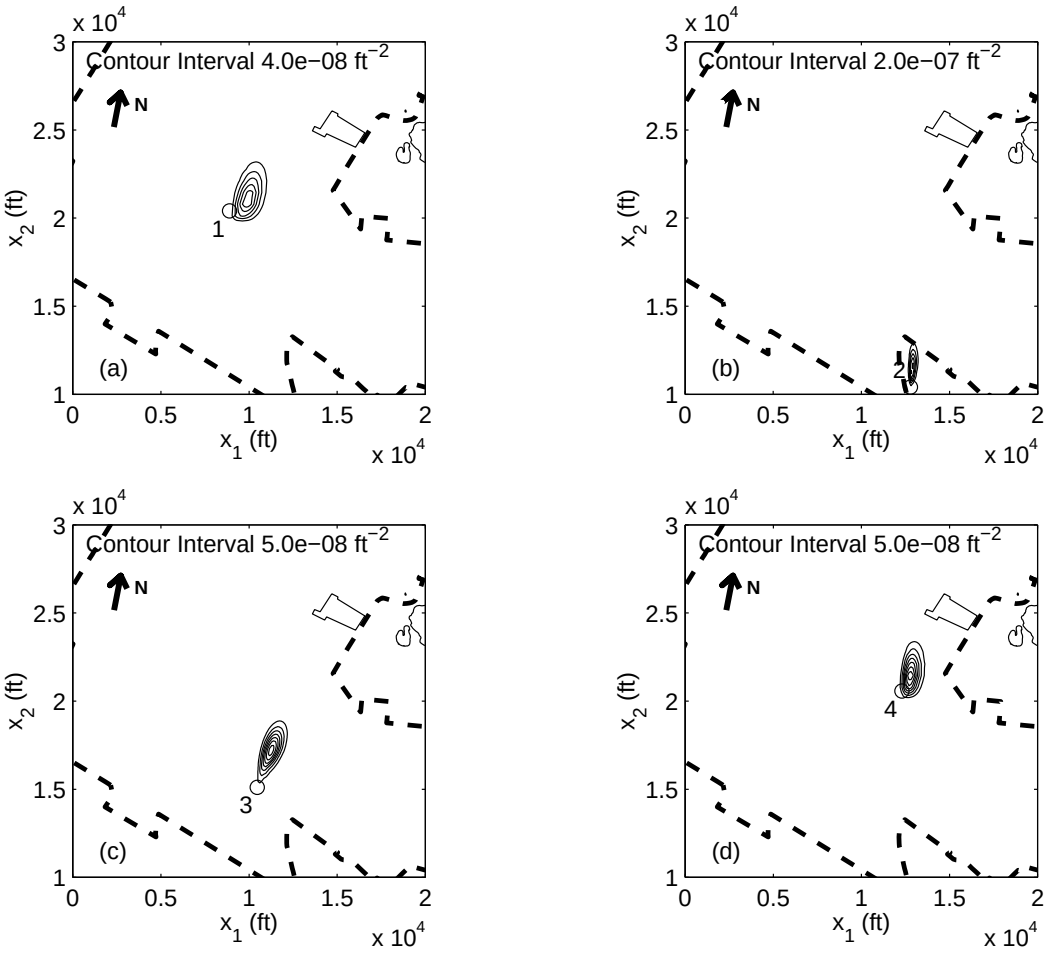

Figure 10.16: Single-detection aqueous phase backward location probability for four samples on January 1, 1988. (a) Sample 1. (b) Sample 2. (c) Sample 3. (d) Sample 4. Sample locations are marked with a circle.

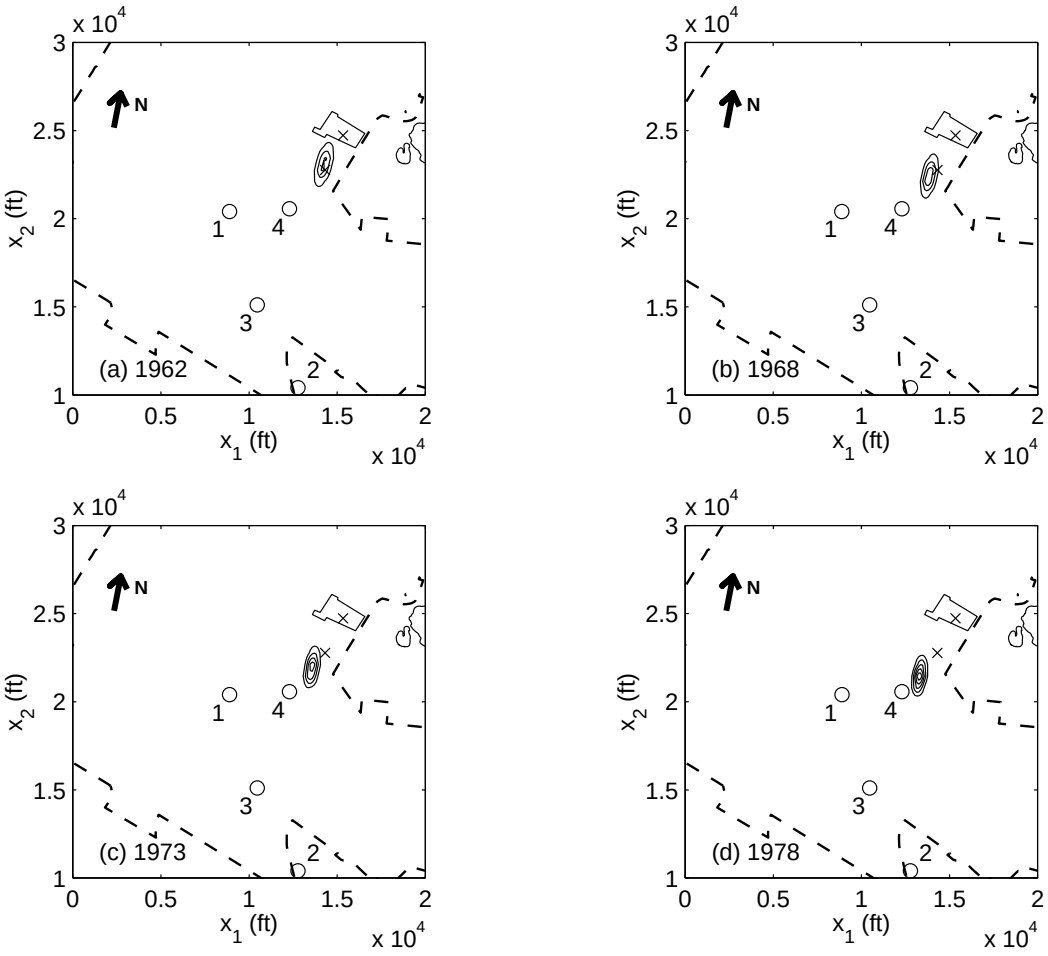

Figure 10.17: Multiple-detection aqueous phase backward location probability distributions. (a) 1962. (b) 1968. (c) 1973. (d) 1978. Contour interval is 2×10^{-7} ft^{-2}. Sample locations are marked with a circle.

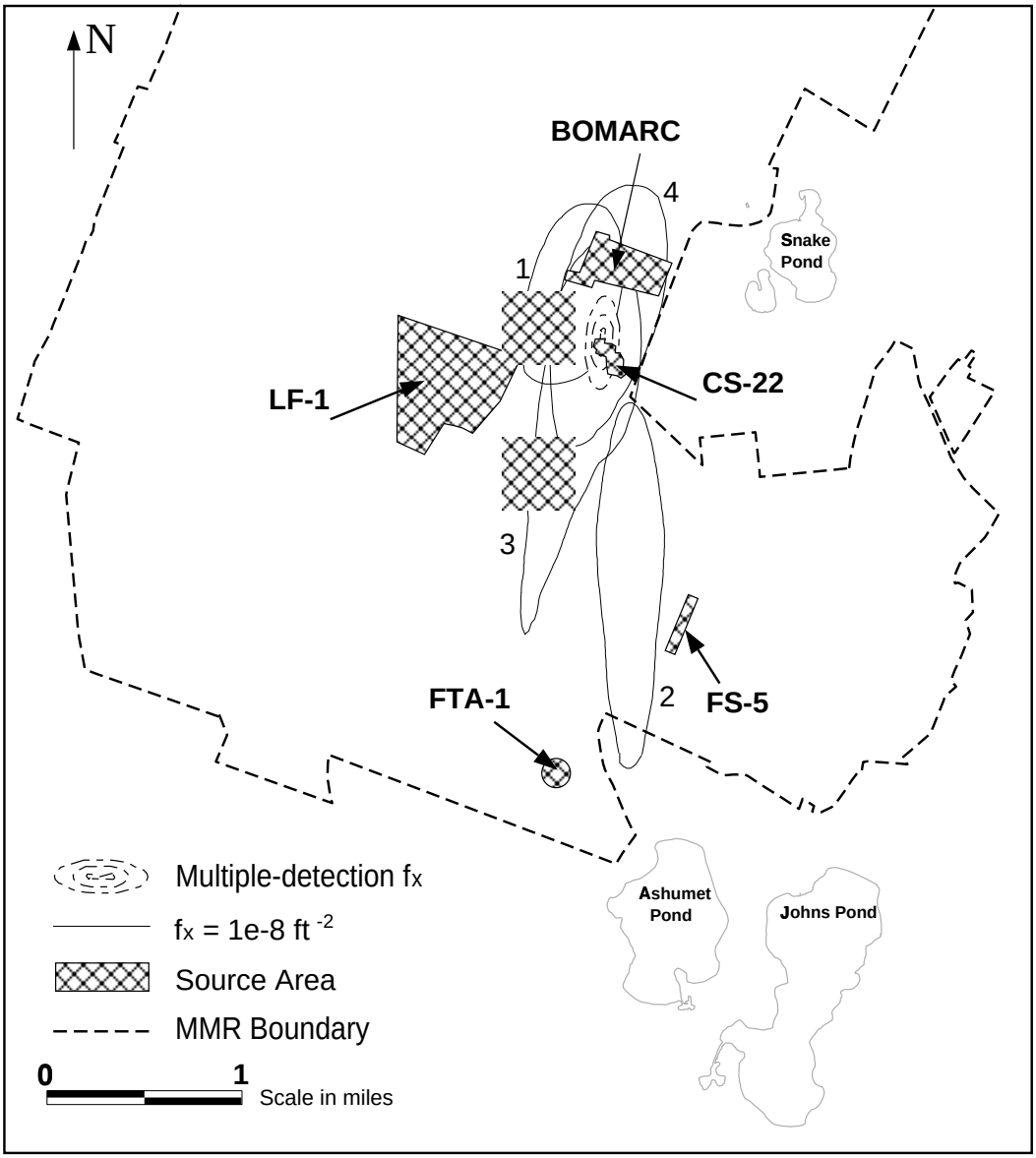

Figure 10.18: Single- and multiple-detection aqueous phase backward location probability distributions for 1962 and possible TCE source locations. The numbers indicate the sample location to which the single-detection probability distribution corresponds. The contour interval for the multiple-detection probability plume is 2×10^{-7} ft^{-2}.

assumption that particles coexisted at the time of interest. Comparison of the probability distributions with and without decay and recharge (Figure 10.19 and 10.17) show very little difference in the results. Therefore, for this case, the final results are insensitive to our choice of eliminating decay and recharge in the backward model.

10.4.2 Backward Travel Time Probability Results

If the source location is known or assumed to be known, backward travel time probability can be used to determine the solute travel time from the source to the detection location. We ran backward travel time probability simulations for the four samples in Table 10.2 using MT3DMS. For each sample, we calculated the single-detection aqueous phase travel time probability for releases in the BOMARC Missile Site area (easting= 862750 ft and northing= 249550 ft) and the CS-22 area (easting= 862119 ft and northing= 247430 ft). Each potential source is denoted by an $\times$ in Figures 10.17 and 10.19. The source areas were each represented by one cell in the x_1, x_2-plane of the model domain, over the entire depth (21 layers). Travel time probability is defined as a flux across a control plane in the source area, perpendicular to groundwater flow; therefore, the magnitude of travel time probability is proportional to the area of this control plane. The height of the control plane is the aquifer thickness (sum of the thicknesses of each of the 21 layers), which was 262 ft for both source areas. The width of the control plane is the length perpendicular to flow in each layer representing the source. Since the actual source areas for the BOMARC Missile Site and CS-22 are unknown, we use a unit width for the control plane and present the results as travel time probability per unit width

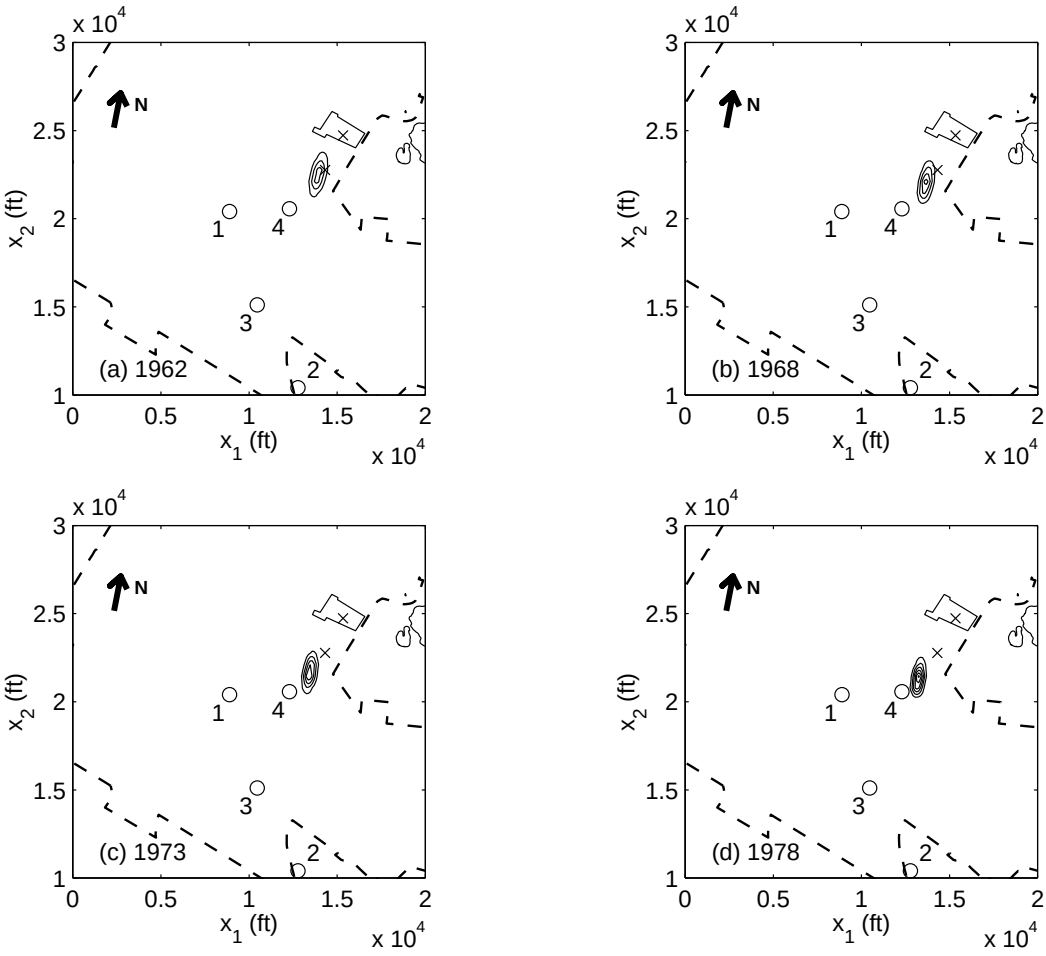

Figure 10.19: Multiple-detection aqueous phase backward location probability distributions using recharge and decay. (a) 1962. (b) 1968. (c) 1973. (d) 1978. Contour interval is 2×10^{-7} ft^{-2}. Sample locations are marked with a circle.

(of the control plane).

The vertically-integrated aqueous-phase backward travel time probabilities for the four samples are plotted in Figure 10.20. The sorbed-phase probability distributions (not shown) have the same shape but are scaled by a factor of $R - 1 = 0.56$. On the plots, $\tau = 0$ corresponds to July 1, 2000. The region between the dashed lines represents the time of operation of the BOMARC Missile Site. The most likely travel times to the sample locations ranges from 43–67 years for the BOMARC site, and from 29–54 years for CS-22. The distributions extend out to 100-200+ years for the BOMARC Site, and to 75–200 years for CS-22. These long travel times are unrealistic. Sample 4 is the only sample of the four that is likely to have originated at the BOMARC Missile Site during site operations; while Samples 1, 3, and 4 have a low, but non-zero, probability of having originated at CS-22 during operations of the BOMARC Missile Site.

These results suggest that of the two pre-selected sites (BOMARC and CS-22), CS-22 is more a likely source of contamination, based on the travel time probabilities during the time of operation of the BOMARC Site. For Sample 2, however, neither site appears to be a likely source. Although Sample 2 has the highest concentration of the samples taken from 1996–2000, it is the most distant sample from either of the pre-selected possible sources. The most likely travel time to Sample 2 is approximately 67 years (release in 1933) from the BOMARC Site and 54 years (release in 1946) from CS-22. These times are prior to the start of BOMARC operations; therefore, it is likely that the source of this contamination is closer to the sampling location or that these areas were contaminated prior to the start of operations at the

BOMARC Missile Site. Alternatively, since the forward model was developed for the remediation conditions, the parameters used in the model may not be accurate for this scenario.

The integral of the backward travel time probability over all times represents the probability that the detected contamination was ever present at the source location. These values are presented in Table 10.3 as travel time probability per unit width of the source area. To obtain the travel time probability for the entire source, they must be multiplied by the width of the source area perpendicular to flow; therefore, these values depend on the source area. Of the four samples, Samples 3 and 4 are the most likely to have ever been present at either of the source areas. Although CS-22 is more likely than the BOMARC Site to be a source of contamination, the values in Table 10.3 are larger for the BOMARC Site. This indicates that if travel time were not a consideration (i.e., ignoring the site history), the detected contamination is more likely to have been at the BOMARC Site than at CS-22 (at any time in the past). This is due to the flow field, which diverges from the northeast in the forward model (see Figure 10.10); therefore, the backward flow lines converge to the northeast. Since the BOMARC Site is located farther northeast of CS-22, a larger percentage of the converging flow passes the BOMARC site (per unit width) than CS-22; therefore, in the absence of a travel time constraint, contamination detected downgradient is more likely to have been near the BOMARC site.

Using the four single-detection aqueous-phase travel time probability distributions, we calculated the multiple-detection travel time probability using (10.12). The result, plotted in Figure 10.21, shows the probability of the time

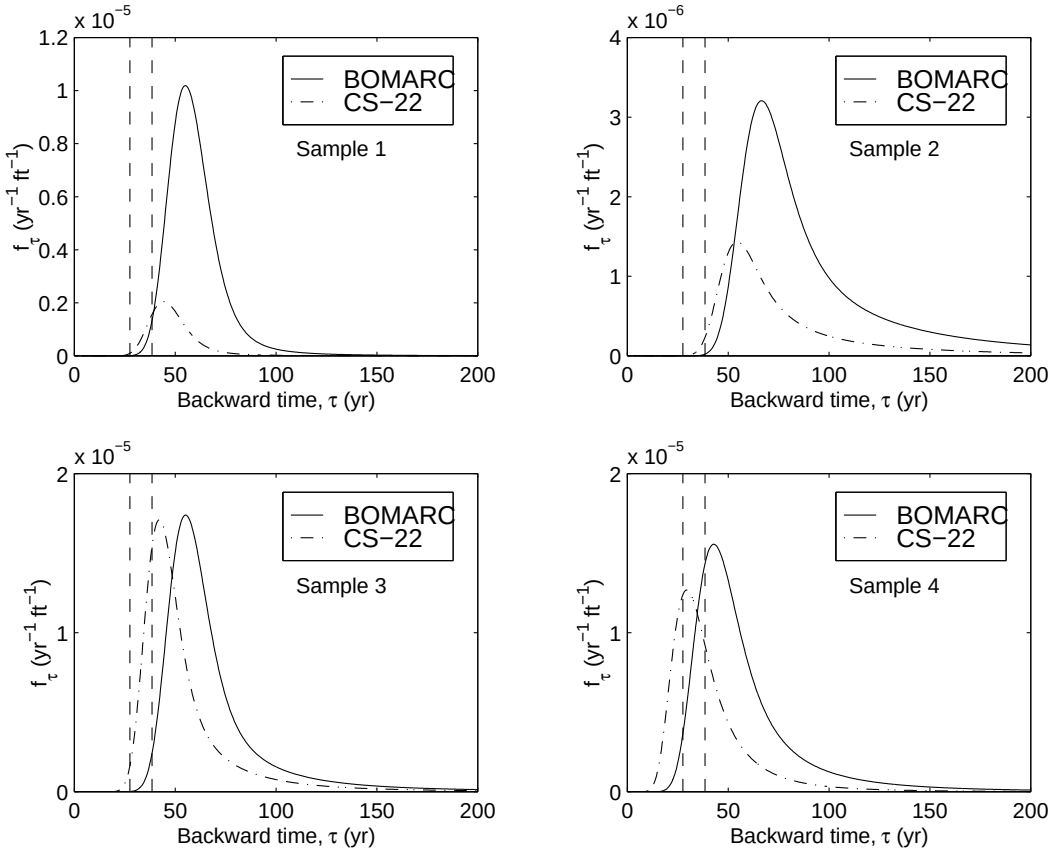

Figure 10.20: Single-detection aqueous phase backward travel time probability distributions (per unit width) from the two suspected source areas for four samples. $\tau = 0$ corresponds to July 1, 2000. Region between the dashed lines represents the time of operation of the BOMARC Missile Site.

Table 10.3: Area under the travel time probability distributions (per unit width) from BOMARC and CS-22 for the four samples.

Sample No.	Area for BOMARC (ft^{-1})	Area for CS-22 (ft^{-1})
1	2.69×10^{-4}	4.75×10^{-5}
2	1.47×10^{-4}	5.72×10^{-5}
3	5.56×10^{-4}	4.65×10^{-4}
4	5.66×10^{-4}	3.73×10^{-4}

that the four contaminant parcels were at the source location, assuming that they were all present at the same location at the same time. The most likely travel times are 57 years from the BOMARC Site (release in 1943) and 45 years from CS-22 (release in 1955). If the contaminant parcels coexisted at the same location, it is unlikely that they were at the BOMARC Missile Site during operations; however, there is a non-zero probability that the particles could have coexisted at CS-22 during the early operations of the BOMARC facility (later backward times). As stated before, these results could indicate that the BOMARC facility was not the source of contamination, but CS-22 may have been; that the model may not be accurate for this scenario; that the BOMARC site was contaminated prior to the start of BOMARC operations; or that there was more than one source.

10.5 Conclusions

Backward-in-time location and travel time probabilities can be used to obtain information about the prior position of contamination that was ob-

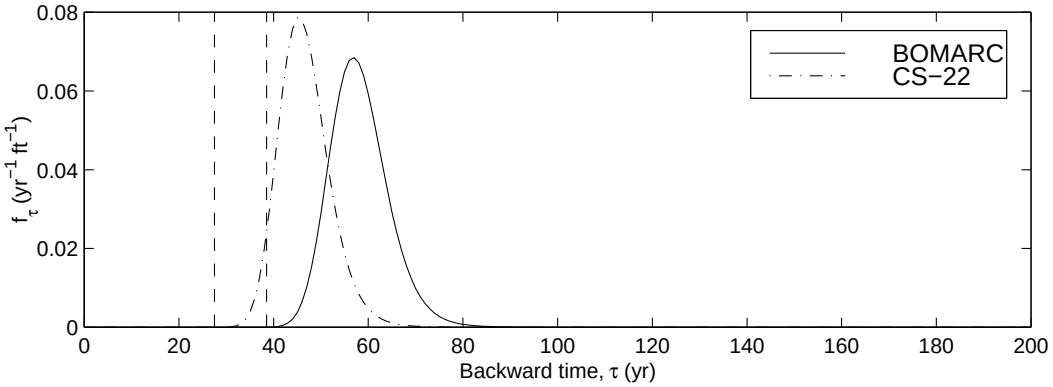

Figure 10.21: Multiple-detection aqueous-phase backward travel time probability distribution from the source area for four samples. $\tau = 0$ corresponds to July 1, 2000. Region between the dashed lines represents the time of operation of the BOMARC Missile Site.

served in an aquifer. For a contaminant parcel that was detected in an aquifer, the backward location probability describes its position at some time prior to sampling and the backward travel time probability describes the amount of time required for it to travel to the sampling location from some upgradient position.

In this paper, we applied the backward modeling approach to a trichloroethylene (TCE) plume at the Massachusetts Military Reservation. The suspected contamination source area is a former missile site that is presently used for maintenance and storage of vehicles. Other spills and releases of chemicals have occurred in this area in the past and have contributed to the contamination. TCE samples have been taken throughout the plume area. We selected four TCE samples to be used in the model. These samples were taken between September 1996 and June 2000 and represent the central and terminal regions of the plume.

The backward probability model treats each detection as a source of probability and simulates the movement of the probability plume upgradient and in reversed time, toward the possible sources. Our numerical model was based on a model developed to simulate the response of the plume to the remediation system [*Zheng*, 1999]. We used MODFLOW-96 to simulate pre-remediation flow conditions using the hydraulic parameters of *Zheng* [1999], and we used MT3DMS to simulate the backward probability movement using transport parameters from the model of *Zheng* [1999].

The single-detection location probability shows the likely prior position of contamination from each of the samples. The results indicate a low probability that the detected contamination originated from the BOMARC Site. The multiple-detection location probability shows the likely positions of the four detected contaminant parcels, assuming their positions coincided at the time of interest. The results also show that it is unlikely that the contamination originated at the BOMARC Missile Site during site operations. This could indicate that the BOMARC facility was not the source of contamination, or that the model calibration, which was based on remediation conditions, may not be accurate for this scenario. Based on the results, the CS-22 area, which is south of the BOMARC facility, is a possible source of contamination.

The single-detection travel time probability describes the likely travel time from an upgradient location to each sampling location. The results indicate that long travel times would be needed for contamination to travel from the BOMARC and CS-22 sites to the sampling locations, especially Sample 2. Only one of the four samples (Sample 4) was likely to have originated at the missile site during site operations, but three of the four samples (Samples 1,

3, and 4), could have originated at CS-22 during BOMARC site operations. This is consistent with a recent report stating that disposal of waste from the BOMARC facility may have occurred at CS-22 [*MMR IRP*, 2000c]. The multiple-detection backward travel time probability distribution shows that if the contaminant parcels were released at the same location, it is unlikely that they were at the released at the BOMARC site during site operations, but it is possible, although with low probability, that they were released at CS-22 during the early operations of the BOMARC site. The probabilities also suggest that the BOMARC site may have been contaminated by some other activity prior to the start of BOMARC operations.

Based on the results of the backward model, it appears that the BOMARC Missile Site may not have been the source of contamination, but that the actual source was southwest of the BOMARC facility. The results indicate that a possible source location is CS-22, an area that has recently been identified as a potential source. If, instead, the BOMARC facility is the source of contamination, the backward model results can be diagnostic of errors in the conceptualization of the model.

Acknowledgments

This research was supported in part by the Geophysical Research Center at New Mexico Tech and in part by the Environmental Protection Agency's STAR Fellowship program under Fellowship No. U-915324-01-0. This work has not been subjected to the EPA's peer and administrative review and therefore may not necessarily reflect the views of the Agency and no official endorsement

should be inferred. Data for the CS-10 TCE plume at MMR was provided by Sarah Stuart of Jacobs Engineering Group Inc. at Otis Air National Guard Base. Spence Smith of the Massachusetts Military Reservation provided information on the TCE contamination and remediation. Chunmiao Zheng of the University of Alabama provided his flow and transport model of the CS-10 TCE plume at MMR.

References

Bagtzoglou, A.C., D.E. Dougherty, and A.F.B. Thompson, Application of particle methods to reliable identification of groundwater pollution sources, *Water Resources Management*, 6, 15–23, 1992.

Bear, J., *Dynamics of Fluids in Porous Media*, American Elsevier Publishing Company, New York, 1972.

Chin, D.A. and P.V.K. Chittaluru, Risk management in wellhead protection, *J. Water Resour. Plan. Manage.*, 120(3), 294–315. 1994.

Harbaugh A.W. and M.G. McDonald, *User's Documentation for MODFLOW-96, an update to the U.S. Geological Survey Modular Finite-Difference Ground-Water Flow Model*, U.S. Geological Survey, Open-File Report 96-485, 1996.

Kavanaugh, M.C., J. Mercer, and A. Leeson, A Technical Review of Groundwater Remedial Actions at Massachusetts Military Reservation, Massachusetts Military Reservation, Installation Restoration Program, 2000.

MMR IRP (Massachusetts Military Reservation, Installation Restoration Program), Chemical Spill 10 (CS-10) Groundwater Plume Fact Sheet, May, 1997, http://www.mmr.org/cleanup/index.htm.

MMR IRP (Massachusetts Military Reservation, Installation Restoration Program), Joint Program Office, Fact Sheet, July, 1998, http://www.mmr.org/cleanup/index.htm.

MMR IRP (Massachusetts Military Reservation, Installation Restoration Pro-

gram), Chemical Spill 10 (CS-10) Source and Plume Update, Fact Sheet #99-08, September, 1999, http://www.mmr.org/cleanup/index.htm.

MMR IRP (Massachusetts Military Reservation, Installation Restoration Program), Chemical Spill 10 (CS-10) Plume Update, Fact Sheet #2000-01, January, 2000a, http://www.mmr.org/cleanup/index.htm.

MMR IRP (Massachusetts Military Reservation, Installation Restoration Program), News Release 2000-24, April 27, 2000b, http://www.mmr.org/cleanup/index.htm.

MMR IRP (Massachusetts Military Reservation, Installation Restoration Program), News Release 2000-51, Sept. 26, 2000c, http://www.mmr.org/cleanup/index.htm.

MMR IRP (Massachusetts Military Reservation, Installation Restoration Program), Site Description, 2000d, http://www.mmr.org/irp/index.htm.

MMR IRP (Massachusetts Military Reservation, Installation Restoration Program), Sites, 2000e, http://www.mmr.org/cleanup/index.htm.

Neupauer, R.M. and J.L. Wilson, Adjoint method for obtaining backward-in-time location and travel time probabilities of a conservative groundwater contaminant, *Water Resour. Res.*, 35(11), 3389–3398, 1999.

Neupauer, R.M. and J.L. Wilson, Adjoint-derived location and travel time probabilities in a multi-dimensional groundwater flow system, *Water Resour. Res.*, in press, 2000.

Uffink, G.J.M., Application of Kolmogorov's backward equation in random

walk simulations of groundwater contaminant transport, in *Contaminant Transport in Groundwater*, H.E. Kobus and W. Kinzelbach, editors, pp. 283–289, A.A. Balkema, Brookfield, Vt., 1989.

USEPA (United States Environmental Protection Agency), Code of Federal Regulations, 40 CFR 141.61, Maximum contaminant levels for organic contaminant, July 1, 1999.

USEPA (United States Environmental Protection Agency), National Priorities List Sites: Massachusetts, EPA/540/8-91/036, Pub. #92005-722A, Office of Emergency and Remedial Response, Washington, D.C., Sept., 1991.

Wilson, J.L. and J. Liu, Backward tracking to find the source of pollution, in *Waste-management: From Risk to Remediation*, edited by R. Bhada *et al.*, ECM Press, Albuquerque, NM, 181–199, 1994.

Wilson, J.L. and J. Liu, Field Validation of the Backward-in-time Advection Dispersion Theory. *Proceedings of the 1996 HSRC/WERC Joint Conf. on the Environment*, Great Plains-Rocky Mountain Hazardous Substance Center, Manhattan, Kansas, http://www.engg.ksu.edu/HSRC/ 96Proceed/wilson.html, 1997.

Zheng, C., Development of Groundwater Flow and Contaminant Transport Models for Remediation System Design Optimization at the Massachusetts Military Reservation (MMR), Technical Report, prepared for the Office of Research and Development, U.S. Environmental Protection Agency, Ada, Oklahoma, October, 1999.

Zheng, C. and P.P. Wang, *MT3DMS: Documentation and User's Guide*, U.S. Army Corps of Engineers, Washington, DC, November, 1999.

CHAPTER 11

CONCLUSIONS AND RECOMMENDATIONS

11.1 Conclusions

If contamination is detected in an aquifer but its source is unknown, contaminant transport modeling can be used to obtain information about the source. With conventional (forward) contaminant transport modeling, we can select several possible source locations, run a forward transport simulation for each, and compare the modeling results with the sampled concentration. If the number of potential sources is large, this approach can result in a significant computational burden since one simulation must be run for each potential source. Furthermore, all potential sources must be pre-identified.

Receptor-based (backward) modeling is a more efficient approach for obtaining information about the source. It produces backward location and travel time probabilities for the contaminant's prior position. Backward location probability describes the position of the contamination at some time prior to sampling, and backward travel time probability describes the amount of time required for the contamination to travel to the sampling location from some upgradient position, such as a known or suspected contamination source. With backward probabilities, the present position of the contamination is known (i.e., the receptor location), and the position of contamination at some time in the

past is desired.

A related concept is forward probability. Forward location probability describes the future position of the contamination at some time after it is released from the source, and forward travel time probability describes the amount of time required for the contamination to travel from its source to a downgradient location. The cumulative distribution function of this forward travel time probability is equivalent to a capture zone. These probabilities can be obtained from conventional forward contaminant transport models; however, if we have only one downgradient location of interest, these forward probabilities can be obtained more efficiently using the backward model.

Although forward and backward probabilities describe similar processes, they have different interpretations. The difference between these two can be best explained with a strong pumping well in a two-dimensional flow field, where flow everywhere is directed toward the pumping well. The forward travel time probability describes the time at which a particle released from the source will arrive at the well. For a particle detected at the pumping well, the backward travel time probability describes the time prior to detection that the particle was at the source. Intuitively, the forward and backward travel time probabilities have the same shape; however, their magnitudes differ. Since flow everywhere is directed toward the well, a particle released at the source will eventually reach the well, but a particle detected at the well might never have been at that particular source, and this is reflected in the lower magnitude of the backward travel time probability.

Backward (receptor-based) modeling is more efficient than forward

modeling in situations in which the number of known or potential sources is greater than the number of detections. The benefit of backward modeling is that, for each detection, we obtain information about all possible prior locations after solving the backward model only once. With forward modeling, we obtain information about all possible future positions for contamination originating from one specified source. Thus, if we have a few detections and many known or possible source locations, backward modeling is computationally more efficient than forward modeling in that fewer simulations must be run (i.e. one simulation for each detection). However, if we have many detections and only a few possible source locations, forward modeling is more computationally efficient. Receptor-based models have a variety of applications, including source characterization, source identification, and capture zone delineation. They can also be used to identify source release times, which is beneficial for assessing liability and for allocating costs of remediation systems.

Wilson and Liu [1994, 1997], *Liu* [1995], and *Liu and Wilson* [1995] heuristically developed a model for backward location and travel time probabilities. The model addressed a single detection of contamination for several flow and transport scenarios including conservative and reactive chemicals, uniform and non-uniform flow fields, homogeneous and heterogeneous aquifers, and one- and multi-dimensional domains. Although they arrived at the appropriate governing equations and boundary conditions, their approach was based more on intuition than on proof.

The main goal of this research was to develop a mathematical modeling technique to efficiently address receptor-based problems (known receptor, unknown source) in complex, three-dimensional, heterogeneous aquifers. We

used the adjoint approach to obtain the governing equations for the backward model. The advantage of the adjoint approach over the heuristic approach is that adjoint theory provides a rigorous mathematical procedure for developing the equations for all aquifer geometries and for all transport processes.

In Chapters 2–6, we illustrated the formal adjoint approach for obtaining the backward model. The development was based on sensitivity analysis, in which the adjoint state can represent the marginal sensitivity of a system state to a system parameter. We showed that the adjoint state for location probability is equivalent to the marginal sensitivity of resident concentration at the detection (system state) to a unit source of contamination (system parameter). Similarly, for travel time probability the system state is flux concentration at the detection. Backward and forward location and travel time probabilities are related to these adjoint states.

We used the advection-dispersion equation (ADE) as the governing equation for contaminant transport, although the approach can be used with other transport equations. The backward governing equation contains the adjoint of the advection-dispersion operator and a load term representing a source of probability. The adjoint is similar to the ADE, with some modifications. In the backward (adjoint) model, the time variable is backward time, or time prior to detection, and the flow field is reversed in both space and time relative to the forward model. The load term on the governing equation in the backward model represents a source of probability, and its functional form depends on the type of probability (location or travel time probability, probability density function or cumulative distribution function) and the sampling device (monitoring well or pumping well). For sorbing solutes, the load term also depends

on whether the contamination was detected in the aqueous or sorbed phase. Another difference between the forward and backward models is in the boundary conditions. First-type boundaries in the forward model remain first-type boundaries in the backward model; however, second-type boundaries in the forward model become third-type in the backward model and vice versa. In the backward model, all boundary and initial conditions are homogeneous.

Using adjoint theory, we formally developed the backward model for several flow and transport scenarios. We addressed one-dimensional flow and transport of a conservative solute in Chapter 2 for a semi-infinite domain representing flow to a pumping well, and in Chapter 3 for an infinite domain representing flow to a monitoring well. The backward location and travel time probability distributions that were developed show the likely position of the contamination at some time prior to detection, or the likely travel time from some upgradient location to the detection. Additional information can be obtained by evaluating the integrals of the probability distributions. The integral of backward location probability over the spatial domain at a specified backward time $\hat{\tau}$ represents the probability that the detected contamination was in the aquifer at time $\hat{\tau}$. If the domain contains no internal sources of water, this integral evaluates to one for a conservative solute because the contamination had to exist at some location. The integral of backward travel time probability over the time domain at a specified location $\mathbf{x}$ represents the probability that the detected contamination was ever at that location. For a conservative solute in a one-dimensional domain with no internal sources of water, this integral evaluates to one for all upgradient locations because the contamination had to exist at $\mathbf{x}$ at some time in the past.

In Chapter 4, we extended the adjoint model to multi-dimensional aquifers with homogeneous properties. In a multi-dimensional domain, a contaminant parcel does not sample all points in the aquifer; therefore, for contamination detected at a well, there is a probability of less than one that it ever was present at a given location $\mathbf{x}$. Since the integral of travel time over the time domain at any location represents the probability that the detected contamination ever was at that location, this integral will evaluate to less than one in a multi-dimensional domain.

In Chapter 5, we extended the model to address heterogenous aquifer properties, spatially-distributed inflows, and non-uniform and transient flow. If the aquifer contains an internal source of water, the spatial integral of location probability at time $\hat{\tau}$ evaluates to less than one because there is a non-zero probability that the detected contamination entered through the source during the time interval $0 < \tau < \hat{\tau}$ and was not in the system at time $\hat{\tau}$. This is observed with areal recharge as a source of water. Similarly, the integral of travel time probability over the time domain at a location $\mathbf{x}$ evaluates to less than one, because there is a non-zero probability that the contamination entered the aquifer downgradient of $\mathbf{x}$ and therefore was never present at $\mathbf{x}$.

In Chapter 6, we extended the backward model to address reactive transport including first-order decay, linear equilibrium sorption, and linear non-equilibrium sorption. Two different interpretations of backward probabilities can be made for decaying contaminants. With one interpretation, we allow probability to decay. This interpretation implies that longer travel times and distant prior location are less likely because contamination originating from these locations and times is likely to have decayed prior to reaching the de-

tection location. In the second interpretation, the probability is conditioned on the contamination reaching the well (i.e., it has not decayed), therefore it does not decay. With the first interpretation, the spatial integral of location probability evaluates to less than one for any time $\tau > 0$; while with the second interpretation, the spatial integral evaluates to one (assuming no internal sources of water).

For sorbing contaminants, the forward model is a system of two equations, one for the sorbed phase and one for the aqueous phase. The backward (adjoint) model is also a system of two equations, with two adjoint states. The backward probabilities depend on the phase of the detected contamination and on the phase of interest at the prior location. The phase of the detected contamination affects the load term, and the phase of interest at the prior location is determined by the combination of the resulting adjoint states used to define probability. The backward probabilities are not obtained directly from adjoint states; however, they can be obtained from a simple integration of the adjoint states. The governing equations for the backward model with linear non-equilibrium sorption are not consistent with the forward model; therefore, we were not able to solve the adjoint model using conventional transport codes.

Because the governing equation for the backward probability model is similar to the forward governing equation, any numerical code that can be used to model contaminant transport should also be capable of modeling backward location and travel time probabilities, with some adjustments. The main adjustments are that the forward flow field must be reversed and the boundary conditions must be modified. Also, since the load term in the backward model contains generalized functions (e.g., Dirac delta function and its derivative), it

cannot be used explicitly in a numerical model and must be approximated. In Chapter 7, we discussed the numerical approximations of the load terms for cell-centered finite difference models and finite element models with linear triangular and prism elements. The procedure can be extended to node-centered finite difference models and to finite element models with other types of elements.

In most practical situations, contamination is detected at more than one location or time. This additional information can improve the characterization of the prior position of contamination by reducing the variance of the probability distributions. The multiple-detection location probability assumes that all particles were at the same location at time τ in the past, and the probability distribution describes the joint position of the particles at time τ. If the contamination was known to have been released at time τ, then this distribution describes the source location probability. The multiple-detection travel time probability assumes that all particles were at location $\mathbf{x}$ at the same time in the past, and the probability distribution describes the time at which the particles were at that location. If we know that $\mathbf{x}$ is the contamination source, then this distribution describes the probability of the source release time.

We examined two different cases of the multiple detection problem. In the first case (Chapter 8), we considered only the existence of the contamination at the detections; and in the second case (Chapter 9), we also used the measured concentrations. For the case of existence only, the multiple-detection probability distributions are related to the single-detection probability distributions through Bayes' theorem and the law of total probability. Because of a normalization that is inherent in the approach, the resulting multiple-detection

probability distributions are conditioned on the fact that the two particles existed at the same location and time. Therefore, we obtain no information about the likelihood that the particles ever existed at the location or time of interest. We showed that the variance of the multiple-detection probability is smaller than the variances of the single-detection probabilities.

To incorporate concentration measurements into the backward probability model, we assumed that the contamination source was an instantaneous point source of unknown location, and that the samples contain unbiased random measurement error with known distribution. The additional information available from the concentration measurements was expected to better characterize the source of contamination, thereby reducing the variance of the probability distributions.

With a known source mass, the location and travel time probability distributions have a smaller variance than the no-concentration distributions. The variance increases as measurement error increases, and in the limit as measurement error becomes large, the probability distributions approach the no-concentration distributions. With an unknown source mass, the variances of the backward location and travel time probability distributions increase as the uncertainty in the source mass increases, and these variances are often larger than the variances of the no-concentration distribution.

In Chapter 10, we illustrated the backward modeling approach using data from a trichloroethylene (TCE) plume at the Massachusetts Military Reservation (MMR) on Cape Cod. The plume, called Chemical Spill 10 (CS-10), is approximately 17,000 ft long, has a maximum width of 4,000 ft, and a

thickness of up to 140 ft. The suspected contamination source area is a former missile site (BOMARC site) that is presently used for maintenance and storage of vehicles. Other spills and releases of chemicals have occurred in this area in the past and have contributed to the contamination. In particular, reports show that disposal of waste from the BOMARC facility may have occurred at an area south of the BOMARC Site (CS-22) [*MMR IRP*, 2000]. TCE samples have been taken throughout the plume area. We selected four TCE samples to be used in the model. These samples were taken between September 1996 and June 2000 and represent the central and terminal regions of the plume.

The backward probability model used in the analysis was a modified version of a model developed to simulate the response of the plume to the remediation system [*Zheng*, 1999]. The model was used to obtain single-detection and multiple-detection location and travel time probability distributions for the four selected samples. The results show that it is unlikely that the contamination originated at the BOMARC Missile Site during site operations. This could indicate that the BOMARC facility was not the source of contamination; that the model calibration, which was based on remediation conditions, may not be accurate for this scenario; that the conceptual model of TCE transport at the site may be inaccurate; or that the conceptualization of the source may be incorrect. Based on the results, the CS-22 area is a more likely source of the contamination.

11.2 Recommendations for Future Work

The general framework for the backward model has been developed and tested. The model can be used to obtain information about the prior position of groundwater contamination in a variety of flow and transport scenarios. Limitations of the existing model inhibit its usefulness in certain practical situations and should be addressed in future work. The future work can be separated into improvements to the existing model and extensions of the model.

11.2.1 Improvements to the Existing Backward Model

The governing equations of the backward model were developed using adjoint theory. Because the form of the adjoint equation is similar to that of the forward equation, any numerical code that solves the forward equation can also be used to solve the backward model. An exception to this is the case of linear non-equilibrium sorption, in which the form of the adjoint equations is different than the form of the forward equation. The forward model is

$$\frac{\partial C}{\partial t} + \frac{\partial C_s}{\partial t} = D\frac{\partial^2 C}{\partial x^2} - v\frac{\partial C}{\partial x} \tag{11.1}$$

$$\frac{\partial C_s}{\partial t} = \alpha_s \left(\frac{K_d \rho_b}{\theta} C - C_s \right) , \tag{11.2}$$

and the backward model is

$$\frac{\partial \psi_a^*}{\partial \tau} = D\frac{\partial^2 \psi_a^*}{\partial x^2} + v\frac{\partial \psi_a^*}{\partial x} + \frac{\alpha_s K_d \rho_b}{\theta}\psi_s^* + \frac{\partial h}{\partial C} \tag{11.3}$$

$$\frac{\partial \psi_a^*}{\partial \tau} + \frac{\partial \psi_s^*}{\partial \tau} = -\alpha_s \psi_s^* + \frac{\partial h}{\partial C_s} , \tag{11.4}$$

(see Section 6.3.3 for a description of the variables). The forward transport equation (11.1) contains two time derivatives, while the backward transport equation (11.3) contains only one, and vice versa for the forward (11.2) and backward (11.4) transfer equations. Since the form of the adjoint equation is different than the forward equation, conventional forward transport codes cannot solve the backward model as written. In his heuristic development of the backward model, *Liu* [1995] obtained equations similar to (11.1) and (11.2); therefore, it is possible that the adjoint equations can be rewritten in a form similar to the forward model and additional work is needed to determine the correct equations.

Multiple-detection location and travel time probabilities are related to the single-detection probabilities through Bayes' theorem and the law of total probability, given by

$$f_x(x_{1_A} = x_1, x_{1_B} = x_1; \tau) = \frac{f_x(x_{1_A} = x_1; \tau) f_x(x_{1_B} = x_1; \tau)}{\int_{x_1} f_x(x_{1_A} = x_1; \tau) f_x(x_{1_B} = x_1; \tau)\, dx_1} \ , \quad (11.5)$$

for two detections (see Section 8.4 for a description of the variables). Because of the normalization, the multiple-detection location probability will always integrate to one over the spatial domain. With a decaying solute or with internal sinks of water, $\int_x f_x(x;\tau)dx < 1$ for $\tau > 0$, indicating a finite probability that the detected particle was not in the system at backward time τ. This provides additional information about the prior position of the detected contamination. With the normalization in (11.5), this additional information is lost. The existing model would be improved if we used a better normalization that preserved this information, and additional work is needed to identify this normalization.

The same problem is observed for backward travel time probability.

If measured concentrations are incorporated into the backward model, the measurement error affects the uncertainty of the backward probability distributions. If the source mass is known, the backward probabilities have small variances for small values of measurement error. As the measurement error increases, the backward probability distributions approach the no-concentration distributions. In other words, as the measured concentration becomes more uncertain, the amount of additional information provided by the concentration measured decreases; in the limit, a completely uncertain concentration measurement provides no additional information. If the source mass is unknown, we would also expect the distributions to approach the no-concentration distribution as the uncertainty in the source mass increases. However, the results presented in Chapter 9 show that the variance of the backward probability distributions increase indefinitely with increasing uncertainty in the source mass. A new approach should be taken so that the use of concentration measurements results in a variance reduction over the no-concentration distributions, regardless of the prior knowledge of the source mass.

11.2.2 Extensions of the Backward Model

An implicit assumption made in the development of the backward model is that the source of contamination is an instantaneous point source, or that it can be represented by a single cell in the numerical model grid. Although this assumption can be relaxed quite easily for the single-detection probabilities, it is inherent in the development of the multiple-detection model.

Since many contamination sources are not instantaneous point sources and must be represented by more than one cell in the numerical grid, the backward model should be extended to addresses distributed sources.

The existing multiple-detection backward model assumes only one source of contamination. Situations exist in which multiple sources of contamination are likely and we need to determine not only the location of the source but also the number of sources. Further developments of the backward model should be made so that the model can provide information about the number of sources.

Often when contamination is detected in an aquifer, samples are taken at many locations to delineate the plume. To adequately identify the plume boundaries, some samples must be taken outside of the plume, resulting in sampled concentrations that are below detection limits. These no-detection measurements provide additional information about the source of the plume; however, the existing backward model does not use this information, and should be extended to account for it.

The backward probability model has been developed for a single dissolved species in groundwater. Many sites are contaminated with multiple species, including decay products. Coupling chemical fate modeling with the backward probability model should improve the source characterization. This might be particularly useful for non-aqueous phase liquid (NAPL) sources which contain multiple components.

The existing backward model was developed only with the classical advection-dispersion equation. Contaminant transport can also be mod-

eled with other equations such as stochastic transport equations [*Dagan*, 1984; *Zhang and Neuman*, 1995; *Zhang et al.*, 2000], a fractional advection-dispersion equation [*Benson et al.*, 2000], or a stochastic-convective equation [*Simmons* 1982; *Jury and Roth*, 1990]. Also, the work presented here deals only with linear systems, and its development was based on linear operator theory. Many transport problems are non-linear, such as vadose zone transport and coupled flow and transport systems with density-dependent flow. To fully address these problems, the backward model should be developed for other transport equations and for non-linear problems.

In the backward model presented here we assumed that all flow and transport parameters were known exactly, and the only unknown parameters were the source location or source release time, and possibly the source mass. Flow and transport parameters always contain uncertainty, which would affect the uncertainty in the backward location and travel time probability distributions. The backward model should be extended to address parameter uncertainty.

Although the focus of this work was contaminant transport in groundwater, the backward probability model can be applied to any environmental media. Some transport processes not included here may be important in other environmental media, such as atmospheric deposition in air pollution. Using adjoint theory, the appropriate governing equations for these backward models can be obtained from the commonly-used equations of forward contaminant transport.

References

Benson, D.A., S.W. Wheatcraft, and M.M. Meerschaert, Application of a fractional advection-dispersion equation, *Water Resour. Res.*, 36(9), 1403–1412, 2000.

Dagan, G., Solute transport in heterogeneous formations, *J. Fluid Mech.*, 145, 151-177, 1984.

Jury, W.A. and K. Roth, *Transfer Functions and Solute Movement through Soil: Theory and Applications*, Birkhauser, Boston, 1990.

Liu, J., *Travel time and location probabilities for groundwater contaminant sources*, Master's thesis, New Mexico Institute of Mining and Technology, Socorro, 1995.

Liu, J. and J.L. Wilson, Modeling travel time and source location probabilities in two-dimensional heterogeneous aquifer. *Proceedings 5th Annual WERC Technology Development Conference*, New Mexico State University, Las Cruces, New Mexico, 59–67, 1995.

MMR IRP (Massachusetts Military Reservation, Installation Restoration Program), News Release 2000-51, Sept. 26, 2000c, http://www.mmr.org/cleanup/index.htm.

Simmons, C.S., A stochastic-convective transport representation of dispersion in one-dimensional porous media systems, *Water Resour. Res.*, 18(4), 1193–1214, 1982.

Wilson, J.L. and J. Liu, Backward tracking to find the source of pollution, in *Waste-management: From Risk to Remediation*, edited by R. Bhada

et al., ECM Press, Albuquerque, NM, 181–199, 1994.

Wilson, J.L. and J. Liu, Field Validation of the Backward-in-time Advection Dispersion Theory. *Proceedings of the 1996 HSRC/WERC Joint Conf. on the Environment*, Great Plains-Rocky Mountain Hazardous Substance Center, Manhattan, Kansas, http://www.engg.ksu.edu/HSRC/ 96Proceed/wilson.html, 1997.

Zhang, D. and S.P. Neuman, Eulerian-Lagrangian analysis of transport con ditioned on hydraulic data, 1, Analytical-numerical approach, *Water Resour. Res.*, 31(1), 39–51, 1995.

Zhang, D., R. Andricevic, A.Y. Sun, X. Hu, and G. He, Solute flux approach to transport through spatially nonstationary flow in porous media, *Water Resour. Res.*, 36(8), 2107–2120, 2000.

Zheng, C. and P.P. Wang, *MT3DMS: Documentation and User's Guide*, U.S. Army Corps of Engineers, Washington, DC, November, 1999.

APPENDIX A

FORTRAN CODE TO REVERSE MODFLOW FLOW FIELD

A.1 Discussion

To run a backward probability model using MT3D, the flow field can be obtained by first generating a flow field for the forward model using MODFLOW and then reversing this flow field. MODFLOW creates a MODFLOW-MT3D link file that contains all of the flow information needed for the transport model. This binary file is written in a format that can be used directly in MT3D. It includes flow components for all cells in the domain. In MODFLOW, the domain is discretized as shown in Figure A.1. The three directions are labeled x, y, and z. The y-direction is discretized into rows indexed as $i = 1, 2, \ldots$, beginning with the back-most row; the x-direction is discretized into columns indexed as $j = 1, 2, \ldots$, beginning with the left-hand column; and the z direction is discretized into layers indexed as $k = 1, 2, \ldots$, beginning with the top layer. The flow data and their descriptions are presented here in the order they are listed in the binary link file [*McDonald and Harbaugh*, 1988; *Zheng*, 1999]:

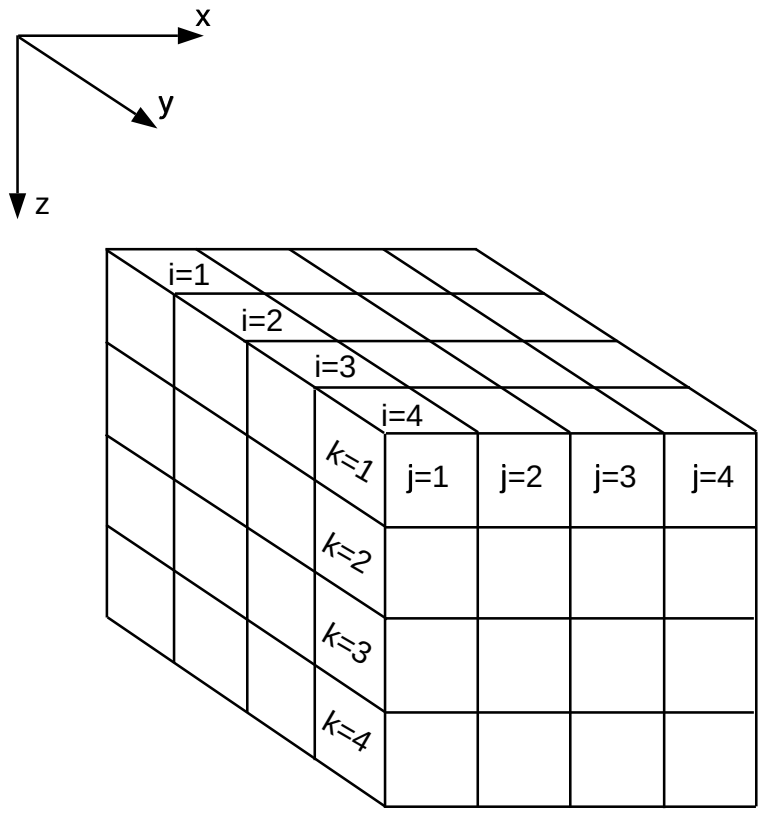

Figure A.1: Sample grid and grid numbering with MODFLOW.

- Saturated thickness

  (one value for each cell in the domain)

  For a confined aquifer, this value is set to -111; for an unconfined aquifer, this value is equal to the saturated thickness of the aquifer at the cell; for an inactive cell, the value is set to 10^{30}.

- Volumetric flow rate in the x-direction

  (one value for each cell in the domain)

  This value quantifies the volumetric flow rate across each front cell face. The flow rate for cell (i, j, k) corresponds to the flow between cells (i, j, k) and $(i + 1, j, k)$. It is positive for flow in the positive x direction.

- Volumetric flow rate in the y-direction

  (one value for each cell in the domain)

  This value quantifies the volumetric flow rate across each right cell face. The flow rate for cell (i, j, k) corresponds to the flow between cells (i, j, k) and $(i, j + 1, k)$. It is positive for flow in the positive y direction.

- Volumetric flow rate in the z-direction

  (one value for each cell in the domain)

  This value quantifies the volumetric flow rate across each lower cell face. The flow rate for cell (i, j, k) corresponds to the flow between cells (i, j, k) and $(i, j, k + 1)$. It is positive for flow in the positive z direction.

- Volumetric flow rate into or out of storage

  (one value for each cell in the domain)

  This value is non-zero only for a transient flow simulation. It is positive for flow out of storage and negative for flow into storage.

- Volumetric flow rate into or out of constant head cells

  (one value for each cell representing a constant-head cell)

  This value represents the volumetric flow rate into or out of a constant head cell, including the exchange between this cell and adjacent cells. It is positive if net flow is out of the constant head cell and negative if net flow is into the constant head cell. (In contrast, the net flow rate calculated by MODFLOW for a constant-head cell does not account for flow into or out of adjacent cells).

- Volumetric flow rate of wells

  (one value for each cell containing a well)

  This value is positive for injections and negative for withdrawals.

- Volumetric flow rate of drains

  (one value for each cell containing a drain)

  This value is always positive.

- Volumetric recharge rate

  (one value for each cell that receives recharge)

  This value is applied to the top-most active cell in each vertical stack of cells. It is always positive.

- Volumetric evapotranspiration rate

  (one value for cell that loses water to evapotranspiration)

  This value is applied to the top-most active cell in each vertical stack of cells. It is always negative.

- Volumetric flow rate of river cells

  (one value for each cell representing a river reach)

  This value is positive for losing reaches and negative for gaining reaches.

- Volumetric flow rate of head-dependent boundary cells

  (one value for each cell representing a general-head boundaries)

  This value is positive for flow into the cell and negative for flow out of the cell.

Only the data required for the simulation are included in the link file. The complete set of required data is written for the first time step, then for the second time step, etc.

The backward probability model requires a reversed flow field. We have written a fortran code that reverses the flow field. The code reads in the data in the MODFLOW-MT3D link file from the forward flow model, and writes a new link file with the flow field reversed. Except for the saturated thickness, all of the data listed above must be reversed in direction and in time. The reversal of direction is accomplished by reversing the sign on the flow rates. The reversal in time is accomplished by rewriting the data into the new link file beginning with the last time step, and ending with the first time step. The code is included in the next section.

A.2 Code

```
      program f2b

c This program converts the MODFLOW-MT3D link file. The file that
c MODFLOW creates is for the forward model; this code reverses the
c flow field and rewrites the file for the equivalent backward model.

c created by: Roseanna M. Neupauer
c created: January 12, 2000
c modified: March 13, 2000 to reverse the flow field in time
c modified: June 7, 2000 to generalize array sizes

      parameter (maxtimes=25,maxrech=200,maxwel=200,maxdrn=200)
      parameter (maxriv=200,maxghb=200,maxcnh=200)
      parameter (maxcol=200,maxrow=200,maxlay=30)
      character*25 fname,oname
      character*11 header
      character*16 label
      dimension thick(maxcol,maxrow,maxlay,maxtimes)
      dimension qxx(maxcol,maxrow,maxlay,maxtimes)
      dimension qyy(maxcol,maxrow,maxlay,maxtimes)
      dimension qzz(maxcol,maxrow,maxlay,maxtimes)
      dimension stor(maxcol,maxrow,maxlay,maxtimes)
      dimension rech(maxcol,maxrow,maxtimes)
      dimension evt(maxcol,maxrow,maxtimes)
      dimension ibuffr(maxcol,maxrow,maxtimes)
      dimension ibuffe(maxcol,maxrow,maxtimes)
      dimension kper(12,maxtimes),kstp(12,maxtimes)
      dimension label(12)
      dimension ncnh(maxtimes),nwel(maxtimes),ndrn(maxtimes)
      dimension nriv(maxtimes),nghb(maxtimes)
      dimension kcnh(maxcnh,maxtimes),icnh(maxcnh,maxtimes)
      dimension jcnh(maxcnh,maxtimes),kwel(maxwel,maxtimes)
      dimension iwel(maxwel,maxtimes),jwel(maxwel,maxtimes)
      dimension kdrn(maxdrn,maxtimes),idrn(maxdrn,maxtimes)
      dimension jdrn(maxdrn,maxtimes),kriv(maxriv,maxtimes)
      dimension iriv(maxriv,maxtimes),jriv(maxriv,maxtimes)
      dimension kghb(maxghb,maxtimes),ighb(maxghb,maxtimes)
      dimension jghb(maxghb,maxtimes)
      dimension qdrn(maxdrn,maxtimes),qwel(maxwel,maxtimes)
      dimension qriv(maxriv,maxtimes),qghb(maxghb,maxtimes)
      dimension qcnh(maxcnh,maxtimes)

      write(*,*)'Enter the name of the MODFLOW-MT3D link file '
      read(*,*) fname
      write(*,*)'Enter the name of the new backward model link file '
      read(*,*) oname
```

```
      open(unit=22,file=fname,form='unformatted',access='sequential')
      open(unit=30,file=oname,form='unformatted')
      rewind(30)

      read(22) header,mtwel,mtdrn,mtrch,mtevt,mtriv,mtghb,
     >     mtchd,mtiss,mtnper
      write(30) header,mtwel,mtdrn,mtrch,mtevt,mtriv,mtghb,
     >     mtchd,mtiss,mtnper

      itimes=0

 10   itimes=itimes+1
      read(22,end=100) kper(1,itimes),kstp(1,itimes),ncol,
     >     nrow,nlay,label(1)

c saturated thickness (unit: l).
      read(22) (((thick(j,i,k,itimes),j=1,ncol),i=1,nrow),k=1,nlay)

c QXX
      if (ncol.ne.1) then
         read(22,end=100) kper(2,itimes),kstp(2,itimes),ncol,
     >     nrow,nlay,label(2)
         read(22) (((qxx(j,i,k,itimes),j=1,ncol),i=1,nrow),k=1,nlay)
      endif
c QYY
      if (nrow.ne.1) then
         read(22,end=100) kper(3,itimes),kstp(3,itimes),ncol,
     >     nrow,nlay,label(3)
         read(22) (((qyy(j,i,k,itimes),j=1,ncol),i=1,nrow),k=1,nlay)
      endif
c QZZ
      if (nlay.ne.1) then
         read(22,end=100) kper(4,itimes),kstp(4,itimes),ncol,
     >     nrow,nlay,label(4)
         read(22) (((qzz(j,i,k,itimes),j=1,ncol),i=1,nrow),k=1,nlay)
      endif
c storage term
      if (mtiss.eq.0) then
         read(22,end=100) kper(5,itimes),kstp(5,itimes),ncol,
     >     nrow,nlay,label(5)
         read(22) (((stor(j,i,k,itimes),j=1,ncol),i=1,nrow),k=1,nlay)
      endif
c constant head boundary cells
      read(22,end=100) kper(6,itimes),kstp(6,itimes),ncol,
     >     nrow,nlay,label(6),ncnh(itimes)
      if (ncnh(itimes).gt.0) then
         do n=1,ncnh(itimes)
            read(22)kcnh(n,itimes),icnh(n,itimes),jcnh(n,itimes),
     >           qcnh(n,itimes)
```

```
         enddo
      endif
c wells
      if (mtwel.gt.0) then
         read(22,end=100) kper(7,itimes),kstp(7,itimes),ncol,
     >     nrow,nlay,label(7),nwel(itimes)
         do n=1,nwel(itimes)
            read(22)kwel(n,itimes),iwel(n,itimes),jwel(n,itimes),
     >           qwel(n,itimes)
         enddo
      endif
c drains
      if (mtdrn.gt.0) then
         read(22,end=100) kper(8,itimes),kstp(8,itimes),ncol,
     >     nrow,nlay,label(8),ndrn(itimes)
         do n=1,ndrn(itimes)
            read(22)kdrn(n,itimes),idrn(n,itimes),jdrn(n,itimes),
     >           qdrn(n,itimes)
         enddo
      endif
c recharge
      if (mtrch.gt.0) then
         read(22,end=100) kper(9,itimes),kstp(9,itimes),ncol,
     >     nrow,nlay,label(9)
         read(22) ((ibuffr(j,i,itimes),j=1,ncol),i=1,nrow)
         read(22) ((rech(j,i,itimes),j=1,ncol),i=1,nrow)
      endif
c evapotranspiration
      if (mtevt.gt.0) then
         read(22,end=100) kper(10,itimes),kstp(10,itimes),
     >        ncol,nrow,nlay,label(10)
         read(22) ((ibuffe(j,i,itimes),j=1,ncol),i=1,nrow)
         read(22) ((evt(j,i,itimes),j=1,ncol),i=1,nrow)
      endif
c rivers and streams
      if (mtriv.gt.0) then
         read(22,end=100) kper(11,itimes),kstp(11,itimes),
     >        ncol,nrow,nlay,label(11),nriv(itimes)
         do n=1,nriv(itimes)
            read(22)kriv(n,itimes),iriv(n,itimes),jriv(n,itimes),
     >           qriv(n,itimes)
         enddo
      endif
c general-head boundaries
      if (mtghb.gt.0) then
         read(22,end=100) kper(12,itimes),kstp(12,itimes),
     >        ncol,nrow,nlay,label(12),nghb(itimes)
         do n=1,nghb(itimes)
            read(22)kghb(n,itimes),ighb(n,itimes),jghb(n,itimes),
```

```
     >           qghb(n,itimes)
            enddo
          endif

          goto 10

 100      continue
          itimes=itimes-1
          close(22)

c start of writing

          do 300 iti=1,itimes
             it=itimes-iti+1

c saturated thickness (unit: l).
             write(30) kper(1,iti),kstp(1,it),ncol,nrow,nlay,label(1)
             write(30) (((thick(j,i,k,it),j=1,ncol),i=1,nrow),k=1,nlay)

c QXX
             if (ncol.ne.1) then
              write(30) kper(2,iti),kstp(2,it),ncol,nrow,nlay,label(2)
              write(30) (((-qxx(j,i,k,it),j=1,ncol),i=1,nrow),k=1,nlay)
             endif
c QYY
             if (nrow.ne.1) then
              write(30) kper(3,iti),kstp(3,it),ncol,nrow,nlay,label(3)
              write(30) (((-qyy(j,i,k,it),j=1,ncol),i=1,nrow),k=1,nlay)
             endif
c QZZ
             if (nlay.ne.1) then
              write(30) kper(4,iti),kstp(4,it),ncol,nrow,nlay,label(4)
              write(30) (((-qzz(j,i,k,it),j=1,ncol),i=1,nrow),k=1,nlay)
             endif
c storage term
             if (mtiss.eq.0) then
              write(30) kper(5,iti),kstp(5,it),ncol,nrow,nlay,label(5)
              write(30) (((-stor(j,i,k,it),j=1,ncol),i=1,nrow),k=1,nlay)
             endif
c constant head boundary cells
             write(30) kper(6,iti),kstp(6,it),ncol,nrow,nlay,label(6),
     >            ncnh(it)
             if (ncnh(it).gt.0) then
                do n=1,ncnh(it)
                   write(30)kcnh(n,it),icnh(n,it),jcnh(n,it),-qcnh(n,it)
                enddo
             endif
c wells
             if (mtwel.gt.0) then
```

```
            write(30) kper(7,iti),kstp(7,it),ncol,
     >           nrow,nlay,label(7),nwel(it)
            do n=1,nwel(it)
               write(30)kwel(n,it),iwel(n,it),jwel(n,it),-qwel(n,it)
            enddo
         endif
c drains
         if (mtdrn.gt.0) then
            write(30) kper(8,iti),kstp(8,it),ncol,
     >           nrow,nlay,label(8),ndrn(it)
            do n=1,ndrn(it)
               write(30)kdrn(n,it),idrn(n,it),jdrn(n,it),-qdrn(n,it)
            enddo
         endif
c recharge
         if (mtrch.gt.0) then
            write(30) kper(9,iti),kstp(9,it),ncol,
     >           nrow,nlay,label(9)
            write(30) ((ibuffr(j,i,it),j=1,ncol),i=1,nrow)
            write(30) ((-rech(j,i,it),j=1,ncol),i=1,nrow)
         endif
c evapotranspiration
         if (mtevt.gt.0) then
            write(30) kper(10,iti),kstp(10,it),ncol,
     >           nrow,nlay,label(10)
            write(30) ((ibuffe(j,i,it),j=1,ncol),i=1,nrow)
            write(30) ((-evt(j,i,it),j=1,ncol),i=1,nrow)
         endif
c rivers and streams
         if (mtriv.gt.0) then
            write(30) kper(11,iti),kstp(11,it),ncol,
     >           nrow,nlay,label(11),nriv(it)
            do n=1,nriv(it)
               write(30)kriv(n,it),iriv(n,it),jriv(n,it),-qriv(n,it)
            enddo
         endif
c general-head boundaries
         if (mtghb.gt.0) then
            write(30) kper(12,iti),kstp(12,it),ncol,
     >           nrow,nlay,label(12),nghb(it)
            do n=1,nghb(it)
               write(30)kghb(n,it),ighb(n,it),jghb(n,it),-qghb(n,it)
            enddo
         endif
 300  continue
      close(30)
      end
```

A.3 References

McDonald, M.G. and A.W. Harbaugh, *A Modular Three-Dimensional Finite-Difference Groundwater Flow Model*, U.S. Geological Survey Techniques of Water-Resources Investigations, Book 6, Chapter A1, 1988.

Zheng, C. and P.P. Wang, *MT3DMS: Documentation and User's Guide*, U.S. Army Corps of Engineers, Washington, DC, November, 1999.